IMOS
Integrated **Marine**
Observing System

State and Trends of Australia's Oceans | Report

IMOS

Integrated **Marine**
Observing System

State and Trends of Australia's Oceans | Report

© Integrated Marine Observing System
Published by the Integrated Marine Observing System

This report is licensed under a Creative Commons Attributional 4.0 International Licence with the exception of the logo of the Integrated Marine Observing System, any other material protected by trademark, content supplied by third parties and any photographs. For information on licence conditions see: https://creativecommons.org/licenses/by/4.0

Data obtained from the Integrated Marine Observing System in the production of this report was accessed under a Creative Commons Attributional 4.0 International Licence. Data that has been sourced from other providers have been appropriately identified.

Disclaimer

While the Integrated Marine Observing System (IMOS) has taken reasonable steps to ensure that the information in this publication is correct, it provides no warranty or guarantee that information provided by the authors is accurate, complete or up-to-date. IMOS does not accept any responsibility or liability for any actions taken as a result of, or in reliance on, information in this publication. Users should check with the originating authors to confirm the accuracy of the information before taking any action in reliance on that information.

If you believe any information in this publication is inaccurate, out of date or misleading, please bring it to our attention by contacting the authors directly or by contatcing the IMOS office.

This publication should be cited as:

Richardson A.J, Eriksen R, Moltmann T, Hodgson-Johnston I, Wallis J.R (2020). State and Trends of Australia's Ocean Report, Integrated Marine Observing System, Hobart.

Editorial team: Anthony J. Richardson, Ruth Eriksen, Tim Moltmann, Jake R. Wallis, Indiah Hodgson-Johnston

Steering Committee: David Smith, Nic Bax and Karen Evans

Visit: www.imosoceanreport.org.au

Comments and questions regarding this document should be addressed to:

Integrated Marine Observing System (IMOS)
University of Tasmania
20 Castray Esplanade
(Private Pag 110)
Hobart TAS 7001, Australia

Phone: (03) 6226 7549
Email: imos@imos.org.au
www.imos.org.au

Australia's Integrated Marine Observing System (IMOS) is enabled by the National Collaborative Research Infrastructure Strategy (NCRIS). It is operated by a consortium of institutions as an unincorporated joint venture, with the University of Tasmania as Lead Agent.

Table of Contents

1. Physical and Chemical Time Series

2.Biological Time Series - Productivity

3. Biological Time Series - Water Quality

4. Biological Time Series - Marine Animals

Introduction

Marine assessments are important tools for examining the state and trends of marine systems at regional, national, and global scales. The most robust assessments are data-driven and underpinned by time series of internationally accepted ecosystem indicators, based on measurement of physical, chemical, and biological variables. The collating, synthesising, and reporting of meaningful indicators of marine ecosystem health provides information in a clear way to a broad, and often non-scientific audience.

The Integrated Marine Observing System (IMOS) is uniquely positioned to provide time series data that can underpin assessments of Australia's vast and valuable marine estate (see "Australia's Integrated Marine Observing System (IMOS)" below).

The national State of the Environment Report, global World Ocean Assessment, and regional Great Barrier Reef Outlook Report are examples of regular reporting and assessment tools that require time series data collected at the scale of IMOS. The State and Trends of Australia's Oceans Report (2019) is intended to provide a baseline for contribution to all such marine assessments into the future.

It is not the role of IMOS to undertake marine assessments. The role of IMOS as a national research infrastructure is to build large datasets and long time series for use and reuse. The process to produce this report is designed to ensure that datasets and time series available within Australia are organised, analysed, and interpreted so that they can be used in relevant assessment and reporting processes as required. Making our datasets and time series 'assessment ready' is part of the IMOS strategy to plan for impact. This includes data collected by IMOS facilities as well as additional data contributed by partners through the Australian Ocean Data Network (AODN).

IMOS
Integrated **Marine**
Observing System

Australia's Integrated Marine Observing System (IMOS)

The Integrated Marine Observing System (IMOS): IMOS is a national research infrastructure funded under the Australian Government's National Collaborative Research Infrastructure Strategy (NCRIS). Since 2006, IMOS has been routinely operating a wide range of observing equipment throughout Australia's coastal and open oceans, making all of its data accessible to the marine and climate science communities, and other stakeholders and users. Significant co-investment is provided by institutional partners, other Australian Government programs, State and Territory Governments, the private sector, and international collaborators. Co-investment comes in the form of cash and in-kind contributions, including provision of additional data accessible through the IMOS-operated Australian Ocean Data Network (AODN). IMOS is a regional alliance of the Global Ocean Observing System (GOOS) and works with many nations to improve the quality, consistency and availability of ocean observations globally.

About this report

The process to develop this report involved over 70 scientists from 16 institutions working with available datasets, mostly of ten years length or longer. New analyses were undertaken to produce scientifically robust information about the state and trends of ecosystem indicators relevant to the Australian marine environment and its bioregions (see "Australian marine bioregions", p 8).

A total of 27 time series datasets were assessed as being appropriate for inclusion in the State and Trends of Australia's Oceans Report (2019). They are grouped into four themes covering indicators of the physical and chemical environment, biological productivity, water quality and marine animals (zooplankton, fish, sharks and marine mammals).

All the time series used are of variables in the water column of the ocean, known as the pelagic zone (see "The pelagic zone", p 9). Before IMOS was established there was no systematic and sustained collection of data in the pelagic zone of Australia's marine environment, limiting our ability to understand the state and trends of key ecosystem indicators. The 2019 report begins to address this huge gap. No variables from the seafloor (benthic zone) are included in this report, though an expanded scope could be considered in the future.

The four themes were not predetermined at the start of the process. Identification of the 27 time series included in the 2019 report was inevitably based on availability of data and willingness of subject matter experts to make time available for analysis. As the editorial team went through the process of synthesising outputs into a single report, this four-theme structure emerged. Different thematic structures could evolve in response to user and stakeholder feedback.

The report contains succinct documents (of 4-6 pages) for each time series that are written in a common format by a group of subject matter experts. There is a Rationale and a section on Implications for people and ecosystems. The analysis Methods used are explained. Results and Interpretation are provided through a combination of brief narratives and downloadable graphs and maps. Data Sources are acknowledged, and References to relevant scientific literature are provided. Each time series document has been assigned its own digital object identifier (DOI).

The goal has been to ensure that the report will be relevant to national, global, and regional marine assessments and therefore useful to the scientific community, government managers and policy makers, and marine industries. The intention has been to establish a process that is repeatable, efficient, and can be timed to feed into future assessment and reporting cycles and take advantage of new data and methods as they become available.

A list of the four themes and 27 time series included in this report is shown below. A summary of key findings is provided in the next section.

Time Series themes

1

Physical & chemical environment

2

Biological productivity

3

Water quality

4

Marine animals

Australian marine bioregions

Australia's ocean territory has been classified into six marine bioregions – South-east, Temperate East, South-west, North-west, North and Coral Sea. Marine bioregional plans have been developed by the Australian Government under the Environment Protection and Biodiversity Conservation Act 1999 (EPBC Act) to improve the way Australia's oceans are managed so they remain healthy and productive.

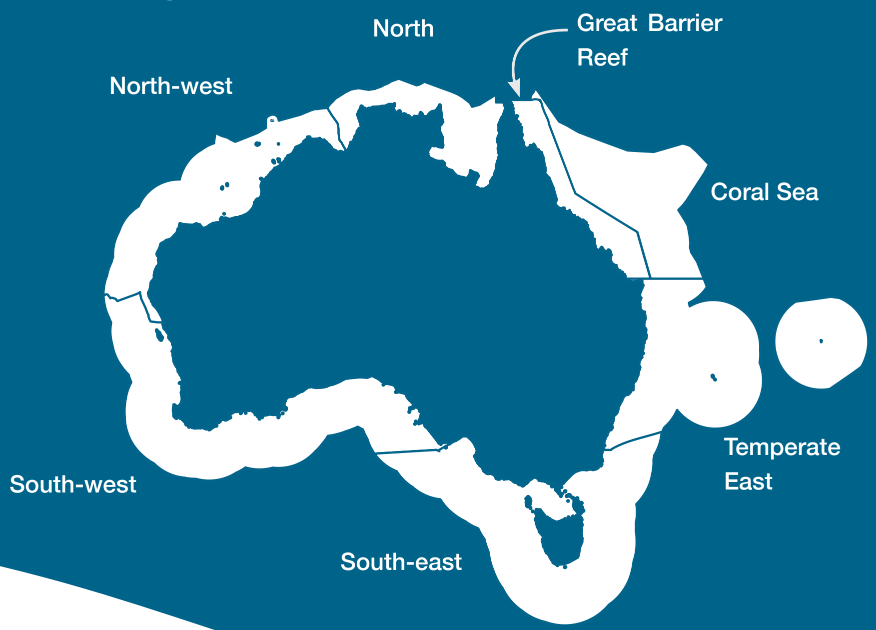

The time Series

1. Physical and chemical environment Time Series

- 1.1 Long-term changes in temperature around Australia
- 1.2 Sea Surface Temperature Variability
- 1.3 East Australian Current Variability
- 1.4 Variability in ocean currents around Australia
- 1.5 Spatial and temporal trends in concentrations of nutrients
- 1.6 Ocean acidification

2. Biological Time Series – Productivity

- 2.1 Spatial and seasonal trends in Chlorophyll a
- 2.2 Spatial and seasonal and trends in net primary production
- 2.3 Contrasting trends of Australia's plankton communities
- 2.4 The seasons of phytoplankton around Australia
- 2.5 Indicators of depth layers important to phytoplankton production
- 2.6 Picophytoplankton: harbingers of change in our coastal oceans
- 2.7 Status of Australian marine microbial assemblages

3. Biological Time Series – Water quality

- 3.1 Water clarity around Australia – satellite and in situ observations
- 3.2 Spatial and seasonal trends in *Trichodesmium*
- 3.3 *Tripos* dinoflagellates as indicators of Australian marine bioregions
- 3.4 Harmful Algal Blooms and the shellfish industry
- 3.5 Harmful Algal Blooms in New South Wales
- 3.6 Range expansion of the red tide dinoflagellate *Noctiluca scintillans*

4. Biological Time Series – Marine animals

- 4.1 The response of the copepod community to long-term warming along the east coast of Australia
- 4.2 The impact on Zooplankton of the 2011 heatwave off Western Australia
- 4.3 Use of Zooplankton communities to estimate the relative strength of the East Australian Current
- 4.4 Ocean acidification and calcifying zooplankton
- 4.5 Sounding out life in Australia's twilight zone
- 4.6 Temporal and spatial changes in larval fish
- 4.7 Continental scale-shark migrations
- 4.8 Tracking elephant seal population trends in the Southern Ocean

The pelagic zone

The pelagic zone is the ecological realm that includes the entire ocean water column. Of all inhabited environments on Earth, it has the largest volume and the greatest vertical range. Pelagic life is found throughout the water column, although the numbers of individuals and species decrease in deeper waters. The regional and vertical distributions of pelagic life are governed by the abundance of nutrients and dissolved oxygen; the presence or absence of sunlight, water temperature, salinity, and pressure; and the presence of continental or submarine topographic barriers.

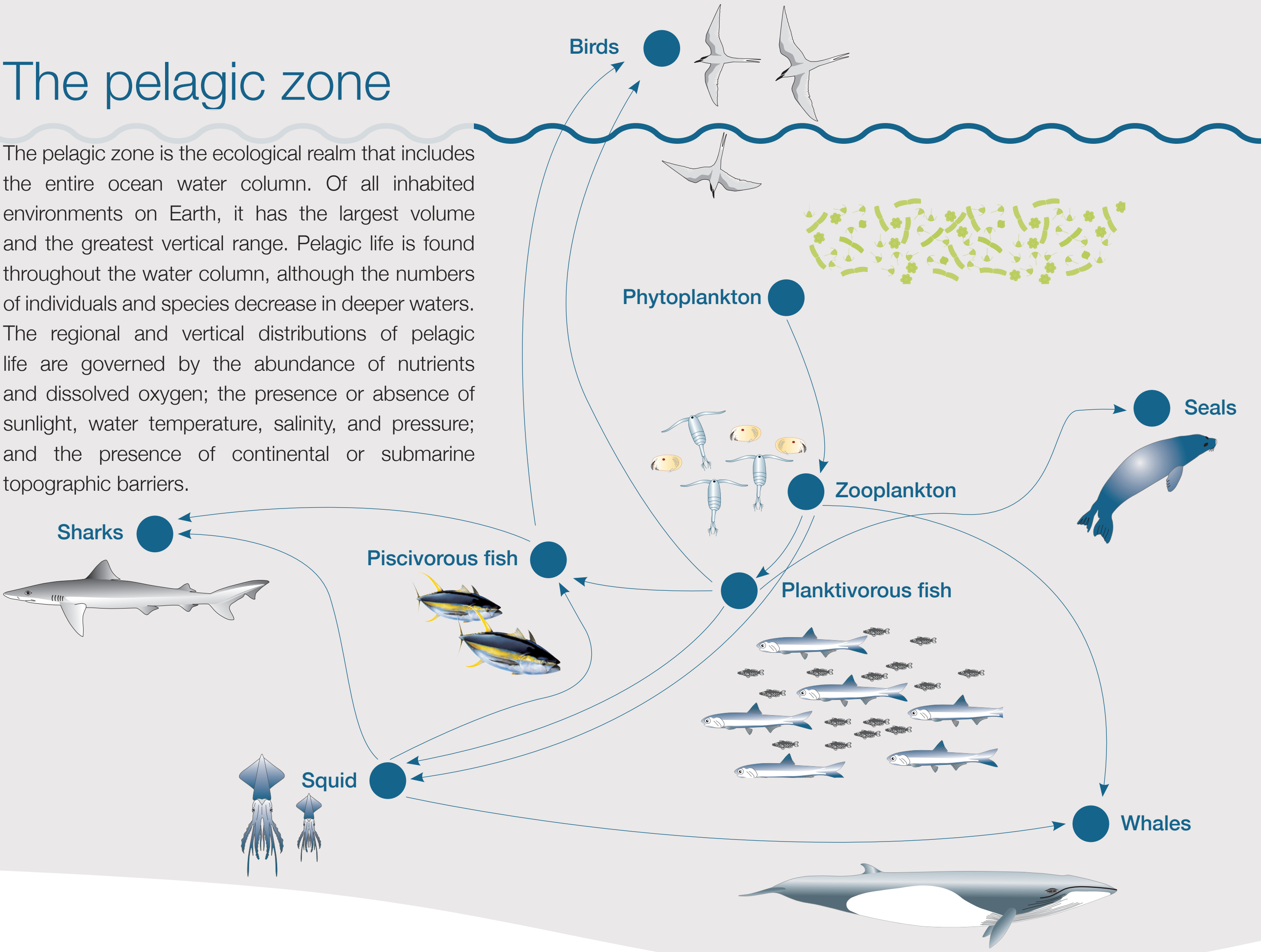

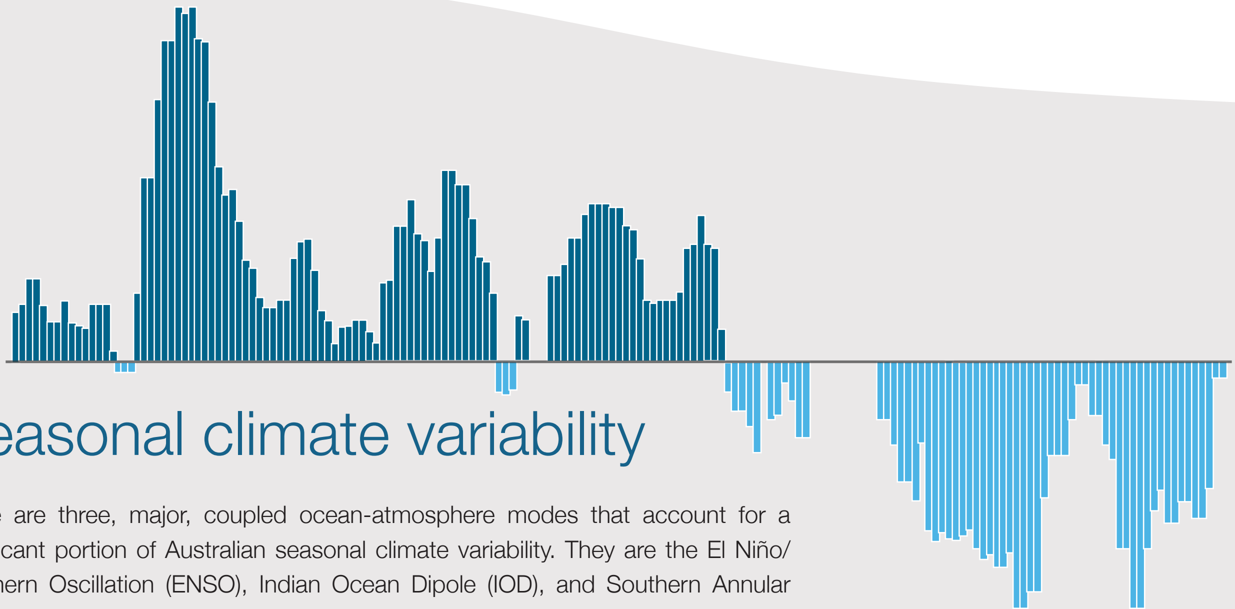

Seasonal climate variability

There are three, major, coupled ocean-atmosphere modes that account for a significant portion of Australian seasonal climate variability. They are the El Niño/ Southern Oscillation (ENSO), Indian Ocean Dipole (IOD), and Southern Annular Mode (SAM). ENSO is the strongest mode both globally and in terms of its impacts on Australian climate. A characteristic of ENSO is the associated pattern of sea surface temperature (SST) variation in the eastern tropical Pacific Ocean, which alternates between a warm phase (El Niño) and a cold phase (La Niña). ENSO has a strong influence on regional rainfall patterns across much of Australia. El Niño are events associated with droughts and La Niña events associated with heavy rainfall.

Key findings

The 27 individual time series include results, interpretations, and implications that will be of use to anyone interested in the variables being observed. Bringing all of these time series together into a single State and Trends of Australia's Oceans Report (2019) creates the potential to get a much more integrated and comprehensive view of what is happening across Australia's marine environment.

It is now possible to do this because of sustained investment in a nationally integrated marine observing system (IMOS) and a national ocean data network (AODN). This report is intended to add value to these investments by providing additional scientific analysis to make available research data more useful to marine assessments that inform government managers and policy makers and marine industries responsible for sustainable development of Australia's marine environment.

Key findings of the State and Trends of Australia's Oceans Report (2019) are summarised below.

1

Physical and chemical environment

Time series of the physical environment (1.1) show steady warming of Australia's oceans over the last century, with some regional variation. Regional variation is strongly influenced by the major ocean currents that flow around the Australian continent (see "Boundary currents around Australia", p 12).

Warming has been fastest in the south, particularly in the South East and Temperate East bioregions. High variability between years, called interannual variability, is also observed (1.2, 1.3, 1.4). This can be related to the major modes of seasonal climate variability impacting the Australian region (see "Seasonal climate variability", p 9). Consistent with global climate models, seasonal, high-temperature extremes called 'marine heatwaves' can now be observed. Marine heatwaves appear to be increasing in frequency and intensity, with implications for marine ecosystems (1.4, 2.6, 4.2).

Bringing these time series together enables investigation of connections between the physical environment, chemical environment, and biological productivity.

Along with rising temperature, increasing acidification of the ocean is observable at a global scale. Time series of chemical variables within the Australian marine environment (1.6) show large decreases in pH of seawater and in concentration of dissolved carbonate ions. These are the internationally accepted measures of ocean acidification. Regional data show interannual variability driven by the combination of seasonal climate and boundary currents. There is no evidence of decline in the abundance of calcifying organisms over the last decade (4.4).

2

Biological productivity

Consistent with ocean warming, there is evidence of declining biological productivity of surface waters across the Australian marine environment. This can be seen in time series of chlorophyll a (2.1), net primary production (2.2), and phytoplankton abundance (2.3). Regional variation can be explained by physical factors e.g. incursion of nutrient-rich sub-Antarctic surface waters in the South East bioregion. Seasonal cycles of productivity are shown to follow latitudinal bands that are temperature dependent (2.4). It is noted that these findings relate to surface waters only, and the importance of sub-surface productivity also needs to be considered in assessing the biological productivity of Australian waters (2.5).

Time series of the biomass and abundance of marine animals that undertake secondary production (called zooplankton) are increasing (2.3), in contrast to the decline in primary production. Possible explanations for this increase include changes to community structure and changes to rates of top-down predation by fish. This interesting finding highlights the value of undertaking integrated analysis of datasets and time series to inform the focus of future research.

Molecular tools have been applied to IMOS sampling programs since 2012 and it is now possible to produce time series of Australian marine microbial assemblages (2.7). As this work matures under the Australian Microbiome Initiative the utility of molecular tools in monitoring, forecasting and managing marine environments will be further investigated.

3

Water quality

Most of Australia's offshore marine environment has relatively high water clarity, with some regional variation but no evidence of long-term change (3.1). The distribution and abundance of microorganisms with the potential to have harmful effects on people, fish, and shellfish is of significant interest to scientists, government managers and policy makers, marine industries, and the community at large. These include various species of dinoflagellates, diatoms, and bacteria.

Time series show changes in distribution and abundance of key species consistent with the physical and chemical effects of ocean warming (3.2, 3.6) and extreme events (3.5). The abundance of major harmful algal bloom species is typically below trigger levels, with some exceptions, though there is evidence that abundance of some key species is increasing (3.4).

A feature of the time series used in this section is the significant contribution of data collected outside of IMOS, by university researchers, State Governments, and the private sector. It is hoped that this report will help to motivate other data custodians to make more marine data findable, accessible, interoperable, and reusable (FAIR) through the AODN so that it can contribute to our collective understanding of the Australian marine environment.

4

Marine animals

Zooplankton are small marine animals that drift with ocean currents. They play a key role in marine food webs as consumers of phytoplankton and other food sources and as a resource for fish and other consumers at higher trophic levels. Time series show zooplankton communities responding to ocean warming, with increased abundance of warm-water taxa and decreased abundance of cold-water taxa (4.1). Marine heatwaves are shown to substantially reduce total zooplankton biomass, abundance, and size, while increasing diversity (4.2). Zooplankton communities have bounced back quite quickly after marine heatwaves, though the effects on higher trophic levels of reduced food availability during these events are currently unknown. Zooplankton community composition is also shown to change in response to variability of the East Australian Current (4.3).

An estimate of the density of smaller fish and larger zooplankton (e.g. squid and jellyfish) that live in the intermediate depths of the ocean (called the mesopelagic zone) can be developed using data from echosounders on fishing vessels and research vessels. Basin-scale time series have been established in the Indian Ocean, Southern Ocean, and Tasman Sea. The data show a significant increasing trend in the Tasman Sea and Southern Ocean (4.5). Further research is required to validate these estimates and understand the mechanisms at play.

The eggs and larvae of most marine fish inhabit surface waters of the ocean as planktonic organisms (called ichthyoplankton). Larval fish data for both the east and west coasts (4.6) show a strong latitudinal gradient for most of the year, with higher diversity and abundance in tropical northern regions and a steep decline below 30°S. Over the last two decades however, this gradient appears to have weakened along the east coast. Larval fish assemblages at northern and southern latitudes have become more similar. This is consistent with southward extension of warm EAC waters, shifting tropical/sub-tropical species poleward. Increased abundance of warm-water larval fish at southern latitudes is also consistent with the trend observed in other zooplankton (see 4.1, above).

Understanding movement and connectivity of larger marine animals (fishes, sharks, marine mammals) is increasingly important as human use and environmental change alter ocean ecosystems. Identifying movement patterns is particularly important for species that move long distances, and animal tracking technologies provide an effective and efficient means to build time series of species distribution. Previously unknown migration of bull sharks between Sydney Harbour and the Great Barrier Reef has been revealed by analysis of data from the continental-scale acoustic telemetry network (4.7). Time series of environmental data collected from satellite tags on elephant seals in the Southern Ocean have been used to describe the water masses in which the animals are feeding, helping to resolve questions about population trends (4.8).

Boundary currents around Australia

The main, large-scale influences on the ocean around Australia arise from the South Pacific basin in the east and the Indian Ocean basin in the west. Australia is therefore influenced by two major ocean current systems at the boundaries of these basins. The East Australian Current (EAC) is a southward-flowing boundary current that is formed by the South Equatorial Current (SEC) crossing the Coral Sea and reaching the coast of Australia off north Queensland. As it flows southward, it splits from the coast just north of Sydney. The majority of the EAC flow moves eastward across the Tasman Sea towards New Zealand, with the remainder flowing southward towards Tasmania (known as the EAC extension). The Leeuwin Current is a boundary current that flows southwards along the coast of Western Australia. It rounds Cape Leeuwin to enter the waters south of Australia where its influence extends as far as Tasmania. The Leeuwin Current is anomalous in that it flows poleward against the prevailing winds.

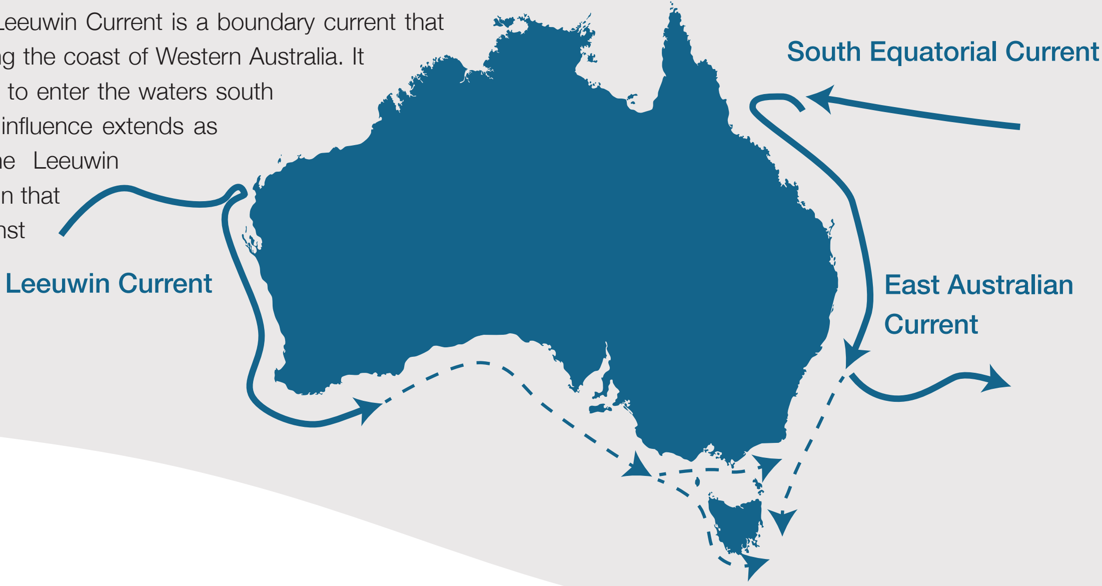

The next steps

The State and Trends of Australia's Oceans Report (2019) is a pilot product.

The concept emerged from within the IMOS community, and preparation of the report has been facilitated through one-off funding of an IMOS Task Team.

It is envisaged that updates of the State and Trends of Australia's Oceans Report would be produced every two years, on a biennial cycle, timed to optimise potential for contribution to major reports and assessments carried out regularly at national, regional and global scales.

Feedback on the first report from the Australian marine management and policy communities is therefore critical to determining next steps. The provision of feedback on this report will be facilitated by the IMOS Office, and stakeholders are encouraged to engage in helping to develop the concept.

For example, the next Australian State of the Environment (SoE) Report will cover the five-year period from 2017 to 2021. Whether or not data and analysis from the State and Trends of Australia's Oceans Report series are used in SoE 2021 will provide one indication of utility.

The large team of over 70 scientists involved in preparing the report found it an interesting and useful process. Many lessons were learnt along the way and any future reports will benefit from this experience. We are confident that the resources required to produce these reports on a routine basis could be marshalled if there is sufficient user and stakeholder demand for the product.

Summary

The time series in this report provide scientifically robust information on state and trends of pelagic ecosystem indicators for Australia's vast and valuable marine estate. Many of these indicators have not been previously available.

Against a background of long-term global ocean warming and acidification, regional variations are elucidated and the influences of seasonal climate variability (e.g. ENSO) and boundary current variability (e.g. EAC) are shown. There is evidence of extreme events (e.g. marine heatwaves) increasing in frequency and intensity.

Importantly, numerous biological responses to change and variability in the physical/chemical environment are shown. Many of these have potential socio-economic and policy implications which are outlined in each of the time series' "implications for people and ecosystems" sections.

There is evidence of declining biological productivity of surface waters across the Australian marine environment. Sub-surface productivity is also shown to be important, though it is currently less well understood at large scale. Decline in primary production is not reflected in time series of secondary production, which is increasing. Explanations for this interesting result are hypothesised and could inform the focus of future research.

Distribution and abundance of harmful algal bloom species is changing. The abundance of major harmful algal bloom species is typically below trigger levels, with some exceptions, though there is evidence that abundance of some key species is increasing.

Communities of microscopic marine animals (e.g. zooplankton) are changing, with evidence of increased abundance of warm-water taxa and decreased abundance of cold-water taxa as the oceans warm. Poleward shifts of tropical/sub-tropical species are also observed. In deeper, colder waters of the Tasman Sea and Southern Ocean, density of larger zooplankton and fish appears to be increasing. New insights into movement patterns of larger marine animals (e.g. bull sharks, elephant seals) are provided, with evidence of patterns changing in response to environmental conditions.

The improved understanding of connections between physical, chemical, and biological variables provided in the State and Trends of Australia's Oceans Report (2019) is a significant step in describing these links and the ongoing changes they face. This in turn increases our confidence in modelling of future states across the Australian marine environment, to inform government managers and policy makers, and marine industries, in the context of sustainable development.

The data behind the Time Series

	Ships of Opportunity	Satellite Remote Sensing	National Mooring Network	Animal Tracking	Deep Water Moorings	Australian Ocean Data Network	Ocean Radar
1. Physical and Chemical Time Series							
1.1 Long-term changes in temperature around Australia		●	●				
1.2 Sea Surface Temperature Variability		●					
1.3 East Australian Current Variability		●			●		●
1.4 Variability in ocean currents around Australia		●					
1.5 Spatial and temporal trends in concentrations of the nutrients N, P, Si			●				
1.6 Ocean acidification			●				
2.Biological Time Series - Productivity							
2.1 Spatial and seasonal trends in Chlorophyll a		●					
2.2 Spatial and seasonal and trends in net primary production		●					
2.3 Contrasting trends of Australia's plankton communities			●				
2.4 The seasons of phytoplankton around Australia		●					
2.5 Indicators of depth layers important to phytoplankton production			●				
2.6 Picophytoplankton: harbingers of change in our coastal oceans			●				
2.7 Status of Australian marine microbial assemblages			●				
3. Biological Time Series - Water Quality							
3.1 Water clarity around Australia – satellite and in situ observations		●	●				
3.2 Spatial and seasonal trends in *Trichodesmium*	●		●				
3.3 *Tripos* dinoflagellates as indicators of Australian marine bioregions	●		●			●	
3.4 Harmful Algal Blooms and the shellfish industry						●	
3.5 Harmful Algal Blooms in New South Wales						●	
3.6 Range expansion of the red tide dinoflagellate *Noctiluca scintillans*	●		●				
4. Biological Time Series - Marine Animals							
4.1 The response of the copepod community to long-term warming along the east coast of Australia	●		●				
4.2 The impact on Zooplankton of the 2011 heatwave off Western Australia			●				
4.3 Use of Zooplankton communities to estimate the relative strength of the East Australian Current	●	●					
4.4 Ocean acidification and calcifying zooplankton			●				
4.5 Sounding out life in Australia's twilight zone	●						
4.6 Temporal and spatial changes in larval fish	●		●				
4.7 Continental-scale shark migrations				●			
4.8 Tracking elephant seal population trends in the Southern Ocean				●			

State and Trends of Australia's Ocean Report

Marine Bioregional Summary

● IMOS National Reference Station

● Coastal Waters

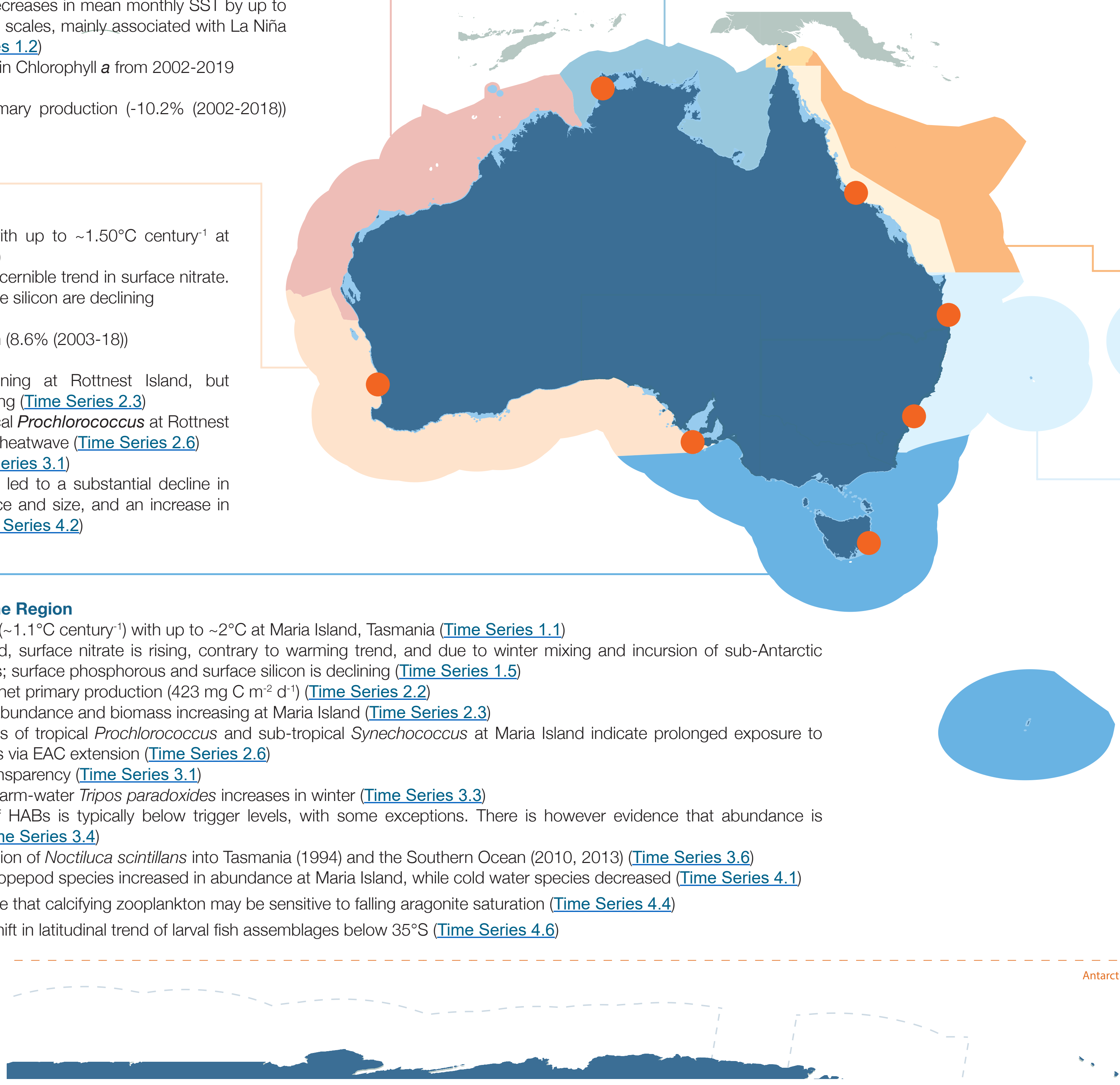

North-west Marine Region

- Ocean warming (~0.6°C century^{-1}) (Time Series 1.1)
- Many increases/decreases in mean monthly SST by up to 2°C at inter-annual scales, mainly associated with La Niña events (Time Series 1.2)
- Significant decline in Chlorophyll ***a*** from 2002-2019 (Time Series 2.1)
- Decline in net primary production (-10.2% (2002-2018)) (Time Series 2.2)

South-west Marine Region

- Warming (~0.99°C century^{-1}), with up to ~1.50°C century^{-1} at Rottnest Island (Time Series 1.1)
- At Rottnest Island there is no discernible trend in surface nitrate. Surface phosphorous and surface silicon are declining (Time Series 1.5)
- Decline in net primary production (8.6% (2003-18)) (Time Series 2.2)
- Phytoplankton biovolume declining at Rottnest Island, but zooplankton abundance increasing (Time Series 2.3)
- Unseasonal appearance of tropical *Prochlorococcus* at Rottnest Island during 2011-2012 marine heatwave (Time Series 2.6)
- High water transparency (Time Series 3.1)
- The 2011 WA marine heatwave led to a substantial decline in zooplankton biomass, abundance and size, and an increase in diversity at Rottnest Island (Time Series 4.2)

South-east Marine Region

- Fast warming (~1.1°C century^{-1}) with up to ~2°C at Maria Island, Tasmania (Time Series 1.1)
- At Maria Island, surface nitrate is rising, contrary to warming trend, and due to winter mixing and incursion of sub-Antarctic surface waters; surface phosphorous and surface silicon is declining (Time Series 1.5)
- Relatively low net primary production (423 mg C m^{-2} d^{-1}) (Time Series 2.2)
- Zooplankton abundance and biomass increasing at Maria Island (Time Series 2.3)
- Summer peaks of tropical *Prochlorococcus* and sub-tropical *Synechococcus* at Maria Island indicate prolonged exposure to warmer waters via EAC extension (Time Series 2.6)
- Low water transparency (Time Series 3.1)
- Presence of warm-water *Tripos paradoxides* increases in winter (Time Series 3.3)
- Abundance of HABs is typically below trigger levels, with some exceptions. There is however evidence that abundance is increasing (Time Series 3.4)
- Range expansion of *Noctiluca scintillans* into Tasmania (1994) and the Southern Ocean (2010, 2013) (Time Series 3.6)
- Warm water copepod species increased in abundance at Maria Island, while cold water species decreased (Time Series 4.1)
- Some evidence that calcifying zooplankton may be sensitive to falling aragonite saturation (Time Series 4.4)
- North/south shift in latitudinal trend of larval fish assemblages below 35°S (Time Series 4.6)

North Marine Region

- Ocean warming (~0.74°C century^{-1}) (Time Series 1.1)
- High Chlorophyll ***a*** (0.537 mg m^{-3}) (Time Series 2.1)
- North bioregion had the greatest primary production at 324 gC m^{-2} y^{-1} (Time Series 2.2)
- Relatively high net primary production (888mg C m^{-2} d^{-1}) (Time Series 2.2)
- Phytoplankton abundance declining at Darwin, but zooplankton abundance and biomass increasing (Time Series 2.3)
- Lowest water transparency and most opaque waters (Time Series 3.1)
- Modest increases in calcifier abundance (Time Series 4.4)

Coral Sea Marine Region

- Warming (~0.8°C century^{-1}) (Time Series 1.1)
- Low Chlorophyll ***a*** (0.084 mg m^{3}) (Time Series 2.1)
- Decline in net primary production (9.1% (2003-2018)) (Time Series 2.2)
- Highest water transparency (Time Series 3.1)

Temperate East Marine Region

- Fast warming (~0.93°C century^{-1}), with up to ~1.50 °C century^{-1} at Port Hacking (Time Series 1.1)
- Linear increase in sea surface temperature along the east coast over 1993-2016 (Time Series 1.2)
- At Port Hacking, surface nitrate is declining - consistent with warming trends and is increasing at depth due to stratification. Surface phosphorous and surface silicon are declining (Time Series 1.5)
- Decline in net primary production (12.9% (2003-2018)) (Time Series 2.2)
- Phytoplankton biovolume and abundance declining significantly at North Stradbroke Island and Port Hacking, and zooplankton biomass declining at North Stradbroke Island (Time Series 2.3)
- Molecular data suggest that strains of *Synechococcus* increase in abundance and those of *Prochlorococcus* decrease in response to coastal upwelling at Port Hacking (Time Series 2.7)
- High water transparency. Validated by North Stradbroke Island NRS (Time Series 3.1)
- Significant decline in abundance of *Trichodesmium* at North Stradbroke Island (Time Series 3.2)
- Abundance of HABs is typically below trigger levels, with some exceptions. There is, however, evidence that abundance is increasing (Time Series 3.4)
- Harmful algal blooms on NSW beaches are seasonal and episodic nature (Time Series 3.5)
- Warm water copepod species increased in abundance at Port Hacking, cold water species decreased (Time Series 4.1)
- North/south shift in latitudinal trend of larval fish assemblages below 35°S (Time Series 4.6)

State and Trends of Australia’s Ocean Report

Regional Summary

Australian Region/EEZ

- Steady warming since 1920, particularly in the south (Time Series 1.1)
- The Leeuwin and East Australian Currents demonstrated strong seasonable and inter-annual variability linked to El Niño and La Niña events (Time Series 1.4)
- Large decreases in both aragonite saturation rate and pH between 1870-99 and 2000-09 (Time Series 1.6)
- Low average Chlorophyll ***a*** (0.25 mg m^3) typical of healthy tropical/ sub-tropical oceans. The average is declining, by 8% in the period 2003-19 (Time Series 2.1)
- Low average net primary production (551 mg C m^{-2} d^{-1}) typical of healthy tropical/sub-tropical oceans. Average declining by 12% in the period 2002-2019 (Time Series 2.2)
- Seasonal cycle of phytoplankton follows latitudinal bands, except in the Leeuwin Current and northeast Indian Ocean (Time Series 2.4)
- Deep chlorophyll maxima deeper than mean mixed layer depths indicating that sub-surface production is important (Time Series 2.5)
- Average Secchi disk depth is 24m (Time Series 3.1)
- Majority of Tripos species exhibit broad temperature range (10-25°C). Restricted group of warm water species identified to enable monitoring of any future range expansion (Time Series 3.3)
- No evidence of decline in calcifying zooplankton at National Reference Stations (Time Series 4.4)

Southern Ocean and Tasman Sea

- Increasing trend in acoustic backscatter in Southern Ocean (77% (2010-2018)) and Tasman Sea (44-105%), likely to reflect change in mesopelagic communities (Time Series 4.5)
- IMOS satellite tagging of elephant seals in the Southern Ocean revealing physical drives of population change (Time Series 4.8)

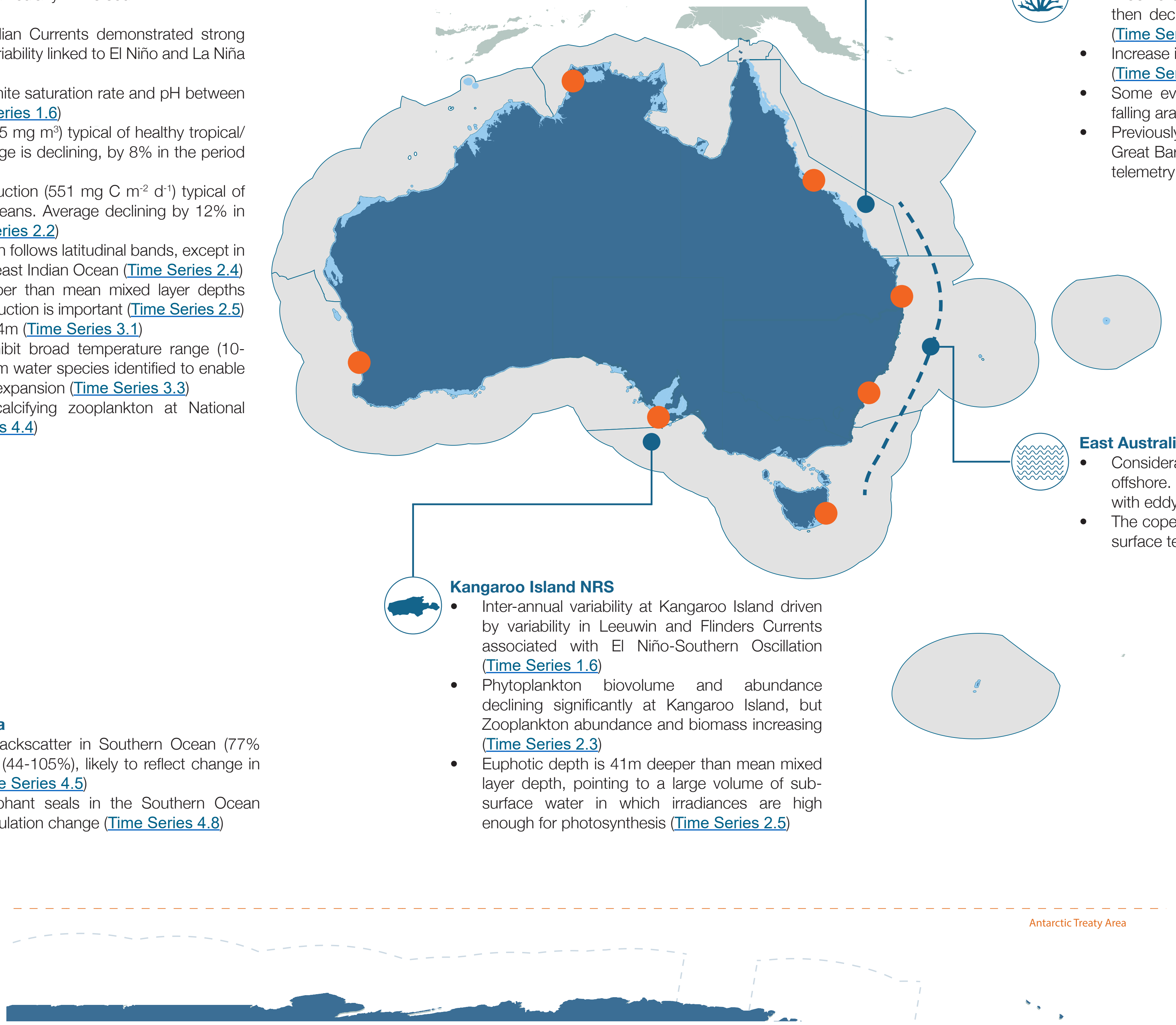

● IMOS National Reference Station

● Coastal Waters

Kangaroo Island NRS

- Inter-annual variability at Kangaroo Island driven by variability in Leeuwin and Flinders Currents associated with El Niño-Southern Oscillation (Time Series 1.6)
- Phytoplankton biovolume and abundance declining significantly at Kangaroo Island, but Zooplankton abundance and biomass increasing (Time Series 2.3)
- Euphotic depth is 41m deeper than mean mixed layer depth, pointing to a large volume of sub-surface water in which irradiances are high enough for photosynthesis (Time Series 2.5)

Great Barrier Reef

- *Prochlorococcus* most abundant at Yongala in spring and summer, then decline rapidly with drop in salinity due to seasonal rainfall (Time Series 2.6)
- Increase in abundance of *Trichodesmium* at Yongala (Time Series 3.2)
- Some evidence that calcifying zooplankton may be sensitive to falling aragonite saturation (Time Series 4.4)
- Previously unknown migration of Bull Sharks between NSW and the Great Barrier Reef revealed by the IMOS continental scale acoustic telemetry network (Time Series 4.7)

East Australian Current

- Considerable variability dominated by movement of the EAC on and offshore. Eastward displacement every 65-100 days associated with eddy shedding (Time Series 1.3)
- The copepod composition index is positive related to trends in sea surface temperature anomaly (2010-2018) (Time Series 4.3)

IMOS
Integrated Marine
Observing System

State and Trends of
Australia's Oceans | Report

1.1 | Long-term changes in temperature around Australia

Anthony J. Richardson[1,2] and Charitha B. Pattiaratchi[3,4]

[1] CSIRO Oceans and Atmosphere, Queensland Biosciences Precinct (QBP), St Lucia, QLD, Australia
[2] Centre for Applications in Natural Resource Mathematics (CARM), School of Mathematics and Physics, The University of Queensland, St Lucia, QLD, Australia
[3] Oceans Graduate School, The University of Western Australia, Perth, WA, Australia
[4] UWA Oceans Institute, The University of Western Australia, Perth, WA, Australia

Summary

Coarse long-term temperature data around Australia from 1870 and fine-scale temperature measurements from the three long-term stations since the 1940s confirm a strong warming trend over the past 100 years, with the strongest warming in the Southeast and the Southwest. This background warming signal is propagating throughout the ecosystem, impacting the physical, chemical and biological characteristics of Australia's marine environment.

Key Data Streams

Satellite Remote Sensing

National Reference Stations

State and Trends of Australia's Ocean Report
www.imosoceanreport.org.au

Time-Series published
10 January 2020

doi: 10.26198/5e169fa949e73

Rationale

The clearest impact of climate change impacts on the ocean is warming, particularly of surface layers that are in closest contact with the atmosphere. Temperature is of fundamental importance to the physics of the ocean. It describes the heat content of the ocean, affects the density and buoyancy of water, and helps distinguish water masses.

Temperature also drives the biology in the ocean. As warming reduces the density of water, and thus enhances stratification, it can lead to lower nutrient concentrations in surface waters, particularly in subtropical and tropical waters. This reduces primary productivity and diminishes phytoplankton and zooplankton biomass. This can then reduce fish biomass in the ocean (Irigoien et al., 2014; Richardson & Schoeman, 2004), especially under climate change (e.g. Galbraith, Carozza, & Bianchi, 2017). Temperature also drives changes in the distribution of marine plants and animals, with most species moving towards cooler temperatures at higher latitudes (Poloczanska et al., 2013). The pace of life in the ocean is also governed by temperature, through its impact on photosynthesis and metabolic rates.

Methods

To investigate long-term changes in sea surface temperature (SST) around Australia, we have used two different datasets. The longest time-scale is from 1870-2018, we used HadISST1, a monthly 1° global product, which is a blend of *in situ* and satellite temperature measurements (Rayner et al., 2003, available from https://www.metoffice.gov.uk/hadobs/hadisst/). We averaged HadISST1 in the six marine bioregions within the Australian EEZ. We also calculated the difference in SST between the present and the past from HadISST data using a linear regression over the entire time series and taking the difference between the estimated temperature in 2017 and that in 1870.

From 1944-2018, we used the longest observed temperature time series in Australia. This is from the three long-term National Reference Stations: Port Hacking, Maria Island and Rottnest Island (AODN dataset: “IMOS - ANMN National Reference Stations - Combined long-term hydrological data product (1944-2014)”).

Results and interpretation

In Australia’s marine bioregions, there was a slight cooling or no change in temperature between 1870 and the early 1900s (**Figure 1**). Since 1920, there has been steady warming, particularly in the south. The greatest warming has been in the South-east (1.1°C century^{-1}), the South-west (0.99°C century^{-1}) and the Temperate East (0.93°C century^{-1}) bioregions, with less warming in the North-west (0.6°C century^{-1}), North (0.74°C century^{-1}) and Coral Sea (0.8°C century^{-1}). The general spatial pattern shows that there has been warming throughout all of Australia since 1870, particularly in the South-east (**Figure 2**).

Data from the long-term National Reference Stations in Australia confirm the surface warming from HadISST1 data, showing strong warming over the past 80 years over all depths in the top 50 m. At Maria Island, all depths show a near-linear increase in temperature, up to ~2°C. Since the 1950s at Port Hacking there has been less warming, ~1.5°C. At Rottnest Island there has been moderate warming of ~0.75°C, including some more recent cooling.

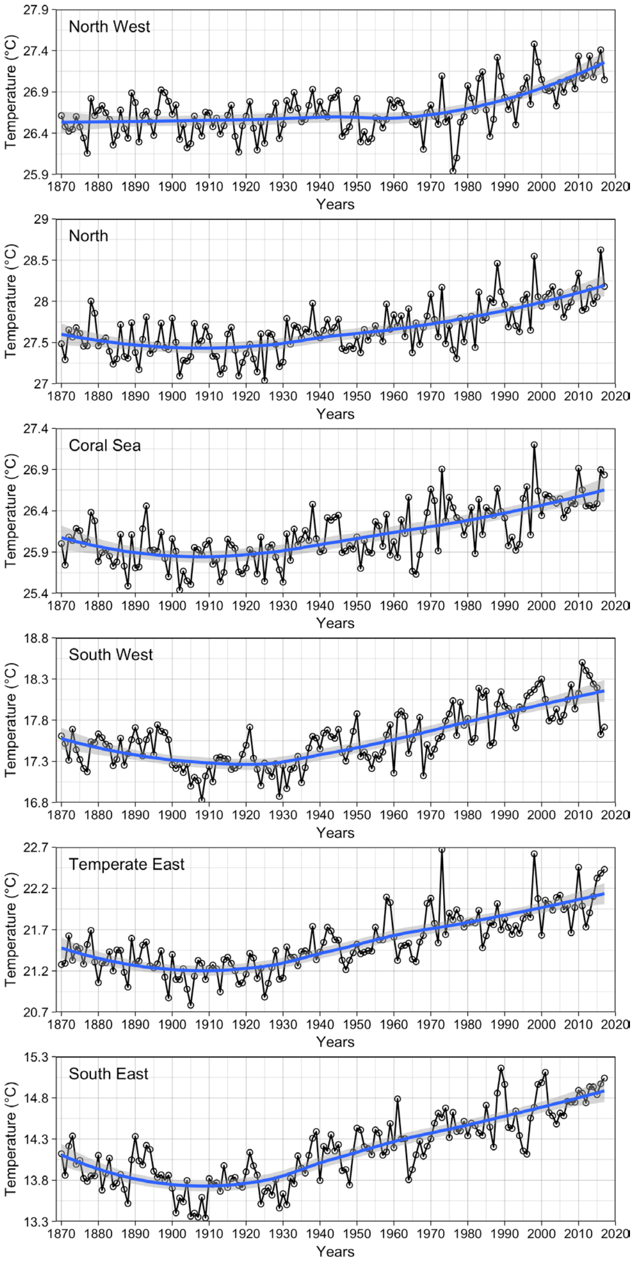

Figure 1. Long-term (since 1870) temperatures (°C) from HadISST in each marine bioregion. Note the different y-axis scales. A loess smoother was included to highlight the long-term pattern

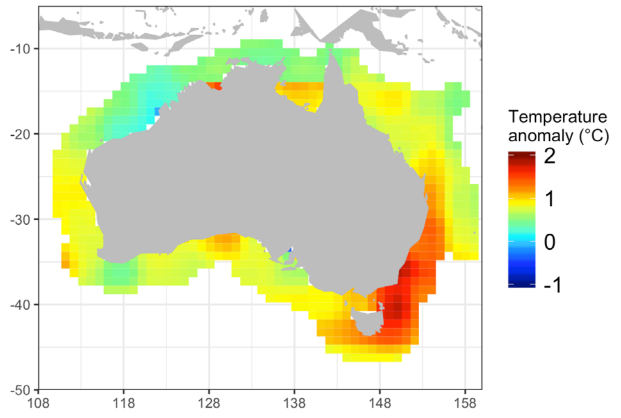

Figure 2. Difference in sea surface temperature between 2017 and 1870, based on a linear trend over the time series.

Implications for people and ecosystems

The HadISST1 data and temperature measurements from the three long-term stations confirm a strong warming trend in Australian waters over the past 150 years. The strength of the warming varies regionally. It is partly a consequence of global warming, amplified by changes of the regional ocean circulation (Ridgway, 2007). The South-east and Temperate East bioregions are warming the fastest because of changes to the path of the East Australian Current, causing increased warm-water incursions into Tasmanian waters (Hill, Rintoul, Coleman, & Ridgway, 2008).

This rapid warming has important implications for the distribution of marine organisms, permitting tropical and subtropical species to survive further south (Johnson et al., 2011; Last et al., 2011). However, resident cold-water coastal species in southern Australia are limited in the extent they can move further south before running out of habitat.

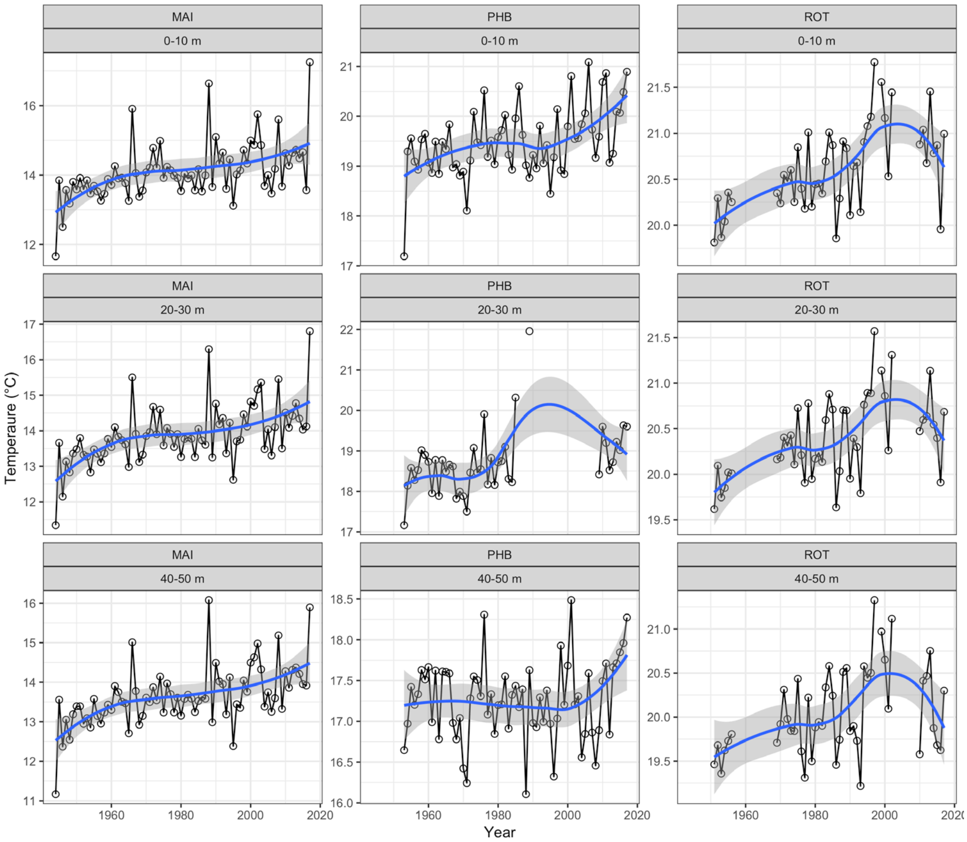

Figure 3. Long-term mean annual temperatures (°C) from Maria Island, Port Hacking and Rottnest Island reference stations in three depth strata in the top 50 m (n=4,500). Note the different y-axis scales. A loess smoother was included to highlight the long-term pattern

Acknowledgements

Data was sourced from Australia's Integrated Marine Observing System (IMOS) which is enabled by the National Collaborative Research Infrastructure Strategy (NCRIS).

Data Sources

IMOS National Reference Stations.
http://imos.org.au/facilities/nationalmooringnetwork/nrs/

IMOS Satellite Remote Sensing.
http://imos.org.au/facilities/srs/

References

Cai, W., Shi, G., Cowan, T., Bi, D., & Ribbe, J. (2005). The response of the Southern Annular Mode, the East Australian Current, and the southern mid-latitude ocean circulation to global warming. *Geophysical Research Letters, 32*(23). doi:L2370610.1029/2005gl024701

Galbraith, E. D., Carozza, D. A., & Bianchi, D. (2017). A coupled human-earth model perspective on long-term trends in the global marine fishery. *Nature Communications, 8*, 7. doi:10.1038/ncomms14884

Hill, K. L., Rintoul, S. R., Coleman, R., & Ridgway, K. R. (2008). Wind forced low frequency variability of the East Australia Current. *Geophysical Research Letters, 35*(8). doi:10.1029/2007gl032912

Irigoien, X., Klevjer, T. A., Rostad, A., Martinez, U., Boyra, G., Acuna, J. L., . . . Kaartvedt, S. (2014). Large mesopelagic fishes biomass and trophic efficiency in the open ocean. *Nature Communications, 5*, 10. doi:10.1038/ncomms4271

Johnson, C. R., Banks, S. C., Barrett, N. S., Cazassus, F., Dunstan, P. K., Edgar, G. J., . . . Taw, N. (2011). Climate change cascades: Shifts in oceanography, species' ranges and subtidal marine community dynamics in eastern Tasmania. *Journal of Experimental Marine Biology and Ecology, 400*(1-2), 17-32. doi:10.1016/j.jembe.2011.02.032

Last, P. R., White, W. T., Gledhill, D. C., Hobday, A. J., Brown, R., Edgar, G. J., & Pecl, G. (2011). Long-term shifts in abundance and distribution of a temperate fish fauna: a response to climate change and fishing practices. *Global Ecology and Biogeography, 20*(1), 58-72. doi:10.1111/j.1466-8238.2010.00575.x

Poloczanska, E. S., Brown, C. J., Sydeman, W. J., Kiessling, W., Schoeman, D. S., Moore, P. J., . . . Richardson, A. J. (2013). Global imprint of climate change on marine life. *Nature Climate Change, 3*, 919. doi:10.1038/nclimate1958

Rayner, N. A., Parker, D. E., Horton, E. B., Folland, C. K., Alexander, L. V., Rowell, D. P., . . . Kaplan, A. (2003). Global analyses of sea surface temperature, sea ice, and night marine air temperature since the late nineteenth century. *Journal of Geophysical Research, 108*.

Richardson, A. J., & Schoeman, D. S. (2004). Climate impact on plankton ecosystems in the northeast Atlantic. *Science, 305*(5690), 1609-1612. doi:10.1126/science.1100958

Ridgway, K. R. (2007). Long-term trend and decadal variability of the southward penetration of the East Australian Current. *Geophysical Research Letters, 34*(13), 1-5. doi:L1361310.1029/2007gl030393

IMOS
Integrated Marine Observing System

State and Trends of
Australia's Oceans
Report

1.2 Sea Surface Temperature Variability

Charitha B. Pattiaratchi[1,2] and Yasha Hetzel[1,2]

[1] Oceans Graduate School, The University of Western Australia, Perth, WA, Australia
[2] UWA Oceans Institute, The University of Western Australia, Perth, WA, Australia

Summary

Variability in sea surface temperature (SST) at seasonal, inter-annual and longer timescales reflect changes in both atmospheric and oceanic processes. SST is a key parameter that influence the heat transfer between the ocean and atmosphere and therefore it is important for regulating climate and its variability, both regionally and globally. SST also have a major influence on marine ecosystem function. Monthly SST and SST anomaly data, derived from satellite data between 1993 and 2018, were used to examine the SST variability in the East Australian and Leeuwin Current regions and indicated strong seasonal and inter-annual variability. There were periods of warm and cool periods where the mean monthly SST changed by up to 2°C at inter-annual scales that were mainly associated with El Niño and La Niña events. In the south-east, the SST has been increasing at a rate of ~1°C per decade whist no longer term changes have been observed along the west coast.

Key Data Streams

Satellite Remote Sensing

State and Trends of Australia's Ocean Report
www.imosoceanreport.org.au

Time-Series published
10 January 2020

doi: 10.26198/5e16a1c649e74

Rationale

Sea surface temperature (SST) reflects processes at the interface between the ocean and atmosphere and is an essential parameter in understanding ocean variability. Patterns of SST variability at seasonal, inter-annual and longer timescales result from a combination of atmospheric and oceanic processes. These SST patterns may be due to atmospheric and ocean circulation variability that imprint upon the SST field. As SST controls the transfer of heat energy from the oceans to the atmosphere, it plays a key role in regulating climate and its variability, both regionally and globally.

The Australian continent is surrounded by surface and subsurface boundary currents that flow along the continental shelf/slope. These currents are components of the sub-tropical gyre circulation in the South Indian and South Pacific oceans and include the East Australian (east coast) and Leeuwin Currents (west coast). Both these currents contribute to the poleward heat and mass transport along the east and west coasts (Wijeratne, Pattiaratchi, & Proctor, 2018). The Indonesian Archipelago, to the north of the Australian continent, allows for the transport of warmer, less saline Pacific Ocean water into the Indian Ocean. This is the only channel in the tropics where there is interocean exchange of water masses. Thus the oceans around the Australian continent are influenced by the dynamics of the tropical Pacific Ocean: the east coast is directly impacted as the western margin of the south Pacific Ocean and the west coast through the Indonesian Archipelago.

Longer-term changes in SST along the west and east coasts are a proxy for the variability in the major current systems. As ocean temperature also influences the physiology and distribution of marine life, changes in SST potentially provides insights into dynamics of marine communities.

Methods

To examine the sea surface temperature (SST) variability in the East Australian Current and Leeuwin Current regions, we used satellite data from the AVHRR sensors (onboard NOAA-11 to NOAA-19) from 1993-2018. We used mean monthly level 3 gridded (0.02° x 0.02° resolution) night skin temperature data (AODN dataset: "IMOS - SRS - SST - L3S - Single Sensor - 1 day - night time – Australia"). The SST climatology developed by Wijffels et al. (2018) was used to obtain monthly SST anomalies (AODN dataset: SST Atlas of Australian Regional Seas (SSTAARS) - Daily climatology fit).

Monthly SST and SST anomaly data were used to obtain the area average in two regions off the east (24°N–37.5°S, 150°–160°E) and west coasts of Australia (21°N–36°S, 108°–116°E, **Figure 1)**.

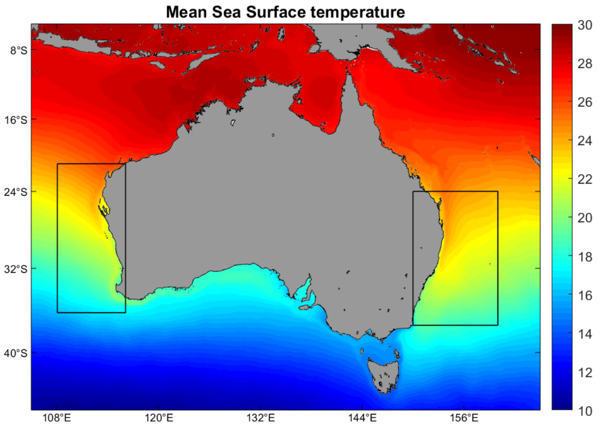

Figure 1. Location of boxes (east and west) used to obtain times series of SST and SST anomalies. The background is the mean SST over the period 1993-2016 obtained from SSTAARS (Wijffels et al., 2018). Units of SST are °C.

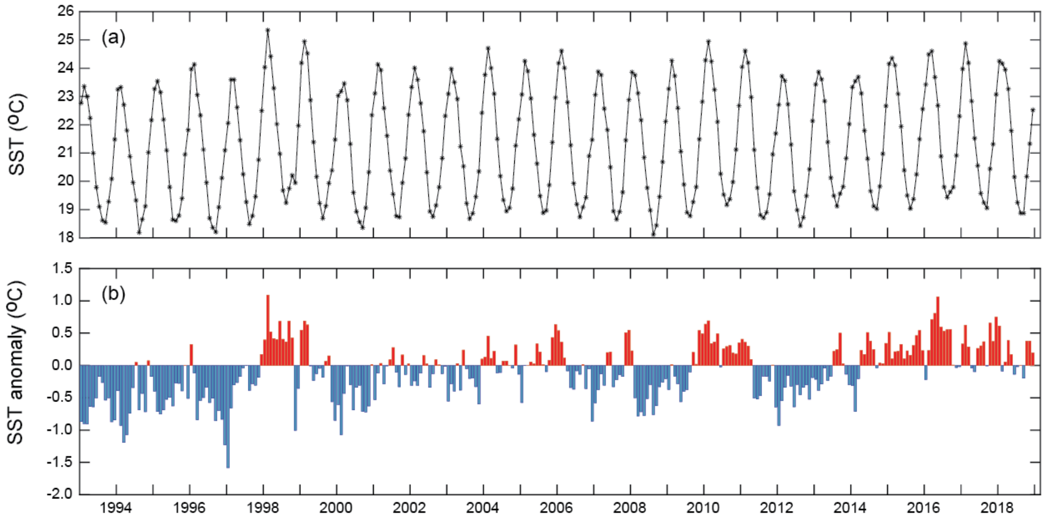

Figure 2. Time series of: (a) monthly sea surface temperature, and (b) monthly sea surface temperature anomaly for the east coast of Australia. Monthly SSTs were averaged over the box shown in Figure 1.

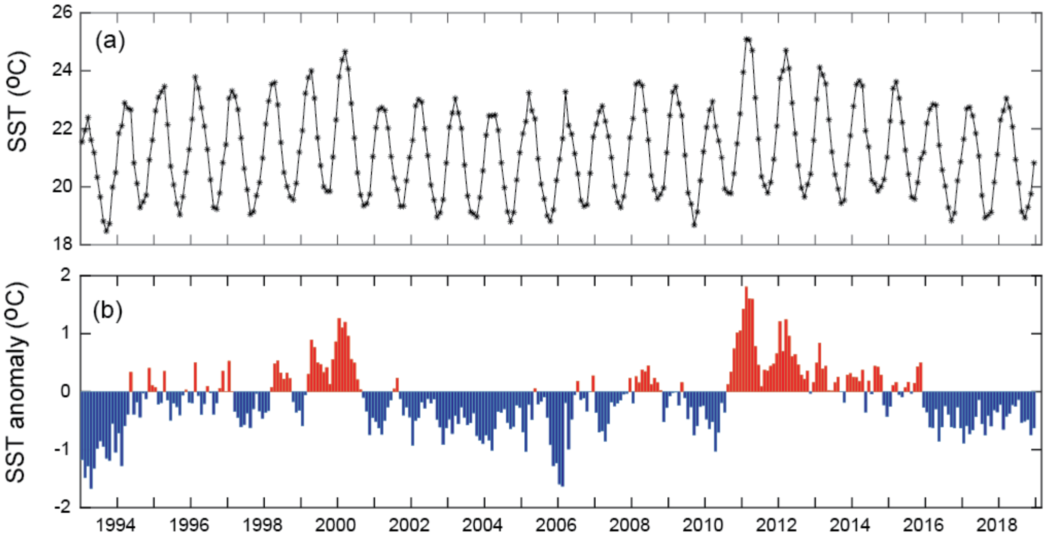

Figure 3. Time series of: (a) monthly sea surface temperature, and (b) monthly sea surface temperature anomaly for the west coast of Australia. Monthly SST anomalies were averaged over the box shown in Figure 1.

Results and interpretation

Monthly mean SSTs indicated strong seasonal variability off both the east and west coasts. Along the east coast, the mean seasonal change is ~5°C (19-24°C), with the annual maximum temperature during February (**Figure 2a**). Along the west coast, the mean seasonal change is ~4°C (19-23°C), with the annual maximum temperature during March (**Figure 3a**).

Over the 1993-2016 period, the mean trend of SST was variable around Australia (**Figure 4**). Along the south-east, the mean trend was positive at ~1°C decade^{-1}, whilst along the west coast the trend was negligible. However, over the 25-year period, there was significant variability along both coasts. Along the east coast, five different changes can be identified (**Figure 2a**): from 1993-1998 there was an increase in the annual maximum SST by ~2°C, with a decrease from 1998-2000 by a similar amount. From 2000-2010 there was a gradual increase in the SST by ~1.5°C, a decrease of ~1.2°C over 2010-2012, and a similar increase from 2012-2017. By contrast, along the west coast, there were only three main changes (**Figure 3a**), each lasting longer: over the period 1993-2000 there was an increase in the annual maximum SST by ~2°C with a rapid decrease from 2000-2001 by a similar amount. From 2001-2010, maximum monthly SST was relatively constant. SST then increased by ~2°C over 1 year (2010-2011) and there was a gradual decrease of ~1.5°C from 2011-2018. These changes were reflected in the mean monthly SST anomalies along both coasts (**Figure 2b**, **Figure 3b**). Increases in SST along both east and west coasts were related to strong La Niña events in 1999 and 2011 when the mean monthly SSTs and associated anomalies were at a maximum. The pattern of mean monthly SST and SST anomalies, along both coasts, indicated that in the years prior to a La Niña event, temperatures increased, with a rapid decrease over a 1-2 year period at the cessation of the event. However, along the east coast, mean monthly SST anomalies have been positive since mid-2014, whilst along the west coast the anomalies have been negative since 2016.

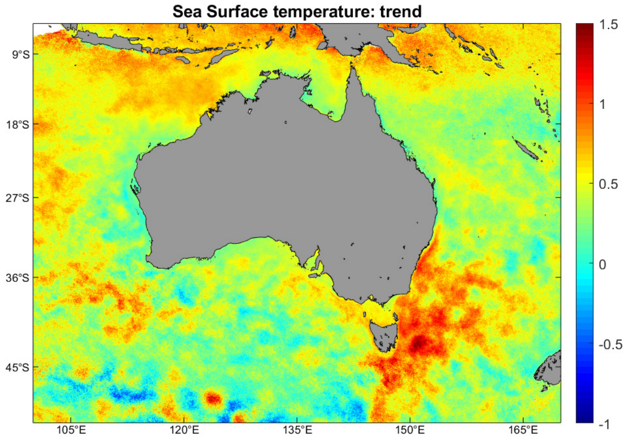

Figure 4. The mean sea surface temperature trend (°C.decade^{-1}) from 1993-2016 (data from Wijffels et al., 2018).

Implications for people and ecosystems

Mean monthly SST and SST anomalies, along both coasts, indicate strong seasonal and inter-annual variability. Although there has been a linear increase in SST along the east coast over the period 1993-2016, no changes have been observed along the west coast. However, there have been many increases/decreases in mean monthly SST by up to 2°C at inter-annual scales, mainly associated with El Niño and La

doi: 10.26198/5e16a1c649e74

Niña events. These changes are comparable to the annual cycle of SST changes (4°C and 5°C along the west and east coasts, respectively).

This SST variability has large influences on coastal ecosystems. For example, the 2011 La Niña event resulted in a severe marine heatwave along the west coast (Pearce & Feng, 2013) that resulted in significant changes to the whole ecosystem (Babcock et al., 2019; Cannell, Thomas, Schoepf, Pattiaratchi, & Fraser, 2019; Wernberg et al., 2013) that included invertebrate fisheries (Caputi et al., 2016) and benthic communities, containing habitat-forming groups such as kelp, seagrass and corals (Kendrick et al., 2019).

Acknowledgements

Data was sourced from Australia's Integrated Marine Observing System (IMOS) which is enabled by the National Collaborative Research Infrastructure Strategy (NCRIS).

Data Sources

IMOS Satellite Remote Sensing.
http://imos.org.au/facilities/srs/

References cited

Babcock, R. C., Bustamante, R. H., Fulton, E. A., Fulton, D. J., Haywood, M. D. E., Hobday, A. J., . . . Vanderklift, M. A. (2019). Severe continental-scale impacts of climate change are happening now: extreme climate events impact marine habitat forming communities along 45% of Australia's coast. ***Frontiers in Marine Science, 6***(411). doi:10.3389/fmars.2019.00411

Cannell, B., Thomas, P. G., Schoepf, V., Pattiaratchi, C., & Fraser, M. W. (2019). ***Impacts of marine heatwaves. In E Techera & G Winter (eds), Marine extremes: ocean safety, marine health and the blue economy***: Routledge, Abingdon, Oxon.

Caputi, N., Kangas, M., Denham, A., Feng, M., Pearce, A., Hetzel, Y., & Chandrapavan, A. (2016). Management adaptation of invertebrate fisheries to an extreme marine heat wave event at a global warming hot spot. ***Ecology and Evolution, 6***(11), 3583-3593. doi:10.1002/ece3.2137

Kendrick, G. A., Nowicki, R. J., Olsen, Y. S., Strydom, S., Fraser, M. W., Sinclair, E. A., . . . Orth, R. J. (2019). A systematic review of how multiple stressors from an extreme event drove ecosystem-wide loss of resilience in an iconic seagrass community. ***Frontiers in Marine Science, 6***, 15. doi:10.3389/fmars.2019.00455

Pearce, A. F., & Feng, M. (2013). The rise and fall of the "marine heat wave" off Western Australia during the summer of 2010/2011. ***Journal of Marine Systems, 111***, 139-156. doi:10.1016/j.jmarsys.2012.10.009

Wernberg, T., Smale, D. A., Tuya, F., Thomsen, M. S., Langlois, T. J., de Bettignies, T., . . . Rousseaux, C. S. (2013). An extreme climatic event alters marine ecosystem structure in a global biodiversity hotspot. ***Nature Climate Change, 3***(1), 78-82. doi:10.1038/nclimate1627

Wijeratne, S., Pattiaratchi, C., & Proctor, R. (2018). Estimates of surface and subsurface boundary current transport around Australia. ***Journal of Geophysical Research-Oceans, 123***(5), 3444-3466. doi:10.1029/2017jc013221

Wijffels, S. E., Beggs, H., Griffin, C., Middleton, J. F., Cahill, M., King, E., . . . Sutton, P. (2018). A fine spatial-scale sea surface temperature atlas of the Australian regional seas (SSTAARS): Seasonal variability and trends around Australasia and New Zealand revisited. ***Journal of Marine Systems, 187***, 156-196. doi:10.1016/j.jmarsys.2018.07.005

IMOS Integrated Marine Observing System

State and Trends of Australia's Oceans | Report

1.3 | East Australian Current Variability

Bernadette M. Sloyan[1], Madeleine Cahill[1],
Moninya Roughan[2] and Ken Ridgway[1]

[1] CSIRO Oceans and Atmosphere, Hobart, TAS, Australia
[2] School of Mathematics and Statistics, University of New South Wales, Sydney, NSW, Australia

Summary

The East Australian Current (EAC) is the complex and energetic western boundary current of the South Pacific Ocean, influencing the lives and economies of people on the eastern seaboard. It is the dominant mechanism for the redistribution of heat between the ocean and atmosphere and has a strong influence on the weather and seasonal climate, coastal ocean circulation and marine ecosystem affecting nearly half the Australian population. IMOS' long-term monitoring of the EAC provides a comprehensive data set that will enable improved understanding and modelling to determine the impact of the EAC on the regional weather and climate, coastal circulation and marine ecosystem.

Key Data Streams

Ocean Radar

Satellite Remote Sensing

Deep Water Moorings

State and Trends of Australia's Ocean Report
www.imosoceanreport.org.au

Time-Series published
10 January 2020
doi: *10.26198/5e16a23f49e75*

Rationale

The East Australian Current (EAC) is the highly energetic western boundary current of the South Pacific Ocean gyre, estimated (27°S) to transport 22.1 ± 7.5 Sverdrups (Sv; 1 Sv=$10^6 m^3 s^{-1}$) of warm tropical water southward (Sloyan, Ridgway, & Cowley, 2016). Any changes in the EAC in both the short-term or long-term will impact waters along south-eastern Australia – Australia's most populated coastline – and the Tasman Sea.

Low frequency (>2 year) variability of the EAC reflects changes in the wind and buoyancy forcing over the South Pacific Ocean (Hu et al., 2015). However, local and regional wind and buoyancy forcing drives higher frequency variability (<1-2 years) of the EAC (Bull, Kiss, Jourdain, England, & van Sebille, 2017). Due to the narrow shelf, EAC meandering has an immediate impact on the shelf circulation. Downstream of the EAC separation zone (~30-31.5°S, Cetina-Heredia, Roughan, van Sebille, & Coleman, 2014), mesoscale eddies are shed, which dominate shelf circulation. Exchange of heat, salt and plankton between the shelf and open ocean is achieved via EAC intrusion, submesoscale and mesoscale eddies, and complex boundary layer and frontal dynamics. Therefore, although the EAC transports oligotrophic Coral Sea water, several key processes still stimulate enrichment, including upwelling associated with the dynamics of the EAC (Roughan & Middleton, 2002), mixing associated with frontal and mesoscale eddies (Roughan et al., 2017), and the dynamic exchange of shelf and boundary current water. These enrichment processes influence the entire marine ecosystem, from planktonic production (Armbrecht, Schaeffer, Roughan, & Armand, 2015), and invertebrate and fish larvae to the distribution of large pelagic fish.

Methods

To summarise the EAC variability, we combine observations from the Integrated Marine Observing System (IMOS) EAC mooring array and satellite sea surface temperature and velocity at 27°S between May 2015 and April 2018. The IMOS EAC mooring array consists of six moorings in water depths of 500 to 4800 m across 152.94 km, from the continental shelf to the deep abyssal plain. In the upper 1200 m, current profiling instruments provide vertical velocity profiles and below 1200 m, point source velocity instruments provide data at discrete depths. IMOS EAC mooring data were interpolated onto a standard vertical grid and time period and the velocity was rotated to the along-, across-slope coordinate frame. We use the Wijffels et al. (2018) annual mean Sea Surface Temperature (SST) and the night-time satellite sea surface temperature to determine the SST anomaly. Sea surface height (SSH) anomaly was from the IMOS gridded satellite product DM00 GSLA.

A high frequency surface radar system is maintained by IMOS centred at 30°S downstream of the EAC mooring array and upstream of the typical EAC separation region. Surface current data were gridded to 1.5 km resolution over a 100 km square area since 2010. Full details of the radar data and its processing are available from Mantovanelli et al. (2017) . EAC jet core speed and position were calculated from the radar derived current data using the methodology of Archer et al. (2017).

Results and interpretation

There is considerable variability of SSH and SST between 2015 and 2018 at 27°S (**Figure 1**). These surface anomalies can extend across the longitudinal extent from the coast to the abyssal basin or partially across the region. There are times when SST and SSH anomalies co-vary, and other times when anomalies are opposed (**Figure 1**).

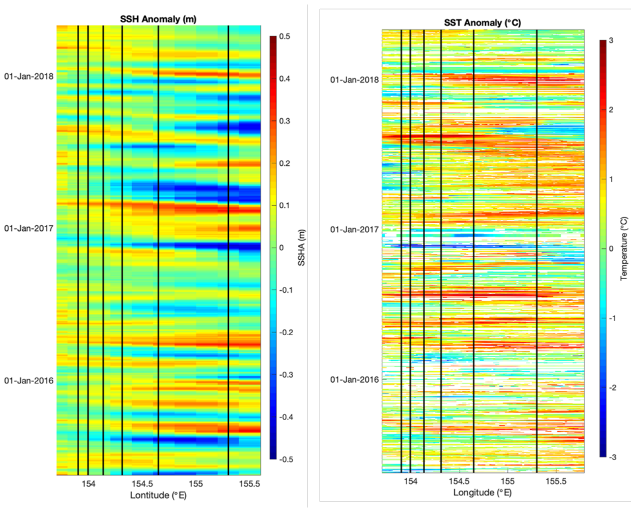

Figure 1. Hovmöller plots (longitude versus time) of the (left) Sea Surface Height (SSH) anomaly and (right) Sea Surface Temperature (SST) anomaly for a region surrounding the IMOS EAC mooring line (~27°S). Thick black lines identify the location of the IMOS EAC mooring array.

To understand the surface anomalies in terms of the EAC, we compare these data with data from the EAC mooring. The mean along-slope velocity vectors show poleward velocity dominates from 60-1500 m. (**Figure 2**). The strongest southward flow is found over the continental shelf, decreasing in strength in deeper water. The variance ellipses show that the largest variability in EAC transport is in the along-shore direction. This indicates that the EAC variability is dominated by the movement of the EAC on- and off-shore. The EAC thus maintains its jet structure as it meanders onshore and offshore adjacent to the continental slope.

While the mean along-shore velocity vectors provide a picture of the mean 3-year EAC, the time series of velocity show that the EAC has a complex and highly variable structure (**Figure 3**).

The EAC 2000 m mooring is located on the continental slope and measures the EAC core (negative along-slope velocity).

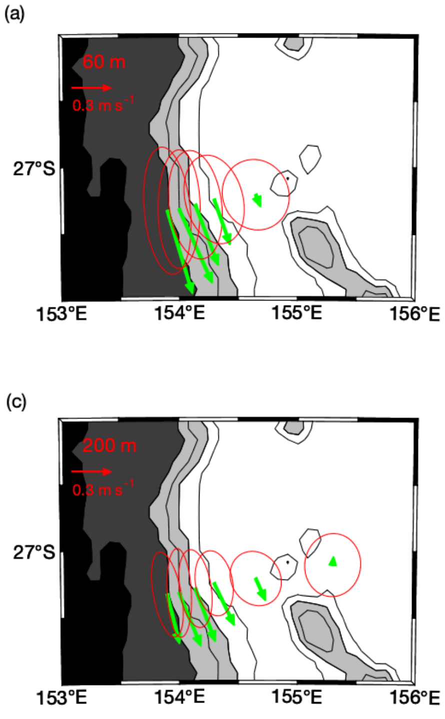

Figure 2. Three-year (May 2015-April 2018) mean along-slope velocity (m/s, green arrow) and velocity variance ellipse (red circle) for (a) 60 m, (b) 120 m, (c) 200 m, and (d) 500 m. The 1000-m, 2000-m, 3000-m, and 4000-m isobaths are contoured and topography shallower than 3000 m is shaded.

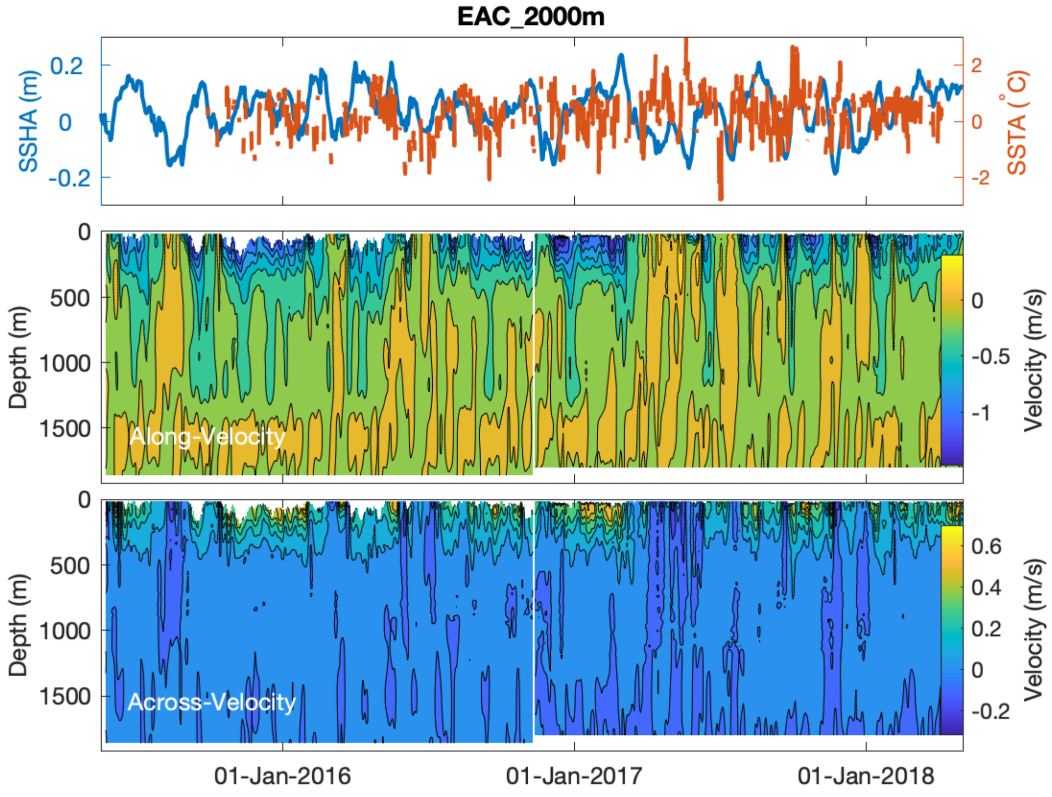

Figure 3. Time series (April 2015-May 2018) of the (top) SSH anomaly (m) and SST (°C) anomaly, (middle) Along-slope velocity (m s-1) and (bottom) Across-Slope velocity (m s-1) at ~ 27°S.

doi: 10.26198/5e16a23f49e75

The strong southward flow is associated with off-shore flow (positive across-slope velocity). While mostly measuring the EAC core, we see times where the flow is northward (positive along-slope velocity). This northward velocity is due to the shelf flow extending from the coast and is generally associated with on-shore flow (negative across-slope velocity). These changes in the direction and strength of the velocity are driven by cyclonic eddies inshore of the jet, and have significant influence on the exchange between the open ocean and shelf waters.

The Coffs Harbour HF Radar shows that the mean EAC jet lies above the 1500 m isobath, ~50 km offshore (Archer et al., 2017). However, the EAC jet strength is highly variable (**Figure 4**, top), with maximum surface velocities >2 m/s, and maximum speed in summer and minimum in winter (Archer et al., 2017) . The EAC meanders onshore and offshore adjacent to the continental slope, covering an offshore excursion of >100 km (**Figure 4**, bottom). The EAC has eastward displacements every 65-100 days, similar to that at 27°S (Sloyan et al., 2016), and is associated with meso-scale eddy shedding at the EAC separation.

Implications for people and ecosystems

The combination of surface and interior observations of the EAC confirm that this current is highly variable and its positions on the shelf influences the exchange between the open and shelf ocean. The interaction between the EAC jet and eddies with prominent topographic features and wind induced upwelling enhances the exchange of nutrient-rich sub-surface water between the open and coastal ocean. These exchanges have a significant influence on the biology of eastern Australian shelf waters and western Tasman Sea.

The long-term EAC mooring arrays at Brisbane (~27°S), Coffs Harbour (~30°S), Sydney (~34°S) and Narooma (~36°S) and the HF radar system at Coffs Harbour provide, unprecedented, comprehensive and valuable information about the EAC and its variability. Although the time series from the EAC mooring array is relatively short currently, over the longer term these observations of temperature and transport will be critical for informing us about how the ocean is responding to climate change, as well as for assessing climate models. The continuation of these observations, coupled with ocean modelling, will improve our understanding of EAC influences on climate, leading to more reliable ocean forecasts for eastern Australia and coastal communities, and help inform management of east coast fisheries.

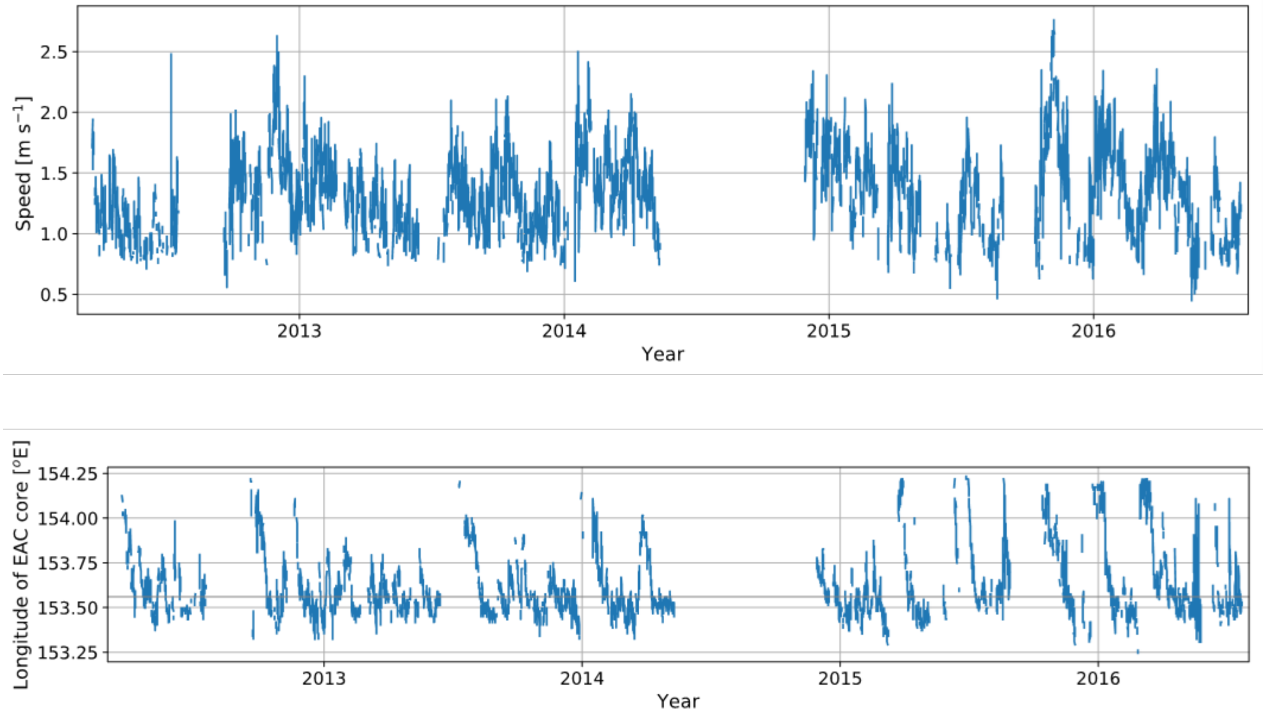

Figure 4. (Top) Speed of the core of the EAC jet calculated from HF radar derived surface velocities centered at 30°S, in a flow following framework (Archer et al. 2017) and (bottom) the position of the core of the EAC jet.

doi: 10.26198/5e16a23f49e75

Acknowledgements

Data was sourced from Australia's Integrated Marine Observing System (IMOS) which is enabled by the National Collaborative Research Infrastructure Strategy (NCRIS).

Data Sources

IMOS Ocean Raddar.
http://imos.org.au/facilities/oceanradar/

IMOS Satellite Remote Sensing.
http://imos.org.au/facilities/srs/

IMOS Deep Water Moorings.
http://imos.org.au/facilities/deepwatermoorings/

References cited

Archer, M. R., Roughan, M., Keating, S. R., & Schaeffer, A. (2017). On the variability of the East Australian Current: jet structure, meandering, and influence on shelf circulation. ***Journal of Geophysical Research-Oceans, 122***(11), 8464-8481. doi:10.1002/2017jc013097

Armbrecht, L. H., Schaeffer, A., Roughan, M., & Armand, L. K. (2015). Interactions between seasonality and oceanic forcing drive the phytoplankton variability in the tropical-temperate transition zone (similar to 30 degrees S) of Eastern Australia. ***Journal of Marine Systems, 144***, 92-106. doi:10.1016/j.jmarsys.2014.11.008

Bull, C. Y. S., Kiss, A. E., Jourdain, N. C., England, M. H., & van Sebille, E. (2017). Wind forced variability in eddy formation, eddy shedding, and the separation of the East Australian Current. ***Journal of Geophysical Research-Oceans, 122***(12), 9980-9998. doi:10.1002/2017jc013311

Cetina-Heredia, P., Roughan, M., van Sebille, E., & Coleman, M. A. (2014). Long-term trends in the East Australian Current separation latitude and eddy driven transport. ***Journal of Geophysical Research-Oceans, 119***(7), 4351-4366. doi:10.1002/2014jc010071

Hu, D. X., Wu, L. X., Cai, W. J., Sen Gupta, A., Ganachaud, A., Qiu, B., . . . Kessler, W. S. (2015). Pacific western boundary currents and their roles in climate. ***Nature, 522***(7556), 299-308. doi:10.1038/nature14504

Mantovanelli, A., Keating, S., Wyatt, L., Roughan, M., & Schaeffer, A. (2017). Lagrangian and Eulerian characterization of two counterrotating submesoscale eddies in a western boundary current. ***Geophysical Research Letters, 122***(6), 4902-4921.

Roughan, M., Keating, S. R., Schaeffer, A., Heredia, P. C., Rocha, C., Griffin, D., . . . Suthers, I. M. (2017). A tale of two eddies: The biophysical characteristics of two contrasting cyclonic eddies in the East Australian Current System. ***Journal of Geophysical Research-Oceans, 122***(3), 2494-2518. doi:10.1002/2016jc012241

Roughan, M., & Middleton, J. H. (2002). A comparison of observed upwelling mechanisms off the east coast of Australia. ***Continental Shelf Research, 22***(17), 2551-2572. doi:10.1016/s0278-4343(02)00101-2

Sloyan, B. M., Ridgway, K. R., & Cowley, R. (2016). The East Australian Current and property transport at 27 degrees S from 2012 to 2013. ***Journal of Physical Oceanography, 46***(3), 993-1008. doi:10.1175/jpo-d-15-0052.1

Wijffels, S. E., Beggs, H., Griffin, C., Middleton, J. F., Cahill, M., King, E., . . . Sutton, P. (2018). A fine spatial-scale sea surface temperature atlas of the Australian regional seas (SSTAARS): Seasonal variability and trends around Australasia and New Zealand revisited. ***Journal of Marine Systems, 187***, 156-196. doi:10.1016/j.jmarsys.2018.07.005

IMOS

Integrated **Marine**
Observing System

IMOS
Integrated Marine Observing System
State and Trends of Australia’s Oceans | Report

1.4 | Variability in ocean currents around Australia

Charitha B. Pattiaratchi[1,2] and Prescilla Siji[1,2]

[1] Oceans Graduate School, The University of Western Australia, Perth, WA, Australia
[2] UWA Oceans Institute, The University of Western Australia, Perth, WA, Australia

Summary

Ocean currents also have a strong influence on marine ecosystems, through the transport of heat, nutrients, phytoplankton, zooplankton and larvae of most marine animals. We used geostrophic currents derived satellite altimetry measurements between 1993 and 2019 to examine the Kinetic Energy (KE, measure of current intensity) and Eddy Kinetic Energy (EKE, variability of the currents relative to a mean) around Australia. The East Australian (EAC) and Leeuwin (LC) current systems along the east and west coasts demonstrated strong seasonal and inter-annual variability linked to El Niño and La Niña events. The variability in the LC system was larger than for the EAC. All major boundary currents around Australia were enhanced during the 2011 La Niña event.

Key Data Streams

Satellite Remote Sensing

State and Trends of Australia’s Ocean Report
www.imosoceanreport.org.au

Time-Series published
10 January 2020

doi: 10.26198/5e16a2ae49e76

Rationale

Ocean currents play a key role in determining the distribution of heat across the planet, not only regulating and stabilising climate, but also contributing to climate variability. Ocean currents also have a strong influence on marine ecosystems, through the transport of phytoplankton (primary producers), zooplankton (grazers on the primary producers and food for higher trophic levels), and larvae of most marine animals. Ocean currents also regulate the physiology and growth of marine life by controlling ambient conditions through the redistribution of heat and nutrients.

The island continent of Australia is surrounded by surface and subsurface boundary currents that flow along the continental shelf and slope. The unique feature of this circulation is that along both east and west coasts, boundary currents transport warm-water southward via the East Australian (EAC) and Leeuwin Currents (LC), respectively (Wijeratne, Pattiaratchi, & Proctor, 2018). These boundary currents are enhanced through inflows from the south Pacific and south Indian Ocean basins. Australia's boundary currents are an important conduit for the poleward heat and mass transport and inter-ocean water exchange in the tropics (Indonesian Throughflow; Sprintall, Wijffels, Molcard, & Jaya, 2009) and the sub-tropics (Tasman outflow; Hu et al., 2015; van Sebille, England, Zika, & Sloyan, 2012). Major surface boundary currents include the Indonesian Throughflow, Holloway, Leeuwin, South Australian, Flinders, Zeehan, East Australian and Hiri currents (**Figure 1**).

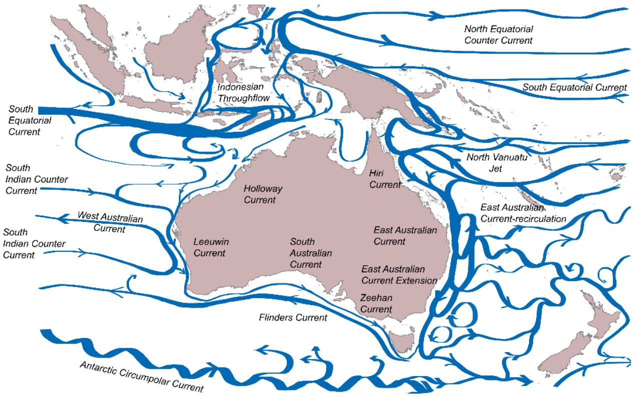

Figure 1. Mean surface currents around Australia (modified from (Wijeratne et al., 2018).

Previous studies have highlighted the seasonal and inter-annual variability associated with the LC, with stronger (weaker) currents during the winter (summer) and La Niña (El Niño) events (Feng, Meyers, Pearce, & Wijffels, 2003; Pattiaratchi & Buchan, 1991; Wijeratne et al., 2018). The ENSO (El Niño Southern Oscillation) signal within the LC is transmitted along the south coast of Australia, where there is enhanced upwelling off Kangaroo Island (Middleton et al., 2007). EAC is stronger during summer and slightly weaker during winter (Wijeratne et al., 2018), with decadal ENSO variations affecting the EAC transport variability (Holbrook, Goodwin, McGregor, Molina, & Power, 2011). Variability associated with ENSO along east coast of Australia appears to be weaker than along the west coast.

Satellite altimeter observations provide a synoptic view of the ocean variability at different time and space scales. Sea surface height data provide information on geostrophic surface flow and thus Kinetic Energy (KE) and the intensity of the surface current variability activity through Eddy Kinetic Energy (EKE, the variance of geostrophic surface velocities). KE is thus a measure of the intensity of currents, whilst EKE provides variability of the currents relative to a mean. Thus, changes in KE and EKE over time determine the inter-annual variability of the ocean currents. Many studies have examined the variability of EKE in the ocean using altimeter data (Caballero, Pascual, Dibarboure, & Espino, 2008; Ducet, Le Traon, & Reverdin, 2000; Ludicone, Santoler, Marullo, & Gerosa, 1998; Pujol & Larnicol, 2005).

Methods

To calculate KE and EKE of ocean currents around Australia, we used global ocean reanalysis of altimeter data (AODN dataset: “IMOS - OceanCurrent - Gridded sea level anomaly - Delayed mode”). For the period January 1993 to December 2010, geostrophic current components were only available on alternative days. Data were interpolated to create a daily mean data set. For the period January 2011 to April 2019, daily mean data were available and no interpolation was necessary. Daily mean data for the period January 1993 to April 2019 were then used to create monthly mean data. The KE for each month was defined as (Caballero et al., 2008):

$$KE = \frac{1}{2}\sqrt{u^2+v^2}$$

where, u and v were the monthly mean of zonal (east-west) and meridional (north-south) geostrophic current components respectively. The EKE was defined as:

$$EKE = \frac{1}{2}\sqrt{u'^2+v'^2}$$

where $u' = u - U$ and $v' = v - V$, with U and V are the monthly climatological means of the zonal and meridional velocity components, respectively.

Monthly KE and EKE were used to obtain the area average in two regions on the east (24°–37.5°S, 150°–160°E) and west coasts of Australia (21°–36°S, 108°–116°E, **Figure 2**).

Results and interpretation

Mean KE from 1993-2019 indicated that all major boundary currents around Australia and inflows were captured in the altimeter data. Boundary currents along the east coast (Hiri, EAC, EAC-extension, EAC-recirculation), as well as the main inflow (North Vanuatu Jet), were well defined (**Figure 2a**). Similarly, boundary currents along the west coast (Holloway, Leeuwin, South Australian and Zeehan Currents), as well as the main inflows (Indonesian Throughflow, central South Indian Counter Current) were also well defined. The EKE also indicated regions of high variability along the east and west coasts of Australia, equatorial regions and the Antarctic Circumpolar Current (**Figure 2b**).

The monthly mean time series of KE and EKE for the regions along the east and west coasts (**Figure 2b**) highlighted the strong seasonal variability (**Figure 3b,c**). The east and west time series were out-of-phase, reflecting that the EAC is strongest in January, whist the LC is strongest in June. It was also noticeable that the seasonal variability (i.e., the seasonal range in both KE and EKE) was higher along the west than the east coast, indicating greater seasonal variability in the LC than the EAC. For example, the maximum seasonal range for KE (EKE) was 370 (350) cm^2s^{-2} for the west coast (in 2013), but only 270 (220) cm^2s^{-2} for the east coast (in 2016). Differences in the seasonal variability between the east and west coasts was more pronounced for EKE than KE (**Figure 3c**).

Over the study period, the range of the KE for east and west coasts were different; for the east coast, the range was 340 cm^2s^{-2} (200-540 cm^2s^{-2}), whilst for the west coast the range was 450 cm^2s^{-2} (90-540 cm^2s^{-2}). Similarly, for EKE, ranges were 310 cm^2s^{-2} (60-370 cm^2s^{-2}) and 440 cm^2s^{-2} (60-500 cm^2s^{-2}), for east and west coasts, respectively (**Figure 3**). This indicates that the inter-annual variability in the LC system was larger than the EAC.

The variability in both KE and EKE demonstrated that the EAC and LC undergo strong inter-annual variability related to ENSO events (Figure 3b). The EAC appears to be stronger towards the waning phase of El Niño events (e.g., January in 1998, 2003, 2010, 2016). For EAC, highest (lowest) KE and EKE were during the 2016 and 2010 El Niño (1998 La Niña) events. By contrast, both KE and EKE increased (decreased) during La Niña (El Niño) events. These periods of strong (weak) KE and EKE correspond to warm (cold) SST anomoloies along both coasts (see State and Trends of Australia's Ocean report 1.2: Sea surface temperature variability).

In addition to variability associated with ENSO events, there were also trends in both KE and EKE time series over a 7-10 year period. In the east, there were decreasing trends in 1993-2000, 2005-2007, 2010-2013 and 2016-2019 (**Figure 3c**). By contrast, there were increasing trends in 2001-2005, 2007-2010 and 2013-2016 (**Figure 3c**). Here, changes in the trend were associated with the occurrence of ENSO events with maxima (minima) during El Niño (La Niña) events. Similar changes were observed in the west, with decreasing trends during 1996-1997, 2000-2004, 2013-2016 and increasing trends during 1993-1993, 1997-2000, 2004-2013 and 2016-2018. Changes in the trends were also associated with ENSO events, but in an opposite sense, with maxima (minima) during La Niña (El Niño) events (**Figure 3c**). An interesting feature along the west coast was that from 2002-2008, both KE and EKE were relatively low over several years, indicating weaker LC during this period.

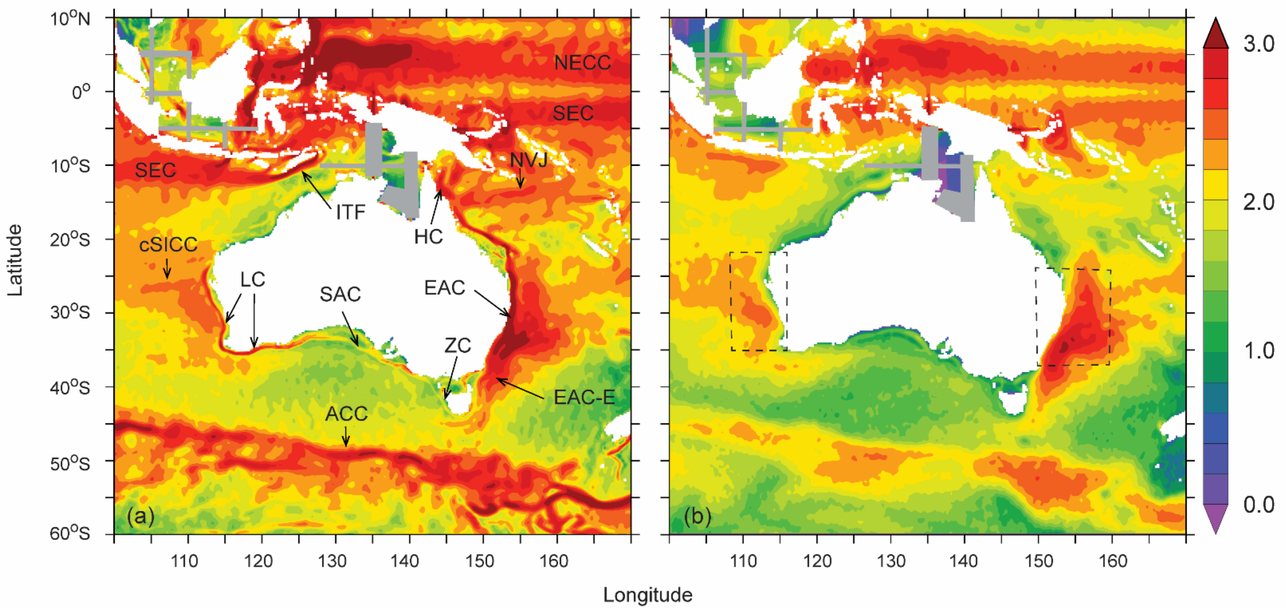

Figure 2. Mean (a) kinetic energy and, (b) eddy kinetic energy for the oceans around Australia over the period 1993-2018. The current systems in (a) are: ITF= Indonesian Throughflow; SEC=South Equatorial Current; HLC=Holloway Current; LC=Leeuwin Current; cSICC= central South Indian Counter Current; ACC=Antarctic Circumpolar Current; SAC=South Australian Current; EAC=East Australian Current; EAC-E=East Australian Current Extension; NVJ=North Vanuatu Jet; HC=Hiri Current; NECC=North Equatorial Counter Current; ZC = Zeehan Current. The location of the boxes where means were calculated are shown in (b) as dashed lines. Grey lines represent missing data

doi: 10.26198/5e16a2ae49e76

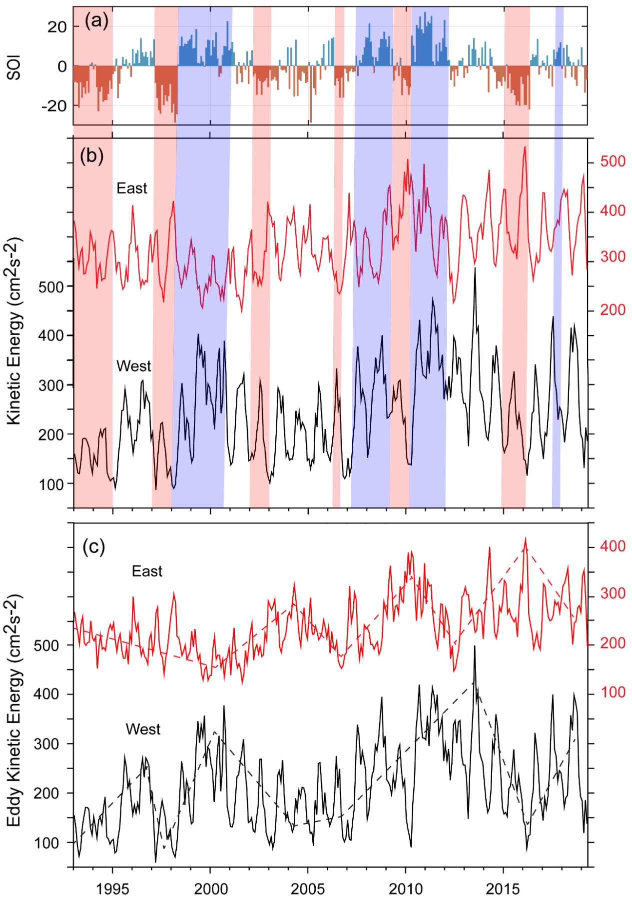

Figure 3. Time series of (a) Southern Oscillation Index (SOI), (b) monthly mean kinetic energy, and (c) eddy kinetic energy from January 1993-April 2019. The red line is for the eastern box and the black line is for the western box. Note that the time series for the eastern box has been shifted by +300 cm^2s^2 to separate the two time series as shown the scale on right. Red and Blue shaded lines represent El Niño and La Niña events, respectively. Dashed lines (c) indicate the linear trend.

The influence of ENSO events around Australia is highlighted by examining the annual mean KE and EKE distributions for 2006 (weak El Niño) and 2011 (La Niña) events (**Figure 4**). A noteworthy feature is that all major boundary currents in the west were enhanced in 2011 compared to 2006. These include the Indonesian Throughflow, LC, and the offshore west coast. However, two regions have significant changes in KE. In the north, the KE associated with the Holloway Current increased during 2011 (cf. **Figure 4a,b**). In the south, KE associated with the LC and South Australian Current increased, with the whole Great Australian Bight having higher KE in 2011 and indicating a northward migration of the LC into the GAB. In the east, the EAC had similar KE values. This was due to the 2011 La Niña following the 2009-10 El Niño, with KE and EKE in the east remaining higher during 2011 (**Figure 3**). The main changes were in the Coral Sea, with higher values in 2011. Similarly, the EKE increased in 2011 compared to 2006 along both the east and west coasts, as well as in the Indonesian Throughflow and Antarctic Circumpolar Current (**Figure 5a,b**).

Implications for people and ecosystems

Ocean currents – with their key role in transporting water with different temperature/salinity characteristics, nutrients and biota – are critical for regional climate and marine ecosystem function. Variability in these current systems has significant influence on year-to-year changes in biomass of marine life. The analysis of KE, as a measure of the intensity of the currents, and EKE as a measure of the variability in the currents over time, provide useful insights into observed

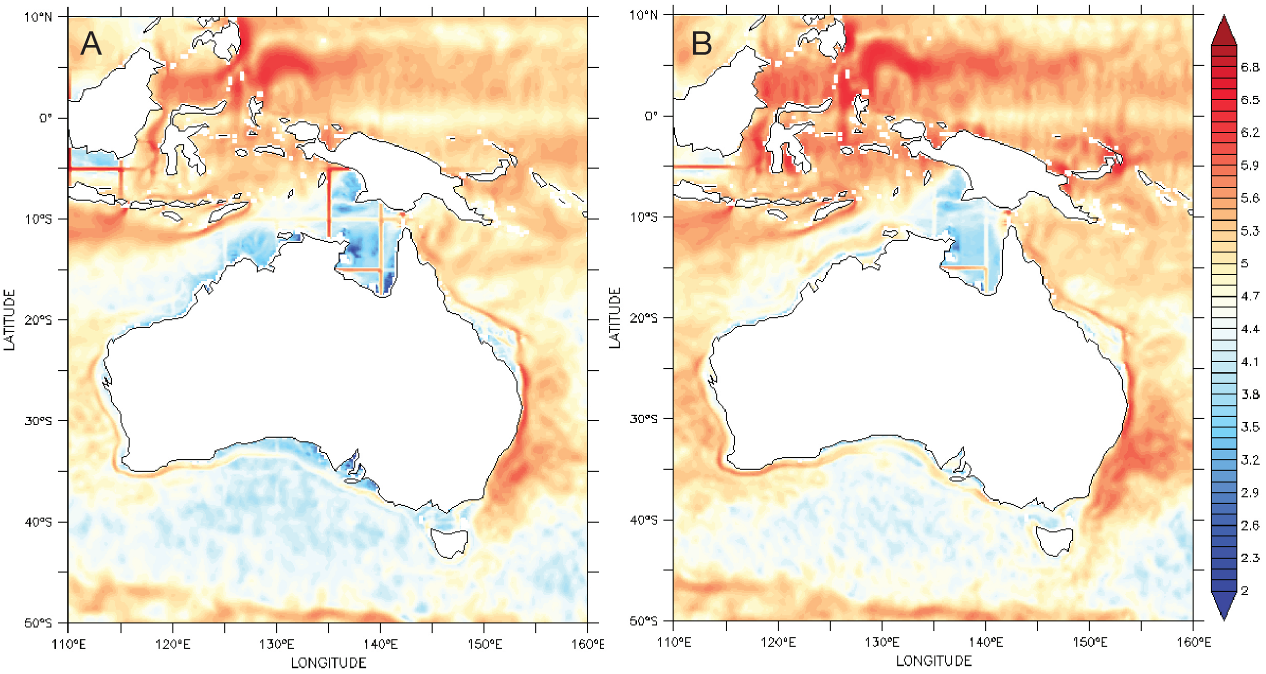

Figure 4. Annual mean kinetic energy for (a) 2006 (El Niño), and (b) 2011 (La Niña). Note the logarithmic scale is with units log(cm2s-2).

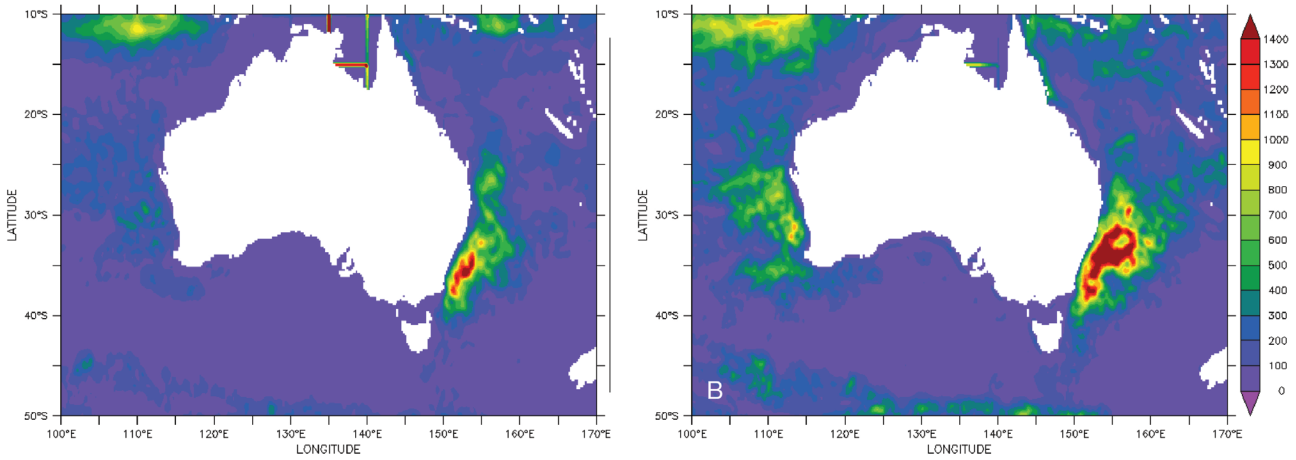

Figure 5. Annual mean eddy kinetic energy for (a) 2006 (El Niño), and (b) 2011 (La Niña). Note the linear scale with units cm^{2}s^{-2}).

changes in marine systems. One of the best examples of the role of ocean currents is their influence on marine heatwaves. that can have devastating effects on the marine environment, and their frequency and intensity appears to be increasing (Babcock et al., 2019). In 2011, an extreme heatwave off the coast of Western Australia had a devastating effect on the marine system, particularly seagrass, rock lobster and scallops. There was also a substantial decline in zooplankton biomass, abundance and size, and an increase in diversity (see State and Trends of Australia's Ocean Report 4.2: The impact on zooplankton of the 2011 heatwave off Western Australia). This was during the 2011 La Niña event, defined as the Ningaloo Niña, where the unseasonal strengthening of the LC occurred earlier in the year (February), transporting warmer water southward. Southerly winds that bring colder water to the surface through upwelling also decreased during this period. The continuing stronger LC through to 2013 maintained the warm water, which continued to impact corals (Babcock et al., 2019). Similarly, warm SST anomalies along the east coast were also associated with the 1997-98 El Niño events and importantly the extended period of warming from 2014 to 2018 were associated with a stronger EAC.

The western rock lobster (*Panulirus Cygnus*) is Australia's most valuable wild-caught commercial fishery. When released, rock lobster larvae (phyllosoma) spend up to 11 months in the deep ocean (offshore LC) before ocean currents transport them to the coast. The abundance of puerulus (late stage phyllosoma) is used as a reliable predictor of the lobster catch for the fishery 3-4 years in advance. For many years, there was a strong relationship between the mean Fremantle sea level, as a proxy for the strength of the Leeuwin Current, and the settlement of puerulus (Pearce & Phillips, 1988). However, since 2001, the relationship between mean sea level and rock lobster recruitment has diminished, with unprecedented low settlement numbers in 2008 (de Lestang et al., 2015). The time series indicate that prior to 2008, both KE and EKE were relatively low, suggesting that lower KE and EKE over several years could have a substantial influence on the cross-shelf transport that contribute to the transport of puerulus onshore.

Acknowledgements

Data was sourced from Australia's Integrated Marine Observing System (IMOS) which is enabled by the National Collaborative Research Infrastructure Strategy (NCRIS).

Data Sources

IMOS Satellite Remote Sensing.
http://imos.org.au/facilities/srs/

References

Babcock, R. C., Bustamante, R. H., Fulton, E. A., Fulton, D. J., Haywood, M. D. E., Hobday, A. J., . . . Vanderklift, M. A. (2019). Severe continental-scale impacts of climate change are happening now: extreme climate events impact marine habitat forming communities along 45% of Australia's coast. *Frontiers in Marine Science, 6*(411). doi:10.3389/fmars.2019.00411

Caballero, A., Pascual, A., Dibarboure, G., & Espino, M. (2008). Sea level and Eddy Kinetic Energy variability in the Bay of Biscay, inferred from satellite altimeter data. *Journal of Marine Systems, 72*(1-4), 116-134. doi:10.1016/j.jmarsys.2007.03.011

De Lestang, S., Caputi, N., Feng, M., Denham, A., Penn, J., Slawinski, D., Pearce, A., How J. (2015). What caused seven consecutive years of low puerulus settlement in the western rock lobster fishery of Western Australia? *ICES Journal of Marine Science, 72,* 59-59.

Ducet, N., Le Traon, P. Y., & Reverdin, G. (2000). Global high-resolution mapping of ocean circulation from TOPEX/Poseidon and ERS-1 and-2. *Journal of Geophysical Research-Oceans, 105*(C8), 19477-19498. doi:10.1029/2000jc900063

Feng, M., Meyers, G., Pearce, A., & Wijffels, S. (2003). Annual and interannual variations of the Leeuwin Current at 32°S. *Journal of Geophysical Research, 108*(C11), 3355. doi:doi:10.1029/2002JC001763

Holbrook, N. J., Goodwin, I. D., McGregor, S., Molina, E., & Power, S. B. (2011). ENSO to multi-decadal time scale changes in East Australian Current transports and Fort Denison sea level: Oceanic Rossby waves as the connecting mechanism. *Deep-Sea Research Part Ii-Topical Studies in Oceanography, 58*(5), 547-558. doi:10.1016/j.dsr2.2010.06.007

Hu, D. X., Wu, L. X., Cai, W. J., Sen Gupta, A., Ganachaud, A., Qiu, B., . . . Kessler, W. S. (2015). Pacific western boundary currents and their roles in climate. *Nature, 522*(7556), 299-308. doi:10.1038/nature14504

Ludicone, D., Santoler, R., Marullo, S., & Gerosa, P. (1998). Sea level variability and surface eddy statistics in the Mediterranean Sea from TOPEX/POSEIDON data. *Journal of Geophysical Research, 103(C2)*, 2995-3011.

Middleton, J. F., Arthur, C., Van Ruth, P., Ward, T. M., McClean, J. L., Maltrud, M. E., . . . Middleton, S. (2007). El Nino effects and upwelling off South Australia. *Journal of Physical Oceanography, 37*(10), 2458-2477. doi:10.1175/jpo3119.1

Pattiaratchi, C. B., & Buchan, S. J. (1991). Implications of long-term climate change for the Leeuwin current. *Journal of the Royal Society of Western Australia, 74*, 133-140.

Pearce, A. F., & Phillips, B. F. (1988). ENSO events, the Leeuwin current, and larval recruitment of the western rock lobster. *Journal Du Conseil, 45*(1), 13-21. Retrieved from <Go to ISI>://WOS:A1988Q548000002

Pujol, M. I., & Larnicol, G. (2005). Mediterranean sea eddy kinetic energy variability from 11 years of altimetric data. *Journal of Marine Systems, 58*(3-4), 121-142. doi:10.1016/j.jmarsys.2005.07.005

Sprintall, J., Wijffels, S. E., Molcard, R., & Jaya, I. (2009). Direct estimates of the Indonesian throughflow entering the Indian Ocean: 2004–2006. *Journal of Geophysical Research (oceans), 114*.

van Sebille, E., England, M. H., Zika, J. D., & Sloyan, B. M. (2012). Tasman leakage in a fine-resolution ocean model. *Geophysical Research Letters, 39*, 5. doi:10.1029/2012gl051004

Wijeratne, S., Pattiaratchi, C., & Proctor, R. (2018). Estimates of surface and subsurface boundary current transport around Australia. *Journal of Geophysical Research-Oceans, 123*(5), 3444-3466. doi:10.1029/2017jc013221

doi: 10.26198/5e16a2ae49e76

IMOS
Integrated Marine Observing System
State and Trends of Australia's Oceans
Report

1.5 Spatial and temporal trends in concentrations of nutrients

Edward Butler[1], Michele Skuza[2] and Christian Lønborg[2]

1 Australian Institute of Marine Science, Arafura Timor Research Facility, NT, Australia
2 Australian Institute of Marine Science, Townsville, QLD, Australia

Summary

Nutrient time series from the seven IMOS NRS show no discernible trends. The three long-term NRS (>50 years) show a decline in silica over multiple decades (most dramatic at MAI), a decline in phosphate more recently, and mixed responses for nitrate.

Key Data Streams

National Reference
Stations

State and Trends of Australia's Ocean Report
www.imosoceanreport.org.au

Time-Series published
10 January 2020

doi: 10.26198/5e16a2ff49e77

Rationale

Marine primary producers, such as phytoplankton, macroalgae, and seagrass, take up their nutrients for growth from the sea. Vitally important are nitrogen (N) and phosphorus (P) as essential building blocks of life, including DNA, proteins and phospholipids (Canfield, Glazer, & Falkowski, 2010; Kitadai & Maruyama, 2018; Ruttenberg, 2014). The next most important nutrient is silicon (Si), which is essential for phytoplankton with siliceous skeletal structures, such as diatoms and silicoflagellates (Tréguer & Rocha, 2013). These nutrients exist in inorganic and organic forms (**Box 1**), with dissolved inorganic forms more easily accessible to plankton organisms than complex organic forms.

In Australian coastal waters distant from urban centres and river mouths, marine primary production is said to be chiefly limited by availability of N (Radke et al., 2017; Thompson et al., 2011). In practice, labile organic N (**Box 1**) and atmospheric N_2-fixation can offset the N deficit; trace elements can also influence growth (**Box 2**). Sustained observations of N, P and Si as part of the Integrated Marine Observing System (IMOS) provide a circum-continental baseline for nutrients that can be used to assess changes from climatic and other anthropogenic pressures.

Nutrient concentrations of Australian surface waters grade from the tropics to the cool temperate regions. They increase with depth below the surface mixed layer as dissolved nutrients are returned to the water column from decomposition of sinking particulate matter and physical processes, such as intrusions of deeper water. Beyond the estuaries and close inshore, they can be characterised broadly into three provinces[1]: North-West (tropical wet/dry climate, macrotidal, broad continental shelf) – low N and P[2], high Si; North-East (tropical wet/dry climate, mesotidal, narrower continental shelf and barrier reef) – very low N and P, intermediate Si; and South (temperate climate, microtidal, seasonal deep mixing) – intermediate N and P, low Si. The transition between these provinces is mediated by the two major, poleward currents on the east (East Australian Current (EAC)) and west (Leeuwin Current (LC)) coasts of Australia and their subsidiary systems. Regional oceanographic influences can be modified by local mechanisms, as observed at Kangaroo Island (van Ruth et al., 2018). Seasonal variability in nutrient concentrations within any year is generally greater than interannual variability.

Methods

Nutrients have been measured at Australia's long-term monitoring sites for up to 70 years. Under IMOS, the National Reference Stations have been extended to key regions around Australia (Lynch et al., 2014). Sampling and analysis methods have been standardised, with discrete samples collected throughout the water column using Niskin bottles, and measured using standard, segmented flow analysis with colorimetric detection (Rees et al., 2019).

The focus of the nutrient time series presented here are the specific forms of N, P and Si measured at the NRS—nitrate (NO_3^-), dissolved reactive phosphorus (DRP) and dissolved reactive silicon (DSi). Nutrient data are presented at each NRS, averaged in 10-m depth bins.

Results and interpretation

IMOS National Reference Stations

For the sub-set of nutrients presented, no trends were discernible at the Yongala (YON), North Stradbroke Island (NSI) and Kangaroo Island (KAI) NRS through 2010–2018, but some features are noteworthy. Peaks in DRP (**Figure 1**) and DSi (**Figure 2**) concentrations at Yongala in 2011 and 2012 likely resulted from widespread flooding or deepwater intrusion events caused by Tropical Cyclone Yasi (February 2011) and a deep tropical low (March 2012). NO_3^- did not respond similarly (**Figure 3**), either because its flood transport was lower, or it was rapidly used by the biota. Higher DSi concentrations at North Stradbroke Island in 2012 might also have resulted from local rivers flooding in March of that year. Kangaroo Island (KAI) had a broad peak in its time series for NO_3^-, DRP and DSi in 2015–17; it is most prominent for DSi throughout the water column, but is only clear for DRP and NO_3^- in deeper samples, and could align with a slight decline in salinity. The upwelling and enrichment mechanism described by van Ruth et al. (2018; Jan–Apr) might be responsible, but at other times of the year storm events causing intrusion of richer, lower salinity waters could have been active. Darwin showed no overall trend between 2011–2018 for NO_3^-, DRP and DSi, but all were higher in 2014 and 2015. Although this did not relate to overall wet-season rainfall, pulses of high nutrients were observed during the wet season when sampling coincided with spring tides and high rainfall events (within preceding 1–3 days). Seasonal cycles of nutrients are not discussed here, but have been included in supplementary information for reference.

Long-term stations

The full records of temperature and salinity at Maria Island, Port Hacking and Rottnest Island[3] (see State and Trends of Australia's Ocean Report 1.1: Long-term changes in temperature around Australia) reveal long-term variability and changes in oceanographic conditions. In south-east Australia, over the past 70 years the EAC extension has transported more water characteristic of subtropical Australian waters to Tasmania (Maria Island). Whereas, off south-western Australia (Rottnest Island), the LC has waxed and waned under the influence of global climate drivers such as the El Niño-Southern Oscillation.

---

[1] This excludes the Gulf of Carpentaria, which remains to be differentiated better for nutrient distributions.

[2] Coastal waters adjacent to the Kimberley coast are possibly intermediate in P concentration (Hayes et al., 2005)

[3] Initiated mid-last century by Rochford and colleagues, before subsequent incorporation into NRS network, see Overall Methods section.

doi: 10.26198/5e16a2ff49e77

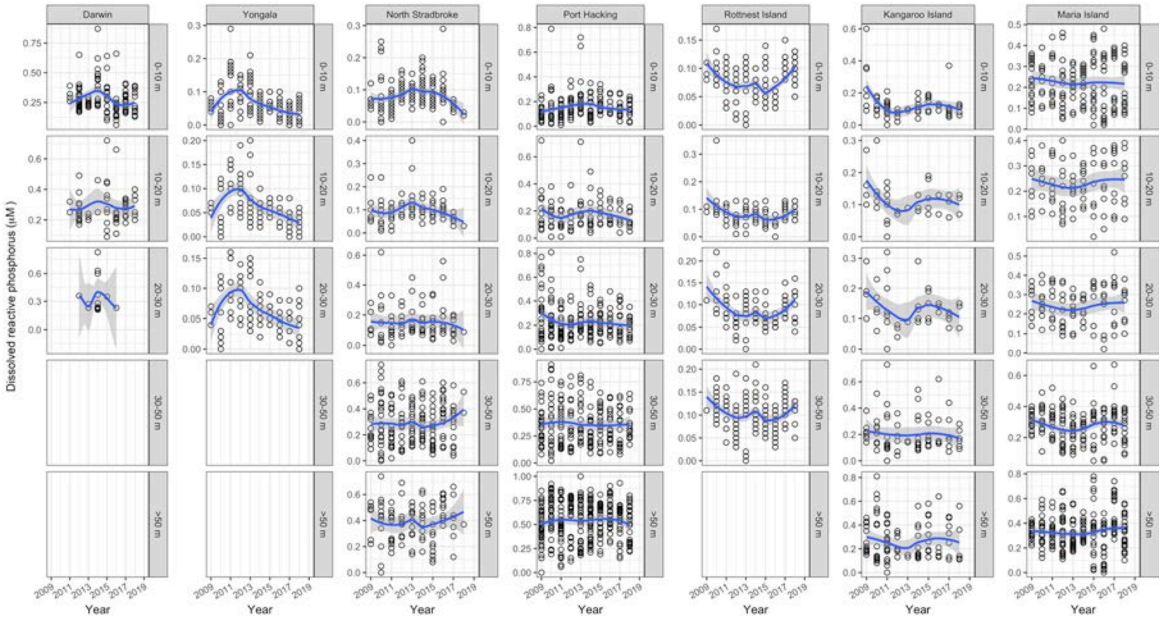

Figure 1. Time series of dissolved reactive phosphorus (DRP) in different depth layers at the 7 IMOS National Reference Stations. Dots represent observed data and the trends are represented by blue lines with grey shaded areas defining 95% confidence intervals of those trends.

NO_3^- concentrations (**Figure 4**) in Maria Island surface waters look to have been rising from the 1970s with temperature and salinity. This is counter to their increased subtropical nature that would imply decreased NO_3^- levels. Instead, rising mean NO_3- concentrations (now ~1.7 µM) suggest enhanced replenishment over time with winter mixing and incursion of sub-Antarctic surface waters, the latter supported by seasonally declining salinity at Maria Island—autumn to early spring—for all sampled depths (related to higher nutrient levels, see Harris et al. (1987)). Over 70 years, NO_3^- levels at the surface at Port Hacking (100-m station, off Sydney) have declined from 1.25 to 0.75 µM, but increased at 40–50 m depth, which could be linked with increased stratification. While the Rottnest Island NO_3^- record shows no long-term trend, a broad peak (0.30–0.50 µM) from 1975 to 1995 suggests a period of diminished LC influence. At 40–50 m depth, all three stations show a similar NO_3^- time series; which might reflect a region-wide oceanographic influence.

DRP concentrations (**Figure 5**) show different behaviour interannually to NO_3^-, which could arise from differences in their supply and assimilation with fluctuating composition of the phytoplankton community. Interpretation of the DRP time series is constrained by data gaps. Maria and Rottnest Islands have similar trends over the full depth range: an initial rise to a peak and a decline to the present. The peak for Maria Island (~0.55 µM at the surface) was in the 1970s; that for Rottnest Island (~0.20 µM at the surface) in the early 1990s. Port Hacking appears to have declined in DRP concentration from a plateau in the mid-1950s to mid-1980s until the last decade (0.20–0.15 µM at the surface). Similar profiles for all three stations are seen at depth (40–50 m) for DRP, as also noted above for NO_3^-.

DSi has a shorter record than NO_3- and DRP (1970 until now), although relatively unbroken (**Figure 6**). Its concentration has declined at all three long-term stations, most markedly at Maria Island, declining at the surface from >3 µM in 1970 to 1 µM now (unlike for NO_3^-, sub-Antarctic waters are depleted in DSi). Port Hacking appears to have declined over the same period from concentrations generally >1 µM to levels < 1 µM now. Apart from an initial anomaly, Rottnest Island has also declined from ~2.5 µM in surface waters to ~2 µM, which could be a consequence of reduced LC flow. Declines in DSi could also plausibly be linked with a mix of other factors—e.g. changes in composition of the phytoplankton community (diatoms have become more active), decrease in supply to coastal waters from terrestrial runoff, and decline in remineralisation rates of biogenic silica.

Implications for people and ecosystems

Human activity influences both the concentration and the relative forms of inorganic and organic nutrients in marine systems directly (e.g. inflow of fertilisers and wastewaters) or indirectly through changes in global climate influencing oceanography, flowing through to primary producers at the base of marine food webs. IMOS NRS data suggest it is mostly meso-scale oceanography that is controlling the patterns in offshore coastal waters around Australia. Time series of annual mean concentrations at long-term stations depict shifts in N, P and Si; they are not in unison one with the other, nor between locations. Nutrient concentrations and proportions of N, P and Si control fertility, the balance of the planktonic and benthic primary producers, and ultimately the composition of marine food webs. Whether changes in nutrient distributions in coastal waters are already causing changes in these food webs, or the nutrients reflect changes caused by other factors (e.g. temperature, stratification) is not clear.

doi: 10.26198/5e16a2ff49e77

For instance, in surface seawaters of Maria Island, increasing NO_3^- and decreasing DSi could favour a shift in phytoplankton from diatoms to dinoflagellates, or it could ensue from DSi removed from seawater by increasing proportions of diatoms stimulated by greater NO_3^- supplies. The former scenario is preferred by Thompson et al. (2009), albeit with DSi in subtropical waters removed upstream by diatoms. We therefore recommend that a future assessment of the impact of these changes should focus on close integration of the poorly constrained biogeochemical processes with changes in plankton and other primary producer communities, and the repercussions for higher-order consumers.

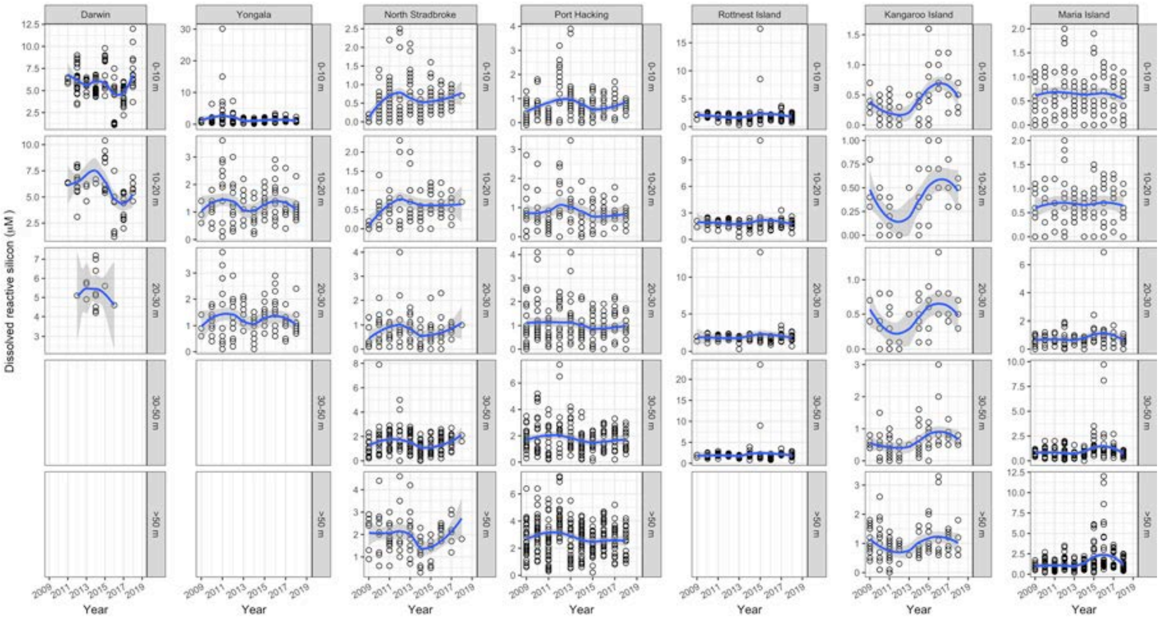

Figure 2. Time series of dissolved reactive silicon (DSi) in different depth layers at the 7 IMOS National Reference Stations. Dots represent observed data and the trends are represented by blue lines with grey shaded areas defining 95% confidence intervals of those trends.

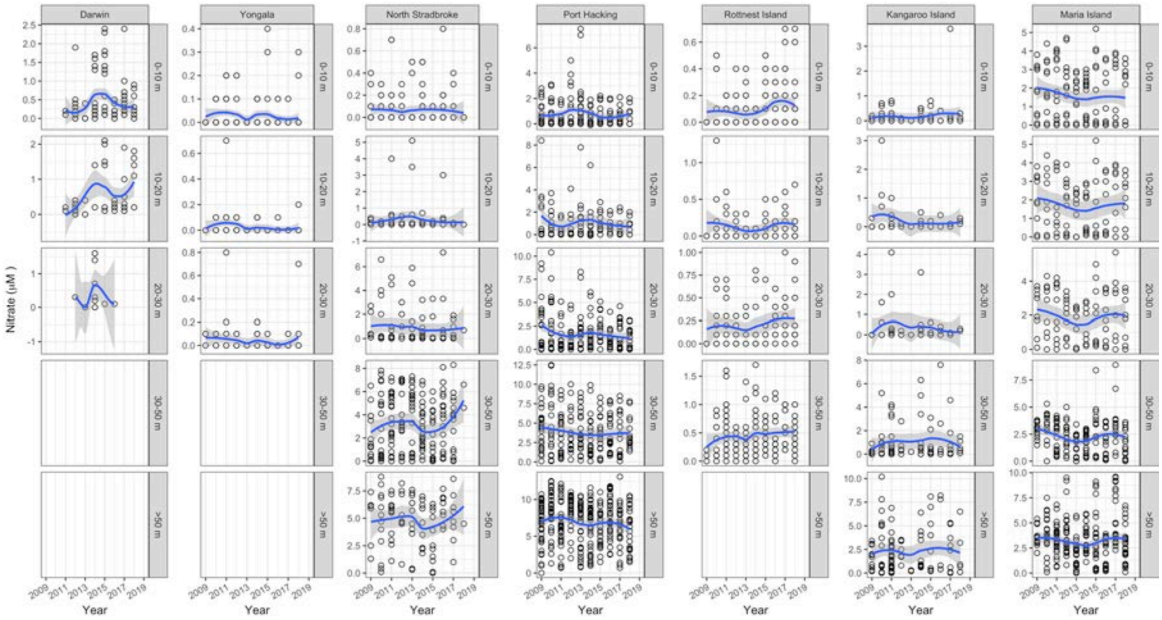

Figure 3 Time series of nitrate (NO_3-) in different depth layers at the 7 IMOS National Reference Stations. Dots represent observed data and the trends are represented by blue lines with grey shaded areas defining 95% confidence intervals of those trends.

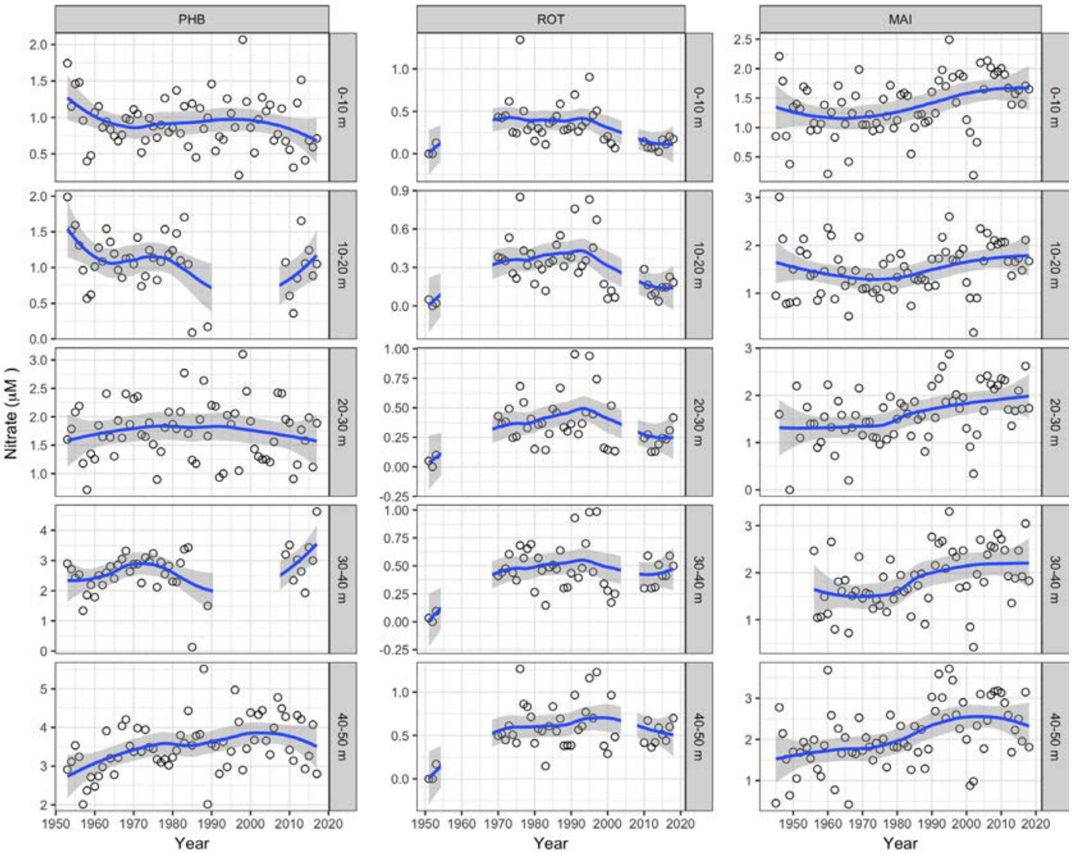

Figure 4 Annual time series of nitrate (NO_3^-) in different depth layers at the three long-term, Australian coastal stations—Port Hacking (100-m station; PHB), Rottnest Island (ROT) and Maria Island (MAI). Dots represent observed data and the trends are represented by blue lines with grey shaded areas defining 95% confidence intervals of those trends. Note data gaps in some time series

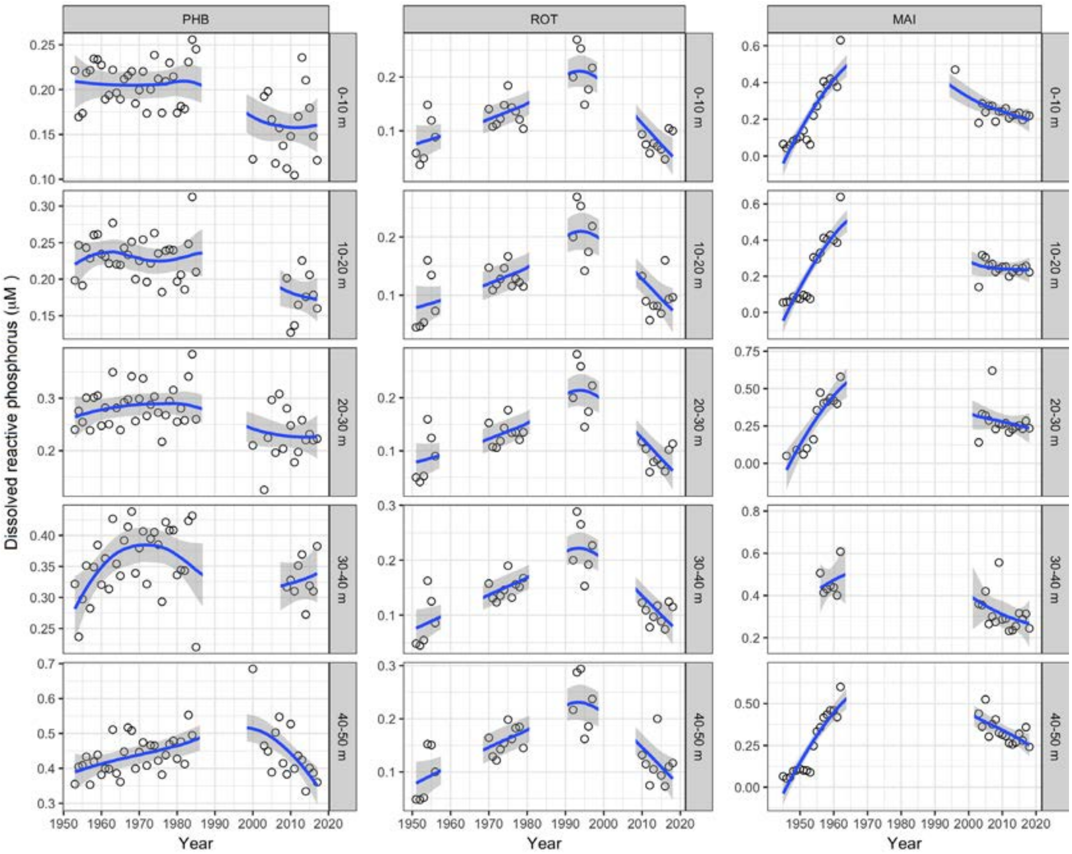

Figure 5. Annual time series of dissolved reactive phosphorus (DRP) in different depth layers at the three long-term, Australian coastal stations—Port Hacking (100-m station; PHB), Rottnest Island (ROT) and Maria Island (MAI). Dots represent observed data and the trends are represented by blue lines with grey shaded areas defining 95% confidence intervals of those trends. Note data gaps in some time series

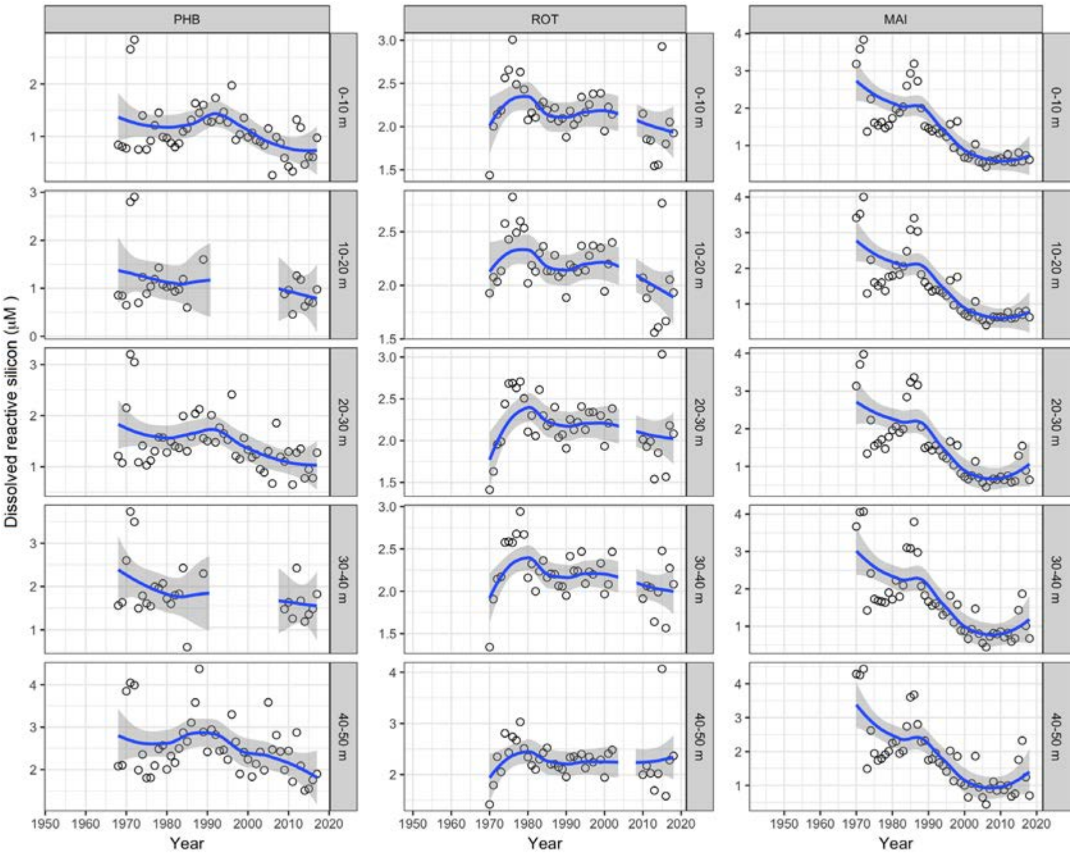

Figure 6. Annual time series of dissolved reactive silicon (DSi) in different depth layers at the three long-term, Australian coastal stations—Port Hacking (100-m station; PHB), Rottnest Island (ROT) and Maria Island (MAI). Dots represent observed data and the trends are represented by blue lines with grey shaded areas defining 95% confidence intervals of those trends. Note data gaps in some time series.

Box 1: The importance of organic nutrients

In marine systems, nitrogen and phosphorus are found in both inorganic and organic forms. Inorganic nutrients are non-living and are present in relatively few chemical forms, with dissolved inorganic N (DIN) found as ammonium (NH_4^+), nitrate (NO_3^-) and nitrite (NO_2^-), with NO_3^- being the most stable and dominant form (Wada & Hattori, 1991). Inorganic P is mostly found as orthophosphate (HPO_4^{2-}) (Cembella, Antia, Harrison, & Rhee, 1984). Dissolved reactive Si exists overwhelmingly as orthosilicate $Si(OH)_4$ or $Si(OH)_3O^-$ (Isshiki, Sohrin, & Nakayama, 1991).

By contrast, organic nutrients are contained in a complex mix of molecules from simple amino acids to highly complex chemical compounds. While inorganic nutrients and a small part of organic nutrients can be directly used for biological growth, most organic nutrients must first be degraded (either biologically by enzymes or abiotically by sunlight) to smaller compounds or inorganic nutrients before they can be used by marine life. These differences in processing steps impact how fast compounds are cycled in the environment. Generally inorganic nutrients are used at short timescales (hours to days), while the organic nutrients are used over a broader range of timescales (hours to years).

Few studies have accounted for the relative importance of both inorganic and organic nutrients. In oligotrophic tropical coastal waters of the Great Barrier Reef where inorganic nutrient levels are low, Lønborg et al. (2018) found that 95% of the nitrogen and 75% of the phosphorus used by marine life were in the organic fraction. This suggests that to understand and manage nutrients in coastal waters, it is important that future work measure and account for both inorganic and organic fractions (**Figure B 1**).

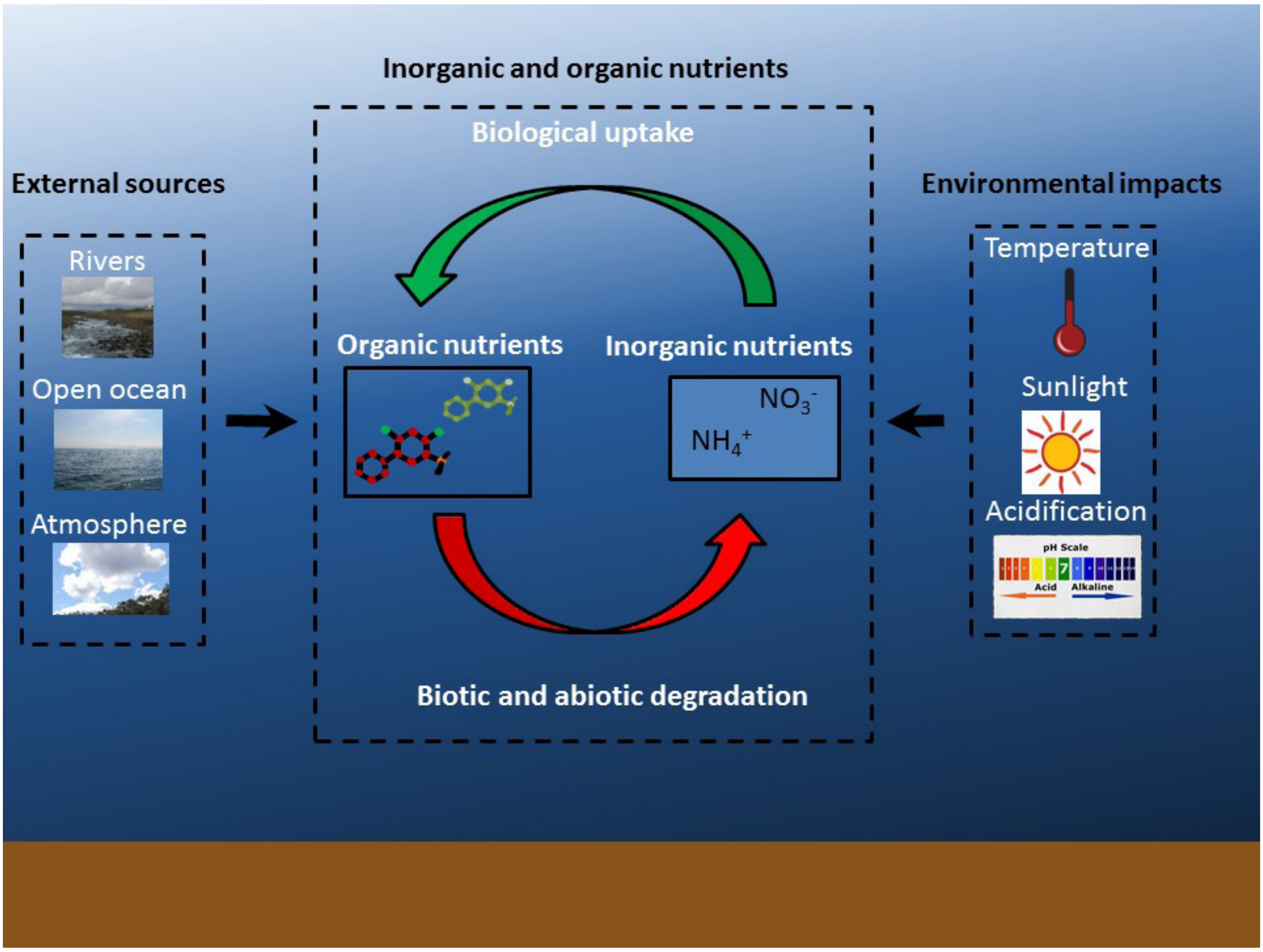

Figure B 1. Schematic overview showing the 1) main external sources, 2) interplay between inorganic and organic nutrients, and 3) some of the main environmental factors impacting this interplay.

Box 2: Micronutrients as modulators

The availability of N, P and Si is not the only nutritional requirement of marine primary producers. Trace elements, especially transition metals of the first row in the Periodic Table, influence productivity at the base of marine ecosystems. These trace elements are characterised as *micronutrients*. Iron (Fe) is universally recognised as the most critical, and can be limiting by itself or limiting jointly with a macronutrient such as N (Tagliabue et al., 2017) . Apart from Fe, micronutrients rarely, if ever, limit primary production (Moore et al., 2013) . More commonly, micronutrients (copper, zinc, cobalt, nickel, manganese, cadmium, selenium, etc.) influence pelagic primary productivity by favouring certain phytoplankton classes, which in turn impact the composition of higher trophic levels.

The influence of micronutrients is manifest among the different classes of phytoplankton, right down to their cellular physiology (**Figure B2**, Morel and Price (2003). Fe is the micronutrient in most demand because it is pivotal in photosynthesis (as a metal centre in photosystems (PSI and PSII) and ferredoxin), an integral component of cytochromes, and specific cellular processes involving the handling of N (e.g. N_2 fixation, nitrate/nitrite reduction). Other micronutrients play more specific roles. Zinc mediates two critical pathways as a metal centre for the enzymes carbonic anhydrase and alkaline phosphatase. Copper is active as a cofactor in photosynthesis and nitrogen cycling (e.g. denitrification, ammonium oxidation). Some micronutrients have a specific role: cobalt is the metal cofactor in Vitamin B_{12}, an important agent for biomethylation; whereas nickel is the metal centre in the enzyme urease, responsible for the decomposition of urea to ammonia and CO_2.

The requirement by phytoplankton for micronutrients is adaptable to prevailing conditions. For example, Zn can be replaced by Co or Cd in carbonic anhydrase (Morel & Price, 2003). The substitution may distinguish different phytoplankton taxa, or it may be a strategy to retain functionality during severe deficiency of the favoured metal at the expense of decreased efficiency. Other physiological strategies involve the substitution by a main-group metal (e.g. alkaline phosphatase variant, with Ca replacing Zn – Sebastian & Ammerman, 2009) or the avoidance of a metal centre altogether (e.g. flavodoxin for ferredoxin – Roche, Murray, Orellana, & Newton, 1995).

Extracellular processes can also favour the acquisition of micronutrients through the excretion of organic compounds (ligands) to sequester essential metals. These ligands (e.g. siderophores) are exuded by some micro-organisms, which have mechanisms to transport the bound metals intracellularly (Vraspir & Butler, 2009).

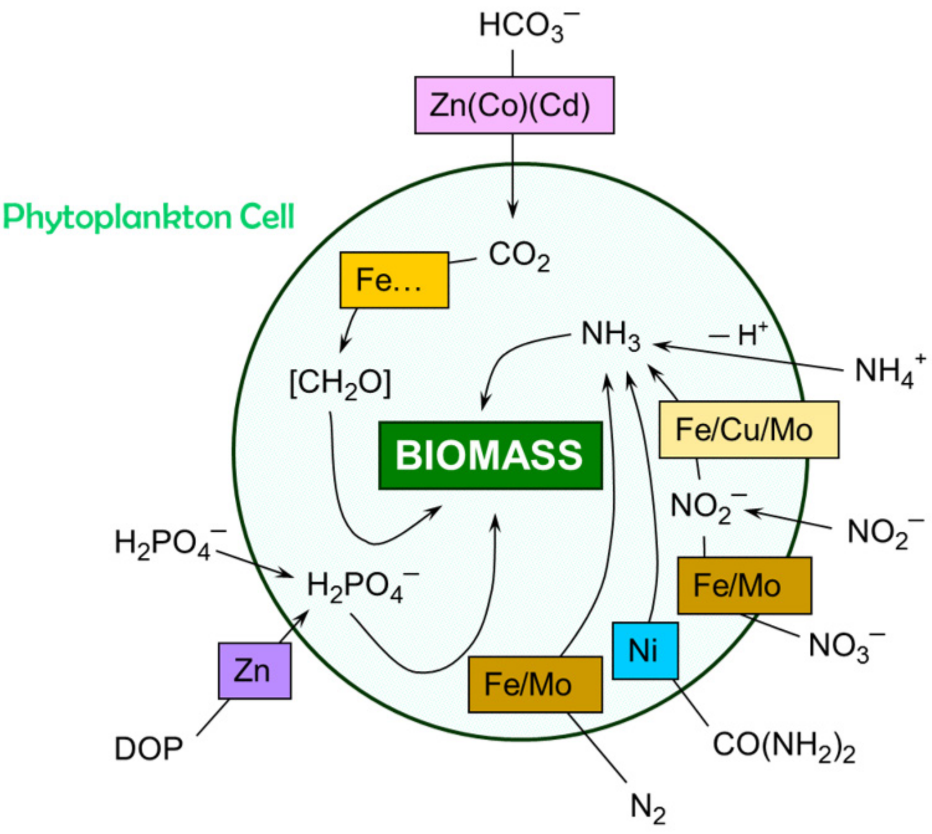

Figure B 2. Micronutrients in key carbon, nitrogen and phosphorus pathways. An ellipsis (e.g. Fe...) indicates other metals of lesser prominence are also cofactors in the pathway. Metals in parenthesis (e.g. (Co)) denote less preferred or less efficient cofactors. A forward slash separates metals active in different steps in a pathway, operating in combination, or having a different function as a cofactor. Modified from original in Morel & Price 2003.

Acknowledgements

Data was sourced from Australia's Integrated Marine Observing System (IMOS) which is enabled by the National Collaborative Research Infrastructure Strategy (NCRIS).

Data Sources

IMOS National Reference Stations.
http://imos.org.au/facilities/nationalmooringnetwork/nrs/

References

Canfield, D. E., Glazer, A. N., & Falkowski, P. G. (2010). The evolution and future of Earth's nitrogen cycle. ***Science 330***, 192–196.

Cembella, A. D., Antia, N. J., Harrison, P. J., & Rhee, G. Y. (1984). The utilization of inorganic and organic phosphorous compounds as nutrients by eukaryotic microalgae: A multidisciplinary perspective: Part 2. ***CRC Critical Reviews in Microbiology, 11***(1), 13-81. doi:10.3109/10408418409105902

Harris, G., Nilsson, C., Clementson, L., & Thomas, D. (1987). The water masses of the east coast of Tasmania: seasonal and interannual variability and the influence on phytoplankton biomass and productivity. ***Australian Journal of Marine and Freshwater Research, 38***, 569-590.

Hayes, D., Lyne, V., Condie, S. A., Griffiths, B., Pigot, S., & Hallegraeff, G. (2005). ***Collation and analysis of oceanographic datasets for National marine bioregionalisation***. A report to the Australian Government, National Oceans Office. CSIRO Marine Research, Hobart. 229 pp.

Isshiki, K., Sohrin, Y., & Nakayama, E. (1991). Form of dissolved silicon in seawater. ***Marine Chemistry, 32***(1), 1-8. doi:10.1016/03044203(91)90021-N

Kitadai, N., & Maruyama, S. (2018). Origins of building blocks of life: A review. ***Geoscience Frontiers, 9***(4), 1117-1153. doi:10.1016/j.gsf.2017.07.007

Lønborg, C., Álvarez–Salgado, X. A., Duggan, S., & Carreira, C. (2018). Organic matter bioavailability in tropical coastal waters: The Great Barrier Reef. ***Limnology and Oceanography, 63***(2), 1015-1035. doi:10.1002/lno.10717

Lynch, T. P., Morello, E. B., Evans, K., Richardson, A. J., Rochester, W., Steinberg, C., . . . Moltman, T. (2014). IMOS National Reference Stations: a continental-wide physical, chemical and biological coastal observing system. ***PLoS ONE, 9***(12), e113652.

Moore, C. M., Mills, M. M., Arrigo, K. R., Berman-Frank, I., Bopp, L., Boyd, P. W., . . . Ulloa, O. (2013). Processes and patterns of oceanic nutrient limitation. ***Nature Geoscience, 6***, 701. doi:10.1038/ngeo1765

Morel, F. M. M., & Price, N. M. (2003). The biogeochemical cycles of trace metals in the oceans. ***Science, 300***(5621), 944. doi:10.1126/science.1083545

Radke, L., Nicholas, T., Thompson, P. A., Li, J., Raes, E., Carey, M., . . . Nichol, S. (2017). Baseline biogeochemical data from Australia's continental margin links seabed sediments to water column characteristics. ***Marine and Freshwater Research, 68***(9), 1593-1617. doi: 10.1071/MF16219

Rees, C., Pender, L., Sherrin, K., Schwanger, C., Hughes, P., Tibben, S., . . . Rayner, M. (2019). Methods for reproducible shipboard SFA nutrient measurement using RMNS and automated data processing. ***Limnology and Oceanography: Methods, 17***(1), 25-41. doi:10.1002/lom3.10294

Roche, J. L., Murray, H., Orellana, M., & Newton, J. (1995). Flavodoxin expression as an indicator of iron limitation in marine diatoms. ***Journal of Phycology, 31***(4), 520-530. doi:10.1111/j.1529-8817.1995.tb02545.x

Ruttenberg, K. C. (2014). 10.13 - The Global Phosphorus Cycle. In H. D. Holland & K. K. Turekian (Eds.), ***Treatise on Geochemistry (Second Edition)*** (pp. 499-558). Oxford: Elsevier.

Sebastian, M., & Ammerman, J. W. (2009). The alkaline phosphatase PhoX is more widely distributed in marine bacteria than the classical PhoA. ***The ISME Journal, 3***(5), 563-572. doi:10.1038/ismej.2009.10

Tagliabue, A., Bowie, A. R., Boyd, P. W., Buck, K. N., Johnson, K. S., & Saito, M. A. (2017). The integral role of iron in ocean biogeochemistry. ***Nature, 543***, 51-59. doi:10.1038/nature21058

Thompson, P., Baird, M., Ingleton, T., & Doblin, M. A. (2009). Long-term changes in temperate Australian coastal waters: implications for phytoplankton. ***Marine ecology progress series, 394***, 1-19.

Thompson, P. A., Bonham, P., Waite, A. M., Clementson, L. A., Cherukuru, N., Hassler, C., & Doblin, M. A. (2011). Contrasting oceanographic conditions and phytoplankton communities on the east and west coasts of Australia. ***Deep Sea Research Part II: Topical Studies in Oceanography, 58***(5), 645-663. doi:10.1016/j.dsr2.2010.10.003

Tréguer, P. J., & Rocha, C. L. D. L. (2013). The world ocean silica cycle. ***Annual Review of Marine Science, 5***(1), 477-501. doi:10.1146/annurev-marine-121211-172346

van Ruth, P. D., Patten, N. L., Doubell, M. J., Chapman, P., Rodriguez, A. R., & Middleton, J. F. (2018). Seasonal- and event-scale variations in upwelling, enrichment and primary productivity in the eastern Great Australian Bight. ***Deep Sea Research Part II: Topical Studies in Oceanography, 157-158***, 36-45. doi:10.1016/j.dsr2.2018.09.008

Vraspir, J. M., & Butler, A. (2009). Chemistry of marine ligands and siderophores. ***Annual Review of Marine Science, 1***(1), 43-63. doi:10.1146/annurev.marine.010908.163712

Wada, E., & Hattori, A. (1991). ***Nitrogen in the Sea: forms, abundances, and rate processes***. Boca Raton, Florida: CRC Press.

Supplement

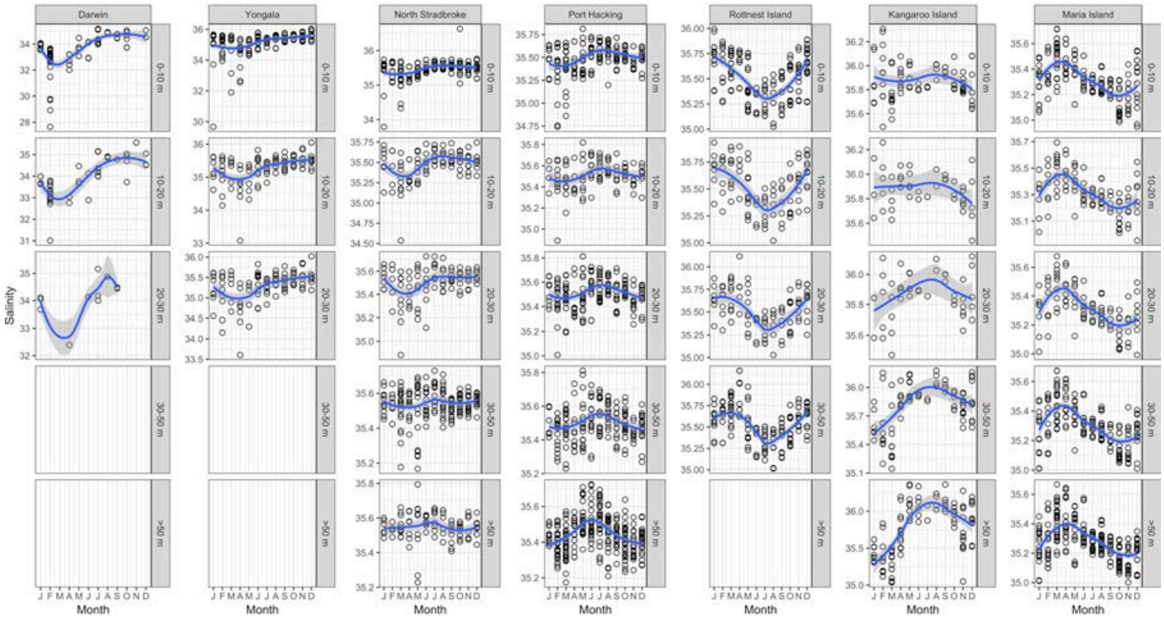

Figure S1. Seasonal cycle of salinity levels in different depth layers at the 7 IMOS National Reference Stations. Dots represent observed data and the trends are represented by blue lines with grey shaded areas defining 95% confidence intervals of those trends.

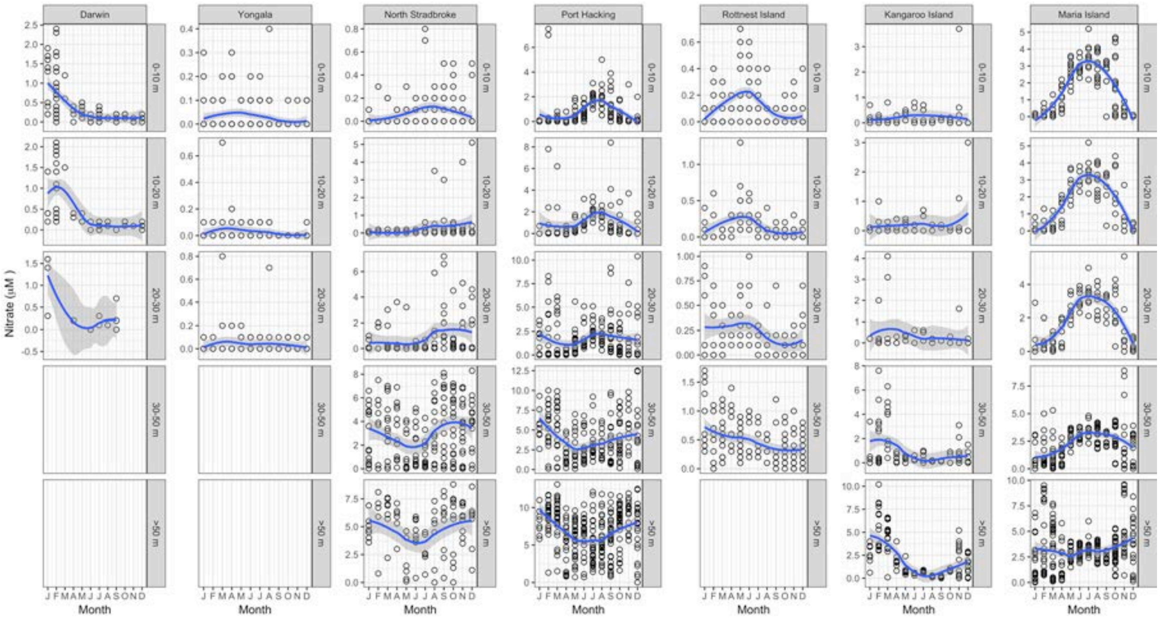

Figure S2. Seasonal cycle of nitrate (NO_3^-) in different depth layers at the 7 IMOS National Reference Stations. Dots represent observed data and the trends are represented by blue lines with grey shaded areas defining 95% confidence intervals of those trends. Time-span of observations presented varies for each NRS, see Overall Methods.

doi: 10.26198/5e16a2ff49e77

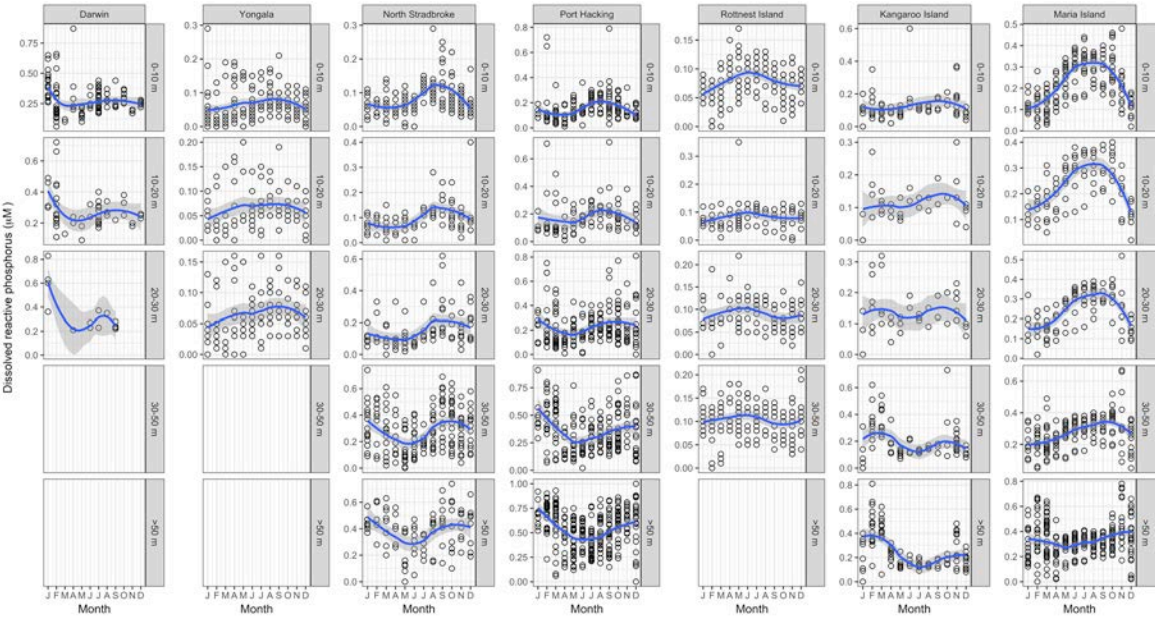

Figure S3. Seasonal cycle of dissolved reactive phosphorus (DRP) in different depth layers at the 7 IMOS National Reference Stations. Dots represent observed data and the trends are represented by blue lines with grey shaded areas defining 95% confidence intervals of those trends. Time-span of observations presented varies for each NRS, see Overall Methods.

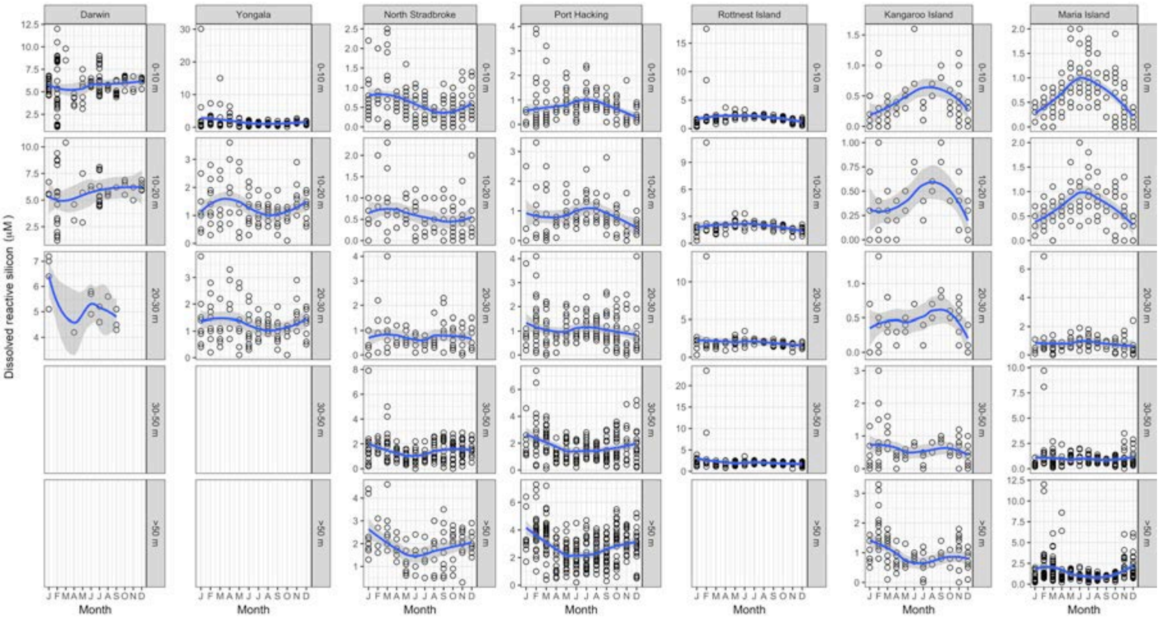

Figure S4. Seasonal cycle of dissolved reactive silicate (DSi) in different depth layers at the IMOS National Reference Stations. Dots represent observed data and the trends are represented by blue lines with grey shaded areas defining 95% confidence intervals of those trends. Time-span of observations presented varies for each NRS, see Overall Methods.

IMOS

Integrated Marine
Observing System

1.6 | Ocean acidification

Bronte Tilbrook[1,2], Erik Van Oiijen[1], Craig Neill[1], Kate Berry[1],
John Akl[1], Abe Passmore[1], James Black[1],
Andrew Lenton[1,2] and Anthony J. Richardson[3,4]

1 CSIRO Oceans and Atmosphere, Hobart, TAS, Australia
2 Australian Antarctic Program Partnership, University of Tasmania, Hobart, TAS, Australia
3 CSIRO Oceans and Atmosphere, Queensland Biosciences Precinct (QBP), St Lucia, QLD, Australia
4 Centre for Applications in Natural Resource Mathematics (CARM), School of Mathematics and Physics, The University of Queensland, St Lucia, QLD, Australia

Summary

The pH and aragonite saturation state of surface seawaters around Australia are influenced by the large-scale circulation, and superimposed on this are the effects of seasonal changes due largely to biological activity and temperature change. Maximum values of aragonite saturation state tend to develop over summer-early autumn, while pH values are typically greatest in winter. Biological production contributes to increases of both pH and aragonite saturation state in the spring-summer, while warming acts to increase the saturation state and decrease pH. Seasonal ranges of both variables are already estimated to be outside the ranges that many of Australia's marine ecosystems are likely to have experienced in the late 1800s.

Key Data Streams

National Reference Stations

Acidification Moorings

State and Trends of Australia's Ocean Report
www.imosoceanreport.org.au

Time-Series published
10 January 2020

doi: 10.26198/5e16a38849e78

Rationale

Ocean acidification results from a change in seawater chemistry due to the oceans taking up about 25% of the current anthropogenic emissions of carbon dioxide (CO_2) to the atmosphere (Hurd et al. 2018). The CO_2 taken up lowers both surface water pH and dissolved carbonate ion concentration and increases dissolved aqueous CO_2 and bicarbonate ion concentrations. The changes are rapid, with a decrease in surface water pH of 0.11 estimated to be ten-fold greater than the rate of change at any in the past 300 million years (Honisch et al., 2012). By 2100, the surface ocean pH is expected to decrease by a further 0.1 to 0.4 units and dissolved carbonate ion concentration by up to 50%, leading to similar decreases in the aragonite saturation state (Gattuso et al., 2015). Superimposed on these large-scale changes, is variability at seasonal and local scales associated with natural processes, which can be large enough to amplify or offset ocean acidification trends, particularly in coastal and shelf environments. Ocean acidification can disrupt marine organisms to different degrees with potential flow-on effects for a broad range of ocean services including shellfish aquaculture, coastal protection, and regional economies dependent on healthy and sustainable marine ecosystems (Tilbrook et al., 2019). Data collected from the Integrated Marine Observing System (IMOS) Ships of Opportunity, Moorings and National Reference Station facilities are providing understanding of how ocean chemistry is changing and is providing a baseline to assess the impact on marine organisms.

Methods

The pH and aragonite saturation state of seawater have been shown to influence the response of marine life to ocean acidification. These two parameters were determined in the waters around Australia using a climatology of the fugacity of dissolved carbon dioxide (fCO_2) combined with total alkalinity values estimated from a salinity-alkalinity relationship for Australian regional seas (Lenton et al., 2016). The carbonate chemistry parameters were averaged for the decade of 2000-2009, and changes since 1870-1889 were calculated assuming changes in fCO_2 of surface waters approximate the increase in atmospheric CO_2 over the same period (Lenton et al., 2016; Pardo et al., 2019; Takahashi et al., 2009). Water samples collected every 1-4 months at IMOS National Reference Stations were used as a check on the values estimated from the climatology, and to provide information on seasonal variability in coastal waters.

Results and interpretation

Regional and long-term change: The aragonite saturation state and pH of surface waters have different patterns of change (**Figure 1**) due to a combination of regional variations in total alkalinity and total dissolved CO_2 concentrations, different sensitivities of the saturation state and pH to temperature, and the large-scale transport and mixing of water masses around Australia (Lenton et al., 2016). The aragonite saturation state for 2000-2009 decreases from values approaching 4 in tropical waters to 2.2 near 45°S, while maximum pH values of about 8.10 to 8.12 are found in subtropical waters. Large decreases have occurred since 1870-1890 for both parameters with changes of up to 0.6 in the aragonite saturation state in subtropical waters and the largest changes in pH of about 0.11 have occurred in temperate and sub-Antarctic waters (**Figure 1**).

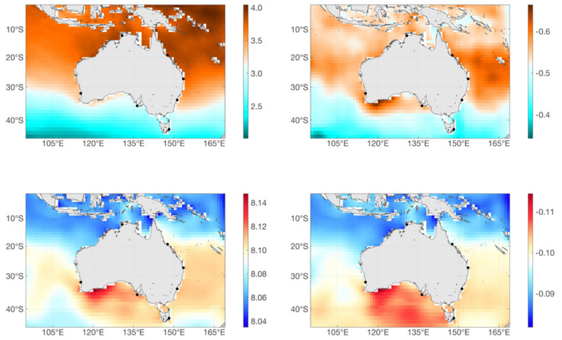

Figure 1. Top left: Mean aragonite saturation state of surface water for the decade 2000-2009; Top right: Estimated change in mean aragonite saturation state of surface waters between 1870-1890 and 2000-2009. Black circles show the location of IMOS National Reference Stations; Bottom left: Mean pH (total scale) of surface water for 2000-2009; Bottom right: Estimated change in average pH of surface waters between 1870-1890 and 2000-2009.

Seasonality: The seasonal cycles of the aragonite saturation state of Australian shelf waters is highlighted by data from the National Reference Stations (**Figure 2**). The east coast and southern shelf sites show a decrease in the aragonite saturation state from North to South, with maxima in Dec-Apr and minima in Jul-Oct (**Figure 2**). Seasonal changes in pH are typically out of phase with aragonite saturation state by up to 6 months. Data from the Darwin National Reference Station are shown, but more frequent sampling is needed to better resolve the seasonal and longer time-scale signals at this site.

The seasonality at the sites is influenced by the development of stable and warmer mixed layers in spring-summer, changes in net production, and seasonal changes in the transport of offshore waters that typically have higher aragonite saturation states and lower pH in the spring-summer period compared to winter-autumn. The sensitivity to these processes varies with the site. High-frequency sampling at KAI and MAI using CO_2 moorings allow more complete assessments of the cause of the changes by decomposing the drivers of the variability (Pardo et al., 2019). At KAI, seasonal warming and cooling tends to dominate the surface fCO2 signal, which covaries with pH, while aragonite saturation state is less sensitive to temperature change and shows only a small range compared to most other locations (**Figure 2**).

Data from this site also shows occasional low fCO_2 (and lower pH) in the summer as upwelling onto the shelf reaches the surface. The seasonality at MAI is also influenced by temperature change, but here the greater transport of warmer and low-CO_2 waters in the spring-summer and their retreat in autumn-winter drives a greater change in the aragonite saturation state and these changes partially offset the temperature effect on pH at this site. The high variability at the MAI site is due in part to the passage of warm and cold core eddies through the site.

The present-day maximum values at the NRS sites are less than the values for the 1870-1890 period, suggesting that for large parts of the year the biota at these sites are already exposed to conditions outside the range of values that existed in preindustrial times.

Interannual change: The 10-year sampling at the sites provides an indication of interannual change (**Figure 3**). De-seasonalised high-frequency mooring data for KAI and MAI (**Figure 4**) do show that changes in circulation and the transport of water masses is driving much of the interannual variability in surface water CO_2 at these two sites. At KAI, the relative strengths of the Leeuwin and Flinders current appear to influence the variability while the interannual changes at MAI are consistent with a greater component of subtropical waters being transported by the East Australian Current into the region over time.

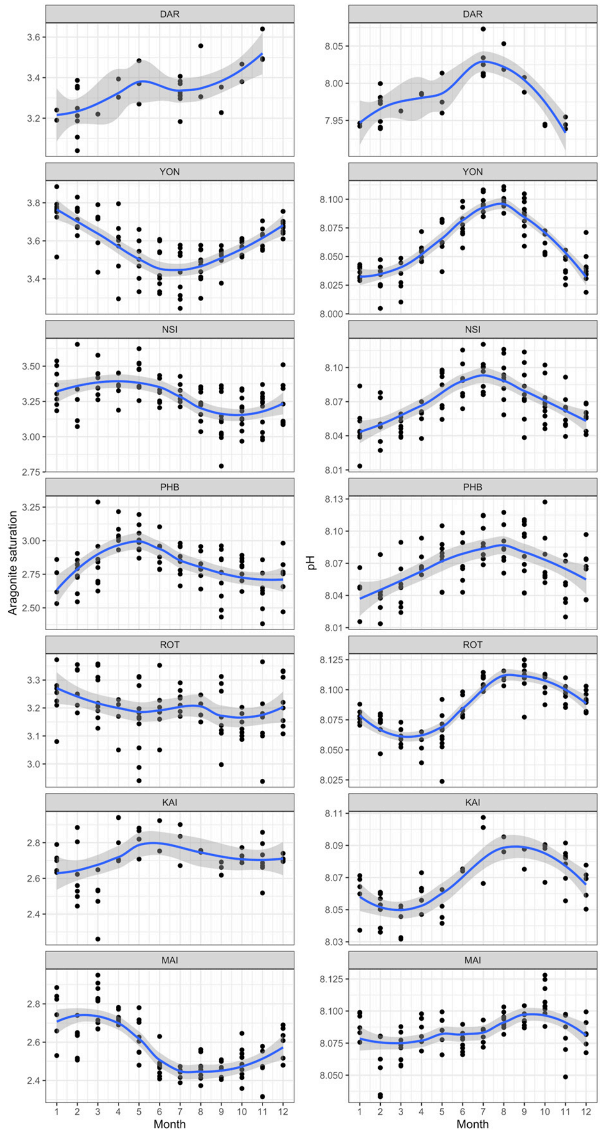

Figure 2. Monthly climatology of aragonite saturation (left) and pH (right) at National Reference Stations Darwin (DAR), Yongala (YON), North Stradbroke Island (NSI), PHB (Port Hacking), ROT (Rottnest Island), KAI (Kangaroo Island) and MAI (Maria Island).

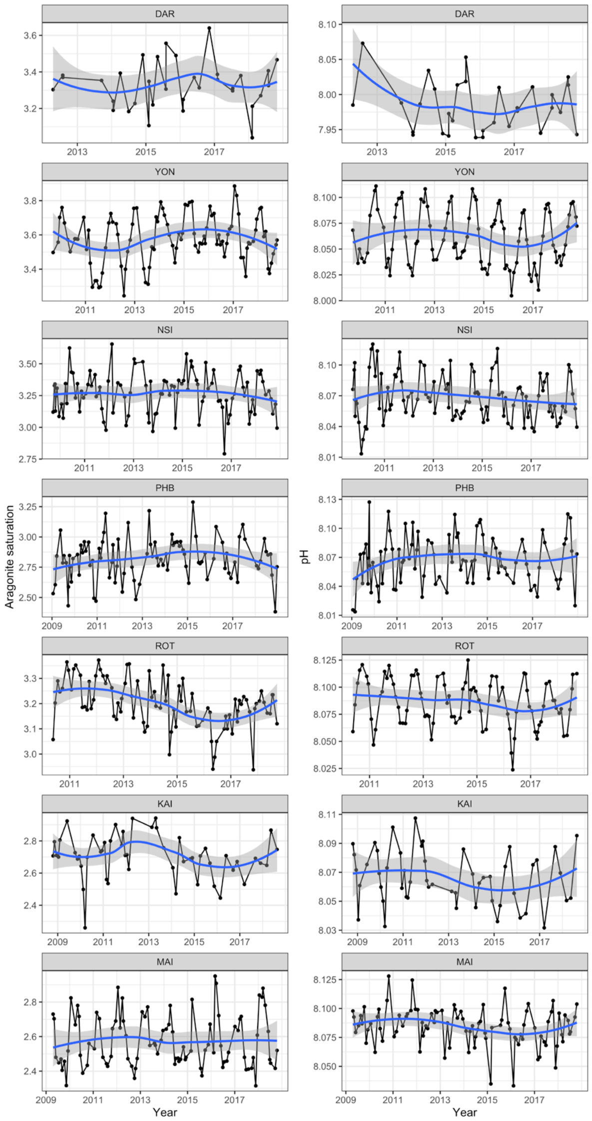

Figure 3. Inter-annual time series of aragonite saturation (left) and pH (right) at National Reference Stations Darwin (DAR), Yongala (YON), North Stradbroke Island (NSI), PHB (Port Hacking), ROT (Rottnest Island), KAI (Kangaroo Island) and MAI (Maria Island).

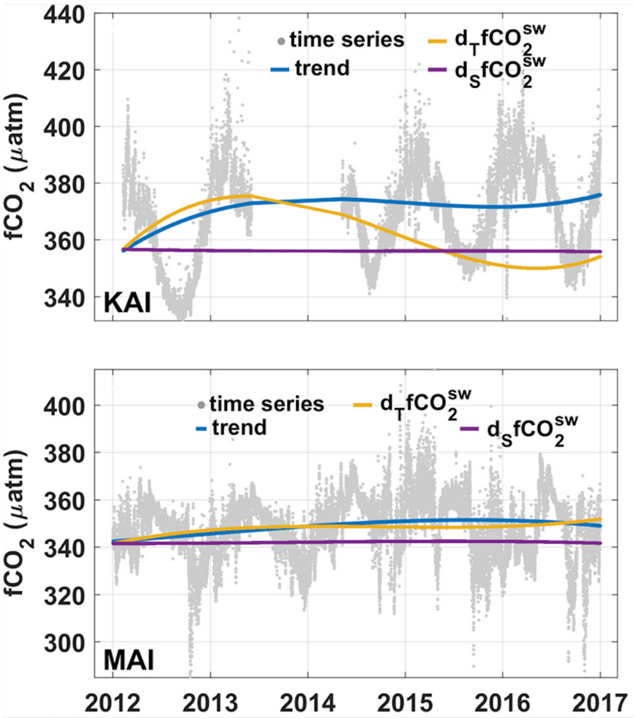

Figure 4. Interannual variability in the carbon system at MAI and KAI. Original data between 2012 and 2016 (grey dots) and de-seasonalised interannual trend (blue line) of surface water fCO$_2$ with the contributions of temperature ($d_T fCO_2^{sw}$, orange line), salinity ($d_S fCO_2^{sw}$, magenta line). Figure adapted from (Pardo et al., 2019) .

Implications for people and ecosystems

As one of the main marine stressors, ocean acidification is expected to impact a wide range of marine organisms in the future, including coral reefs and wild and farmed shellfisheries that generate substantial income and support local communities. The range of seawater pH and aragonite saturation state values that occur for large parts of the year are already outside the range of values that were likely in the late 1800s. These data will provide a foundation to assess the response of benthic and pelagic biota to the changes, and for understanding how ocean carbon cycling is evolving in Australia's seas, including in the major boundary current regions.

Acknowledgements

Data was sourced from Australia’s Integrated Marine Observing System (IMOS) which is enabled by the National Collaborative Research Infrastructure Strategy (NCRIS).

Data Sources

IMOS National Reference Stations.
http://imos.org.au/facilities/nationalmooringnetwork/nrs/

IMOS Acidification Moorings
http://imos.org.au/facilities/nationalmooringnetwork/acidificationmoorings/

References

Gattuso, J. P., Magnan, A., Bille, R., Cheung, W. W. L., Howes, E. L., Joos, F., . . . Turley, C. (2015). Contrasting futures for ocean and society from different anthropogenic CO2 emissions scenarios. ***Science, 349***(6243), 11. doi:10.1126/science.aac4722

Honisch, B., Ridgwell, A., Schmidt, D. N., Thomas, E., Gibbs, S. J., Sluijs, A., . . . Williams, B. (2012). The geological record of ocean acidification. *Science, 335*(6072), 1058-1063. doi:10.1126/science.1208277

Hurd, C. L., Lenton, A., Tilbrook, B., & Boyd, P. W. (2018). Current understanding and challenges for oceans in a higher-CO2 world. *Nature Climate Change, 8*(8), 686-694. doi:10.1038/s41558-018-0211-0

Lenton, A., Tilbrook, B., Matear, R. J., Sasse, T. P., & Nojiri, Y. (2016). Historical reconstruction of ocean acidification in the Australian region. *Biogeosciences, 13*(6), 1753-1765. doi:10.5194/bg-13-1753-2016

Pardo, P. C., Tilbrook, B., van Ooijen, E., Passmore, A., Neill, C., Jansen, P., . . . Trull, T. W. (2019). Surface ocean carbon dioxide variability in South Pacific boundary currents and Subantarctic waters. *Scientific Reports, 9*, 12. doi:10.1038/s41598-019-44109-2

Takahashi, T., Sutherland, S. C., Wanninkhof, R., Sweeney, C., Feely, R. A., Chipman, D. W., . . . de Baar, H. J. W. (2009). Climatological mean and decadal change in surface ocean pCO(2), and net sea-air CO2 flux over the global oceans. *Deep-Sea Research Part Ii-Topical Studies in Oceanography, 56*(8-10), 554-577. doi:10.1016/j.dsr2.2008.12.009

Tilbrook, B., Jewett, E. B., DeGrandpre, M. D., Hernandez-Ayon, J. M., Feely, R. A., Gledhill, D. K., . . . Telszewski, M. (2019). An enhanced ocean acidification observing network: from people to technology to data synthesis and information exchange. *Frontiers in Marine Science, 6*, 21. doi:10.3389/fmars.2019.00337

State and Trends of
Australia's Oceans
Report

2.1 Spatial and seasonal trends in Chlorophyll *a*

Peter Thompson[1], David Antoine[2] and Edward King[1]

[1] CSIRO Oceans and Atmosphere, Hobart, TAS, Australia
[2] Remote Sensing and Satellite Research Group, School of Earth and Planetary Sciences, Curtin University, Perth, WA, Australia

Summary

The concentration of chlorophyll a, a measure of phytoplankton biomass has seen an overall declined by 8% in Australian waters over the past 17 years. Despite this general marked decrease, large parts of the ocean south and southeast of Australia and the coastal zone along the east coast of Australia have seen significant increases in chlorophyll a concentration. Declines in chlorophyll a close to shore along the North West shelf and throughout the Great Australian Bight may significantly impact these coastal ecosystems and the fisheries they support.

Key Data Streams

Satellite Remote
Sensing

State and Trends of Australia's Ocean Report
www.imosoceanreport.org.au

Time-Series published
10 January 2020

doi: 10.26198/5e16a44a49e79

Rationale

Chlorophyll ***a*** is a pigment present in all photosynthetic phytoplankton species. The amount of chlorophyll ***a*** in water is internationally recognized as a simple but worthwhile measure of phytoplankton biomass. Chlorophyll enables phytoplankton to grow by capturing energy from the sun, thus earning phytoplankton the name “grass of the sea”. Without phytoplankton there would be almost no other life in the ocean – they provide oxygen, food for higher trophic levels, are important in carbon sequestration as they sink into the deep ocean and, therefore, are of great ecological significance (Sournia, 1978).

Chlorophyll ***a*** can be monitored relatively easily, but the use of satellites to measure chlorophyll ***a*** has revolutionized our ability to observe the spatial and temporal dynamics, especially large scales. These dynamics include seasonal patterns of phytoplankton abundance, climate cycles and any longer-term changes. Trends in chlorophyll ***a*** tend to reflect changes in the ocean’s physical and chemical dynamics as temperature plus light and nutrient availability are the primary determinants of phytoplankton growth. Temperature, light and nutrient concentrations have a range of natural cycles that drive most of the temporal variation in phytoplankton. This means that any longer-term climate-driven trends can be difficult to detect without a sufficiently long time series of measurements to apportion phytoplankton variation to the right driver.

Methods

Phytoplankton pigments are a major source of colour in the world’s oceans and satellite technology has made it possible to obtain global estimates of this colour many times a year. The temporal and spatial sampling achieved by satellites produces a marvellous global estimate of phytoplankton biomass using well established empirical relationships. Research continues to reduce the small errors associated with variation in absorption and backscattering properties of phytoplankton and effects of coloured-dissolved organic matter and minerals (Dierssen, 2010).

Here we have used sixteen years of satellite data (2003-2018) from the MODerate resolution Imaging Spectroradiometer (Aqua-MODIS) sensor that estimates the near-surface concentration of chlorophyll ***a*** using an empirical relationship derived from in situ measurements of chlorophyll ***a*** and blue-to-green band ratios of in situ remote sensing reflectances. Full details can be found at https://modis.gsfc.nasa.gov/data/dataprod/chlor_a.php.

Satellite data were processed using the SeaDAS software with the OCI chlorophyll algorithm (Hu, Lee, & Franz, 2012). Data were analysed to give monthly composite maps of the chlorophyll ***a*** concentration. Linear temporal trends were extracted across a range of spatial scales from 4 km^2 to the Australian region (50°S to equator, 100°E to 170°E), including analysis of the de-trended time series (the time series from which the mean seasonal cycle was removed).

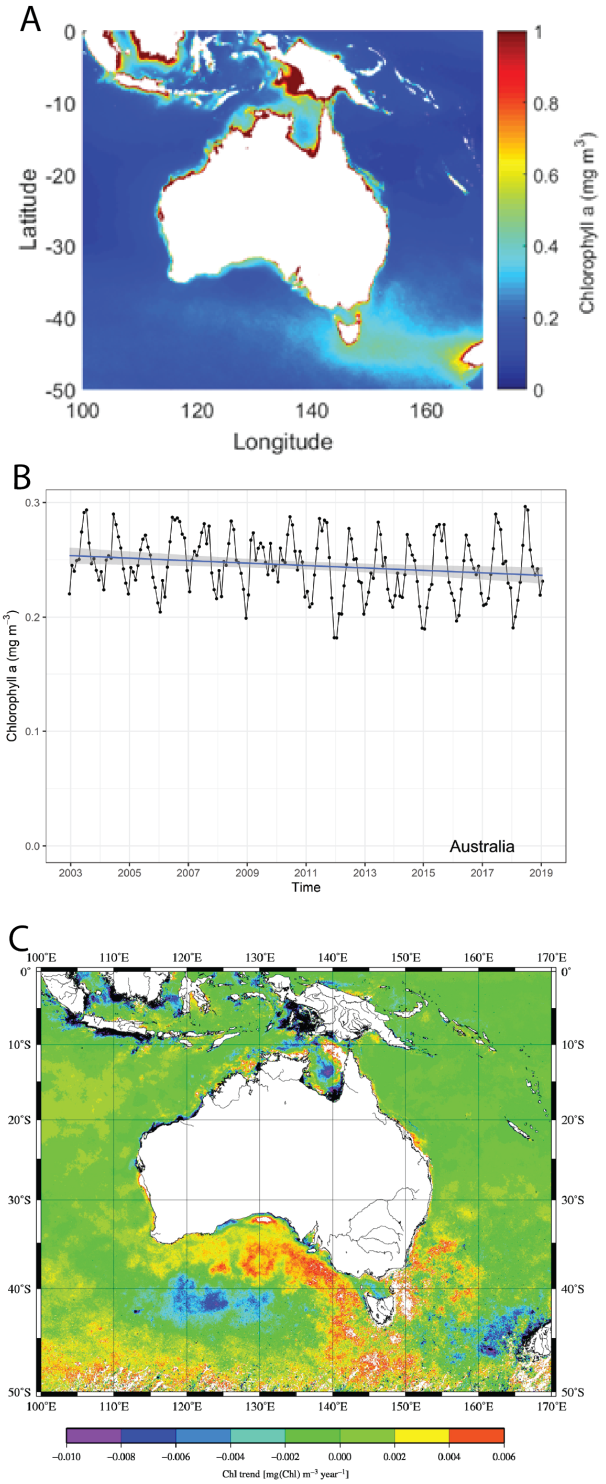

Figure 1. a) The mean Chlorophyll a (mg. m^{-3}) across the Australian region (50°S to equator, 100°E to 170°E) from 2003 to 2019. b) mean monthly Chlorophyll a (mg. m^{-3}) with a linear regression fitted showing trend at the same spatial scale. c) Trends in Chlorophyll a (mg. m^{-3} y^{-1}) for each 4 km^2 across the entire Australian region (50°S to equator, 100°E to 170°E) from 2003 to 2019.

doi: 10.26198/5e16a44a49e79

Results and Interpretation

Chlorophyll a within the Australian region

The mean chlorophyll ***a*** concentration in surface waters across the Australian region between the beginning of 2003 and the end of 2018 was 0.25 mg. m^{-3} (**Figure 1a**). This is a low concentration typical of healthy tropical and subtropical oceanic waters. Areas of markedly higher chlorophyll ***a*** include the coastal zone around Australia, seas between Australia and its northern neighbours, and waters between Tasmania and New Zealand.

The mean monthly chlorophyll ***a*** concentration varied seasonally and inter-annually (**Figure 1b**). There was, however, a significant (P<0.006) negative trend across the entire region over the period from 2003-2019 (**Figure 1b**), with the Chlorophyll ***a*** concentration declining ~8%. By contrast, there were large parts of the ocean south and southeast of Australia, and in the coastal zone along the eastern seaboard plus smaller patches throughout the shallow seas north of Australia there were significant gains in Chlorophyll ***a***. (**Figure 1c**). Within the region the most significant (**Figure S1**) downward trends in Chlorophyll ***a*** were found between 120 and 130°E near 40°S, near the centre of the Gulf of Carpentaria and nearshore in two regions; parts of the North West Shelf and throughout much of the Great Australian Bight.

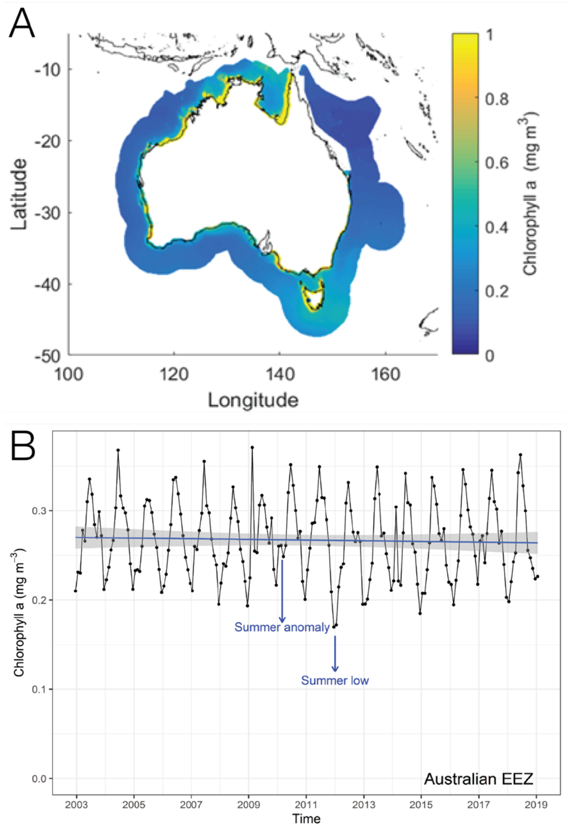

Figure 2. a) The mean Chlorophyll a (mg. m^{-3}) within the Australian Economic Exclusion Zone (EEZ) from 2003-2019 (the EEZ extends 200 nautical miles from the territorial sea baseline). b) mean monthly EEZ chlorophyll a fitted with a linear regression showing the long-term trend. Some anomalous summer months are circled. They demonstrate the interannual variability associated with climate cycles such as ENSO.

Chlorophyll a within the Australian EEZ

Within Australia's continental EEZ the mean chlorophyll ***a*** concentration was 0.26 mg m^{-3} (**Figure 2a**). Chlorophyll ***a*** tended to be low in the tropical and subtropical oceanic regions; greater in the coastal zone, the shallow seas between Australia and its northern neighbours and around Tasmania.

As with the broader regional trend the overall EEZ has declined significantly in chlorophyll ***a*** (P<0.006) over the period from 2003 to 2019. The rate of decline was similar at ~8% over 16 years. The inter-annual variation shows the summer of 2011-12 was much lower in chlorophyll ***a*** than the summer of 2009-10 (see grey circles **Figure 2b**).

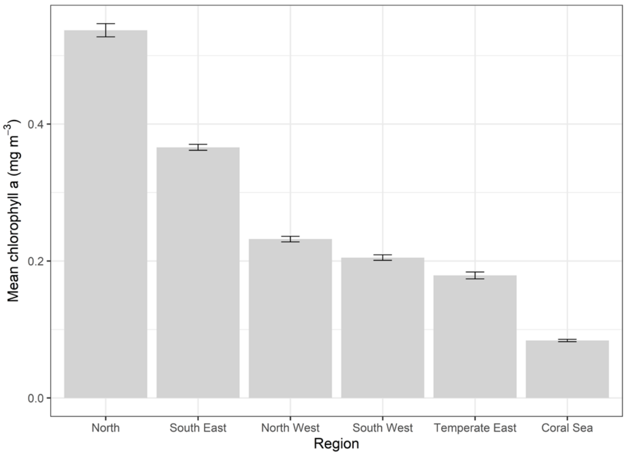

Figure 3. The mean Chlorophyll a (mg m^{-3}) within each bioregion, from 2003 to 2019.

Chlorophyll a within the Australian bioregions

Australia has six marine bioregions around the continent plus several around islands such as Christmas, Cocos, Lord Howe, Macquarie and another along the Antarctic coast. In this report we assess the six bioregions around the continent (**Figure 3a**). They showed distinct differences in the mean state and trends for chlorophyll ***a***, net primary production and turbidity.

Table 1. Mean Chlorophyll a (mg m^{-3}) within each of Australia's six bioregions from 2003 -2019.

Bioregion	Mean (mg m^{-3})	Standard Deviation	Standard error of the mean
Southeast	0.366	0.0596	0.00428
Coral Sea	0.0839	0.0232	0.00167
North west	0.232	0.0565	0.00406
Temperate east	0.179	0.0699	0.00502
North	0.537	0.134	0.00962
South west	0.205	0.0562	0.00404

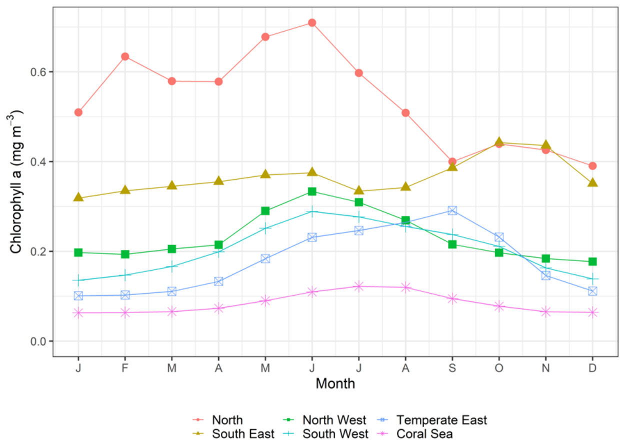

Figure 4. Monthly mean concentrations of Chlorophyll a (mg. m^{-3}) within each of Australia's six bioregions from 2003 -2019.

All of the six bioregions have distinctly different ($p<0.05$) mean chlorophyll ***a*** concentrations (**Figure 3b**). The North bioregion has more than 6 times the mean chlorophyll ***a*** of the nearby Coral Sea (**Table 1**). The second greatest mean chlorophyll ***a*** is found in the southeast, in waters around Tasmania. All bioregions showed some seasonal variability in chlorophyll ***a*** concentration, with the largest variability seen in the North bioregion where chlorophyll ***a*** peaked at 0.7 mg m^{-3} in July (**Figure 4**). The Coral Sea and both west coast bioregions (NW and SW) tended to reach peak chlorophyll ***a*** concentrations during winter. Both the Temperate East and the Southeast bioregions experienced spring blooms of phytoplankton. The Temperate East phytoplankton bloom reached peak biomass in September and the Southeast spring bloom peaked in October.

State and trends in chlorophyll ***a*** were assessed for each of the six bioregions (**Figure 5**). Mean values for each bioregion are all different (**Table 1**) and so are the trends (**Table 2**). There were no statistically significant positive trends in any bioregion. The Coral Sea, Temperate East and Northwest Bioregions all showed significant declines from 2002-2019.

Table 2. Assessment of linear trends for seasonally corrected (the average monthly mean is subtracted from each monthly value) chlorophyll a concentrations in 6 Australian bioregions over the period 2003 to 2019.

Bioregion	Annual change (mg m^{-3} y^{-1})	error	Student's t	P
Temperate East	-0.0008	0.000275	-2.898	0.004
NW	-0.00103	0.000356	-2.906	0.004
North	-0.00106	0.001296	-0.816	0.415
SW	+0.000166	0.000268	0.620	0.536
Coral Sea	-0.00055	0.000120	-4.563	<0.001

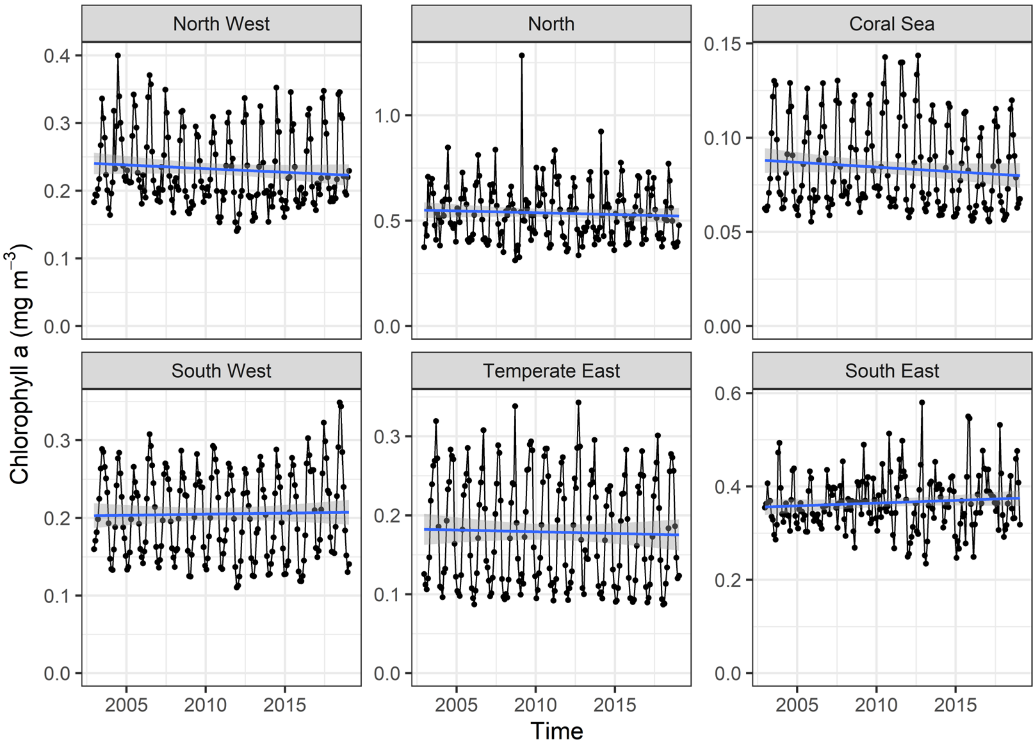

Figure 5. Mean monthly chlorophyll a concentrations (mg. m^{-3}) for the six Australian bioregions from 2003 to 2019 including a linear regression showing the trend for each bioregion.

doi: 10.26198/5e16a44a49e79

Implications for people and ecosystems

The phytoplankton biomass around Australia is relativley low; a situation typical of most tropical and subtropical waters. Unlike most continents, Australia does not have large-scale upwelling along its west coast as it is supressed by the southward-flowing Leeuwin Current.

The North, Northwest, Southwest and Coral Sea all experienced greatest phytoplankton biomass in winter. By contrast, the Temperate East and Southeast regions show classic spring blooms during September or October. These periods of high phytoplankton biomass provide periods of peak food availability for zooplankton and are often the most important period for larval fish recruitment. The capacity for our marine ecosystems to sustain our existing biodiversity is dependent upon both the amount of phytoplankton present and the timing of the greatest biomass.

Although the spatial patterns of change in Chlorophyll ***a*** are patchy from 2002-2019, the rate of change averaged over the region, the continental EEZ, and within 3 of the 6 bioregions was significantly negative. If the overall rate of decline is sustained at 0.5% per year, it will eventually cause a dramatic impact on the region's marine ecology and is very likely to cause a reduction in many regional fish stocks. Declines in Chlorophyll ***a*** close to shore along the North West Shelf and throughout much of the Great Australian Bight are of considerable concern given the potential impacts on our coastal ecosystems. A longer time series and more in-situ monitoring should reveal whether this decline is caused by a climate cycle or is likely to persist if the planet continues to warm.

Acknowledgements

Data was sourced from Australia's Integrated Marine Observing System (IMOS) which is enabled by the National Collaborative Research Infrastructure Strategy (NCRIS).

Data Sources

IMOS Satellite Remote Sensing.
http://imos.org.au/facilities/srs/

References

Dierssen, H. M. (2010). Perspectives on empirical approaches for ocean color remote sensing of chlorophyll in a changing climate. *Proceedings of the National Academy of Sciences of the United States of America, 107*(40), 17073-17078. doi:10.1073/pnas.0913800107

Hu, C., Lee, Z., & Franz, B. (2012). Chlorophyll a algorithms for oligotrophic oceans: A novel approach based on three-band reflectance difference *Journal of Geophysical Research, Oceans, 117*, C01011. doi:10.1029/2011jc007395

Sournia, A. (1978). ***Phytoplankton manual***. Retrieved from Paris: United Nations Educational, Scientific and Cultural Organization.

Supplemental figure

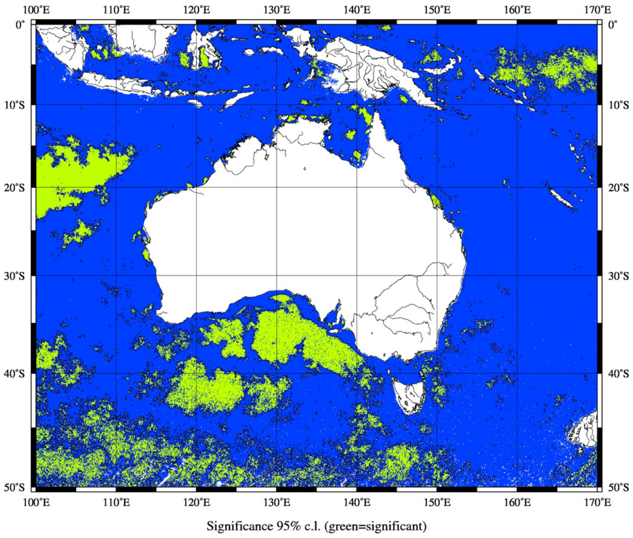

Figure S1. The statistical significance of the trends shown in Figure 1c (Student test, 95% confidence level).


IMOS
Integrated Marine
Observing System

IMOS
Integrated Marine
Observing System

State and Trends of
Australia's Oceans
Report

2.2 Spatial and seasonal trends in net primary production

Peter Thompson[1] and Karlie McDonald[1]

[1] CSIRO Oceans and Atmosphere, Hobart, TAS, Australia

Summary

Net primary productivity varies greatly around Australia, with highest rates in coastal zones and in seas between Australia and its northern neighbours. Although there is a strong seasonal trend, increasing during spring-summer and decreasing in autumn-winter, average net primary productivity has declined in Australian waters by 12 % in the past 17 years (2002-2019). Given that primary production sets the carrying capacity of higher trophic levels (zooplankton, fish, birds and mammals), this decrease is likely to cause a reduction in the size of Australia's fisheries.

Key Data Streams

Satellite Remote
Sensing

State and Trends of Australia's Ocean Report
www.imosoceanreport.org.au

Time-Series published
10 January 2020

doi: 10.26198/5e16a4a749e7a

Rationale

Plants use sunlight to grow and this growth supports all animal life. The growth is often measured as the conversion of carbon dioxide (CO_2) into plant biomass (= primary production) per unit time. Total net primary production on Earth exceeds 100 billion tons of carbon per year and plays a profound role in the global carbon cycle. Phytoplankton in the oceans provide almost half of this productivity. Satellites have made it possible to have much more precise estimates of global primary production because of their ability to observe the entire planet every few days. The productivity of phytoplankton in our ocean pastures regulates the abundance of fish.

Methods

Although there are direct measurements of primary production from Australian waters (Everett & Doblin, 2015; Furnas & Carpenter, 2014; Jitts, 1967; Lourey et al., 2013; McLaughlin et al., 2019; Waite et al., 2007), they do not provide comprehensive spatial resolution or interannual resolution. Therefore, we are reliant on data from satellites. Converting satellite estimates of phytoplankton biomass derived from ocean colour to chlorophyll ***a*** and into primary production uses conceptual and mathematical models that originated in the 1950s (Ryther, 1956; Ryther & Yentsch, 1957; Talling, 1957). A more recent model uses satellite-based estimates of phytoplankton carbon concentration (Behrenfeld et al., 2005) derived from light scattering properties (Behrenfeld & Boss, 2003, 2006; Durand & Olson, 1996; Green & Sosik, 2004; Green et al., 2003; Loisel et al., 2001; Stramski et al., 1999) and improved information on particulate backscattering coefficients, phytoplankton pigment absorption, and coloured dissolved organic carbon absorption (Garver & Siegel, 1997; Maritorena et al., 2002; Siegel et al., 2002). We use this carbon-based approach here. Data and further description of the methods can be found at http://www.science.oregonstate.edu/ocean.productivity/.

Results and interpretation

The mean net primary production across the Australian region between 2002 and 2019 was 551 mgC m^{-2} d^{-1}. This is a relatively low productivity, typical of healthy tropical and subtropical oceanic waters. Areas of higher net primary production in the region include the coastal zone and seas between Australia and its northern neighbours (**Figure 1**).

Across the Australian region, the net primary production (NPP) varied seasonally and inter-annually (**Figure 2**). NPP was elevated during the summer of 2009-10 and reduced in the summer of 2011-12 (**Figure 2**). There was, however, a significant ($p<0.001$) negative trend in NPP across this region. From 2002 to 2019, the mean annual NPP declined 12%.

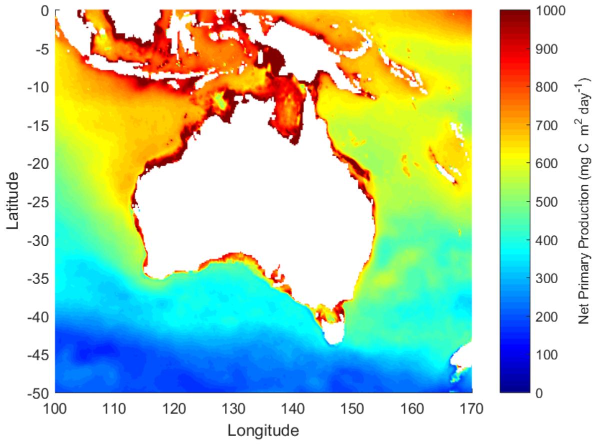

Figure 1. Estimated mean net primary production (mgC m^{-2} d^{-1}) for the Australian region (0-50°S and 100-170°E) from December 2002 to January 2019.

Within Australia's continental EEZ, the mean net primary production was 606 mgC m^{-2} d^{-1}. Net primary production was lower further south (**Figure 3**). Net primary production was greater in the coastal zone, the shallow seas between Australia and its northern neighbours, and through Bass Strait to Tasmania.

Similar to the broader regional trend, the net primary production in the Australian EEZ has declined significantly ($p<0.0009$) from 2002 to 2019 (**Figure 4**). The rate of decline was similar at 0.6% per year or ~10% over the elapsed period from 2002 to 2019. There was substantial inter-annual variation (Fig. 4). For example, summer 2009-10 was less productive than the summer of 2010-11 (**Figure 4**).

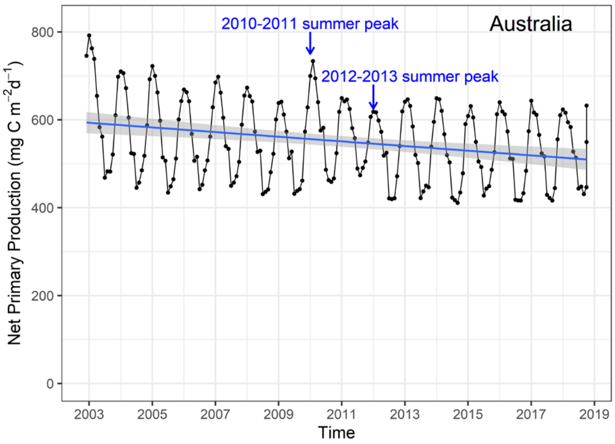

Figure 2. Estimated mean monthly net primary production (mgC m^{-2} d^{-1}) for the Australian region (0-50°S and 100-170°E) from December 2002 to January 2019. Strong seasonal, inter-annual and long-term variability are evident (grey ellipses show differences between peak primary production in 2010-11 and 2012-13), with the long-term trend estimated as significantly negative ($P<0.001$).

doi: 10.26198/5e16a4a749e7a

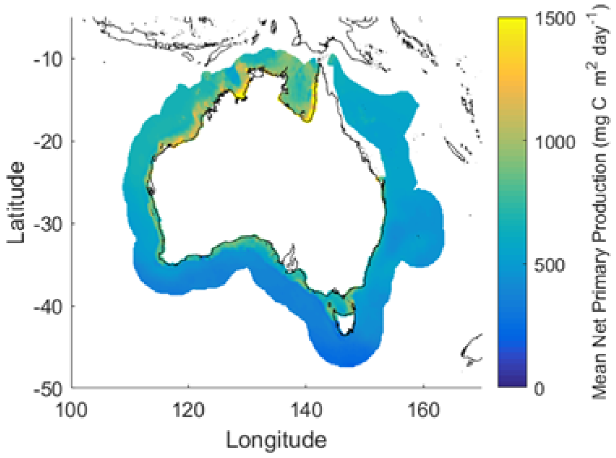

Figure 3. Estimated mean net primary production (mgC m^{-2} d^{-1}) for the Australian EEZ for December 2002 to January 2019.

All six bioregions around the coast of Australia were significantly different from each other in terms of their net primary production ($p<0.001$), except for the Temperate East, which was not different from the South East (**Figure 5**). The North bioregion had the greatest primary production followed by the North West and then the Coral Sea. The three bioregions further south, Temperate East, South West and South East had lower primary production. Across all bioregions, the range in estimated primary production was a factor of ~2 between the North and South East regions (**Table 1**).

All bioregions showed seasonal variability in net primary production, with largest seasonal changes in more southern bioregions (**Figure 6**). The South East bioregion had the largest seasonal variation, with a relatively high mean primary production of ~800 mgC m^{-2} d^{-1} during summer, declining to <200 mgC m^{-2} d^{-1} during winter for an annual range of 642 mgC m^{-2} d^{-1}. The smallest average annual range of only 87 mgC m^{-2} d^{-1} was in the North West bioregion, where there was a winter minimum followed by small spring and autumn increases in primary production.

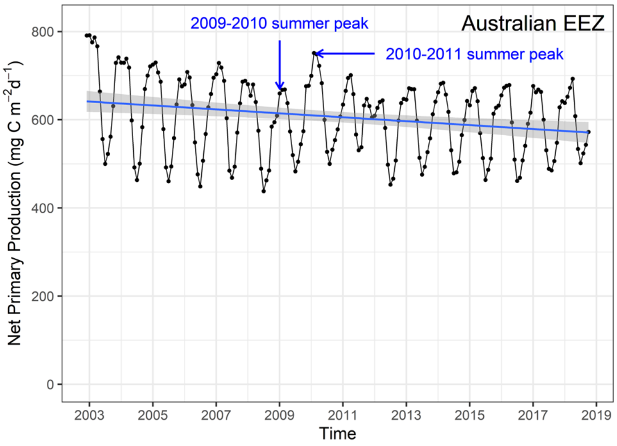

Figure 4. Estimated mean monthly net primary production (mgC m^{-2} d^{-1}) for the Australian EEZ for December 2002 to January 2019. Strong seasonal, inter-annual and long-term variability are evident (grey ellipses show differences between peak primary production in 2009-10 and 2010-11) with the long-term trend estimated as significantly negative ($P<0.0009$).

Table 1. Mean 2003-2018 daily net primary production in each bioregion (mgC m^{-2} d^{-1}), its overall decline, and the probability the rate of decline is zero (p). SD = Standard Deviation

Bioregion	Mean	SD	Standard error of the mean	% decline 2003 to 2018	p
North	888	43	11	-7.1%	0.074
Temperate East	510	28	7	-12.9%	0.001
North West	758	36	9	-10.2%	0.004
South West	491	25	6	-8.6%	0.032
South East	423	28	7	-7.6%	0.158

Trends in net primary production from 2002 to 2019 were negative in each of the six bioregions, although only statistically significant for four (the Coral Sea, Temperate East, South West, North West bioregions, **Table 1**). Rates of decline in net primary production ranged from 7-13% over 15 years across the 6 bioregions and averaged 9% overall or 0.6% per year across all bioregions. The rate of decline as a percent of total net primary production was greatest in the Temperate East and least in the North (**Table 1**).

Although there are few net primary production estimates in the Australian region, the North bioregion has been relatively well studied using conventional ^{14}C measurements for primary production (Furnas & Carpenter 2016). These data, collected between 1990 and 2013, had a mean of 1048 ± 109 mgC m^{-2} d^{-1} (mean ± 95% CI). Based on our results, the estimated mean for the entire region between 1990 and 2013 was 924 mgC m^{-2} d^{-1}, with monthly means that varied from 684 to 1165 mgC m^{-2} d^{-1}. Thus, estimates here from satellite and observed point estimates from ^{14}C measurements are in reasonable agreement, given differences in spatial-temporal sampling.

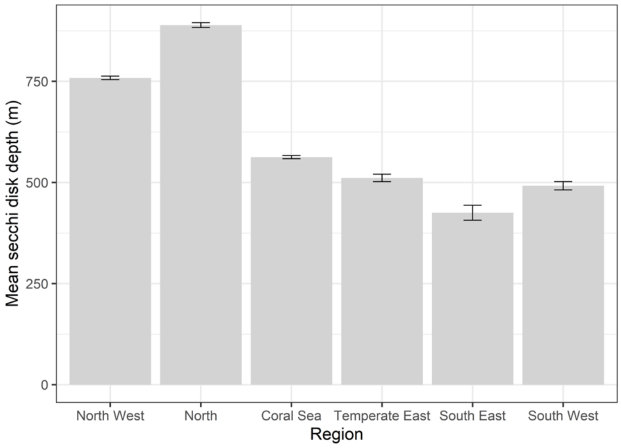

Figure 5. Estimated mean annual net primary production for the six bioregions around Australia (mean ± standard error).

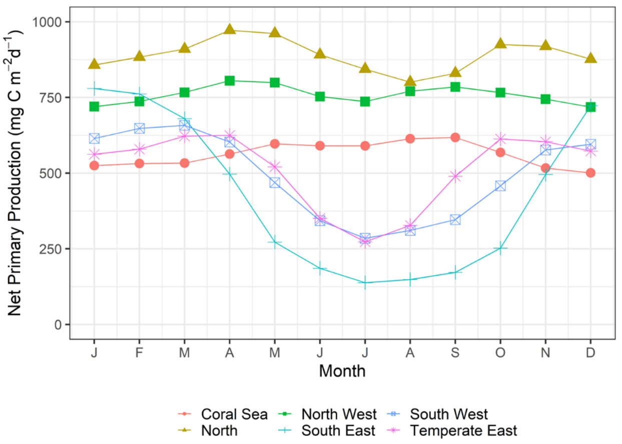

Figure 6. The average monthly net primary production for the six bioregions around Australia.

Implications for people and ecosystems

From 2002 to 2019, there was a significant decline in net primary production in the continental EEZ and four of the six bioregions. Both the carbon-based model and the ocean colour-based model of primary production are likely to indicate significant declines in primary production. These downwards trends in primary production are also similar to those observed elsewhere using other observational methods such as long-term measurements by Secchi Disk (e.g. Falkowski & Wilson, 1992). This decline in primary production is consistent with the observed declines in chlorophyll ***a*** (see State and Trends of Australia's Ocean Report 2.1: Spatial and seasonal trends in Chlorophyll a), phytoplankton abundance and phytoplankton biovolume (see State and Trends of Australia's Ocean Report 2.3: Contrasting trends of Australia's plankton communities).

The conventional understanding of primary production around Australia has changed dramatically in the last decade. Early estimates based on ocean colour from the coastal zone colour scanner, the SeaWiFs, and MODIS satellites e.g. (Behrenfeld & Falkowski, 1997) indicated that the greatest primary production was in the Tasman Sea (**Figure 7**). These early models have been widely used to estimate global primary production (e.g. (Field, Behrenfeld, Randerson, & Falkowski, 1998). Here net primary production was calculated based on the satellite-derived measures of phytoplankton carbon. This carbon-based approach is considered an improvement (Behrenfeld & Boss, 2003, 2006) . Using the new temperature-corrected and carbon-based model suggests northern Australian waters are more productive than previously thought (**Figure 7**). The new approach estimates the North bioregion has the greatest annual primary production at 324 gC m^{-2} y^{-1} and Southeast bioregion with the least at only 154 gC m^{-2} y^{-1} (Table 1).

All the Australian bioregions had estimated primary production values within ±100 gC m^{-2} d^{-1} of the global mean of measurements from 131 coastal or estuarine water bodies of 252 gC m^{-2} d^{-1} (Cloern et al., 2014). The relatively high measured values of primary production using ^{14}C from the North (e.g. Furnas & Carpenter, 2014) would suggest that newer carbon-based models (Behrenfeld & Boss, 2003, 2006) provide better estimates of primary production in our northern waters than models based on ocean colour. At this time there are no data to substantiate whether these new models are also better for the Tasman Sea.

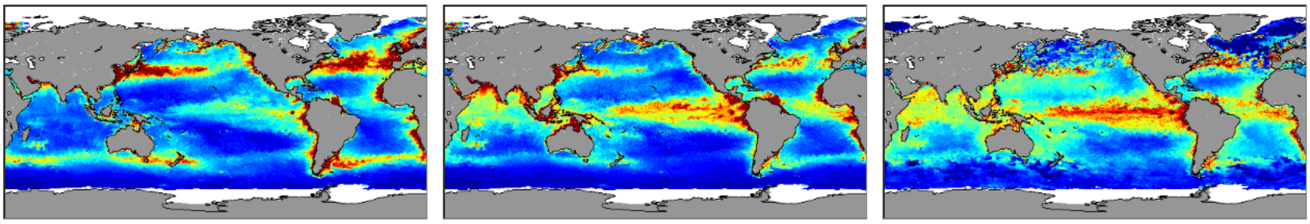

Figure 7. Modified from **http://www.science.oregonstate.edu/ocean.productivity/custom.php**. (accessed May 17 2019). All panels show estimated net primary production (NPP) with blue (= low) to red (= high) derived from MODIS satellite data. The Left panel shows conventional NPP, the centre panel shows temperature adjusted NPP, the right panel is NPP from a spectral and depth resolved carbon-based model.

Data Sources

Oregon State University

http://sites.science.oregonstate.edu/ocean.productivity/

References

Behrenfeld, M. J., & Boss, E. (2003). The beam attenuation to chlorophyll ratio: an optical index of phytoplankton physiology in the surface ocean? *Deep-Sea Research Part I-Oceanographic Research Papers, 50*(12), 1537-1549. doi:10.1016/j.dsr.2003.09.002

Behrenfeld, M. J., & Boss, E. (2006). Beam attenuation and chlorophyll concentration as alternative optical indices of phytoplankton biomass. *Journal of Marine Research, 64*(3), 431-451. doi:10.1357/002224006778189563

Behrenfeld, M. J., Boss, E., Siegel, D. A., & Shea, D. M. (2005). Carbon-based ocean productivity and phytoplankton physiology from space. *Global Biogeochemical Cycles, 19*.

Behrenfeld, M. J., & Falkowski, P. G. (1997). A consumer's guide to phytoplankton primary productivity models. *Limnology and Oceanography, 42*(7), 1479-1491. doi:10.4319/lo.1997.42.7.1479

Cloern, J. E., Foster, S. Q., & Kleckner, A. E. (2014). Phytoplankton primary production in the world's estuarine-coastal ecosystems. *Biogeosciences, 11*(9), 2477-2501. doi:10.5194/bg-11-2477-2014

Durand, M. D., & Olson, R. J. (1996). Contributions of phytoplankton light scattering and cell concentration changes to diel variations in beam attenuation in the equatorial Pacific from flow cytometric measurements of pico-, ultra- and nanoplankton. *Deep-Sea Research Part Ii-Topical Studies in Oceanography, 43*(4-6), 891-906. doi:10.1016/0967-0645(96)00020-3

Everett, J. D., & Doblin, M. A. (2015). Characterising primary productivity measurements across a dynamic western boundary current region. *Deep-Sea Research Part I-Oceanographic Research Papers, 100*, 105-116. doi:10.1016/j.dsr.2015.02.010

Falkowski, P. G., & Wilson, C. (1992). Phytoplankton productivity in the North Pacific ocean since 1900 and implications for absorption of anthropogenic CO2. *Nature, 358*(6389), 741-743. doi:10.1038/358741a0

Field, C. B., Behrenfeld, M. J., Randerson, J. T., & Falkowski, P. (1998). Primary production of the biosphere: Integrating terrestrial and oceanic components. *Science, 281*(5374), 237-240. doi:10.1126/science.281.5374.237

Furnas, M. J., & Carpenter, E. J. (2014). Primary production in the tropical continental shelf seas bordering northern Australia. *Continental Shelf Research, 129*, 33-48. doi:10.1016/j.csr.2016.06.006

Garver, S. A., & Siegel, D. A. (1997). Inherent optical property inversion of ocean color spectra and its biogeochemical interpretation .1. Time series from the Sargasso Sea. *Journal of Geophysical Research-Oceans, 102*(C8), 18607-18625. doi:10.1029/96jc03243

Green, R. E., & Sosik, H. M. (2004). Analysis of apparent optical properties and ocean color models using measurements of seawater constituents in New England continental shelf surface waters. *Journal of Geophysical Research-Oceans, 109*(C3), 17. doi:10.1029/2003jc001977

Green, R. E., Sosik, H. M., & Olson, R. J. (2003). Contributions of phytoplankton and other particles to inherent optical properties in New England continental shelf waters. *Limnology and Oceanography, 48*(6), 2377-2391. doi:10.4319/lo.2003.48.6.2377

Jitts, H. R. (1967). Seasonal variations in the Indian Ocean along 110°E IV. Primary Production. *Australian Journal Marine and Freshwater Research, 20*, 65-75.

Loisel, H., Bosc, E., Stramski, D., Oubelkheir, K., & Deschamps, P. Y. (2001). Seasonal variability of the backscattering coefficient in the Mediterranean Sea based on Satellite SeaWiFS imagery. *Geophysical Research Letters, 28*(22), 4203-4206. doi:10.1029/2001gl013863

Lourey, M. J., Thompson, P. A., McLaughlin, M. J., Bonham, P., & Feng, M. (2013). Primary production and phytoplankton community structure during a winter shelf-scale phytoplankton bloom off Western Australia. *Marine Biology, 160*(2), 355-369. doi:10.1007/s00227-012-2093-4

Maritorena, S., Siegel, D. A., & Peterson, A. R. (2002). Optimization of a semianalytical ocean color model for global-scale applications. *Applied Optics, 41*(15), 2705-2714. doi:10.1364/ao.41.002705

McLaughlin, M. J., Lourey, M. J., Hanson, C. E., Cherukuru, N., Thompson, P. A., & Pattiaratchi, C. B. (2019). Biophysical oceanography of tidally-extreme waters of the southern Kimberley coast, Western Australia. *Continental Shelf Research, 173*, 1-12. doi:10.1016/j.csr.2018.12.002

Ryther, J. H. (1956). Photosynthesis in the ocean as a function of light intensity *Limnology and Oceanography, 1*(1), 61-70. doi:10.4319/lo.1956.1.1.0061

Ryther, J. H., & Yentsch, C. S. (1957). Optimization of a semianalytical ocean color model for global-scale applications. *Limnology Oceanography, 2*, 281-286.

Siegel, D. A., Maritorena, S., Nelson, N. B., Hansell, D. A., & Lorenzi-Kayser, M. (2002). Global distribution and dynamics of colored dissolved and detrital organic materials. *Journal of Geophysical Research-Oceans, 107*(C12), 14. doi:10.1029/2001jc000965

Stramski, D., Reynolds, R. A., Kahru, M., & Mitchell, B. G. (1999). Estimation of particulate organic carbon in the ocean from satellite remote sensing. *Science, 285*(5425), 239-242. doi:10.1126/science.285.5425.239

Talling, J. F. (1957). The phytoplankton population as a compound photosynthetic system. . *New Phytologist, 56*, 133-149.

Waite, A. M., Pesant, S., Griffin, D. A., Thompson, P. A., & Holl, C. M. (2007). Oceanography, primary production and dissolved inorganic nitrogen uptake in two Leeuwin Current eddies. *Deep-Sea Research Part Ii-Topical Studies in Oceanography, 54*(8-10), 981-1002. doi:10.1016/j.dsr2.2007.03.001

IMOS

Integrated **Marine**
Observing System

State and Trends of Australia's Oceans | Report

2.3 Contrasting trends of Australia's plankton communities

Jason D. Everett[1,2,4], Anthony J. Richardson[1,2],
Claire Davies[3] and Ruth Eriksen[3]

[1] CSIRO Oceans and Atmosphere, Queensland Biosciences Precinct (QBP), St Lucia, QLD, Australia

[2] Centre for Applications in Natural Resource Mathematics (CARM), School of Mathematics and Physics, The University of Queensland, St Lucia, QLD, Australia

[3] CSIRO Oceans and Atmosphere, Hobart, TAS, Australia

[4] School of Biological, Earth and Environmental Sciences, University of New South Wales, Sydney, NSW, Australia

Summary

We show that around Australia, phytoplankton are, on average, decreasing in their abundance, a trend consistent with other observations including both chlorophyll a and primary production. Despite this trend in phytoplankton, zooplankton have generally been increasing in their abundance and biomass, with implications for the fish communities they can potentially support.

Key Data Streams

National Reference
Stations

State and Trends of Australia's Ocean Report
www.imosoceanreport.org.au

Time-Series published
10 January 2020

doi: 10.26198/5e16a4e849e7b

Rationale

The magnitude and distribution of fish caught in the ocean depends on the biomass of phytoplankton (microscopic photosynthetic "plants") and zooplankton (animal drifters) at the base of the food web (Chassot et al., 2010; Irigoien et al., 2014). Changes in phytoplankton biomass will constrain future fish biomass (Lam, Cheung, Reygondeau, & Sumaila, 2016). Under climate change, global models show an overall decline in global phytoplankton biomass (C. A. Stock, Dunne, & John, 2014; Woodworth-Jefcoats, Polovina, & Drazen, 2017), but with increases in some regions and declines in others. However, the idea that reduced phytoplankton biomass directly translates to reduced fish biomass ignores the complex phytoplankton-zooplankton role. As the intermediate trophic link in the ocean, zooplankton graze on phytoplankton, heterotrophic microbes, and each other, and are eaten by fish, seabirds and marine mammals. They are thus pivotal in the transfer of energy to higher trophic levels.

Methods

Here we present 10 years (2009-2019) of phytoplankton and zooplankton abundance and biomass data from the seven Integrated Marine Observing System (IMOS) National Reference Stations (NRS) to investigate long-term changes in the two lowest trophic levels in the ocean. We use multiple lines of evidence to investigate changes in phytoplankton. We use two measures to represent change in the phytoplankton: changes in biovolume of phytoplankton and changes in abundance. These measures are based on phytoplankton samples collected by Niskin bottles at several depths, mixed into a single sample, and counted in the laboratory (Eriksen et al., 2019). We also use two measures to represent change in the zooplankton: changes in biomass and changes in the abundance. These measures are based on zooplankton samples collected with a 100 µm mesh drop net and counted (for abundance) or dried and weighed (biomass) in the laboratory.

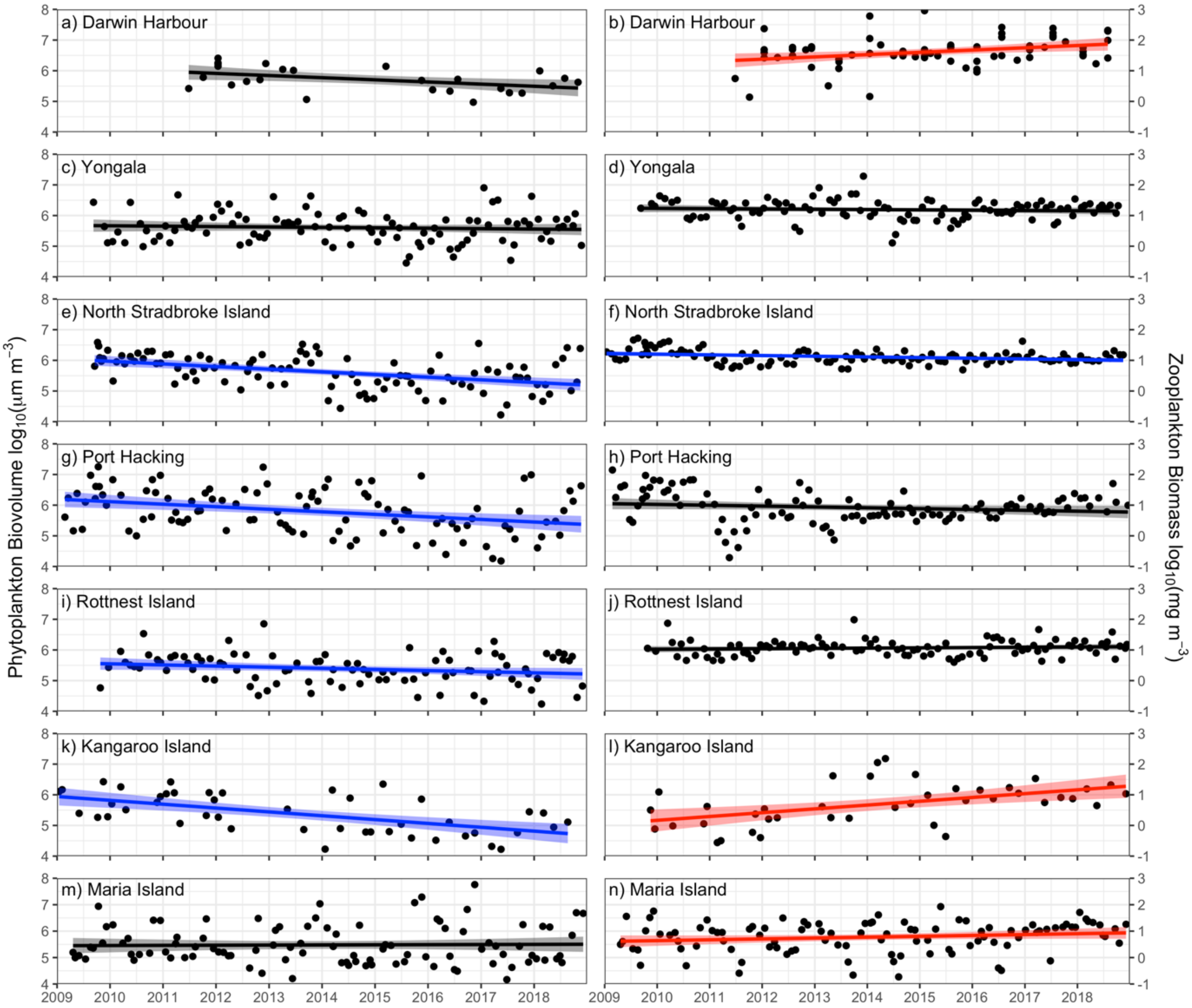

Figure 1. Phytoplankton biovolume ($\log_{10}$ µm^3 m^{-3}; left column) and Zooplankton Biomass ($\log_{10}$ mg m^{-3}; right column). Data are plotted with blue (decreasing) and red (increasing) trendlines indicating a significant change. Black trendlines indicate no statistically significant change.

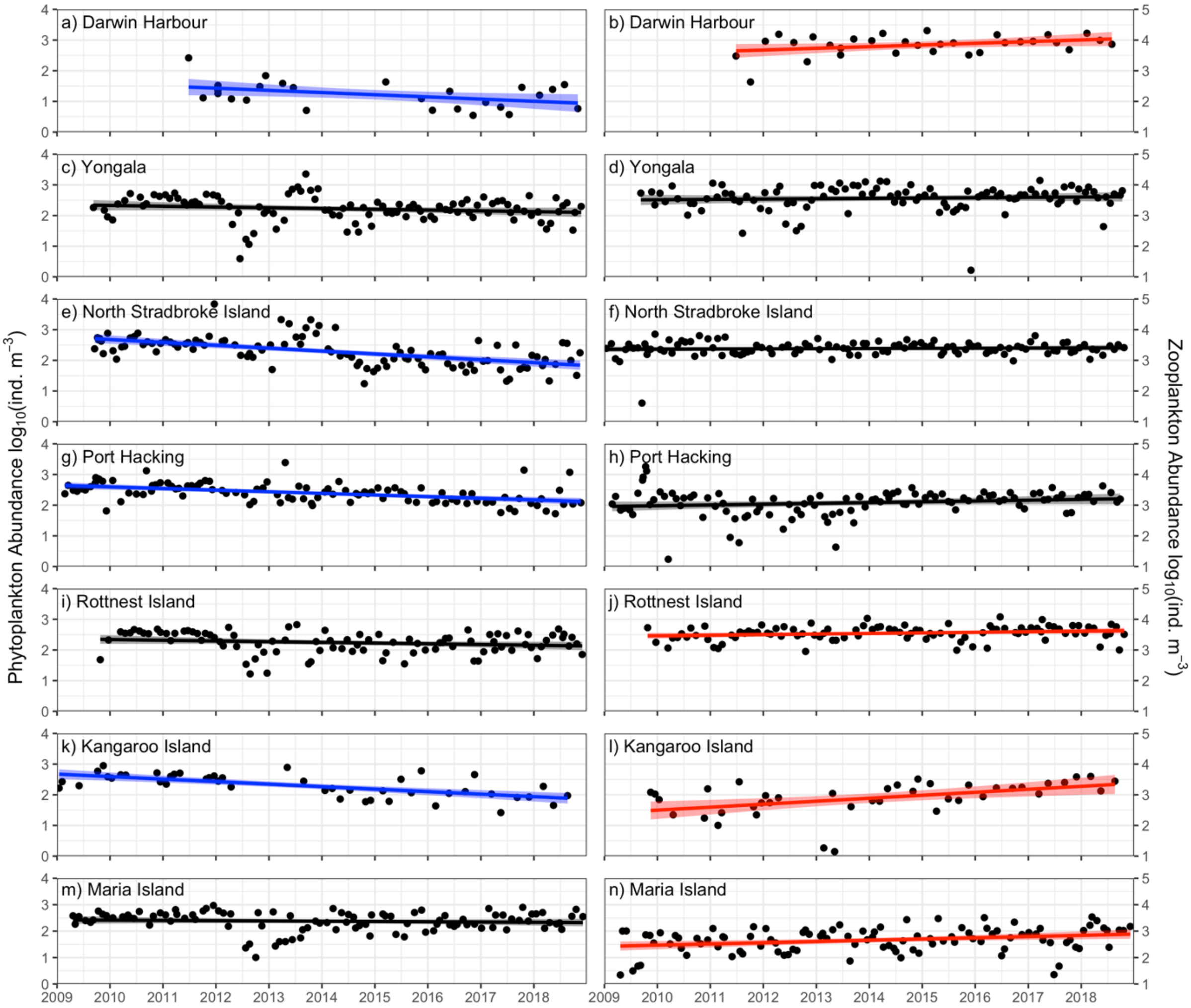

Figure 2. Phytoplankton (left column) and zooplankton (right column) abundance ($\log_{10}$ counts m^{-3}) at each NRS. Data are plotted with blue (decreasing) and red (increasing) trendlines indicating a significant change. Black trendlines indicate no statistically significant change.

Data were analysed using a linear model with the response variable being either Abundance or Biomass/Biovolume, and predictors being Date (continuous) and Month (a fixed factor). Including Month in the model adjusts for the temporal autocorrelation. Based on visual inspection of the diagnostic plots, a $\log_{10}$ transformation of the response improved the normality and homogeneity of variance assumptions.

All data were sourced from the IMOS Australian Ocean Data Network (AODN) (https://portal.aodn.org.au/; see the datasets IMOS National Reference Station (NRS) - Phytoplankton Abundance and Biovolume", "IMOS National Reference Station (NRS) - Zooplankton Abundance", "IMOS National Reference and "IMOS National Reference Station (NRS) - Zooplankton Biomass")

Results and Interpretation

Both phytoplankton biovolume (**Figure 1**, **column 1**) and abundance (**Figure 2**, **column 1**) are declining significantly at North Stradbroke Island, Port Hacking and Kangaroo Island NRS. Phytoplankton biovolume is also declining at Rottnest Island, and abundance is declining at Darwin. Kangaroo Island had the largest relative decline in biovolume (-96% decade^{-1}, -579,271 µm^{3} m^{-3} decade^{-1}) and a 76% decade^{-1} decline in abundance (-267 cells m^{-3} decade^{-1}). North Stradbroke Island had a 93% decade^{-1} decline in abundance (-389 cells m^{-3} decade^{-1}) and Port Hacking had a significant decline in both abundance (54% decade^{-1}, -209 cells m^{-3} decade^{-1}) and biovolume (-80% decade^{-1}, -717,364 µm^{3} m^{-3} decade^{-1})

By contrast, zooplankton abundance (**Figure 1**, **column 2**) and biomass (**Figure 2**, **column 2**) are increasing at Darwin (174 mg m^{-3} decade^{-1}; 9372 individuals m^{-3} decade^{-1}), Kangaroo Island (25 mg m^{-3} decade^{-1}; 2630 individuals m^{-3} decade^{-1}) and Maria Island (19 mg m^{-3} decade^{-1}; 359 individuals m^{-3} decade^{-1}). Zooplankton abundance, but not biomass, is increasing at Rottnest Island (1277 individuals m^{-3} decade^{-1}). The biomass of zooplankton is declining at North Stradbroke Island (-5 mg m^{-3} decade^{-1}), making it the only station that shows a consistent pattern (decline or increase) between phytoplankton and zooplankton, and the only station that has a declining zooplankton biomass (albeit only a small decline).

Implications for people and ecosystems

Around Australia, we found that phytoplankton are generally decreasing in abundance. This is consistent with observed declines in chlorophyll-a (see State and Trends of Australia's Ocean Report 2.1: Spatial and seasonal trends in Chlorophyll a and primary production).

Somewhat surprisingly, therefore, we found that zooplankton are not decreasing in response to the phytoplankton decline, but are generally increasing. Over large time and space scales, zooplankton abundance and biomass typically follow changes in phytoplankton, their primary food source (Richardson & Schoeman, 2004). Recent work has shown that differences in fish catch across the ocean far exceed differences in phytoplankton production, indicating that zooplankton is playing a major role (Stock et al., 2017). The increase in zooplankton despite the decline in phytoplankton could be because of increases in microzooplankton (not measured in this analysis), which are grazed upon by larger omnivorous zooplankton. An alternative theory is that there is a relaxation of top-down control of zooplankton. For instance, fewer planktivorous fish (small fish species that eat zooplankton such as mado, yakka and anchovy) could reduce the predation pressure on zooplankton and lead to them increasing in abundance. Despite being more common on coastal reefs (Bellwood et al., 2018), we know little about planktivorous fish in most coastal regions of Australia.

An outstanding question is whether these substantial changes in lower trophic levels are impacting coastal fish communities. Typically, higher zooplankton biomass supports higher fish biomass (Chassot et al., 2010; Ware & Thomson, 2005). Whether these trends in phytoplankton and zooplankton continue is an outstanding question, and one that IMOS is well placed to answer in the future.

Acknowledgements

Data was sourced from Australia's Integrated Marine Observing System (IMOS) which is enabled by the National Collaborative Research Infrastructure Strategy (NCRIS).

Data Sources

IMOS National Reference Stations.
http://imos.org.au/facilities/nationalmooringnetwork/nrs/

References

Bellwood, D. R., Streit, R. P., Brandl, S. J., & Tebbett, S. B. (2018). The meaning of the term 'function' in ecology: A coral reef perspective. *Functional Ecology, 0*(0). doi:10.1111/1365-2435.13265

Chassot, E., Bonhommeau, S., Dulvy, N. K., Mélin, F., Watson, R., Gascuel, D., & Le Pape, O. (2010). Global marine primary production constrains fisheries catches. *Ecology Letters, 13*(4), 495-505. doi:10.1111/j.1461-0248.2010.01443.x

Eriksen, R. S., Davies, C. H., Bonham, P., Coman, F. E., Edgar, S., McEnnulty, F., . . . Richardson, A. J. (2019). Australia's long-term plankton observations: the Integrated Marine Observing System National Reference Station network. *Frontiers in Marine Science*.

FAO. (2016). *The State of World Fisheries and Aquaculture 2016. Contributing to food security and nutrition for all.* Retrieved from Rome:

Irigoien, X., Klevjer, T. A., Røstad, A., Martinez, U., Boyra, G., Acuña, J. L., . . . Kaartvedt, S. (2014). Large mesopelagic fishes biomass and trophic efficiency in the open ocean. *Nature Communications, 5*, 3271. doi:10.1038/ncomms4271

Lam, V. W. Y., Cheung, W. W. L., Reygondeau, G., & Sumaila, U. R. (2016). Projected change in global fisheries revenues under climate change. *Scientific Reports, 6*, 32607. doi:10.1038/srep32607

Richardson, A. J., & Schoeman, D. S. (2004). Climate impact on plankton ecosystems in the northeast Atlantic. *Science, 305*(5690), 1609-1612. doi:10.1126/science.1100958

Stock, C. A., Dunne, J. P., & John, J. G. (2014). Drivers of trophic amplification of ocean productivity trends in a changing climate. *Biogeosciences, 11*(24), 7125-7135. doi:10.5194/bg-11-7125-2014

Stock, C. A., John, J. G., Rykaczewski, R. R., Asch, R. G., Cheung, W. W. L., Dunne, J. P., . . . Watson, R. A. (2017). Reconciling fisheries catch and ocean productivity. *Proceedings of the National Academy of Sciences, 114*(8), E1441-E1449. doi:10.1073/pnas.1610238114

Ware, D. M., & Thomson, R. E. (2005). Bottom-Up Ecosystem Trophic Dynamics Determine Fish Production in the Northeast Pacific. *Science, 308*(5726), 1280. doi:10.1126/science.1109049

Woodworth-Jefcoats, P. A., Polovina, J. J., & Drazen, J. C. (2017). Climate change is projected to reduce carrying capacity and redistribute species richness in North Pacific pelagic marine ecosystems. *Global Change Biology, 23*(3), 1000-1008. doi:10.1111/gcb.13471

IMOS
Integrated Marine Observing System

State and Trends of
Australia's Oceans | Report

2.4 The seasons of phytoplankton around Australia

David Antoine[1], Nicolas Mayot[2] and Edward King[3]

[1] Remote Sensing & Satellite Research Group, School of Earth and Planetary Sciences, Curtin University, Perth, WA, Australia
[2] School of Environmental Sciences, University of East Anglia, Norwich, United Kingdom
[3] CSIRO Oceans and Atmosphere, Hobart, TAS, Australia

Summary

An analysis using satellite observations shows how phytoplankton amounts evolve along seasons around Australia, revealing broad areas of distinct seasonal patterns. These different phenology traits determine the functioning of the entire ecosystem, inasmuch as phytoplankton is the base of the entire oceanic foodweb.

Key Data Streams

Satellite Remote
Sensing

State and Trends of Australia's Ocean Report
www.imosoceanreport.org.au

Time-Series published
10 January 2020

doi: 10.26198/5e16a91249e7c

Rationale

The study of naturally recurring events is known as “phenology” and has been largely developed and used in terrestrial ecosystem studies. Such events can be, for instance, the onset and duration of the spring growing season. Similar studies are now carried out for ocean ecosystems, with a particular emphasis on phytoplankton, which is the base of the marine foodweb and an important component of the marine carbon cycle. Here we characterise regional patterns of phytoplankton seasonal cycles, which is crucial to understanding relationships between climate (environment) forcing and marine ecosystems.

Methods

Our analysis used sixteen years (2003-2018) of satellite ocean colour observations from the NASA Aqua-MODIS sensor. Individual satellite images were processed using the SeaDAS software and applying the OCI chlorophyll algorithm (Hu, Lee, & Franz, 2012). Images were combined spatially and temporally into 4-km monthly composite maps of the chlorophyll concentration, further aggregated into twelve climatological monthly composite maps. A k-means based cluster analysis (D'Ortenzio & Ribera d'Alcalà, 2009) was then applied at each of the 4-km grid cell of these monthly climatological chlorophyll maps, after the data in each of these cells were normalised by their maximum. This technique groups pixels with similar seasonal cycles, without being overly influenced by the dominant signal from changes of the chlorophyll concentration. The optimal number of clusters was determined through a “silhouette” analysis (Rousseeuw, 1987). The mean within each cluster is then computed and provides the typical seasonal cycle representative of the group. Resulting mapping reveals broad ocean areas – referred to here as bioregions – where seasonal changes in phytoplankton are similar. These bioregions are likely to have similar underlying physical mechanisms and ecosystem responses. Depths shallower than 100 m have been excluded from the analysis.

Results and interpretation

The cluster analysis suggested six bioregions (**Figure 1**), with each having a distinctive seasonal cycle (**Figure 2**). Overall, the bioregions follow latitudinal bands, except in the Leeuwin Current and in the northeast Indian Ocean. Mid-latitude areas show a single seasonal maximum in July or August (bioregions #3 and #4). When moving further south, two maxima appear, in June and September for region #2, and June and November for region #5, which essentially matches the subtropical convergence. Interestingly the same seasonal pattern (#5) also appears further south in the western part of the study region, and corresponds to the Antarctic convergence.

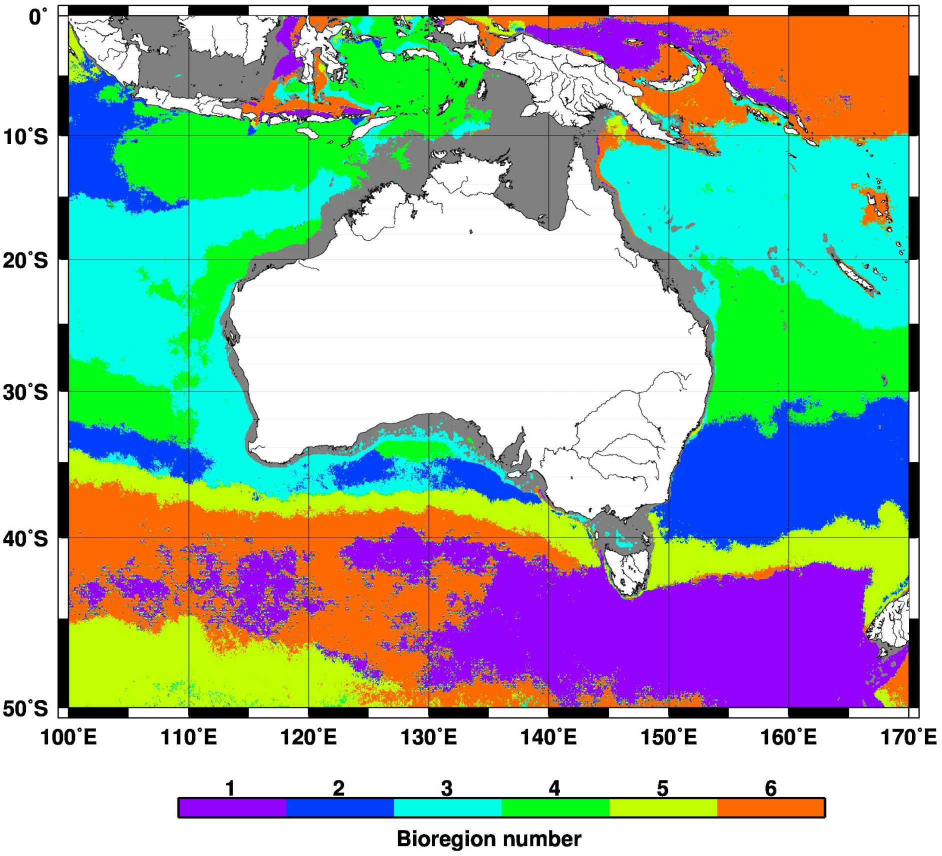

Figure 1. The 6 “bioregions” determined from the phenology of phytoplankton. The average normalised seasonal cycles are shown in Figure 2 (same colour coding). Shallow waters (depth <100m) where the satellite chlorophyll is less reliable have been excluded from the analysis and appear white on this map.

doi: 10.26198/5e16a91249e7c

The area in-between these two major features of the physical oceanography of the Southern Ocean is split into two distinct bioregions around a longitude of 135°E. West of this, the seasonality is weak with a maximum in March, whereas the maximum is in February and the seasonal amplitude larger east of 135°E. Region #2 is quasi-absent west of the Australian continent. Consequently, the Leeuwin Current flowing south along the west coast of Australia includes only two major bioregions (#3 and #4), while the East Australian current crosses regions #3, #4 and #2. As for low-latitude areas (<10°S), an area of essentially low seasonality extends east of Papua New Guinea, whereas the Banda Sea (between Indonesia and Papua New Guinea) is entirely assigned to region #4, with a strong seasonal cycle showing a maximum in August. This same pattern appears south of Java.

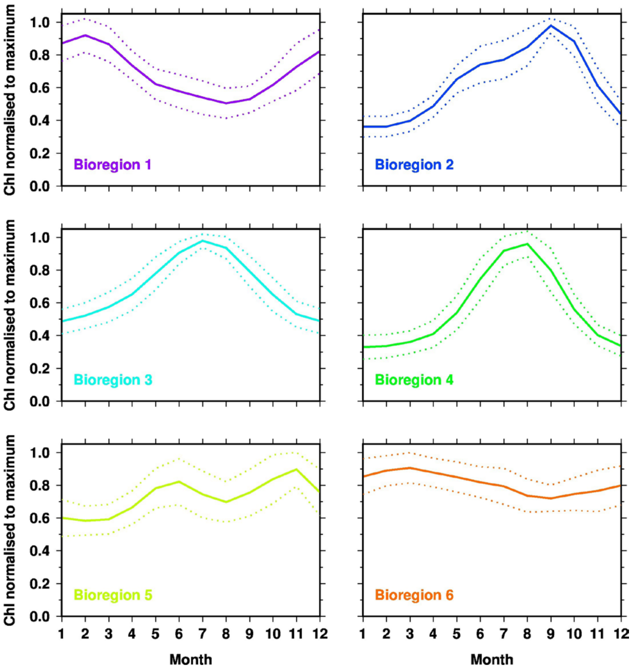

Figure 2. Mean normalised seasonal cycles for the 6 "bioregions" mapped in Figure 1 (same colour coding applies). The upper and lower curves in each panel indicate the standard deviation within the data cluster from which the average seasonal cycle (middle curve) was derived.

Implications for people and ecosystems

Interactions between physics and biology in the ocean are complex. To some extent, delineating bioregions based on a simple indicator such as the shape of the seasonal cycle, captures this complexity and allows us to summarise it graphically.

The phenology of phytoplankton and the importance to fisheries production is encapsulated in the match-mismatch hypothesis (Cushing, 1989). This hypothesis states that the degree of match and mismatch in the timing of fish larval abundance and the production of their food (both phytoplankton and zooplankton) explains much of the variability in recruitment of fish. Thus, if fish spawn and larvae emerge when phytoplankton (and zooplankton) are high, then there is a match in timing and there is higher likelihood of fish larval survival because of good feeding conditions. By contrast, if fish spawn and larvae emerge when phytoplankton (and zooplankton) are low, then there is a mismatch in timing and there is higher mortality of fish larvae because of starvation. Thus, knowing the seasonality of phytoplankton is key to understanding whether higher trophic levels can find sufficient food at the right time of the year. Although the climatology presented here cannot address interannual variability, the same analyses can be performed on shorter and successive time periods to identify changes in the spatial distributions of bioregions.

A practical application of defining bioregions is to guide oceanographic sampling. The significant effort that is put into sampling the ocean is inevitably limited with respect to its vastness. Therefore, when designing research voyages or planning for deployment of autonomous profiling floats, maps such as the one derived here can help avoid oversampling some areas while missing others, in view of optimising the use of our sampling capability. They could also help when delineating boundaries of marine parks or marine protected areas.

Acknowledgements

Data was sourced from Australia's Integrated Marine Observing System (IMOS) which is enabled by the National Collaborative Research Infrastructure Strategy (NCRIS).

Data Sources

IMOS Satellite Remote Sensing.
http://imos.org.au/facilities/srs/

References

Cushing, D. H. (1989). A difference in structure between ecosystems in strongly stratified waters and in those that are only weakly stratified. *Journal of Plankton Research, 11*(1), 1-13.

D'Ortenzio, F., & Ribera d'Alcalà, M. (2009). On the trophic regimes of the Mediterranean Sea: a satellite analysis. *Biogeosciences, 6*(2), 139-148. doi:10.5194/bg-6-139-2009

Hu, C., Lee, Z., & Franz, B. (2012). Chlorophyll a algorithms for oligotrophic oceans: A novel approach based on three-band reflectance difference *Journal of Geophysical Research, Oceans, 117*, C01011. doi:10.1029/2011jc007395

Rousseeuw, P. J. (1987). Silhouettes: A graphical aid to the interpretation and validation of cluster analysis. *Journal of Computational and Applied Mathematics, 20*, 53-65. doi: 10.1016/0377-0427(87)90125-7

IMOS

Integrated **Marine**
Observing System

IMOS
Integrated Marine Observing System

State and Trends of Australia's Oceans
Report

2.5 Indicators of depth layers important to phytoplankton production

Paul van Ruth[1], Ana Redondo Rodriguez[1], Claire Davies[2] and Anthony J. Richardson[3,4]

[1] Aquatic Science Centre, South Australia Research and Development Institute, SA, Australia
[2] CSIRO Oceans and Atmosphere, Hobart, TAS, Australia
[3] CSIRO Oceans and Atmosphere, Queensland Biosciences Precinct (QBP), St Lucia, QLD, Australia
[4] Centre for Applications in Natural Resource Mathematics (CARM), School of Mathematics and Physics, The University of Queensland, St Lucia, QLD, Australia

Summary

Monthly climatologies of mixed layer depth, euphotic depth, and the depth of the chlorophyll maximum highlight the importance of subsurface production to total water column productivity at outer-shelf IMOS National Reference Stations. Trends in the time-series data at these sites reveal changes in these depth layers that are indicative of strengthening turbulent mixing processes, increased solar intensities, and shifts in enrichment pathways, which have implications for primary production and total ecosystem productivity.

Key Data Streams

National Reference Stations

State and Trends of Australia's Ocean Report
www.imosoceanreport.org.au

Time-Series published
10 January 2020

doi: 10.26198/5e16a98549e7d

Rationale

Production by phytoplankton – the rate of growth at the base of the open ocean food web – ultimately controls the abundance of higher trophic levels including fish, marine mammals and seabirds. Phytoplankton are microscopic plants, which produce food for higher trophic levels via photosynthesis. Critical to this process is the availability of nutrients and light. Mixing processes such as upwelling and vertical mixing promote phytoplankton productivity by bringing nutrients from great depths into well-lit surface waters where they can be used in photosynthesis. Mixing processes, however, can also influence the amount of light available for photosynthesis. During periods of strong/deep mixing, phytoplankton may spend significant periods in waters where irradiances are too low for photosynthesis to proceed. There are several layers in the ocean that together regulate phytoplankton production. The first is the depth of the mixed layer, the depth to which active turbulence from winds and tides homogenises the top layer of the ocean. The deeper it is, the deeper that phytoplankton are mixed, which will take them away from the light required for photosynthesis. A second depth layer is the euphotic zone, which is the layer from the surface to the depth at which irradiances are 1% of the surface irradiance. The deeper the euphotic depth, the deeper the layer in which photosynthesis and phytoplankton production can occur. A third important depth is that of the chlorophyll maximum, which is the depth of maximum phytoplankton biomass. The deeper the chlorophyll maximum, the less light phytoplankton will generally receive, and growth will be slower. However, phytoplankton are then closer to the nutrient-rich bottom-water and can often migrate to use it.

The interplay between mixed layer depth, (MLD) the euphotic depth (Z_{eu}), and the depth of the chlorophyll maximum (DCM) regulates primary production. The proximity of the depth of the chlorophyll maximum, relative to the mixed layer depth and the euphotic depth, reflects the importance of processes in the surface mixed layer to water column primary production, and may be indicative of changes in nutrient supply processes from surface sources (e.g., terrestrial run-off, surface flows) to more oceanic (e.g. upwelling/uplift/vertical mixing).

Information regarding the depth of the chlorophyll maximum is particularly important because satellites only see near-surface layers (to the optical depth of the satellite (Behrenfeld & Falkowski, 1997)). However, deep chlorophyll biomass (i.e., biomass below the surface mixed layer) contributes significantly to depth integrated primary production in many regions, such as the eastern Great Australian Bight (van Ruth, Ganf, & Ward, 2010a, 2010b; van Ruth et al., 2018). A better understanding of long-term trends in, and the climatology of, mixed layer depth, euphotic depth, and deep chlorophyll maxima will help improve modelled estimates of primary production. It will also help facilitate an accurate assessment of long-term trends in total water column primary production at IMOS National Reference Stations.

Methods

We examined variation in ecologically relevant depth layers using a decade (2008 – 2018) of profiling data collected from the five outer-shelf IMOS National Reference Stations (North Stradbroke Island, Port Hacking, Maria Island, Kangaroo Island, Rottnest Island) using conductivity, temperature, depth recorders (CTDs) fitted with fluorometers. Data from more coastal National Reference Stations (Darwin Harbour, Yongala) were not included in the analysis, since the shallow water depths characteristic of these sites resulted in mixed layer and euphotic depths regularly extending to the seafloor.

All data were processed according to standard IMOS procedures using the CTD Toolbox produced by the Australian Ocean Data Network. The deep chlorophyll maximum was the depth of the fluorescence maximum from each CTD profile. Mixed layer depths were calculated using potential density depth profiles according to the hybrid method modified from the algorithm of Holte and Talley (2009). This method calculates a number of possible mixed layer depths, based on a threshold, gradient or the shape of the profile, and then analyses the patterns to select a final depth estimate. Euphotic depth was calculated from profiles of photosynthetically active radiation, where available. The coefficient of downwelled irradiance (K_d) was derived from the slope of the semi-log plot of irradiance versus depth. Euphotic depth was calculated by substituting K_d into the Beer-Lambert equation (Kirk, 1994) :

$$Z_{eu} = \frac{1}{K_d} \text{X} \ln\left(\frac{100}{1}\right)$$

Monthly climatologies for each variable were produced by calculating monthly means from all observations across the time series at each site. Most sites have not collected light profiles, so euphotic depth could only be analysed for Kangaroo Island.

To examine longer-term changes in depths of the deep chlorophyll maximum, mixed layer depth and euphotic depth, we fitted linear models. For the deep chlorophyll maximum and mixed layer depth models (each was the response), predictors were Station (with five levels of National Reference Station: NSI, PHB, MAI, KAI, ROT), Year (as a linear trend), and Month (the seasonal cycle modelled as a harmonic of superimposed sine and cosine waves). We included the interaction of Station:Year, allowing different slopes for each Station. We also included the interaction of Station:Month, allowing different seasonal cycles for each Station. As euphotic depth was only available for KAI, we did not include the Station effect or its interactions. We visually inspected model residuals using diagnostic plots and observed that homogeneity of variance assumptions and normality were reasonably met for deep chlorophyll maximum and the euphotic depth, but residuals for the mixed layer depth increased with predicted values. We thus used a generalised linear model with a Gamma error structure with a log-link function, which improved the distribution of residuals in the diagnostic plots.

Results and interpretation

There was a range of trends in the time series examined at the National Reference Stations (**Figure 1**). For all sites, mean deep chlorophyll maxima across the time series were deeper than mean mixed layer depths (**Table 1**). This suggests that sub-surface production, below the surface mixed layer, is an important component of integrated water column primary production at Integrated Marine Observing System (IMOS) National Reference Stations (NRS).

The irradiance data from KAI showed that the euphotic depth was 41 m deeper than the mean mixed layer depth (**Table 1**), which indicates that there was a large volume of water below the surface mixed layer in which irradiances were high enough for photosynthesis. During the characteristic summer/autumn upwelling at KAI, this water is likely to be rich in nutrients and promote substantial sub-surface primary production. This assertion is supported by the fact that the mean deep chlorophyll maximum at KAI is found in the bottom layer, mid-way between the mixed layer depth and the euphotic depth (**Table 1**).

Table 1. Time series mean (+/- standard deviation) for ecologically relevant depth layers at IMOS NRS derived from CTD profile data collected between 2008 and 2018.

National Reference Station	Deep chlorophyll maximum (m)	Euphotic depth (m)	Mixed layer depth (m)
NSI	35 (+/- 15.7)		20 (+/- 8.7)
PHB	30 (+/- 12.8)		23 (+/- 13.8)
MAI	33 (+/- 17.2)		30 (+/- 21.9)
KAI	43 (+/- 18.5)	65 (+/- 15.3)	24 (+/- 19.4)

Monthly climatologies highlighted differences in physical characteristics among sites. In general, mixed layers were shallower in summer, becoming deeper through autumn into winter (due to increased winter mixing), then shallower again through spring (**Figure 2**). However, this pattern was most pronounced at Maria Island and Kangaroo Island, and least evident at Rottnest Island.

Monthly euphotic depth at Kangaroo Island remained relatively constant, aside from an abrupt deepening in June that coincided with the shallowest deep chlorophyll maximum (**Figure 2D**). Euphotic depth ranged between 57.8 m in November and 96.6 m in June. The depth of the euphotic zone at Kangaroo Island was always deeper than the mixed layer, from 59.6 m deeper in June to 4.5 m deeper in July.

Figure 1. Time series for the depth of the chlorophyll (fluorescence) maximum, euphotic depth, and mixed layer depth at the five the five outer shelf NRS. Dashed lines indicate linear regressions through the data points for each variable.

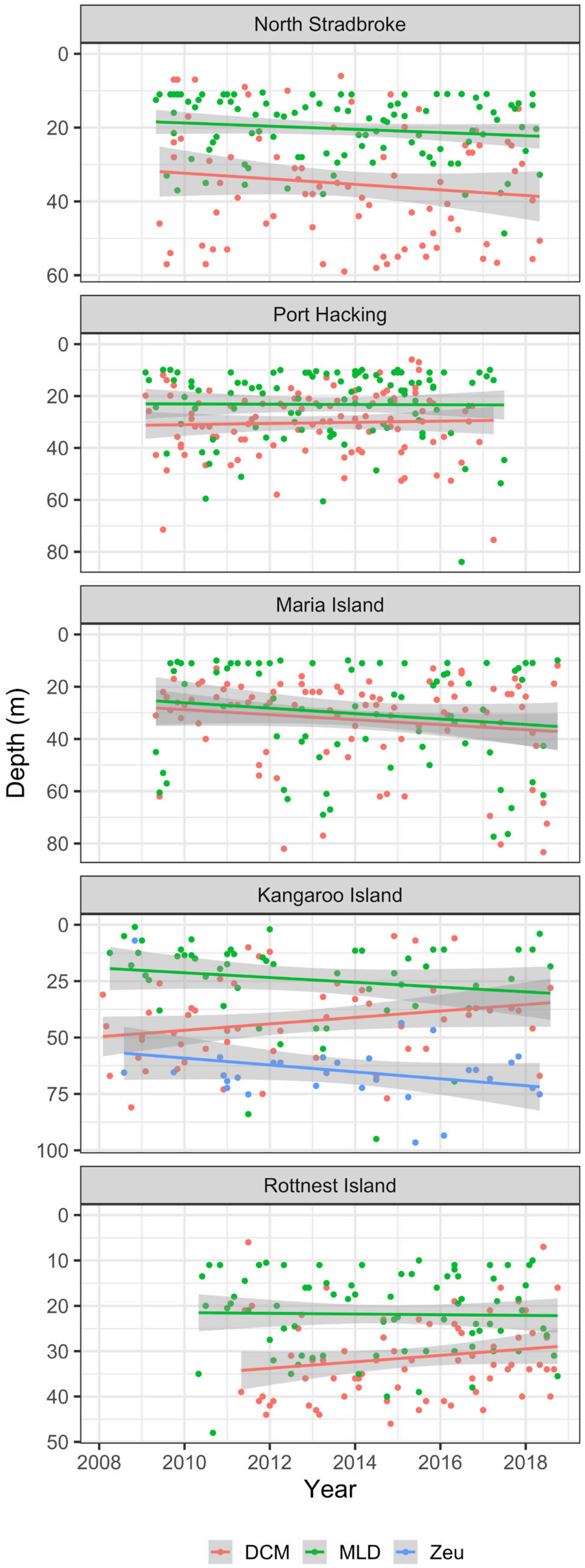

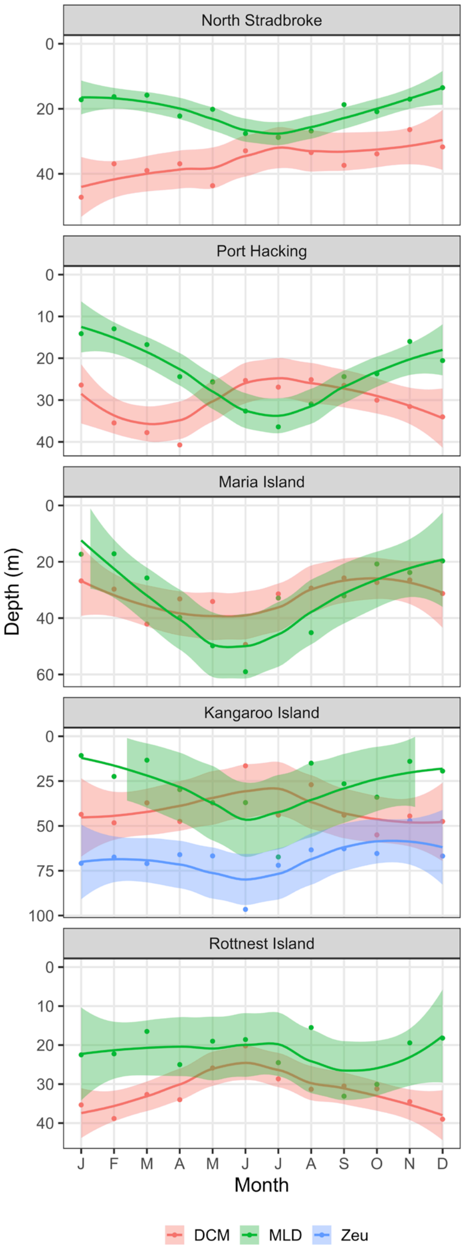

Figure 2. Monthly climatologies (means ± standard deviation) for the depth of the chlorophyll (fluorescence) maximum, euphotic depth, and mixed layer depth at the five the five outer shelf NRS.

Deep chlorophyll maximum model

In the final linear model for the deep chlorophyll maximum, the interaction Station:Month and the main effect of Month, were not significant. The final model included the interaction Station:Year, indicating that trends over time in the deep chlorophyll maximum were variable among Stations (**Figure 3**). The deep chlorophyll maximum is deepening at both NSI (0.9 m yr^{-1}) and MAI (1.02 m yr^{-1}). By contrast, it is shallowing at PHB (0.16 m yr^{-1}), KAI (1.50 m yr^{-1}) and ROT (0.69 m yr^{-1}). The deep chlorophyll maxima are between 30-35 m for all National Reference Stations, except for KAI, which is 41.9 m.

Mixed layer depth model

The final generalised linear model for the mixed layer depth at the National Reference Stations had non-significant interactions for Year:Station (implying the yearly trend was the same at all stations) and Month:Station (implying the seasonal cycles were the same at all stations) (**Figure 4**). The Year effect was marginally significant ($p<0.058$), and indicated that the mixed layer depth is deepening by 1.02 m yr^{-1} across all the National Reference Stations. MLDs were shallowest in autumn and spring. The mean mixed layer depths for the were 20-25 m for all stations, except MAI, which was 30.2 m (in June 2013).

Euphotic depth model

For the euphotic depth model Year was marginally significant ($p<0.084$), but Month was not significant. The Year effect showed that euphotic depth deepened at KAI by 1.70 m yr^{-1} (**Figure 5**).

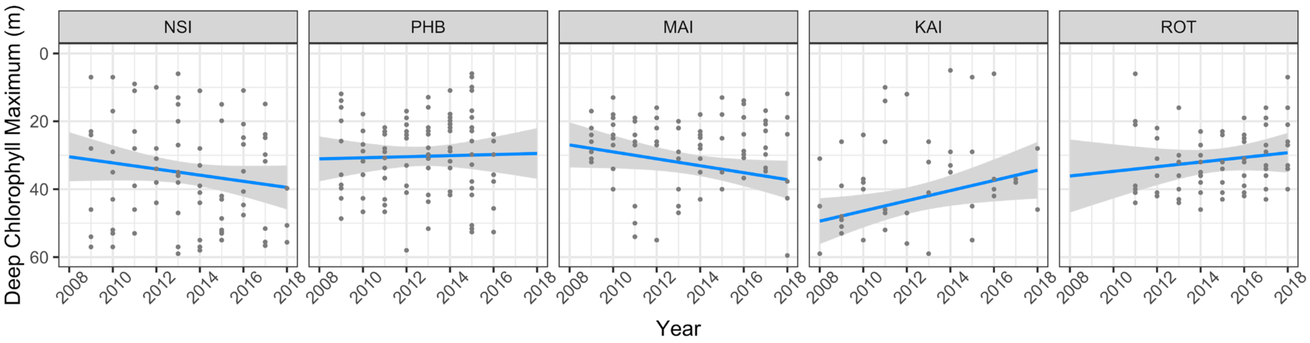

Figure 3. The final linear model for the Deep Chlorophyll Maximum (m) at the National Reference Stations. The interaction between Station and Year was significant. The Deep Chlorophyll Maximum is deepening at NSI and MAI, and shallowing at KAI and ROT, with little change at PHB.

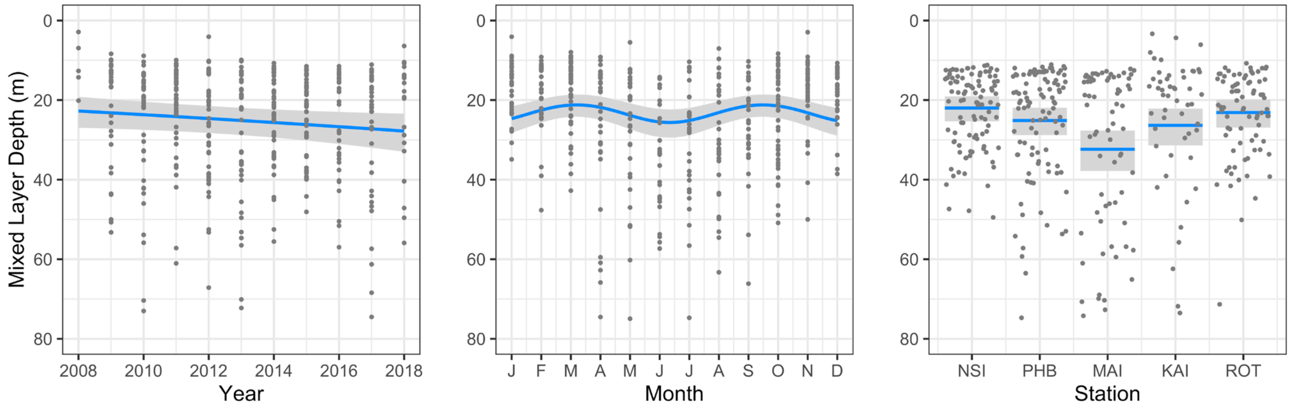

Figure 4. The final linear model for the Mixed Layer Depth (m) at the National Reference Stations. The main effects Year, Month and Station were significant. The Mixed Layer Depth is deepening across the National Reference Stations.

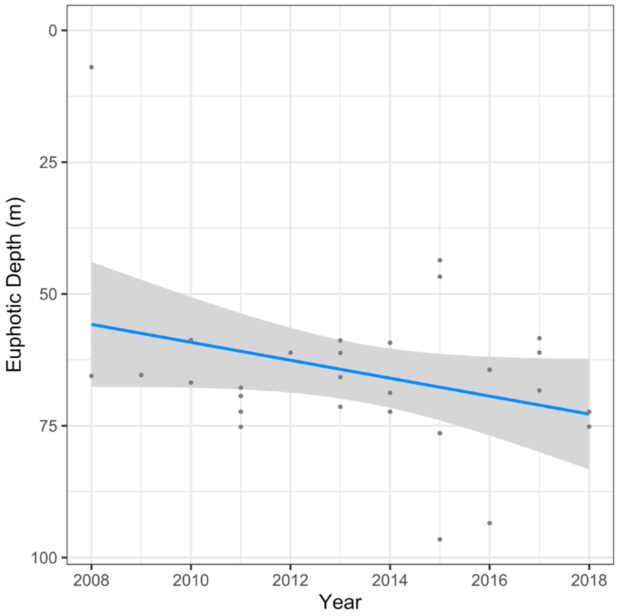

Figure 5. The final linear model for the Euphotic Depth (m) at Kangaroo Island. The Euphotic Depth is deepening.

Implications for people and ecosystems

An examination of long-term variation in water column integrated primary production – probably the best estimate of food available at lower trophic levels – requires an understanding of variations in depth layers relevant for phytoplankton. This information feeds directly into depth-integrated models of primary production.

Monthly climatologies presented here highlight the importance of subsurface production throughout the annual cycle at North Stradbroke Island and Rottnest Island, and through spring, summer and autumn at Port Hacking, Maria Island, and Kangaroo Island. Data from Kangaroo Island indicate that there is always (perhaps with the exception of July) a significant volume of water below the surface mixed layer that is still within the euphotic zone. This means that deeper nutrient-rich water still has sufficient light for photosynthesis. Consideration of the phytoplankton below the mixed layer and within the euphotic zone is critical for robust estimates of integrated water column production, particularly through the summer upwelling season, and the autumn and spring transitions to and from winter.

Trends in the time series data at the IMOS National Reference Stations suggest that turbulent mixing processes from winds and tides are getting stronger at all sites. The deepening trend in euphotic depths at Kangaroo Island imply that either the water column is becoming clearer, with less suspended matter, or solar irradiances are becoming more intense. Trends in the depth of the chlorophyll maximum may be indicative of changes in the influence of oceanic enrichment processes like upwelling, uplift and vertical mixing, which may be weakening at NSI and MAI, and strengthening at PHB, ROT, and more significantly at KAI. However, while generally due to increased biomass from photosynthesis, deep chlorophyll maxima may also be caused by an increase in phytoplankton chlorophyll content per cell in response to low irradiances (i.e. phytoplankton produce more of the light capturing pigment to enable them to capture as much light as possible when there is not much light available). This generally occurs at depths close to the euphotic depth (Kirk, 1994) . In the absence of irradiance data and euphotic depths at National Reference Stations other than Kangaroo Island, care must be taken in interpreting trends in the depth of the chlorophyll maximum.

While inferences can be made about probable euphotic depth from other available data, such as fluorescence (Lund-Hansen, 2004) or remotely-sensed data (Lee et al., 2007) , the lack of light profiles at NRS other than Kangaroo Island represents a significant gap in the IMOS dataset that should be filled. Light profiles in other regions would not only provide the data to make robust national comparisons of integrated primary production, but could assist in the validation of regional remote sensing algorithms.

Together, the trends highlighted in this analysis above have implications for primary production, and consequently ecosystem productivity. They also highlight the need for more in-depth, integrative analysis of IMOS time series, with careful consideration of the data streams and products required to best assist in the management of Australia's marine resources.

Acknowledgements

Data was sourced from Australia’s Integrated Marine Observing System (IMOS) which is enabled by the National Collaborative Research Infrastructure Strategy (NCRIS).

Data Sources

IMOS National Reference Stations.
http://imos.org.au/facilities/nationalmooringnetwork/nrs/

References

Behrenfeld, M. J., & Falkowski, P. G. (1997). A consumer's guide to phytoplankton primary productivity models. *Limnology and Oceanography, 42*(7), 1479-1491. doi:10.4319/lo.1997.42.7.1479

Holte, J., & Talley, L. (2009). A new algorithm for finding mixed layer depths with applications to argo data and subantarctic mode water formation. *Journal of Atmospheric and Oceanic Technology, 26*(9), 1920-1939. doi:10.1175/2009jtecho543.1

Kirk, J. T. O. (1994). *Light and photosynthesis in aquatic ecosystems*. Cambridge: Cambridge University Press

Lee, Z., Weidemann, A., Kindle, J., Arnone, R., Carder, K. L., & Davis, C. (2007). Euphotic zone depth: Its derivation and implication to ocean-color remote sensing. *Journal of Geophysical Research-Oceans, 112*(C3). doi:10.1029/2006jc003802

Lund-Hansen, L. C. (2004). Diffuse attenuation coefficients K-d(PAR) at the estuarine North Sea-Baltic Sea transition: time-series, partitioning, absorption, and scattering. *Estuarine Coastal and Shelf Science, 61*(2), 251-259. doi:10.1016/j.ecss.2004.05.004

van Ruth, P. D., Ganf, G. G., & Ward, T. M. (2010a). Hot-spots of primary productivity: An Alternative interpretation to Conventional upwelling models. *Estuarine Coastal and Shelf Science, 90*(3), 142-158. doi:10.1016/j.ecss.2010.08.009

van Ruth, P. D., Ganf, G. G., & Ward, T. M. (2010b). The influence of mixing on primary productivity: A unique application of classical critical depth theory. *Progress in Oceanography, 85*(3-4), 224-235. doi:10.1016/j.pocean.2010.03.002

van Ruth, P. D., Patten, N. L., Doubell, M. J., Chapman, P., Rodriguez, A. R., & Middleton, J. F. (2018). Seasonal- and event-scale variations in upwelling, enrichment and primary productivity in the eastern Great Australian Bight. *Deep Sea Research Part II: Topical Studies in Oceanography, 157-158*, 36-45. doi: 10.1016/j.dsr2.2018.09.008

Integrated Marine Observing System

State and Trends of
Australia's Oceans | Report

2.6 Picophytoplankton: harbingers of change in our coastal oceans

Paul G. Thomson[1,2], Dion M. F. Frampton[3],
Lesley A. Clementson[3] and Chari B. Pattiaratchi[1,2]

[1] Oceans Graduate School, The University of Western Australia, Crawley, WA, Australia
[2] UWA Oceans Institute, The University of Western Australia, Crawley, WA, Australia
[3] CSIRO, Oceans and Atmosphere, Hobart, Tasmania, 7000, Australia

Summary

Strengthening boundary currents and episodic marine heatwaves are carrying tropical and subtropical picophytoplankton species such as *Prochlorococcus* and *Synechococcus* far into temperate southern waters around Tasmania and South West Australia, with implications for both people and ecosystems. As biomarkers for warmer currents, the picophytoplankton are sensitive indicators of tropical/subtropical microbial communities and thus may 1) afford us a glimpse of future microbial communities in our warming southern oceans and 2), help us model the spread of viral diseases, pathogens and other microbes along our coastlines. Using sensitive biomarkers such as the picophytoplankton will help us understand changes in marine microbial communities at the base of the marine food chain and subsequent impacts on the environment and marine industry such as aquaculture.

Key Data Streams

National Reference Stations

State and Trends of Australia's Ocean Report
www.imosoceanreport.org.au

Time-Series published
10 January 2020

doi: 10.26198/5e16a9dd49e7e

Rationale

Australia's' coastal oceans are changing. Our major boundary currents, the southward-flowing East Australian Current off the east coast and the Leeuwin Current off the west coast are changing and are penetrating warm tropical water further south, sometimes resulting in devastating marine heatwaves (Oliver et al., 2017). These changes have led to the 'tropicalisation' of Australia's southern coastlines and are responsible for the loss of seagrass meadows, kelp forests, species translocations, and impacts on fisheries and aquaculture (Babcock et al., 2019, Oliver et al., 2018, Wernberg et al., 2016). However, little is known of the changes within the less visible, marine microbial communities that form the base of the marine food web. Here we show that the smallest size class of the phytoplankton, the picophytoplankton, are being carried southwards. As sensitive biomarkers of change, their appearance in southern waters may be indicative of future marine microbial communities, with implications for our blue economy.

The picophytoplankton, *Prochlorococcus* and *Synechococcus*, are small (< 2µm diameter) photosynthetic, cyanobacterial cells that contribute most of the primary productivity to the world's open oceans (Worden et al., 2004). Both genera inhabit specific niches. *Prochlorococcus* flourishes in warm, tropical waters with few nutrients and abundant light, and tends to be intolerant of coastal waters. By contrast, *Synechococcus* is distributed further into subtropical zones and is most abundant in upwelling areas or coastal regions where waters are nutrient replete and more turbid. Being so small, picophytoplankton have a large surface area to volume ratio, which places them in intimate contact with surrounding seawater. This results in the cells being able to rapidly access nutrients, allowing them to respond quickly to changing environmental conditions. Picophytoplankton are also light and buoyant, rendering them capable of being carried long distances by ocean currents. Picophytoplankton are thus sensitive indicators of change in our coastal oceans.

Methods

We used samples from the Integrated Marine Observing System (IMOS) National Reference Stations (NRS) at Yongala, Maria Island and Rottnest Island to analyse the abundance of picophytoplankton between 2009 and 2018. These sites were chosen as they represented regions that were strongly influenced by Australia's boundary currents. Triplicate 1 ml seawater samples for the picophytoplankton were collected monthly from pooled water samples over several depths, fixed to a final concentration of 0.5% gluteraldehyde, and frozen in liquid nitrogen until analysis. Picophytoplankton abundance was analysed by standard flow cytometric methods where populations of *Prochlorococcus* and *Synechococcus* were discriminated based on their relative autofluorescence of chlorophyll-a (red) and phycoerythrin (orange) pigments (Marie et al., 2005). A Beckton Dickinson FacsCanto flow cytometer analysed samples from 2009, but a CytoSense cytometer was used from September 2015. Counts between the two instruments were calibrated by determining the relationship between replicate samples taken over a four-year period from 2013 to 2017, and calculating a corresponding conversion factor (Frampton et al., 2019). We used the accessory pigment divinyl chlorophyll-a (a marker for *Prochlorococcus*) from simultaneous water samples to help correct for false detections. Where divinyl chlorophyll-a was not detected, we removed counts resulting from particle and electronic noise. We matched picophytoplankton abundances to seawater temperature and salinity time series from the IMOS NRS stations and known events impacting the station such as cyclones, monsoonal rainfall and marine heatwaves.

Results and interpretation

Yongala, North Queensland

At the Yongala NRS, seasonal patterns of seawater temperature, salinity and picophytoplankton abundance illustrate the preferential niche of the picophytoplankton (**Figure 1**). *Prochlorococcus* is generally most abundant during spring and summer, when seawater temperatures are rising under the influence of the warm, clear Pacific waters feeding the source of the EAC.

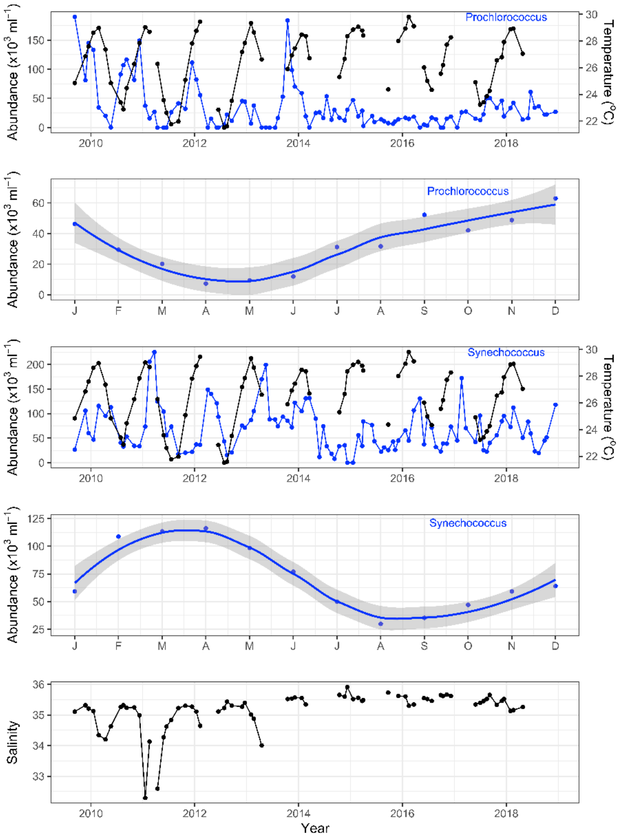

Figure 1. Picophytoplankton abundances and seasonal cycles at the IMOS Yongala National Reference Station. Also shown are temperature and salinity time series from the mooring. Note that there are missing data when the mooring has been damaged.

Prochlorococcus abundance, however, declines abruptly early in the year, with relatively large decreases in seawater salinity caused by either rainfall from cyclones (e.g., Tropical Cyclone Yasi in 2011) or the monsoon season between December to March. Cyclones and high rainfall also result in mixing and sediment runoff, which increase both nutrient concentrations and turbidity (data not shown), conditions not favourable for *Prochlorococcus*. Conversely, *Synechococcus* abundances increase from late summer through to autumn, before declining with cooler temperatures into winter, confirming their preference for warm, turbid and nutrient-rich seawater. Over the longer term, patterns of picophytoplankton abundance appear to be influenced by the El Niño–Southern Oscillation (ENSO), where abundances can be higher during La Niña or neutral years (2009 – 2014) than in El Niño years (2015 onwards).

Rottnest Island, Western Australia

At the Rottnest Island NRS, seawater temperatures ranged between 18°C to 23°C between 2009 and 2018, with the exception of periods in 2011 and 2012 when temperatures reached 25°C (**Figure 2**). Elevated temperatures beginning in February 2011 were a result of a record strength Leeuwin Current and a severe marine heatwave, which persisted into 2012 (Feng et al., 2013). This is confirmed by the lower salinity seawater (a marker of the Leeuwin Current water) evident into 2012.

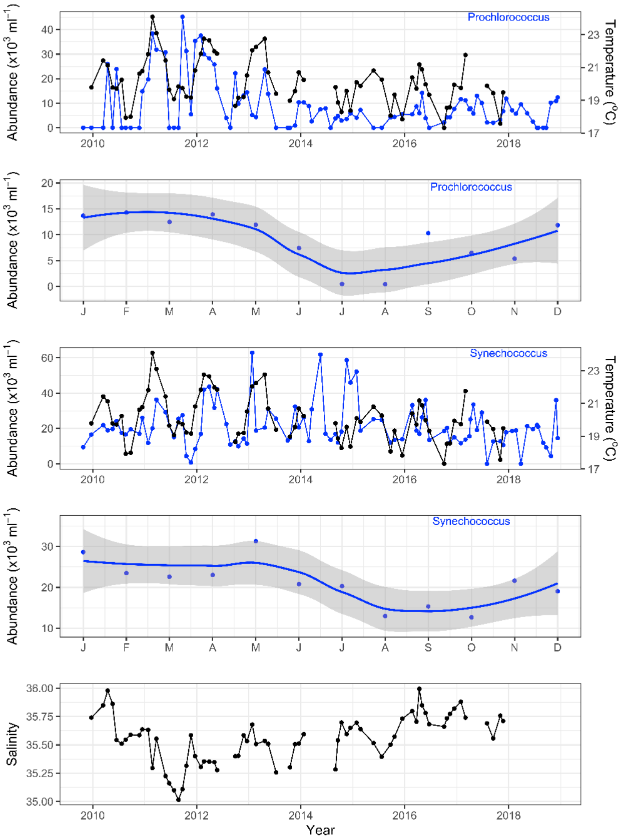

Figure 2. Picophytoplankton abundances and seasonal cycles at the IMOS Rottnest Island National Reference Station. Also shown are temperature and salinity time series from the mooring. Note that there are missing data when the mooring has been damaged.

An immediate effect of the heatwave was the unseasonal appearance of the tropical *Prochlorococcus* at the Rottnest Island NRS, at abundances at least twice the values observed outside the heatwave conditions. Further, *Prochlorococcus* abundance remained elevated throughout 2011 and into 2012, carried by the persistent Leeuwin Current. At this site, *Synechococcus* abundances correlated poorly with the marine heatwave conditions and appeared influenced more by coastal upwelling water of the inshore northward flowing Capes Current.

Maria Island, Tasmania

At the Maria Island NRS, seawater temperature has distinct seasonal cycles and peaks in late summer each year (**Figure 3**).

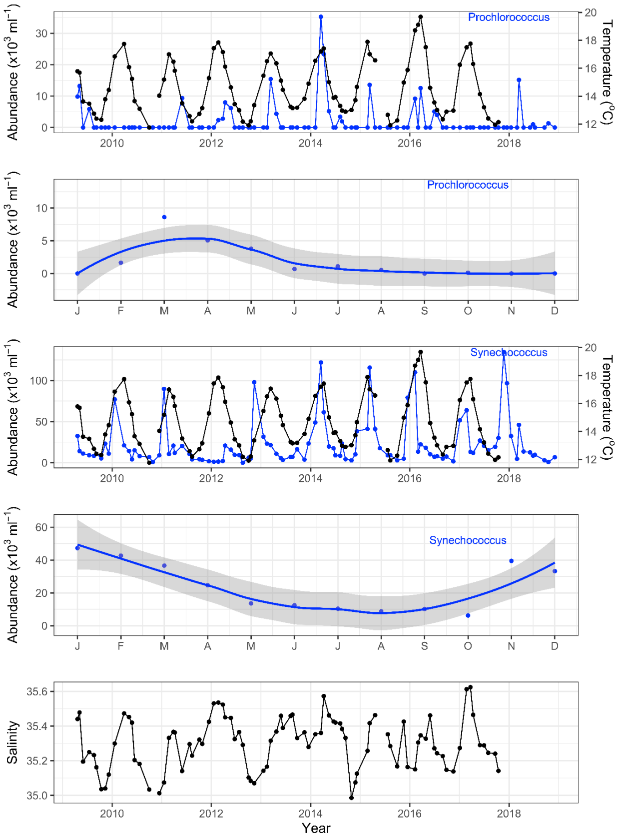

Figure 3. Picophytoplankton abundances and seasonal cycles at the IMOS Maria Island National Reference Station. Also shown are temperature and salinity time series from the mooring. Note that there are missing data when the mooring has been damaged.

Since 2009 at this temperate site, there have been small peaks in abundance of the tropical *Prochlorococcus* of up to 40 000 cells ml^{-1} most summers. The subtropical *Synechococcus* was also recorded most summers and appears to increase in abundance to 2014, before remaining at stable but elevated concentrations through to the most recent observations. Further, peaks in *Synechococcus* abundance were only found in a single month prior to 2014, but were found over at least two successive months from 2014, indicating prolonged exposure to tropical waters. A warming trend has been recorded at the Maria Island NRS over the past 50 years

(Ridgway, 2007, Kelly et al., 2015, Kelly et al., 2016), and the east coast of Tasmania has experienced marine heatwaves since 2015 until present day (Oliver et al., 2018). Both the gradual warming and the marine heatwaves have been attributed to the increasing strength of the EAC extension to 2014 and the impact of its' eddies that have intensified from 2015. Thus, the appearance of the tropical and subtropical picophytoplankton appear to be a direct result of transport by the EAC southwards along the Tasmanian coast.

Implications for people and ecosystems

Data from the IMOS NRS show that picophytoplankton are sensitive biomarkers of environmental conditions. Picophytoplankton have specific environmental niches and respond quickly to changing conditions, such as decreasing salinity resulting from rainfall and the passage of cyclones. We have provided evidence that tropical and subtropical picophytoplankton are increasing in abundance in southern Australian waters, either as a result of episodic marine heatwaves and/or through strengthening boundary currents. These increases in abundance represent an immediate ecological impact and are consistent with other impacts of warming along our southern coastlines, such as abalone mortality, fish kills, species translocations and the loss of kelp forests (Oliver et al., 2017, Wernberg et al., 2016, Pearce and Feng, 2013).

What is the significance of the picophytoplankton? As biomarkers for warmer currents, these light and buoyant cells can be used as proxies for understanding the spread of viral diseases, pathogens and other microbes along our coastlines, as well as impacts of marine heatwaves. For example, oyster aquaculture in Tasmania was severely impacted for the first time by the Pacific Oyster Mortality Syndrome (POMS) in 2015. Previously POMS was only known in NSW (Green et al., 2014). Was this virus spread to Tasmanian waters by the EAC? The transport of the picophytoplankton southwards makes this and the translocation of other pathogens a possibility. Further, as picophytoplankton are biomarkers for tropical seawater, it is likely they are markers for tropical microbial communities, possibly of a different size class, species composition and nutritional quality than found locally. While the stress of hotter temperatures during marine heatwaves can impact wild shellfish (including fished species) and aquaculture shellfish such as farmed oysters, it is likely that a change in the underlying microbial community is responsible for additional, chronic stress to higher trophic levels. Finally, like our southern coastlines undergoing tropicalisation, the picophytoplankton biomarkers may also be giving us a glimpse of future microbial communities in our warming southern oceans.

Acknowledgements

Data was sourced from Australia's Integrated Marine Observing System (IMOS) which is enabled by the National Collaborative Research Infrastructure Strategy (NCRIS).

Data Sources

IMOS National Reference Stations.
http://imos.org.au/facilities/nationalmooringnetwork/nrs/

References

Babcock, R. C., Bustamante, R. H., Fulton, E. A., Fulton, D. J., Haywood, M. D. E., Hobday, A. J., . . . Vanderklift, M. A. (2019). Severe continental-scale impacts of climate change are happening now: extreme climate events impact marine habitat forming communities along 45% of Australia's coast. *Frontiers in Marine Science, 6*(411). doi:10.3389/fmars.2019.00411

Feng, M., McPhaden, M. J., Xie, S.-P., & Hafner, J. (2013). La Niña forces unprecedented Leeuwin Current warming in 2011. *Scientific Reports, 3*, 1277. doi:10.1038/srep01277. https://www.nature.com/articles/srep01277#supplementary-information

Frampton, D., Thomson, P. G., & Clementson, L. (2019). *IMOS flow cytometry instrument comparison*.

Green, T. J., Montagnani, C., Benkendorff, K., Robinson, N., & Speck, P. (2014). Ontogeny and water temperature influences the antiviral response of the Pacific oyster, Crassostrea gigas. *Fish & Shellfish Immunology, 36*(1), 151-157. doi:https://doi.org/10.1016/j.fsi.2013.10.026

Kelly, P., Clementson, L., Davies, C., Corney, S., & Swadling, K. (2016). Zooplankton responses to increasing sea surface temperatures in the southeastern Australia global marine hotspot. *Estuarine Coastal and Shelf Science, 180*, 242-257. doi:10.1016/j.ecss.2016.07.019

Kelly, P., Clementson, L., & Lyne, V. (2015). Decadal and seasonal changes in temperature, salinity, nitrate, and chlorophyll in inshore and offshore waters along southeast Australia. *Journal of Geophysical Research-Oceans, 120*(6), 4226-4244. doi:10.1002/2014jc010646

Oliver, E. C. J., Benthuysen, J. A., Bindoff, N. L., Hobday, A. J., Holbrook, N. J., Mundy, C. N., & Perkins-Kirkpatrick, S. E. (2017). The unprecedented 2015/16 Tasman Sea marine heatwave. *Nature Communications, 8*(1), 16101. doi:10.1038/ncomms16101

Oliver, E. C. J., Donat, M. G., Burrows, M. T., Moore, P. J., Smale, D. A., Alexander, L. V., . . . Wernberg, T. (2018). Longer and more frequent marine heatwaves over the past century. *Nature Communications, 9*(1), 1324. doi:10.1038/s41467-018-03732-9

Pearce, A. F., & Feng, M. (2013). The rise and fall of the "marine heat wave" off Western Australia during the summer of 2010/2011. *Journal of Marine Systems, 111*, 139-156. doi:10.1016/j.jmarsys.2012.10.009

Ridgway, K. R. (2007). Long-term trend and decadal variability of the southward penetration of the East Australian Current. *Geophysical Research Letters, 34*(13), 1-5. doi:L1361310.1029/2007gl030393

Wernberg, T., Bennett, S., Babcock, R. C., de Bettignies, T., Cure, K., Depczynski, M., . . . Wilson, S. (2016). Climate-driven regime shift of a temperate marine ecosystem. *Science, 353*(6295), 169. doi:10.1126/science.aad8745

Worden, A. Z., Nolan, J. K., & Palenik, B. (2004). Assessing the dynamics and ecology of marine picophytoplankton: The importance of the eukaryotic component. *Limnology and Oceanography, 49*(1), 168-179. doi:10.4319/lo.2004.49.1.0168

doi: 10.26198/5e16a9dd49e7e

IMOS
Integrated Marine Observing System

State and Trends of Australia's Oceans | Report

2.7 Status of Australian marine microbial assemblages

Martin Ostrowski[1], Justin Seymour[1], Lauren Messer[2], Deepa Varkey[3], Kirianne Goosen[4], Matthew Smith[5], Andrew Bissett[4], Jodie Van de Kamp[4], Levente Bodrossy[4] and Mark Brown[6]

[1] Climate Change Cluster, University of Technology, Sydney, Sydney, NSW, Australia
[2] Australian Centre for Ecogenomics, University of Queensland, Brisbane, QLD, Australia
[3] Department of Molecular Sciences, Macquarie University, Sydney, NSW, Australia
[4] CSIRO Oceans and Atmosphere, Hobart, TAS, Australia
[5] CSIRO, National Collections and Marine Infrastructure, Hobart, TAS, Australia
[6] School of Environmental and Life Sciences, University of Newcastle, Callaghan, NSW, Australia

Summary

Using molecular approaches to monitoring microbial assemblages, we found that cyanobacterial microbes generally show less seasonal and interannual variation in the subtropics compared to temperate waters. *Synechococcus* was found to increase and *Prochlorococcus*, decrease in abundance due to coastal upwelling at Port Hacking, highlighting the ability to interpret underlying changes in environment (nutrients, heat and light) from molecular microbial time series.

Key Data Streams

National Reference Stations

State and Trends of Australia's Ocean Report
www.imosoceanreport.org.au

Time-Series published
10 January 2020

doi: 10.26198/5e16aa3e49e7f

Rationale

Despite being invisible to the naked eye, microbes have long been recognised as the planet's consummate recyclers of dead and decaying matter (Azam, 1998). Their diverse metabolic activities contribute to the resupply of nutrients to the base of marine food webs, effectively repriming the production that sustains all Ocean life. This important, but narrow, view has expanded rapidly over the past four decades, leading to the realisation that microbes 'drive global biogeochemical cycles' (Falkowski, Fenchel, & DeLong, 2008). The vast numbers of microbes and their metabolic diversity has only recently been unveiled by a rapid expansion of molecular techniques, fuelled by advances in fluorescence and low-cost sequencing technologies. Numerous discoveries within this new dimension have fundamentally changed our understanding of how marine food webs function (Worden et al., 2015).

Here we use molecular tools to distinguish tiny, planktonic, single-celled bacteria, archaea and microbial eukaryotes that constitute 90% of all biomass in the ocean, but lack distinguishing external features. We analyse some of the sustained molecular observations from three Integrated Marine Observing System (IMOS) National Reference Stations since 2012, highlighting some of the time series of key microbial components and their dynamics. Observations span marker genes and metagenomes. Marker genes reveal the complex dynamics and interactions among three domains of life (archaea, bacteria and eukaryotes). Metagenomes provide additional insight into functional adaptations that underpin how individual single-celled microbes adapt to diverse marine environments.

Methods

We used the publicly available bacterial single nucleotide variant 16S rRNA gene sequence dataset from the Australian Microbiome Initiative (AMI) to observe the relative abundance of microbial taxa for the three longest time series at the IMOS National Reference Stations, Maria Island, Port Hacking and North Stradbroke Island. The relative abundance of taxa was square-root transformed to reduce the dominance of abundant taxa in the analysis. The relationship among samples was visualised in two dimensions using non-metric multidimensional scaling and unsupervised clustering (simprof) based on the Bray-Curtis similarity measure of the microbial assemblage. Community structure was investigated using concomitant environmental data (see the AODN dataset "IMOS National Reference Station (NRS) - Salinity, Carbon, Alkalinity, Oxygen and Nutrients (Silicate, Ammonium, Nitrite/Nitrate, Phosphate").

Photosynthetic populations detected in the 16S rRNA were analysed at the Order (Chloroplast and Cyanobacteria), and phylotype level (*Synechococcus* and *Prochlorococcus*) by assigning single nucleotide variants to ecologically-defined genotypes (Farrant et al., 2016; Mazard, Ostrowski, Partensky, & Scanlan, 2012). Where possible, proportions of each type were scaled to absolute abundances obtained from the AODN flow cytometry analyses (see Section "Picophytoplankton: harbingers of change in our coastal oceans" by Thomson et al.).

Results and Interpretation

Discrete microbial assemblages inhabit each of the IMOS National Reference Stations (**Figure 1,** (Brown et al., 2018)), with several common abundant order-level taxonomic groups displaying different relative abundances that vary spatially, seasonally and interannually. Pelagibacteriales (SAR11), Rhodobacterales and SAR86 are the most abundant heterotrophic groups, constituting ~50% of the sequences from surface waters at each station. Phototrophic taxa include cyanobacteria as well as eukaryote phytoplankton (detected by the 16S rRNA gene in their chloroplasts) and their relative abundance provides important indicators to monitor changes in the dynamics of microbial primary production at each site.

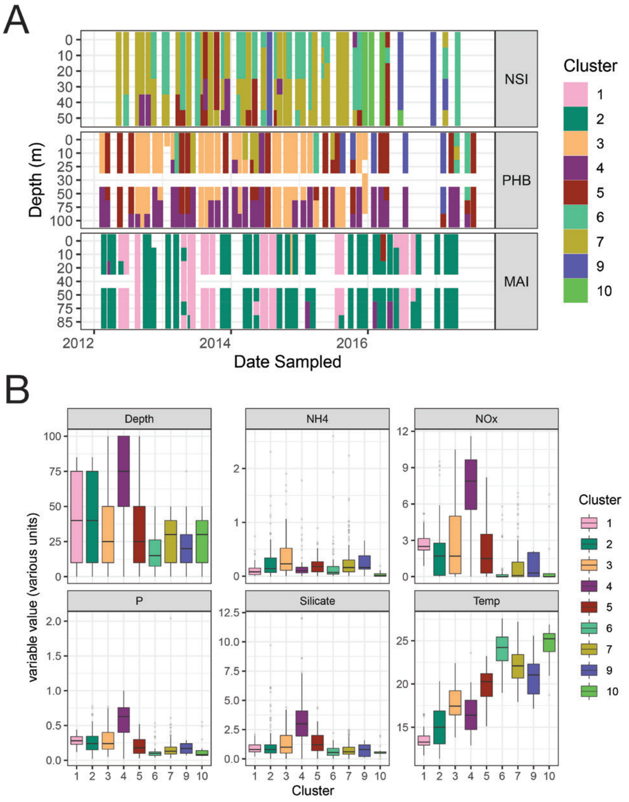

Figure 1. Temporal changes in microbial assemblages at three IMOS National Reference Stations: North Stradbroke Island, Port Hacking and Maria Island. A. Microbial communities were classified by hierarchal clustering (Bray-Curtis distance) and the distribution of nine distinct types were plotted over time at each of the depths sampled. B. The relationship between each community type and physico-chemical conditions at the time of sampling. Abbreviations and units. NH4: Ammonium (μmol L^{-1}); NOx: Nitrate plus Nitrite (μmol L^{-1}); P: Phosphate (μmol L^{-1}), Silicate (μmol L^{-1}), Temperature (˚C).

North Stradbroke Island, Queensland

At the North Stradbroke Island National Reference Station, cyanobacteria are an order of magnitude more abundant than chloroplast sequences over time (**Figure 2**), indicating that prokaryotes may be the largest contributor to primary production in this region. At a higher taxonomic resolution, *Synechococcus* clade II and *Prochlorococcus* High-Light II (HLII) are the major components of the cyanobacteria and their genetic composition shows little variation seasonally or over time. Fluctuations in overall abundance of cyanobacteria may be linked to warmer temperatures and nutrients, which correspond to peaks in the abundance of *Prochlorococcus* and *Synechococcus*. Sequences of the keystone nitrogen-fixing cyanobacterium *Trichodesmium* spp. (not shown here) are sporadically detected in the data in low relative abundance (see Section "Spatial and seasonal trends in *Trichodesmium*" by Davies et al.).

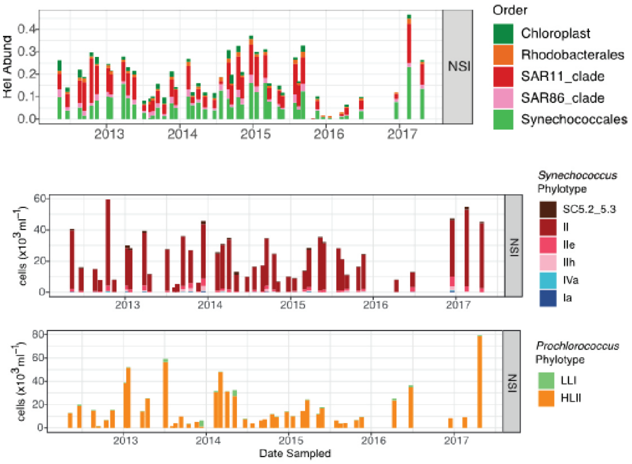

Figure 2. North Stradbroke Island NRS relative abundances of eukaryote (Chloroplast) and prokaryote (Synechococales) sequences grouped at the Order level. Abundances of *Synechococcus* and *Prochlorococcus* phylotypes. (note different Y axes, which were scaled to absolute counts by comparison with flow cytometry data).

Maria Island, Tasmania

The most southerly IMOS National Reference Station (Maria Island) has a higher proportion of chloroplast sequences, with picoeukaryote species *Ostreococcus* and *Micromonas* contributing most (Brown et al., 2018). At Maria Island, the relative proportion of chloroplasts peaks in winter, with their highest relative proportions in 2013 and 2014, representing up to 20% of all bacterial 16S sequences (**Figure 3**). The late-winter, early-spring peak in chloroplasts is followed by an increase in the abundance of the heterotrophic *Rhodobacterales*. This group is widespread in coastal and oceanic environments, displays diverse interactions with phytoplankton, and has metabolic capabilities associated with post-bloom recycling of organic matter (Moran et al., 2007). By contrast with northerly National Reference Stations, *Synechococcus* sub clade I and IV are the most abundant phylotypes at Maria Island, and their abundance peaks in February/March each year, reaching similar numbers as observed in the sub-tropical National Reference Stations. Seasonally, *Synechococcus* steadily increases from November and declines from April, with the appearance of the subtropical clade II and IIe phylotypes as distinct markers of the influence of warmer sea surface temperatures, and potentially indicators of the southerly extension of the East Australia Current.

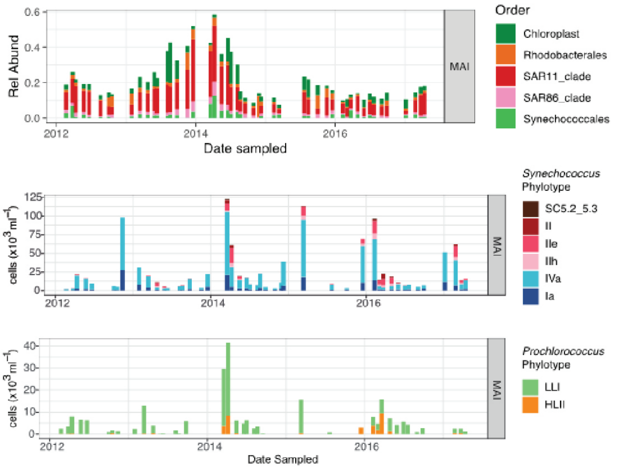

Figure 3. IMOS Maria Island NRS Relative abundances of eukaryote (Chloroplast) and prokaryote (Synechococales) sequences grouped at the Order level. Abundances of *Synechococcus* and *Prochlorococcus* phylotypes. Also shown are the (note different Y axes, which were scaled to absolute counts by comparison with flow cytometry data).

Port Hacking, New South Wales

The composition of communities at the Port Hacking National Reference Station varies considerably over time, reflecting the complex oceanography at this site. For example, the elevated abundance of *Prochlorococcus* is closely coupled to the influence of the East Australian Current (**Figure 4**).

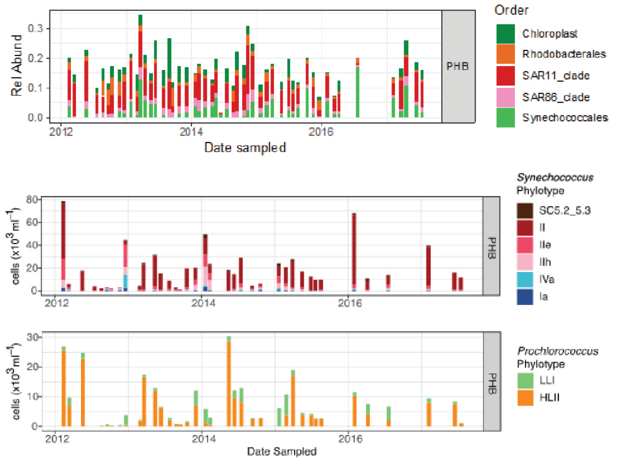

Figure 4. Port Hacking NRS abundances of eukaryote (Chloroplast) and prokaryote (Synechococales) sequences grouped at the Order level. Abundances of *Synechococcus* and *Prochlorococcus* phylotypes (note different Y axes, which were scaled to absolute counts by comparison with flow cytometry data).

doi: 10.26198/5e16aa3e49e7f

The sub-tropical *Synechococcus* clade II is the most abundant. However, the episodic appearance of phylotypes (IIe and IIh), hypothesised to represent lineages adapted to the intermediate conditions found at the boundaries between water masses at Maria Island, and the inverse at Port Hacking, highlight the presence of a major ecological transition between subtropical and temperate communities in this region. Appearances of the temperate *Synechococcus* clades (I and IV) are correlated with a decrease of *Prochlorococcus* HLII and appear to indicate coastal upwelling (see Section "Picophytoplankton: harbingers of change in our coastal oceans" by Thomson et al.).

Implications for people and ecosystems

We show that molecular approaches can now be used to monitor changes in key species; here we focused on cyanobacterial primary producers. This is an important group, because many of these are small and not visible with light microscopy (e.g., *Prochlorocochus*, *Synecococchus*) or have cryptic species (*Trichodesmium*). *Procholorococcus* and *Synechococcus* are the most abundant photosynthetic species in the ocean, responsible for ~25% of all primary production in the ocean, and their numbers are predicted to change substantially over the next decades in response to climate change (Flombaum et al., 2013).

For the cyanobacterial microbes investigated here, there was generally less seasonality in subtropical waters (North Stradbroke Island) than in temperate waters (Maria Island) (**Figure 5**). Similar to the seasonality, the interannual variation of most clades was lower in the subtropics (North Stradbroke Island) than in cooler regions (Maria Island and Port Hacking). We found that at Port Hacking, molecular data suggest that strains of *Synechococcus* increase in abundance and those of *Prochlorococcus* decrease in response to coastal upwelling.

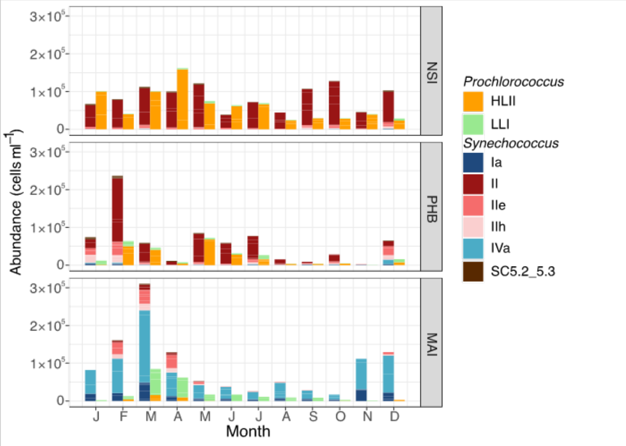

Figure 5. Seasonal abundances of *Synechococcus* and *Prochlorococcus* phylotypes at the IMOS five IMOS National Reference Stations.

Microbes are the primary biological determinants of ocean health and the first responders to ecosystem change. The high-resolution dataset housed at the Australian Microbiome Initiative describes seasonal and interannual marine microbial diversity and dynamics across the seven IMOS National Reference Stations and the greater southern hemisphere region. This dataset provides a valuable baseline against which changes in microbial assemblages in response to climate change can be assessed.

The use of molecular tools to generate time series and their use in ecosystem assessments is still in its infancy. The recent establishment of the microbe facility within IMOS will facilitate the development of novel tools to monitor, forecast and sustainably manage marine resources. Ongoing observations will help document shifts in distributions of organisms, which result from changes in ocean currents (e.g., East Australia Current dynamics), basin-scale climatic events, or climate change. In particular, a number of species associated with harmful algal blooms are detected within the microbial data (*Alexandrium*, *Noctiluca* and *Gymnodinium*), which highlights the potential to enhance understanding of bloom dynamics within the context of a holistic record of microbial community structure (Brown et al., 2018).

Supplement: Microbial Methods and the Australian Marine Microbial Biodiversity Initiative

Sustained temporal observations of microbial dynamics in Australian waters was formally established through an IMOS partnership with the Australian marine microbiology community in 2012, with the establishment of the Australian Marine Microbial Biodiversity Initiative (AMMBI). Data and protocols from this project have recently become an integral part of the Australian Microbiome Initiative (https://www.australianmicrobiome.com/) (AMI). This initiative draws core funding from IMOS, Bioplatforms Australia, CSIRO and Parks Australia. AMI provides publicly available, methodologically standardised, continental scale, phylogenetic amplicon and metagenomic sequencing data describing the temporal and spatial dynamics of *bacteria*, *archaea* and microbial *eukarya* assemblages in Australian, and more broadly, southern hemisphere waters ranging the Antarctic ice edge to the equator.

As part of the IMOS National reference Station facility, samples for microbial analysis are collected from seven IMOS NRS: Darwin Harbour (Northern Territory; depths 0, 10, 20 m), Yongala (Queensland; depths 0, 10, 20, 26 m), North Stradbroke Island (Queensland; depths 0, 10, 20, 30, 40, 50 m), Rottnest Island (Western Australia; depths 0, 10, 20, 30, 40, 46 m), Port Hacking (New South Wales; depths 0, 10, 25, 50, 75, 100 m), Kangaroo Island (South Australia; depths 0, 10, 20, 50, 75, 100 m), Maria Island (Tasmania; depths 0, 10, 20, 50, 75, 85 m). Oceanographic samples have been collected during Marine National Facility (MNF) supported voyages on the RV Southern Surveyor, RV Investigator and the RV Aurora Australis. The current AMI pelagic marine dataset contains data from 3381 samples and describes microbial assemblages in the southern hemisphere from Latitudes 0 to 66.3S, temperatures -1.6 and 31.4 and depths 0 to 6,015 m.

Further, metagenomic datasets are generated from a subset of these samples. This method involves the sequencing of random fragments of DNA from a sample to provide a snapshot of functional genetic diversity. Metagenomic data is parsed into taxonomic marker gene tables and functional gene-abundance tables, and also enables the targeted reconstruction of population genomes of specific, potentially uncultivated taxa.

All data are housed at the National Centre for Biotechnology Information under bioproject PRJNA385736 and also through the AMI data portal (https://data.bioplatforms.com/organization/about/australian-microbiome).

To allow for the highest possible flexibility for users, the AMI provides searchable, fully processed amplicon data in the form of single nucleotide variants, partially-processed data in the form of a unique sequences table, and unprocessed data in the form paired end read (R1, R2) and indexed read (I1, I2) data in .fastq. It is important to note that due to the methods used, which are current best practice, including multiplexing of samples, different data formats may be more suitable or desirable to users asking different scientific questions.

Acknowledgements

Data was sourced from Australia's Integrated Marine Observing System (IMOS) which is enabled by the National Collaborative Research Infrastructure Strategy (NCRIS).

Data Sources

IMOS National Reference Stations.
http://imos.org.au/facilities/nationalmooringnetwork/nrs/

References

Azam, F. (1998). Microbial control of oceanic carbon flux: The plot thickens. *Science, 280*(5364), 694-696. doi:10.1126/science.280.5364.694

Brown, M. V., van de Kamp, J., Ostrowski, M., Seymour, J. R., Ingleton, T., Messer, L. F., . . . Bodrossy, L. (2018). Data Descriptor: Systematic, continental scale temporal monitoring of marine pelagic microbiota by the Australian Marine Microbial Biodiversity Initiative. *Scientific Data, 5*. doi:10.1038/sdata.2018.130

Falkowski, P. G., Fenchel, T., & DeLong, E. F. (2008). The microbial engines that drive earth *Biogeochemical Cycles, 3*, 1034-1040.

Farrant, G. K., Dore, H., Cornejo-Castillo, F. M., Partensky, F., Ratin, M., Ostrowski, M., . . . Garczarek, L. (2016). Delineating ecologically significant taxonomic units from global patterns of marine picocyanobacteria. *Proceedings of the National Academy of Sciences of the United States of America, 113*(24), E3365-E3374. doi:10.1073/pnas.1524865113

Flombaum, P., Gallegos, J. L., Gordillo, R. A., Rincon, J., Zabala, L. L., Jiao, N. A. Z., . . . Martiny, A. C. (2013). Present and future global distributions of the marine Cyanobacteria Prochlorococcus and Synechococcus. *Proceedings of the National Academy of Sciences of the United States of America, 110*(24), 9824-9829. doi:10.1073/pnas.1307701110

Mazard, S., Ostrowski, M., Partensky, F., & Scanlan, D. J. (2012). Multi-locus sequence analysis, taxonomic resolution and biogeography of marine Synechococcus. *Environmental Microbiology, 14*(2), 372-386. doi:10.1111/j.1462-2920.2011.02514.x

Moran, M. A., Belas, R., Schell, M. A., González, J. M., Sun, F., Sun, S., . . . A., B. (2007). Ecological genomics of marine roseobacters. *Applied and Environmental Microbiology 73*(14).

Worden, A. Z., Follows, M. J., Giovannoni, S. J., Wilken, S., Zimmerman, A. E., & Keeling, P. J. (2015). Rethinking the marine carbon cycle: factoring in the multifarious lifestyles of microbes. *Science, 347*(6223).

IMOS

Integrated **Marine**
Observing System

IMOS
Integrated Marine Observing System

State and Trends of Australia's Oceans | Report

3.1

Water clarity around Australia – satellite and in situ observations

Peter Thompson[1] and Karlie McDonald[1]

[1] CSIRO Oceans and Atmosphere, Hobart, TAS, Australia

Summary

Water clarity, an indicator of water quality is highest offshore and lowest in coastal waters due to sediments and phytoplankton biomass. Northern areas typically have the lowest water clarity due to tidal re-suspension of sediments and high seasonal runoff.

Key Data Streams

National Reference Stations

Satellite Remote Sensing

State and Trends of Australia's Ocean Report
www.imosoceanreport.org.au

Time-Series published
10 January 2020

doi: 10.26198/5e16aafe49e80

Rationale

Water clarity is a fundamental measure of water quality used to help protect our marine environment. There are many ways it can be measured and reported. One of the best is to measure the reduction in light with depth over many metres (Lee et al., 2015). This integrating method improves the scientific value of the measurement so that we can better understand the state and trends in water quality. Although old technology, the Secchi Disk is an excellent tool for this type of observation (Hou, Lee, & Weidemann, 2007; Preisendorfer, 1986). Generally, Australian marine waters are low in turbidity, low in colour and high in transparency. Much of our flora and fauna are adapted to these conditions and a deterioration in transparency puts these communities and populations at increased risk of stress and impaired conditions. In oceanic and outer continental shelf waters, the major determinants of turbidity, transparency and colour is the biomass of phytoplankton (Yentsch, 1960). Most waters off Australian shores are low in phytoplankton and we thus have some of the clearest waters on the planet. Light penetrates deeply, allowing phytoplankton to grow down to >100 m. Nearshore regions of the continental shelf often have benthic communities dominated by coral or aquatic plants (e.g. seagrasses and macrophytes) that are dependent upon sunlight reaching the bottom.

Methods

The Secchi Disk method was invented in the 1800s by P.A. Secchi (first published in ‘Relazione delle esperienze fatte a bordo della pontificia pirocorvetta l’Immacolata concezione per determinare la trasparenza del mare; Memoria del P. A. Secchi’ in Il Nuovo Cimento December 1864, Volume 20, Issue 1, pp 205–238). It has a long history of use by many institutions and the length of time means it is a valuable measure of change in water transparency over long periods (Wernand, 2010). The technique involves lowering a plain white (or black and white) circular disk 30 cm in diameter on a line. The depth at which the disk is no longer visible is known as the Secchi depth and is a measure of the transparency of the water column or turbidity.

With a modest amount of training, the easy-to-use Secchi disk can provide accurate data and has been adopted in citizen science programs (for example, see http://www.secchidisk.org/). It has been applied in many scientific studies of phytoplankton productivity (Falkowski & Wilson, 1992). Because of the value of Secchi disk data, modern satellites have an algorithm to estimate Secchi depth, which is comparable to in situ measurements. The advantage of satellites is that they provide an excellent global picture of water clarity by scanning all oceans every 3 days. Here we have used Secchi Disk Depth data from NASA’s MODerate resolution Imaging Spectroradiometer (MODIS) satellite estimated using the algorithm of Morel et al. (2007).

Here we analyse the Secchi disk depth on three different scales: a regional scale (10-50°S and 100-170°E), Australia’s six bioregions (see Common Methods), and the Integrated Marine Observing System (IMOS) National Reference Stations (https://portal.aodn.org.au/; see the dataset “IMOS National Reference Station (NRS) - Total Suspended Solids (TSS) and Secchi Depth”).

Results and interpretation

Trends across the region

On a regional scale around Australia, water transparency declines strongly toward shore (**Figure 1**) due to increased sediment and greater phytoplankton biomass. Areas of greatest water clarity are offshore in the Indian and Pacific Oceans. Tropical rivers in areas of high rainfall also supply large amounts of sediment to the coastal zone, increasing turbidity especially in northern seas between Australia and Indonesia (**Figure 1**). These turbid waters can have strong seasonality, with the turbidity increasing by up to 3 orders of magnitude during the tropical monsoon season and can cover extensive areas in our tropical seas. During tropical cyclones, both runoff and bottom disturbance by waves can also generate substantial turbidity in shallow areas such as the Gulf of Carpentaria. Waves also contribute to turbidity, and shallow water bodies with a large fetch are more turbid than deeper water bodies or those with lower wind speed or fetch. Areas with large tides (e.g. NW coast) or tidally flushed creeks can also have high turbidity and shallow Secchi depth.

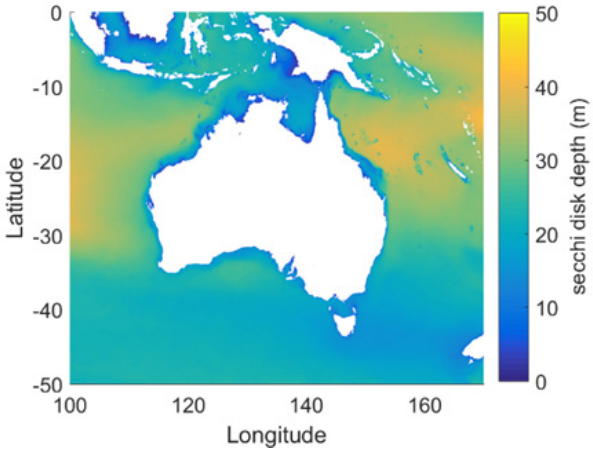

Figure 1. Water transparency as estimated by MODIS satellite across the Australian region (50°S to equator, 100°E to 170°E) from 2003 to 2019.

Water clarity within the Australian EEZ

Within Australia’s continental EEZ, the average Secchi disk depth was 24 m. Water clarity was best and the depth greatest in the NE, particularly the Coral Sea. Secchi depth was generally much lower nearshore, low in the Gulf of Carpentaria, and low through Bass Strait and around Tasmania (**Figure 3**). The temporal pattern of Secchi depth in the EEZ was similar to the broader region.

doi: 10.26198/5e16aafe49e80

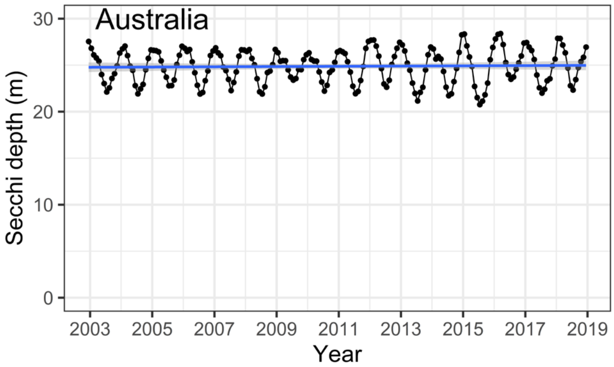

Figure 2. Estimated mean monthly Secchi disk depth (m) across the Australian region (0-50°S, 100-170°E) from December 2002 to January 2019. Blue dashed line is least squares regression. Moderate seasonal and inter-annual is evident. There was no significant long-term trend in water transparency.

Over the entire EEZ, Secchi depth was similar to that within the Australian region but minimum seasonal values were lower, possibly reflecting the reduction in the relative amount of open ocean. While seasonal variation was also high in the EEZ, there was no long-term trend detected (**Figure 4**).

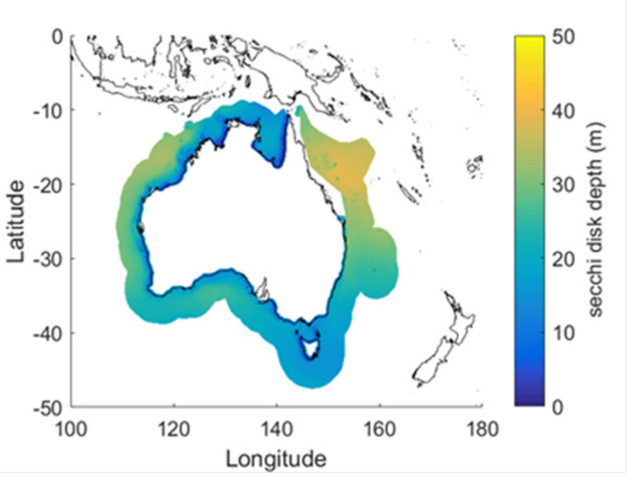

Figure 3. Estimated mean Secchi disk depth (m) across the Australian EEZ from December 2002 to January 2019.

Water clarity in Australia's six bioregions

All six bioregions around the coast of Australia were significantly different from each other in terms of their mean water clarity (P<0.01), except the Temperate East (mean Secchi depth = 26 m) and North West bioregions (mean = 26.2 m, **Figure 5**, **Table 1**). The North bioregion had the lowest Secchi depth – i.e. the lowest water transparency and the most opaque waters. The Coral Sea had the clearest waters, followed by the North West and Temperate East (**Table 1**). All bioregions showed some seasonal variability in Secchi depth, with largest seasonal changes in the Temperate East, North West and Coral Sea (**Figure 6**). The North and the South East bioregions had the lowest Secchi depth and the least seasonality (**Table 1**). There were no significant long-term trends in Secchi depth from 2002 to 2019 in any bioregion (**Figure 7**).

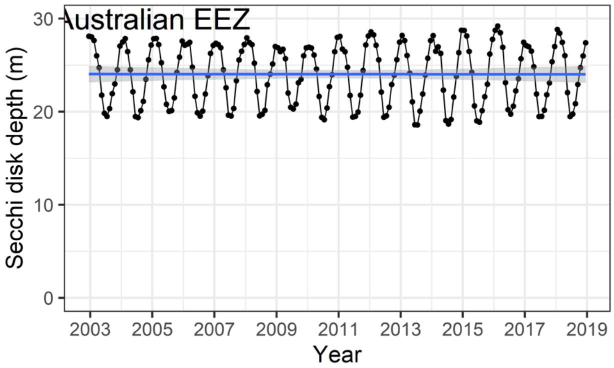

Figure 4. Estimated mean monthly Secchi Disk Depth (m) for the Australian EEZ from December 2002 to January 2019. Blue dashed line is least squares regression. No long-term trend was detected.

The IMOS National Reference Stations (NRS)

From the IMOS NRS stations around Australia, Darwin had the lowest Secchi depth and North Stradbroke Island had the greatest (**Figure 8**), a pattern broadly reflecting satellite observations and providing much needed validation of patterns detected by satellites.

Table 1. Secchi disk depth data from 2003-2018 in each bioregion.

Bioregion	Mean SDD (m)	Minimum monthly mean SDD (m)	Maximum monthly mean SDD (m)	Range in monthly mean SDD (m)
North	15.8	10.7	21.0	10.3
Temperate East	26.0	18.1	36.3	18.3
North West	26.2	17.0	32.7	15.6
South West	23.1	16.6	30.1	13.5
South East	17.2	13.6	21.5	7.9
Coral Sea	35.8	27.0	41.9	15.0

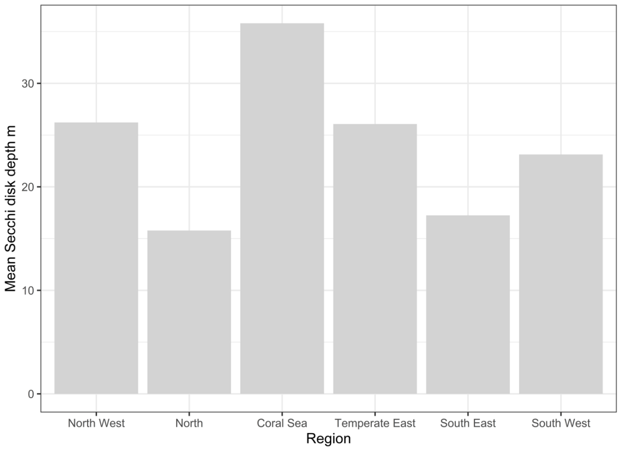

Figure 5. Mean Secchi Disk Depth (m) for each bioregion over the period of analysis (2002-2019).

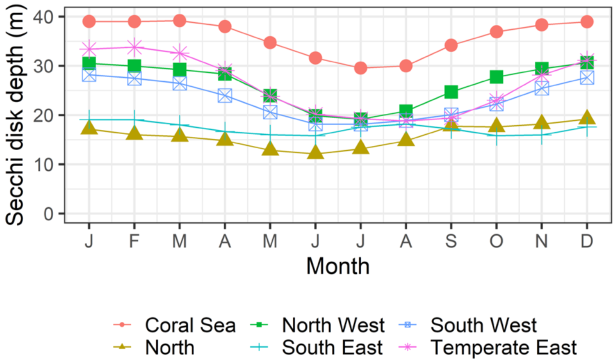

Figure 6. Seasonal cycle of water clarity estimated as Secchi Disk Depth (SDD, m) for Australia's 6 bioregions (2003 – 2018).

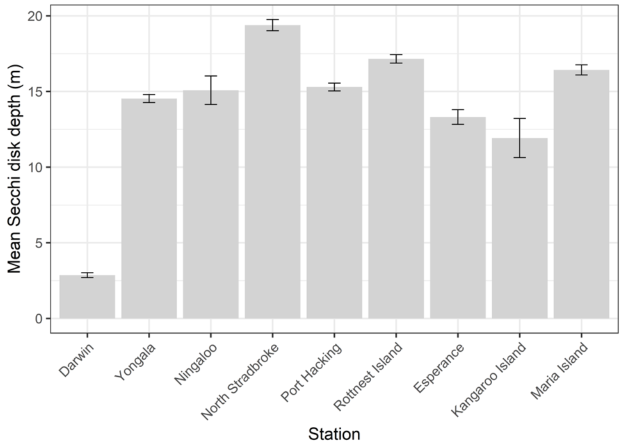

Figure 7. Monthly average estimated Secchi disk depth (m) for each of the six Australian bioregions, from 2003 to 2018.

Implications for people and ecosystems

In this study there were significant spatial differences in water clarity around Australia with northern areas having low Secchi depths in association with tidal re-suspension of sediments and high seasonal runoff. Seasonal differences in Secchi depth tended to be greatest in the Temperate East, North West and Coral Sea. There were no long-term trends evident in the data.

One of the most widely used measures of water quality is transparency. Most of Australia's marine waters are highly transparent (i.e, a large secchi depth). Exceptions can be found in many estuaries and some coastal areas with high tidal currents that resuspend sediments. The high transparency is critical to the growth of organisms that are crucial to marine ecology such as phytoplankton, seagrass, seaweeds and corals. All marine animals depend on these organisms for food or habitat or both.

Because of its ease of use, low cost and integrating nature, the Secchi disk is a valuable tool for the assessment of water quality. It is well suited to citizen science projects and can provide robust assessments of water quality to help protect our aquatic ecosystems from degradation. It is particularly suited to monitoring in lakes, streams, rivers, estuaries and the coastal zone, where many pressures are causing widespread declines in water quality. More observations in different habitats would improve our knowledge of where more attention is needed to reduce any developing problems in water quality.

doi: 10.26198/5e16aafe49e80

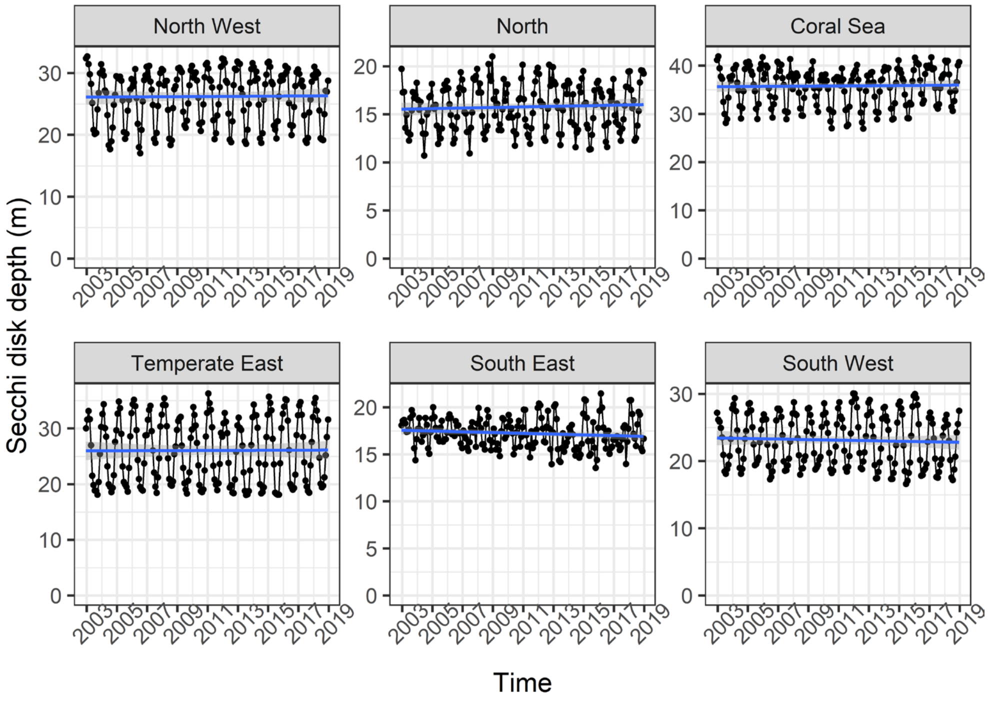

Figure 8. Mean measured Secchi Disk Depth (m) from monthly IMOS National Reference Stations from 2008 to 2017. Note that monitoring at Ningaloo (NIN) and Esperance (ESP) ceased in 2013 and that Kangaroo Island (KAI) and Darwin (DAR) have a quarterly sampling program.

Data Sources

IMOS National Reference Stations.

http://imos.org.au/facilities/nationalmooringnetwork/nrs/

NASA MODIS

https://modis.gsfc.nasa.gov/data/

References

Falkowski, P. G., & Wilson, C. (1992). Phytoplankton productivity in the North Pacific ocean since 1900 and implications for absorption of anthropogenic CO2. *Nature, 358*(6389), 741-743. doi:10.1038/358741a0

Hou, W., Lee, Z., & Weidemann, A. D. (2007). Why does the Secchi disk disappear? An imaging perspective. *Optics Express, 15*(6), 2791-2802. doi:10.1364/OE.15.002791

Lee, Z., Shang, S., Hu, C., Du, K., Weidemann, A., Hou, W., . . . Lin, G. (2015). Secchi disk depth: A new theory and mechanistic model for underwater visibility. *Remote Sensing of Environment, 169*, 139-149. doi:10.1016/j.rse.2015.08.002

Morel, A., Huot, Y., Gentili, B., Werdell, P. J., Hooker, S. B., & Franz, B. A. (2007). Examining the consistency of products derived from various ocean color sensors in open ocean (Case 1) waters in the perspective of a multi-sensor approach. *Remote Sensing of Environment, 111*(1), 69-88. doi: 10.1016/j.rse.2007.03.012

Preisendorfer, R. W. (1986). Secchi disk science: Visual optics of natural waters. *Limnology and Oceanography, 31*(5), 909-926. doi:10.4319/lo.1986.31.5.0909

Wernand, M. R. (2010). On the history of the Secchi disc. *Journal of the European Optical Society - Rapid publications; Vol 5 (2010)*. Retrieved from https://www.jeos.org/index.php/jeos_rp/article/view/10013s

Yentsch, C. S. (1960). The influence of phytoplankton pigments on the colour of sea water. *Deep Sea Research (1953), 7*(1), 1-9. doi: 10.1016/0146-6313(60)90002-2

IMOS

Integrated **Marine**
Observing System

IMOS
Integrated Marine
Observing System

State and Trends of
Australia's Oceans

Report

3.2

Spatial and seasonal trends in *Trichodesmium*

Claire Davies[1], Ruth Eriksen[1] and Anthony J. Richardson[2,3]

[1] CSIRO Oceans and Atmosphere, Hobart, TAS, Australia

[2] CSIRO Oceans and Atmosphere, Queensland Biosciences Precinct (QBP), St Lucia, QLD, Australia

[3] Centre for Applications in Natural Resource Mathematics (CARM), School of Mathematics and Physics, The University of Queensland, St Lucia, QLD, Australia

Summary

Trichodesmium is an important nitrogen fixer especially in oligotrophic areas of the oceans and a major component of primary production. Monitoring the changes in abundances and seasonal variations in *Trichodesmium* around Australia help us to understand which environmental variables are driving abundance and distribution. It appears that sea surface temperature and phosphate availability are the major drivers for increased abundances in the GBR. The increased abundances we are seeing over time at the Yongala National Reference Station may be a response to climate change and will have implications for nutrient cycling in the region.

Key Data Streams

Ships of Opportunity

National Reference Stations

State and Trends of Australia's Ocean Report
www.imosoceanreport.org.au

Time-Series published
10 January 2020

doi: 10.26198/5e16abb949e81

Rationale

Trichodesmium is a large filamentous marine cyanobacterium (**Figure 1**), notable for its ability to fix atmospheric nitrogen. It forms extensive, high biomass surface blooms visible from space. These blooms are known in Australia as “sea sawdust” and were noted by Captain James Cook sailing down the Great Barrier Reef in 1770. *Trichodesmium* blooms can be a major contributor to primary production in tropical systems. By fixing atmospheric nitrogen, *Trichodesmium* introduces “new” nitrogen into the low-nutrient waters (Blondeau-Patissier et al., 2018), supplementing the limited regenerated nitrogen. *Trichodesmium* is important in the global nitrogen cycle and is the only genus resolved in the eReefs biogeochemical model of the Great Barrier Reef (Skerratt et al., 2019).

When present in high densities, *Trichodesmium* can provide food and habitat for a diverse range of organisms including zooplankton (O'Neil, 1998) (**Figure 1**). *Trichodesmium* produces potent neurotoxins, causing respiratory distress and contact dermatitis in humans (Schock et al., 2011). *Trichodesmium* thus has potential for significant environmental and economic impacts. Large blooms or surface expressions of *Trichodesmium* typically indicate cells and filaments no longer actively growing, and have ceased their characteristic vertical migration in the water column they use to search for optimal nutrient conditions (Villareal and Carpenter, 1990).

Whilst strongly associated with the tropics due to its preference for warm waters (the mean Species Temperature Index is 26.1°C from IMOS records), the genus is widely observed in the IMOS Continuous Plankton Recorder and National Reference Station samples (typically at low concentrations but occasionally in blooms) around Australia. A variety of morphological forms are observed, but true species diversity is poorly understood, and is currently the focus of genetic studies.

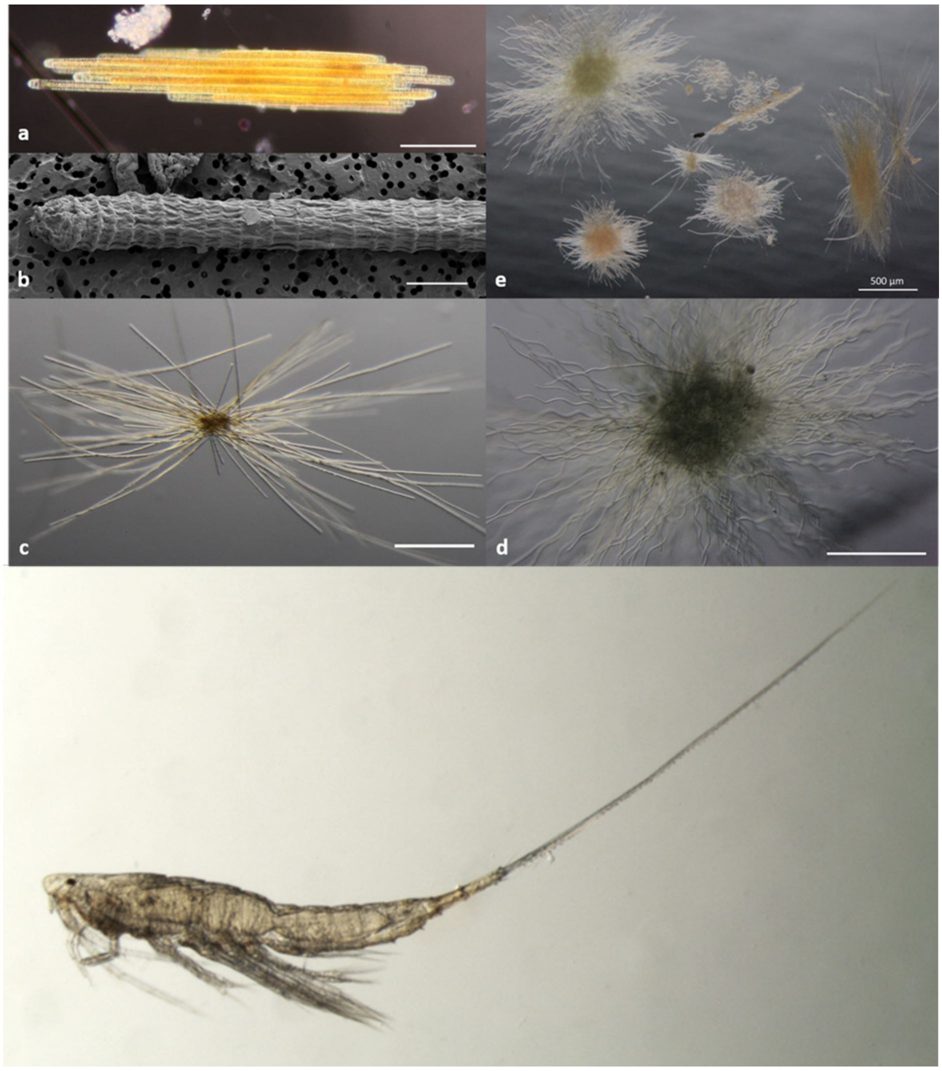

Figure 1. *Trichodesmium* morphology from the east coast of Australia. Straight filamentous forms from Yongala viewed under a) a light microscope (scale bar 100 µm) and b) a scanning electron microscope (scale bar 10 µm).c) A “Tuft” form from Yongala (scale bar 100 µm) and d) a “puff” form from Port Hacking (scale bar 100 µm). e) A composite collection of various forms of filamentous cyanobacteria from Port Hacking (scale bar 500 µm). Images a) Ruth Eriksen CSIRO, b) Gustaaf Hallegraeff IMAS, c-e) Julian Uribe Palomino CSIRO (see Robson et al. in prep.). f) The marine copepod *Macrosetella gracilis*, which uses *Trichodesmium* as a food source and physical substrate for all aspects of its life-cycle (image: A. Slotwinki CSIRO).

Methods

Time-series observations of *Trichodesmium* around Australia were compiled from counts at the IMOS National Reference Stations (Eriksen et al. (2019) and the Australian Continuous Plankton Recorder survey. At the IMOS National Reference Stations, we used counts from zooplankton net samples rather than abundance estimates from phytoplankton bottles as is more typical. This was because zooplankton net samples (volume of water sampled = 10s of m^3 water sampled) had far fewer absences of *Trichodesmium* than phytoplankton bottle samples (several litres) because of the larger volume sampled. We used additional observations of *Trichodesmium* from the Australian Phytoplankton Database available on the AODN (Davies et al., 2016). All data were sourced from the AODN (https://portal.aodn.org.au/; see the datasets "IMOS National Reference Station (NRS) - Zooplankton Abundance", "IMOS - AusCPR: Phytoplankton Abundance", and "The Australian Phytoplankton Database (1844 - ongoing) - abundance and biovolume").

As *Trichodesmium* is most abundant at the Yongala National Reference Station, we explored its environmental drivers there. We used a linear model to investigate how abundance is related to a suite of environmental drivers including sea surface temperature, phosphate concentration, mixed layer depth, and month at this site. We used a harmonic term – a mix of sine and cosine waves – to model the seasonal cycle. SST data were sourced from GHRSST (http://rs-data1-mel.csiro.au/thredds/catalog.sstL3Syts.html?dataset=l3s_sst_day_1dts) and Chl-a data from MODIS (http://rs-data1-mel.csiro.au/thredds/dodsC/imos-srs/oc/aqua/). Phosphate concentration and mixed layer depth were from concurrent measurements at Yongala (https://portal.aodn.org.au/; see the dataset "IMOS National Reference Station (NRS) - Salinity, Carbon, Alkalinity, Oxygen and Nutrients (Silicate, Ammonium, Nitrite/Nitrate, Phosphate"). Predictors were retained in the model based on AIC (Akaike's Information Criterion).

To investigate the spatial distribution of *Trichodesmium* around Australia and how it varies seasonally, we developed a species distribution model using a generalised linear model using a suite of environmental predictors, including sea surface temperature, phosphate concentration, water column depth (bathymetry) and month. We used a negative binomial error structure, which can better model count data with a preponderance of zeros than a more typical Poisson distribution.

Results and Interpretation

Trichodesmium has been observed at almost all locations sampled around the Australian coastline, although it is rare outside tropical waters. Its presence in more southerly and seasonally cooler waters is often the result of prevailing winds and currents. In tropical waters of Yongala, *Trichodesmium* has been observed in all but one of the monthly net samples collected since 2009 (n = 120), and an increase in abundance has been observed over the monitoring period (**Figure 2**). Abundances at Darwin, Rottnest Island, North Stradbroke Island and Port Hacking are generally lower, and vary more seasonally than at Yongala (**Figure 2**). Overall, abundances have declined significantly at North Stradbroke Island over the past decade. *Trichodesmium* is rarely observed in southern Australia, with one occurrence at Kangaroo Island and it has never been seen at Maria Island.

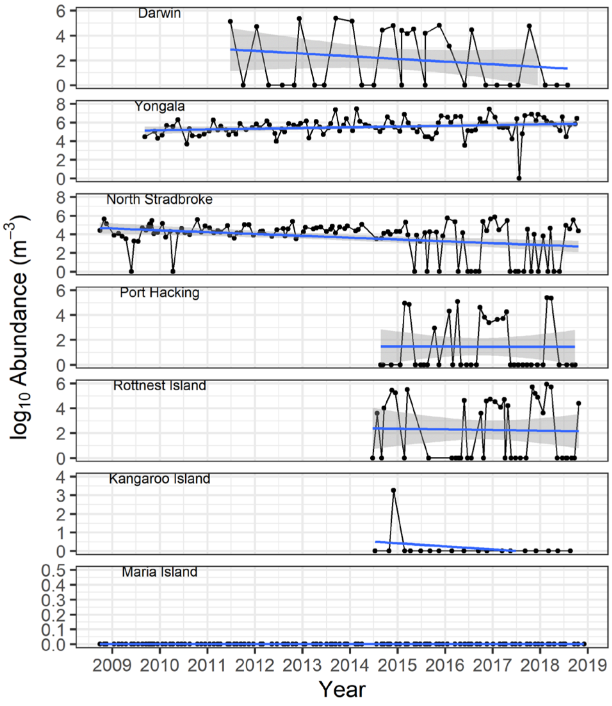

Figure 2. *Trichodesmium* abundance at the IMOS National Reference Stations, based on counts of monthly zooplankton net samples.

At Yongala, the strongest predictor of *Trichodesmium* abundance was the seasonal cycle, with abundance increasing in spring, dipping slightly in summer, before increasing again in autumn and declining in winter (**Figure 3**). The next most important predictor was Year, exhibiting a strong increasing trend in *Trichodesmium* abundance. We also found that more phosphate and deeper mixed layers corresponded to higher *Trichodesmium* abundances. SST, chlorophyll-a and iron concentration were not significant.

The generalised linear model of *Trichodesmium* around Australia showed that the more tropical National Reference Stations (Yongala and North Stradbroke Island) had higher *Trichodesmium* abundance compared with other areas (**Figure 4**). The decline in abundance from northern to southern areas is evident. There was also a marked seasonal cycle, very similar to that observed at Yongala. There were high abundances in spring and autumn, with a slight dip in summer, and a large dip in winter. There is evidence for vertical migration, with higher *Trichodesmium* abundances at night (note that we could not test for this at Yongala because all samples were collected during the day). In terms of bathymetry, the *Trichodesmium* abundance declines strongly offshore. *Trichodesmium* is rare in water <20°C, peaks in water of ~23°C, then the abundance declines gently to 31°C. This is similar to other studies that have found a preferred temperature niche of 24-29°C (Bergman et al., 2013).

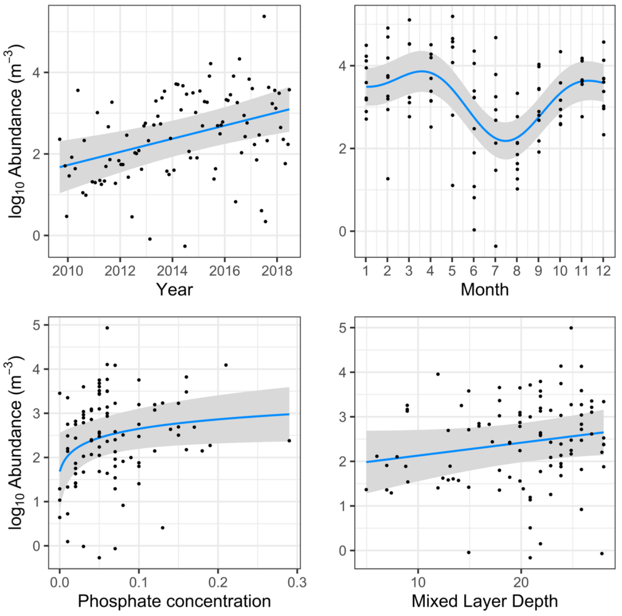

Figure 3. Effect plots for the linear model at the Yongala NRS, showing the influence of key parameters on *Trichodesmium* abundance.

Counterintuitively, *Trichodesmium* was inversely related to phosphate concentration, in contrast to the model from Yongala alone. *Trichodesmium* abundance increases with iron concentration, similar to the model for Yongala. *Trichodesmium* abundance increased with chlorophyll-a concentration, whereas chlorophyll-a was found not to be important at Yongala.

The map of the distribution of *Trichodesmium* based on the generalised linear model shows a tropical inshore distribution (**Figure 5**). Temperature was the most significant driver, and bathymetry was also important in determining *Trichodesmium* abundance (**Figure 4**). The model provides an integrated picture of the seasonal distribution of *Trichodesmium*, as well as expected abundance in areas that have not been sampled, or only sampled infrequently such as the North West Coast (**Figure 5**). It is clear that *Trichodesmium* extends further south during summer.

Implications for people and ecosystems

We found a significant increase in *Trichodesmium* abundance at Yongala. This increase will enhance the capture of new nitrogen into the oligotrophic waters of the region and will undoubtedly have implications for nutrient cycling. The increase is consistent with hypothesised impacts of climate change on phytoplankton communities in nutrient-poor regions.

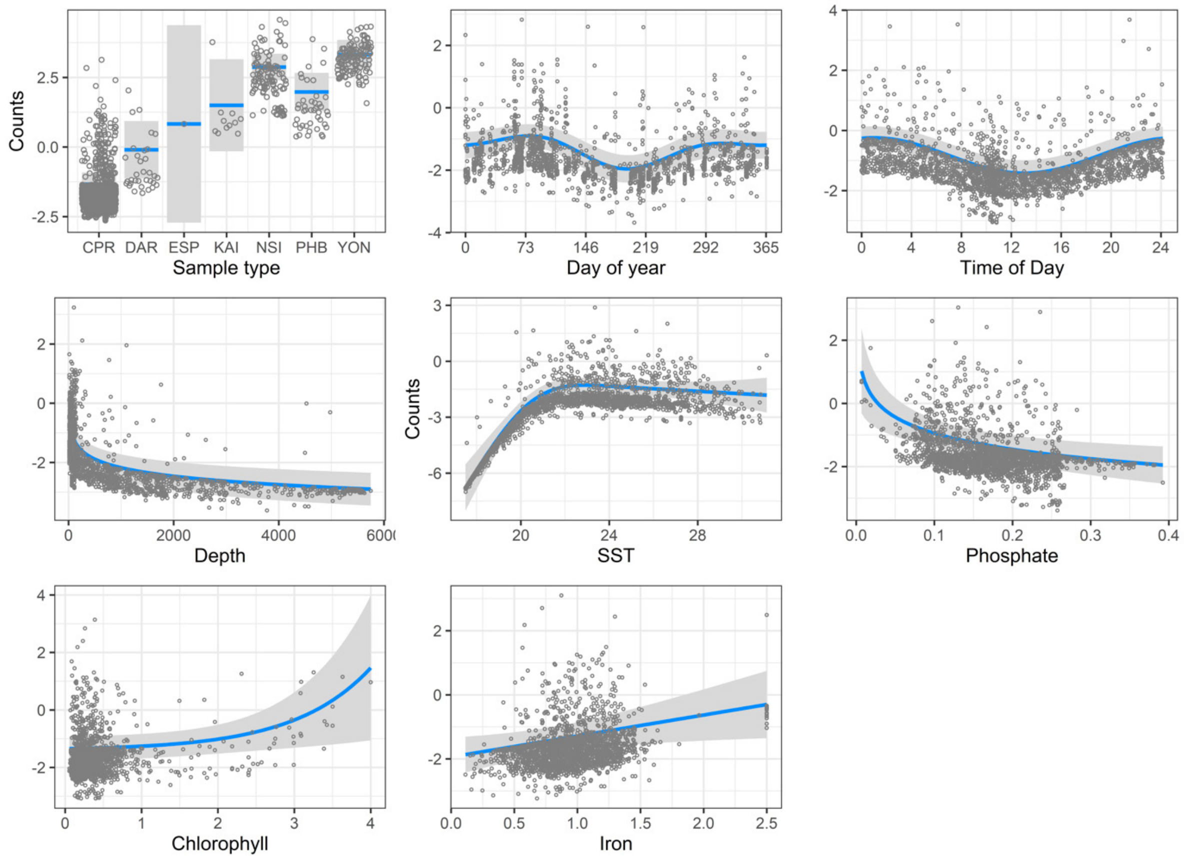

Figure 4. Negative binomial model output for distribution and abundance of *Trichodesmium* around Australia.

doi: 10.26198/5e16abb949e81

Because of enhanced stratification and the subsequent decline in surface nutrient conditions with climate change, nitrogen fixers such as *Trichodesmium* are expected to benefit (Beardall and Stojkovic, 2006).

Although surface expressions of *Trichodesmium* may extend for many hundreds of kilometres (Blondeau-Patissier et al., 2018) it is currently unknown whether the increase in *Trichodesmium* at Yongala is indicative of a broader phenomenon across the Great Barrier Reef. We also noted an overall decline in *Trichodesmium* abundance at North Stradbroke Island, although causes of this change are unclear. Although changes in *Trichodesmium* abundance can have large effects on nutrient cycling, the degree to which *Trichodesmium* is used directly by higher trophic levels is also a subject of debate. There is a small but obligate community that lives on it, which includes the harpacticoid copepod, *Macrosetella gracilis* (**Figure 1f**). This species uses the filaments as a food source and as a protective substrate when young (O'Neil 1998).

Our observations confirm that *Trichodesmium* is a tropical species, with high abundances at warmer temperatures and in warmer months (although slightly lower in the middle of summer). We see the distribution of *Trichodesmium* extending further south during summer and receding north during winter. The southerly extent of *Trichodesmium* could be a good indicator of climate change. We will be monitoring whether it is making more frequent and deeper incursions into southerly areas. This is similar to the red tide species *Noctiluca*, which we have seen increase its range further south.

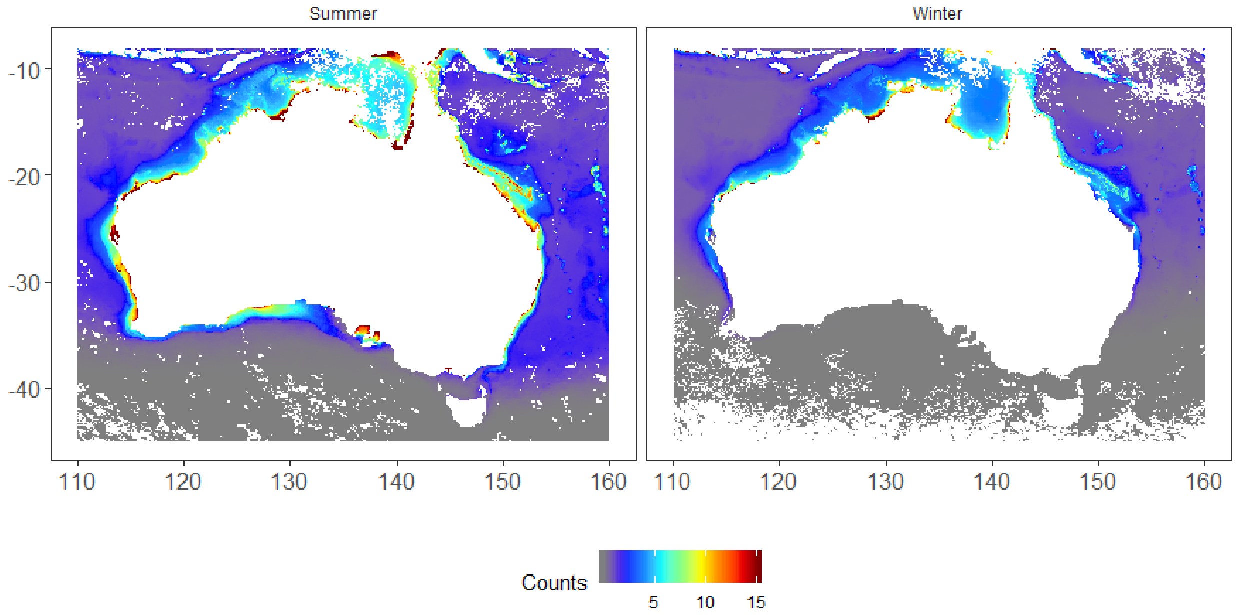

Figure 5. Seasonal distribution maps of *Trichodesmium* abundance, based on a negative binomial error structure with a suite of environmental predictors.

doi: 10.26198/5e16abb949e81

Acknowledgements

Data was sourced from Australia's Integrated Marine Observing System (IMOS) which is enabled by the National Collaborative Research Infrastructure Strategy (NCRIS).

Data Sources

IMOS National Reference Stations.
http://imos.org.au/facilities/nationalmooringnetwork/nrs/

IMOS Ships of Opportunity.
http://imos.org.au/facilities/shipsofopportunity/

References cited

Beardall, J., & Stojkovic, S. (2006). Microalgae under global environmental change: Implications for growth and productivity, populations and trophic flow. ***ScienceAsia, 32***. doi:10.2306/scienceasia1513-1874.2006.32(s1).001

Bergman, B., Sandh, G., Lin, S., Larsson, J., & Carpenter, E. J. (2013). Trichodesmium– a widespread marine cyanobacterium with unusual nitrogen fixation properties. ***FEMS Microbiology Reviews, 37***(3), 286-302. doi:10.1111/j.1574-6976.2012.00352.x

Blondeau-Patissier, D., Brando, V. E., Lønborg, C., Leahy, S. M., & Dekker, A. G. (2018). Phenology of Trichodesmium spp. blooms in the Great Barrier Reef lagoon, Australia, from the ESA-MERIS 10-year mission. ***PLoS ONE, 13***(12), e0208010. doi:10.1371/journal.pone.0208010

Davies, C. H., Coughlan, A., Hallegraeff, G., Ajani, P., Armbrecht, L., Atkins, N., . . . Richardson, A. J. (2016). A database of marine phytoplankton abundance, biomass and species composition in Australian waters. ***Scientific Data, 3***, 160043. doi:10.1038/sdata.2016.43

Eriksen, R. S., Davies, C. H., Bonham, P., Coman, F. E., Edgar, S., McEnnulty, F., . . . Richardson, A. J. (2019). Australia's long-term plankton observations: the Integrated Marine Observing System National Reference Station network. ***Frontiers in Marine Science***.

O'Neil, J. M. (1998). The colonial cyanobacterium Trichodesmium as a physical and nutritional substrate for the harpacticoid copepod Macrosetella gracilis. ***Journal of Plankton Research, 20***(1), 43-59. doi:10.1093/plankt/20.1.43

Schock, T., Huncik, K., Beauchesne, K., Villareal, T., & Moeller, P. (2011). Identification of Trichotoxon, a novel chlorinated compound associated ith the bloom forming cyanobacterium ***Trichodesmium thiebautii***. ***Environmental Science & Technology, 45***, 7503-7509. doi:dx.doi.org/10.1021/es201034r

Skerratt, J. H., Mongin, M., Wild-Allen, K. A., Baird, M. E., Robson, B. J., Schaffelke, B., . . . Steven, A. D. L. (2019). Plankton and nutrient dynamics on the Great Barrier Reef: Skill assessment and analysis of the eReefs biogeochemical model. ***Journal of Marine Systems, 192***, 51-74.

Villareal, T., & Carpenter, E. (1990). Diel buoyancy regulation in the marine diazotrophic cyanobacterium ***Trichodesmium thiebautii***. ***Limnology and Oceanography, 35***(8), 1832-1837.

doi: 10.26198/5e16abb949e81

IMOS
Integrated Marine Observing System
State and Trends of Australia's Oceans | Report

3.3 *Tripos* dinoflagellates as indicators of Australian marine bioregions

Gustaaf Hallegraeff[1], Claire Davies[2] and Ruth Eriksen[2]

[1] Institute for Marine and Antarctic Studies, University of Tasmania, Hobart, TAS, Australia
[2] CSIRO Oceans and Atmosphere, Hobart, TAS, Australia

Summary

While the distributions of a large number of the total of 50+ Australian *Tripos* dinoflagellate species have remained remarkably stable over the past 60-80 years, we identified a group of 8 rare tropical species that deserve careful attention in monitoring for range expansions, changes in seasonality or incursion of deep tropical waters.

Key Data Streams

Ships of Opportunity

National Reference Stations

Australian Ocean Data Network

State and Trends of Australia's Ocean Report
www.imosoceanreport.org.au

Time-Series published
10 January 2020

doi: 10.26198/5e16ac0f49e82

Rationale

Dinoflagellates belonging to what used to be referred to as the genus *Ceratium*, now redesignated *Tripos*, are widespread in marine waters, particularly outside the polar waters. The genus exhibits an amazing morphological diversity, with >77 species and numerous varieties and forms documented globally, and with numerous regional taxonomic monographs (**Figure 1**). Many studies hint at the potential of using *Tripos* species as water mass indicators to detect environmental change, which has been quantitatively explored for the North Atlantic (Dodge & Marshall, 1994) and the Mediterranean Sea (Tunin-Ley, Ibanez, Labat, Zingone, & Lemée, 2009). Previous comprehensive *Tripos* surveys of Australian species include Wood's (1954) dinoflagellate monograph of 71 taxa. These early studies produced the first conclusive biological evidence for what is now called the Leeuwin Current, which occasionally transports dinoflagellates from the Indian Ocean all the way to the west coast of Tasmania. Huisman (1989) focused on *Tripos* in 7 years (1979-1985) of net samples from Bass Strait (32 taxa). In adjoining Indian Ocean waters, Taylor (1976) characterized 56 *Tripos* taxa. In the period 1978-1984, as part of a series of CSIRO Division of Fisheries & Oceanography cruises, Hallegraeff and co-workers (1984) reported *Tripos* species from New South Wales coastal waters, East Australian Current eddies, the Coral Sea, North West Shelf and Gulf of Carpentaria. Here we summarise *Tripos* species in Australian tropical, subtropical, temperate and Southern Ocean environments.

Methods

Observations since 2007 were based on 614 Integrated Marine Observing System (IMOS) National Reference Station and 4263 Continuous Plankton Recorder samples from the Australian and Southern Ocean Continuous Plankton Recorder Surveys, and the phytoplankton and zooplankton samples from the IMOS National Reference Stations (Eriksen et al., 2019). Historical records of *Tripos* were obtained from the Australian Phytoplankton Database (8818 records) (Davies et al., 2016). All data were sourced from the AODN (https://portal.aodn.org.au/; see the datasets IMOS National Reference Station (NRS) - Phytoplankton Abundance and Biovolume", "IMOS - AusCPR: Phytoplankton Abundance", and "The Australian Phytoplankton Database (1844 - ongoing) - abundance and biovolume").

Results and Interpretation

Tripos in Australian waters exhibit a striking species richness, with most offshore sample locations containing 5-10 species. *Tripos* is best collected by phytoplankton or zooplankton nets, such as the surface to 100 µm drop nets in the Coral Sea, which also catch deep "shade" species (Sournia (1982). Tunin-Ley et al. (2009) in the Mediterranean Sea determined that a minimum sample volume of 70 L was needed for a sound estimate of *Tripos* species richness. The traditional bottle sampling of phytoplankton is insufficient.

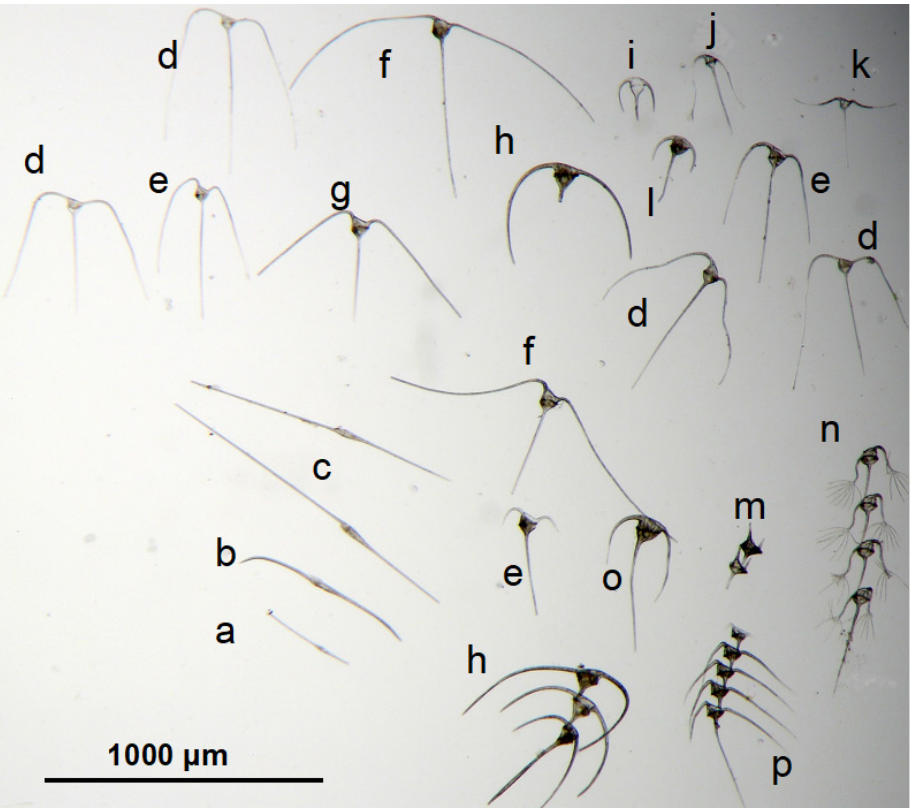

Figure 1. A selection of Tripos dinoflagellate species from the Port Hacking station off Sydney, Australia, hand-picked, sorted and photographed on the same scale (1000 µm). a. *Tripos fusus*; b. *T. falcatus*; c. *T. biceps*; d. *T. trichoceros*; e. *T. macroceros*; f. *T. carriensis*; g. *T. massiliensis*; h. *T. lunula*; i. *T. symmetricus*; j. *T. claviger*; k. *T. patentissimus*; l. *T. muelleri*; m. *T. candelabrus*; n. *T. ranipes*; o. *T. muelleri var. atlanticus*; p. *T. vultur. Micrograph* J. Uribe-Palomino.

doi: 10.26198/5e16ac0f49e82

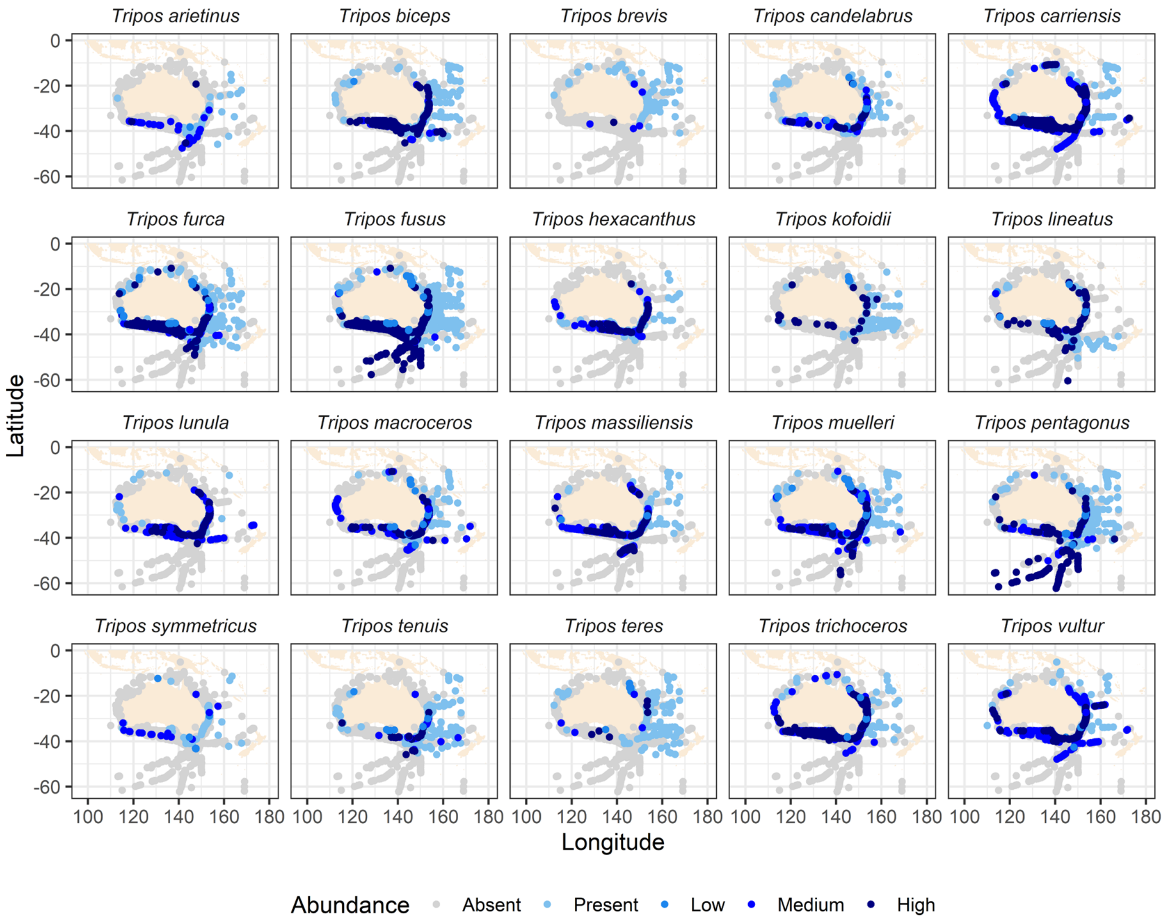

Figure 2. Collation over the period 1940-2019 of Australia-wide distribution records of 20 Tripos species.

Some apparent decadal shifts in Australian distribution patterns (**Figure 2**) simply reflect the fact that Wood's sampling focus was on the East Coast of Australia, while IMOS sampling covered the entire region.

The majority of *Tripos* species exhibit broad temperate to subtropical to tropical temperature preference (10-25°C), which essentially covers all Australian waters. This limits the use of *Tripos* indicator species in the Australian region. This is well demonstrated by the distributions of *Tripos carriense, T. falcatus, T. furca, T. fusus, T. gibberus, T. hexacanthus, T. limulus, T. massiliense, T. muelleri, T. platycornis,* and *T. ranipes*, which have remained remarkably stable in Australian waters over the past 60-80 years (**Figure 3**, **Figure 4**). It is noted that some species which are used as warm-water indicators in the North Atlantic (e.g. *T. hexacanthus*, 7-30°C, but "prefers higher temperature") are not necessarily diagnostic for warm waters of the Australian region (**Figure 4**). Similarly, Tunin-Ley et al. (2009) observed some strictly warm-water species such as *T. digitatus* in winter in the Mediterranean Sea.

Using the strict definition of stenothermal tropical species, agreed to by both Dodge & Marshall (1994) and Taylor (1976), we identified a restricted group of warm-water species including *T. belone, T. cephalotus, T. dens, T. digitatus, T. gravidus, T. incisus, T. paradoxides, and T. praelongus* (**Figure 5**).

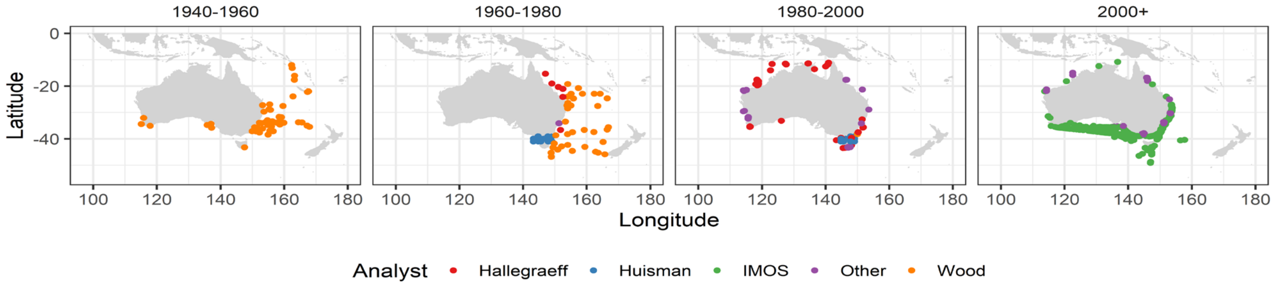

Figure 3. Sixty+ years of Australian distribution records of the widespread Tripos furca reflect temporal shifts in sampling efforts.

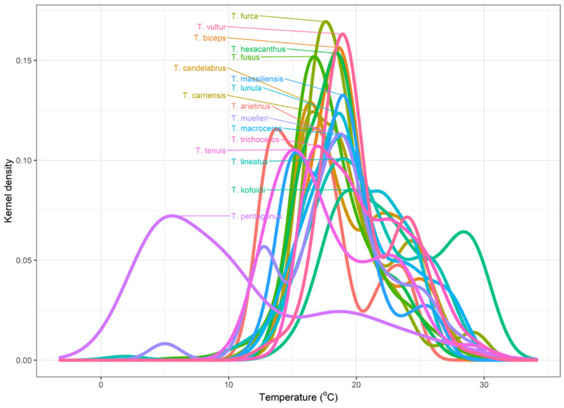

Figure 4. Thermal preferences of *Tripos* species estimated from IMOS data using kernel density. The temperature which gives the highest kernel density value is the Species Temperature Index (STI) and is a measure of whether a species prefers warm or cold water.

These tropical species are commonly encountered off Sydney (*T. digitatus, T. gravidus*), and more rarely down to Eden and Batemans Bay (*T. praelongus,* Sept 84) or Bass Strait (Huisman 1989: *T. gravidus, T. paradoxides*), but have occasionally been observed as far south as King Island (*T. cephalotus*, August 84) and even Tasmania off Maria Island (*T. gravidus* Sept 84) and the Huon River (*T. gravidus* Dec 2013, Nov 2018). These comparatively rare tropical Australian *Tripos* species are probably carried south on the East Australian Current and deserve careful attention in monitoring for future range expansions, changes in seasonality (**Figure 6**), or signs of upwelling/incursion of deep tropical waters (Sournia, 1982).

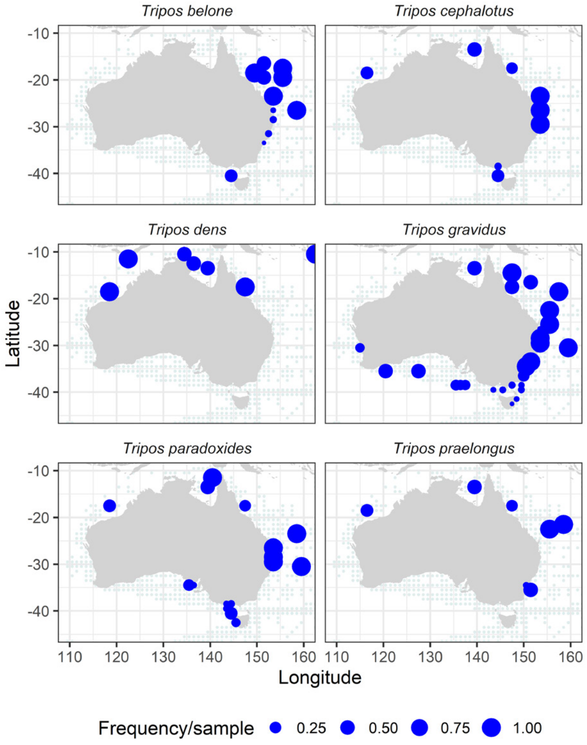

Figure 5. Australian distribution records of 6 stenothermal warm-water *Tripos* species.

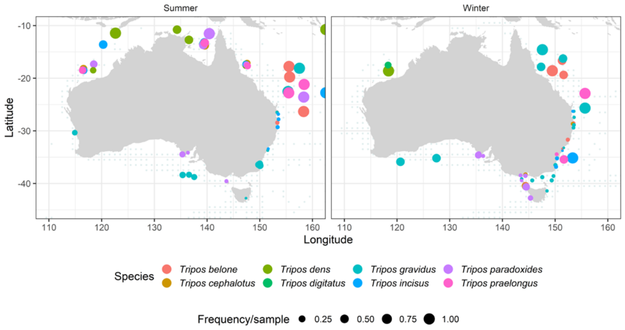

Figure 6. Seasonality of stenothermal warm-water *Tripos* species reflects upwelling in the Coral Sea, East Australian Current activity in summer, and Leeuwin Current activity in winter, as first postulated by Wood 1954.

Implications for people and ecosystems

Phytoplankton have been used successfully to increase our knowledge of the extent of water mass circulation by acting as indicator species. The ability to monitor changes in the extent and persistence of changes in water mass circulation relies heavily on long-term biological time-series, with sufficient taxonomic resolution to provide quantitative evidence of species range shifts or thermal niches (Buchanan, Swadling, Eriksen, & Wild-Allen, 2013; Eriksen et al., 2019). *Tripos* is a valuable indicator in this regard, but it is only through the careful curation of historical datasets, and species level data that these lines of evidence can be utilised. Shifts in species ranges due to changes in environmental conditions in the pelagic environment can have impacts on the food availability for higher trophic levels, potentially affecting the commercial and recreational fisheries that depend upon these food resources. Now that we have a validated dataset on *Tripos* from the 1940s to the present, the next step will be to derive indicators of change that are robust to the different sampling methods and focal regions.

Acknowledgements

Data was sourced from Australia's Integrated Marine Observing System (IMOS) which is enabled by the National Collaborative Research Infrastructure Strategy (NCRIS).

Data Sources

IMOS National Reference Stations.
http://imos.org.au/facilities/nationalmooringnetwork/nrs/

IMOS Ships of Opportunity.
http://imos.org.au/facilities/shipsofopportunity/

Australian Phytoplankton Database available through the AODN.
https://portal.aodn.org.au/search?uuid=75f4f1fc-bee3-4498-ab71-aa1ab29ab2c0

References

Buchanan, P. J., Swadling, K. M., Eriksen, R. S., & Wild-Allen, K. (2013). New evidence links changing shelf phytoplankton communities to boundary currents in southeast Tasmania. ***Reviews in Fish Biology and Fisheries***. doi:DOI 10.1007/s11160-013-9312-z

Davies, C. H., Coughlan, A., Hallegraeff, G., Ajani, P., Armbrecht, L., Atkins, N., . . . Richardson, A. J. (2016). A database of marine phytoplankton abundance, biomass and species composition in Australian waters. ***Scientific Data, 3***. doi:10.1038/sdata.2016.43

Dodge, J. D., & Marshall, H. G. (1994). Biogeographic analysis of the armored plankton dinoflagellate ***Ceratium*** in the North Atlantic and adjacent seas. ***Journal of Phycology, 30***(6), 905-922. doi:10.1111/j.0022-3646.1994.00905.x

Eriksen, R. S., Davies, C. H., Bonham, P., Coman, F. E., Edgar, S., McEnnulty, F., . . . Richardson, A. J. (2019). Australia's long-term plankton observations: the Integrated Marine Observing System National Reference Station network. ***Frontiers in Marine Science, 6***(Article 161), 17.

Hallegraeff, G. M., & Jeffrey, S. W. (1984). Tropical phytoplankton species and pigments of continental shelf waters of north and northwest Australia. ***Marine Ecology Progress Series, 20***(1-2), 59-74. Retrieved from <Go to ISI>://A1984TT15600007

Huisman, J. M. (1989). The genus *Ceratium* Dinophyceae in Bass Strait and adjoining waters Southern Australia. ***Australian systematic botany, 2***(4), 425-454. Retrieved from <Go to ISI>://ZOOREC:ZOOR12600052147

Sournia, A. (1982). Is there a shade flora in the marine plankton? ***Journal of plankton research, 4***(2), 391-399.

Taylor, F. J. R. (1976). ***Dinoflagellates from the International Indian Ocean Expedition: A report on material collected by the R.V. "Anton Bruun" 1963-1964***. ***Bibliotheca Botanica, 132,*** 1-234.

Tunin-Ley, A., Ibanez, F., Labat, J.-P., Zingone, A., & Lemée, R. (2009). Phytoplankton biodiversity and NW Mediterranean Sea warming: Changes in the dinoflagellate genus Ceratium in the 20th century, ***Marine Ecology Progress Series, 375***, 85-90.

Wood, E. J. F. (1954). Dinoflagellates in the Australian region. ***Australian Journal of Marine and Freshwater Research, 5***((2)), 171-351. Retrieved from <Go to ISI>://ZOOREC:ZOOR09100014862

doi: 10.26198/5e16ac0f49e82


IMOS
Integrated Marine
Observing System

3.4 Harmful Algal Blooms and the shellfish industry

Steve Brett[1], Claire Davies[2], Ruth Eriksen[2] and Anthony J. Richardson[3,4]

[1] Microalgal Services, Ormond, VIC, Australia
[2] CSIRO Oceans and Atmosphere, Hobart, TAS, Australia
[3] CSIRO Oceans and Atmosphere, Queensland Biosciences Precinct (QBP), St Lucia, QLD, Australia
[4] Centre for Applications in Natural Resource Mathematics (CARM), School of Mathematics and Physics, The University of Queensland, St Lucia, QLD, Australia

Summary

We found that HAB species of concern to the Australian shellfish industry are widely distributed in Southeast Australia. The dinoflagellate species most commonly above levels that trigger an industry response are *Dinophysis acuminata* and *Dinophysis caudata*. While *Prorocentrum lima* is often recorded above trigger levels, elevated toxins have not been detected in association with these events. Key HAB species have increased in abundance slightly over the past 10 years in Southern and Northern NSW, but are stable in Central NSW and Port Phillip Bay.

Key Data Streams

Australian Ocean Data Network

State and Trends of Australia's Ocean Report
www.imosoceanreport.org.au

Time-Series published
10 January 2020

doi: 10.26198/5e16ac8149e83

Rationale

Harmful Algal Blooms (HABs) occur when toxic or nuisance species of phytoplankton grow rapidly, leading to high abundances that can impact human health and marine life, and can often cause substantial economic losses to aquaculture, tourism, and hospitality industries. The most common problems with HABs in Australia are the accumulation of toxins in seafood that is then ingested by people, and fish kills from the toxins or from low dissolved oxygen in the water associated with the breakdown of phytoplankton blooms. Some phytoplankton species are problematic at low cell concentrations, i.e., even without a visible bloom. Because toxins can accumulate in the food chain, there is regular monitoring of marine species, particularly for shellfish harvest, to prevent impacts on human health. Monitoring usually includes a combination of phytoplankton community composition, environmental parameters, and analysis of toxin profiles in seafood products destined for human consumption.

Although HABs are natural, some might be exacerbated by global change, including eutrophication, climate change, and translocation (Wells et al., 2015, Hallegraeff, 2010).

Globally, the Intergovernmental Oceanographic Commission (Moestrup et al., 2009-2019) maintains a list of ~180 harmful phytoplankton species. Locally, public health, seafood safety and export agencies maintain lists of species deemed to be a risk in each particular region. These key species form the basis of monitoring programs. Here we analyse weekly phytoplankton data from a range of monitoring programs from the coast of mainland Southeast Australia to identify problem species, where they are found, their interannual trends and how often their levels exceed regulatory guidelines. Ultimately it is hoped that these data will help us understand the environmental triggers of blooms and toxin production.

Methods

We analysed weekly data on HAB species collated in the Australian Phytoplankton Database (Davies et al., 2016) focusing on mainland Southeast Australia from 2003-2019. This includes data from shellfish industry monitoring programs and State and local government monitoring programs outside of aquaculture areas. This database compilation represents the largest publicly-available HAB dataset in Australia, and includes species that produce toxins accumulated by shellfish, as well as species that may cause other harmful or nuisance effects to fish or people. A subset of species monitored by the shellfish industry in Australia is shown in **Table 1**. It focuses on potentially harmful dinoflagellate species where robust species-level data are available through routine monitoring programs. Also shown are the relevant trigger levels or thresholds for each species. When the abundance of a HAB species is above its trigger level, further investigations including tissue testing of potentially affected shellfish is undertaken. Trigger levels were sourced from the NSW Phytoplankton Action Levels (NSW Food Authority, 2015) (**Table 1**).

For regional and seasonal analysis, we focused on 12 dinoflagellate species from five of the most common dinoflagellate genera. Southeast Australia was divided into four subregions that reflect the major areas of shellfish industry for which data are publicly available: Northern NSW, Central NSW, Southern NSW and Port Phillip Bay Victoria. We used Principal Components Analysis (PCA) to describe interannual and seasonal patterns in these regions for selected HAB dinoflagellate species. We used a hellinger transformation so that abundant species did not dominate. The 1st principal component scores were plotted so that most species had positive loadings (i.e., positive correlations with PC1).

Results and Interpretation

Over the 15 years of sampling in Southeast Australia, 20 HAB genera that produce toxins or cause problems for aquaculture or public amenity have been observed (**Figure 1**). The most common genus is the diatom *Pseudo-nitzschia*, although only some species in this group are toxic, and species-level detection is difficult with standard microscopy alone. Other common genera are the dinoflagellates *Prorocentrum, Alexandrium* and *Dinophysis*, which have many toxic species. Six genera are also associated with fish kills; viz. *Amphidinium, Fibrocapsa, Heterosigma, Karenia, Karlodinium*, and *Takayama*.

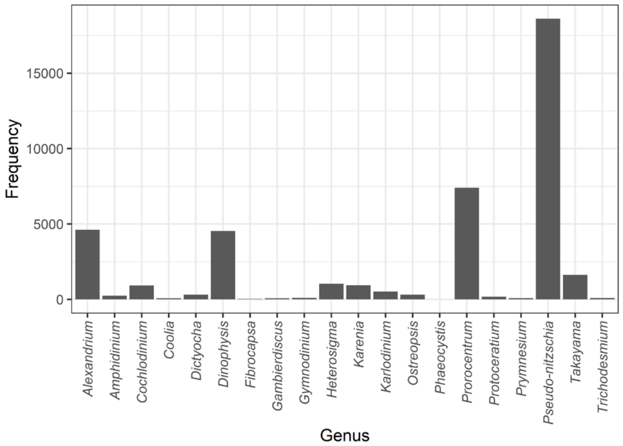

Figure 1. The frequency of occurrence of harmful algal bloom genera around the coast of mainland Southeast Australia. Not all genera are associated with toxin production, other effects include gill irritation in fish, visual impacts and skin or respiratory irritation.

Our analysis of 12 dinoflagellates routinely discriminated to species level show there are some notable patterns in the seasonal distribution of these harmful species (**Figure 2**). In general, the dinoflagellate HAB species in the regions are not highly seasonal with most species found in all seasons, even in the colder waters of the south.

Table 1. Summary of dinoflagellate species included in this analysis, and their associated shellfish toxin syndrome or other major impacts (see [1] for more details). Trigger levels listed for shellfish are based on the NSW Marine Biotoxin Management Plan (2015)[2]. Discrimination of the species listed is based on stable morphological characteristics that can be routinely observed by microscopy, by suitably trained personnel.

Species	Toxin syndrome	Symptoms	Trigger level	Comment
Alexandrium pacificum (formerly *A. catanella*)	Paralytic Shellfish Poisoning (PSP)	Nausea, vomiting, diarrhoea, abdominal pain, tingling or burning lips, gums, face, neck, legs and toes	200 cells L^{-1}	Toxic in Australia
A. minutum	PSP		200 cells L^{-1}	Toxic in Australia
A. ostendfeldii	PSP		200 cells L^{-}1	Toxicity of local strains have not been verified
A. australiense (formerly *A. tamarense*)	PSP		200 cells L^{-1}	Toxic in Australia
Gymnodinium catenatum	PSP		1000 cells L^{-1} (see 3) 2000 cells L^{-1} (see 4)	Toxic in Australia
Karenia mikimotoi	Fish killer	NA	NA (See 5)	Unknown toxicity in Australia
Dinophysis acuminata	Diarrhetic Shellfish Poisoning (DSP)	Diarrhea, nausea, vomiting, cramps	1000 cells L^{-1}	Toxic in Australia, no fatalities recorded to date.
D. acuta	DSP		500 cells L^{-1}	No reports of DSP associated with these species to date
D. caudata	DSP		500 cells L^{-1}	
D. fortii	DSP		500 cells L^{-1}	
D. tripos	DSP		500 cells L^{-1}	
Prorocentrum lima	DSP		500 cells L^{-1}	Rare, probably a species complex.

[1] Ajani, P and Murray, S (2016) “A Review of Toxic Algal Species towards Improving Management of Toxic Blooms in New South Wales” Climate Change Cluster University of Technology Sydney

[2] NSW Food Authority. (2015). Marine Biotoxin Management Plan: http://www.foodauthority.nsw.gov.au/_Documents/industry/marine_biotoxin_management_plan.pdf

[3] Mussels

[4] Other shellfish

[5] Victorian Marine Biotoxin Management Plan (2015) management protocol for the *Karenia/Karlodinium* group recommends a warning issued to growers when concentrations for *Karenia* species other than *K. brevis* reach 100,000 cells/L.

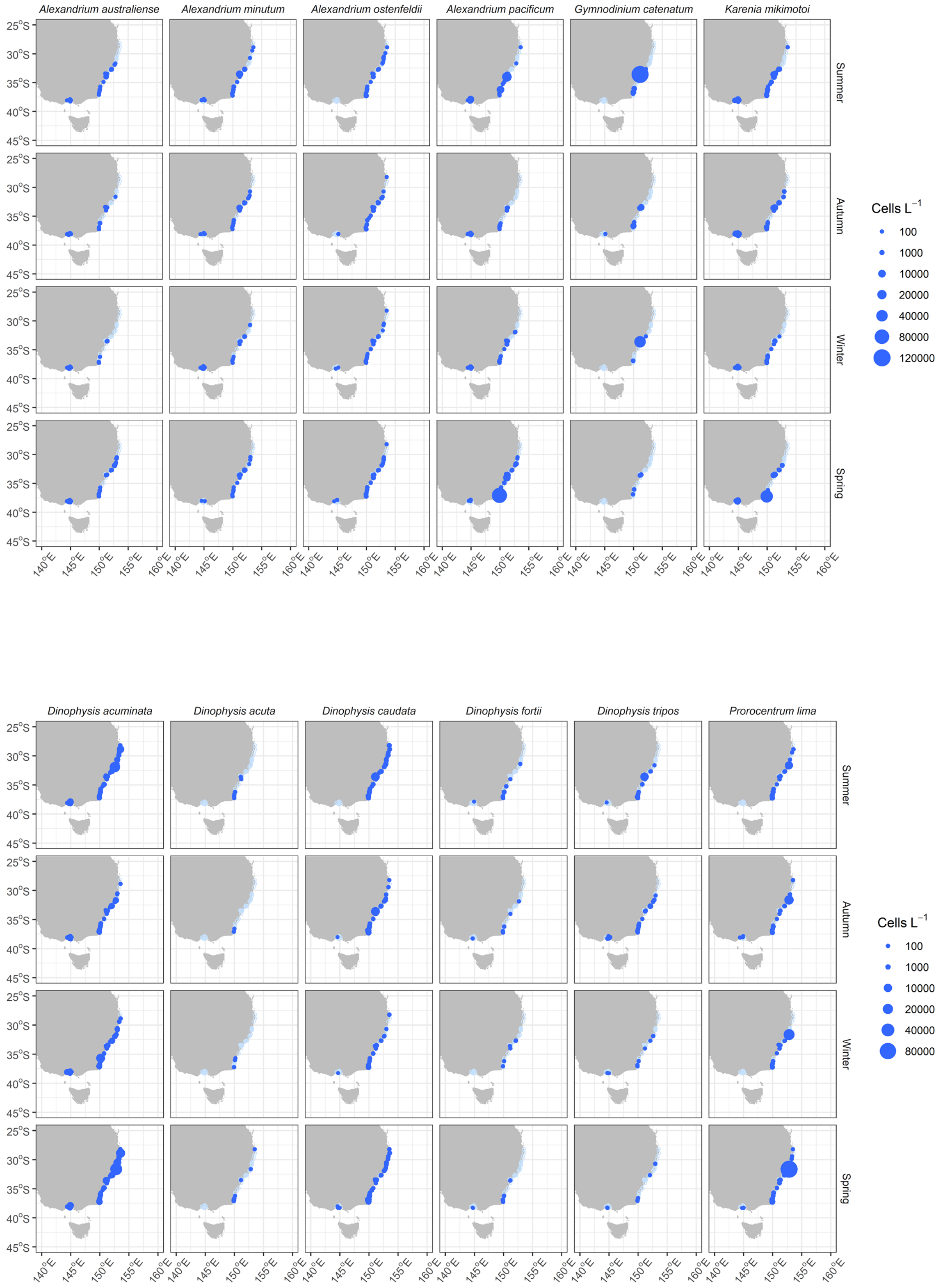

Figure 2. Spatial distribution of key HAB dinoflagellate species by season, across mainland Southeast Australia. Empty circles (light blue) represent samples collected and analysed but no cells were detected for that species.

doi: 10.26198/5e16ac8149e83

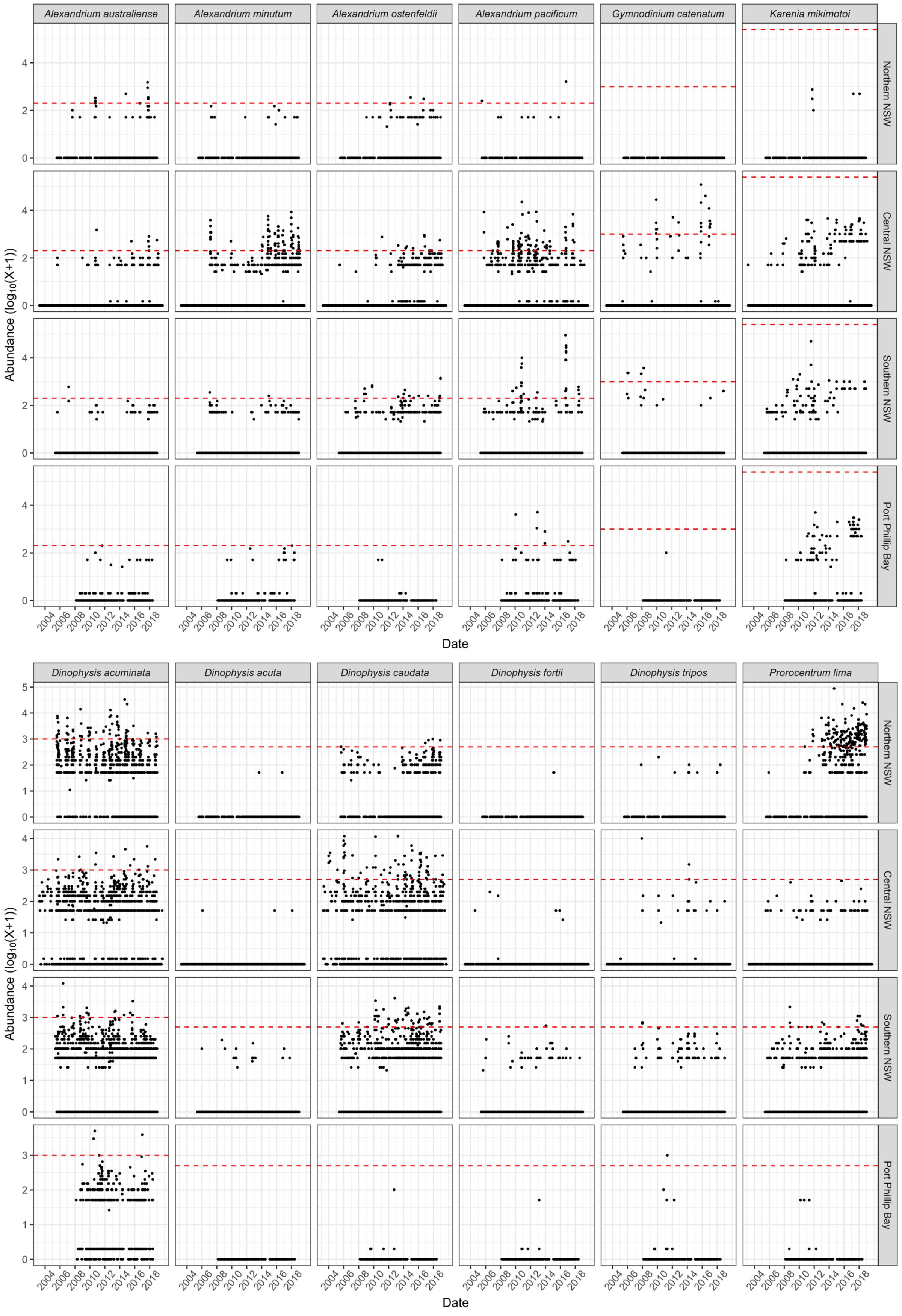

Figure 3. Trends in the abundance of selected dinoflagellate HAB species in Southeast Australia, in relation to their trigger levels for warning growers and further testing of shellfish in aquaculture areas. Note the dots representing zero abundance for each HAB species, and that abundances are $\log_{10}$ transformed.

Occasionally there is a large increase in one species e.g *Gymnodinium catenatum* in summer, *Alexandrium pacificum* and *Prorocentrum lima* in spring, however the increase is at a small number of sites rather than across the whole region. The most abundant species is *Dinophysis acuminata,* which is present throughout the year. *Dinophysis caudata* is found in modest numbers throughout all regions, in all seasons. Some species are relatively rare, including *Dinophysis acuta*[6], *Dinophysis fortii* and *Dinophysis tripos*. *Karenia mikimotoi*, predominantly associated with fish-kills, has been observed in routine monitoring, in all regions.

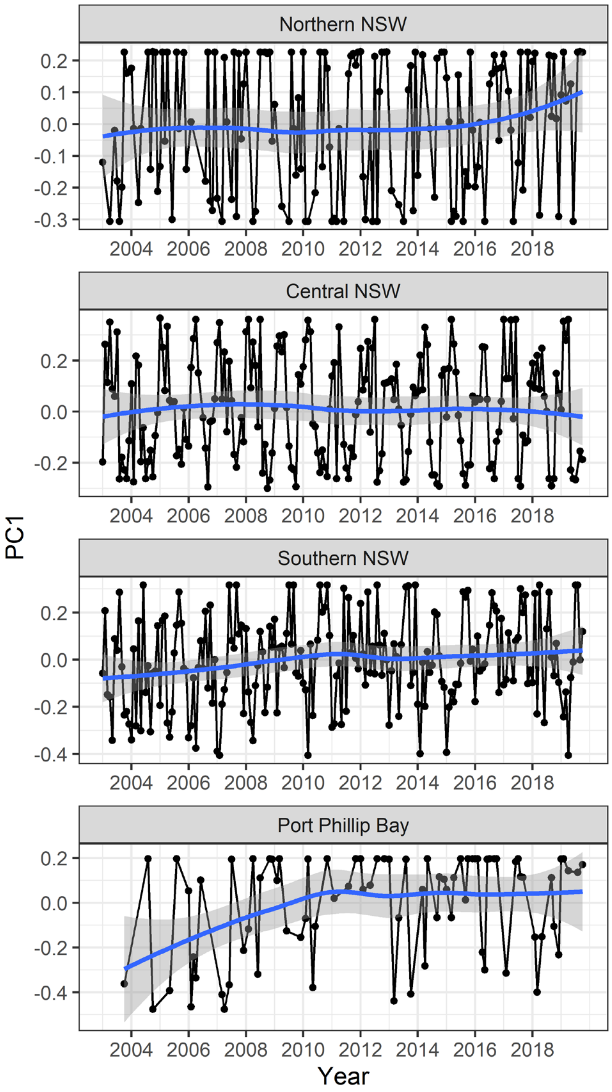

Figure 4. The first principal component (PC1) representing abundance of the dinoflagellate HAB species through time, in the four subregions in Southeast Australia.

Regionally, Central NSW appears to be a hotspot for HABs (**Figure 3**) with regular blooms of *Alexandrium minutum, Alexandrium pacificum, Dinophysis caudata* and *Gymnodinium catenatum*. In Northern NSW *Gymnodinium catenatum* has not been observed to date, and the four *Alexandrium* species of concern (*A. australiense, A. minutum, A. ostenfeldii* and *A. pacificum*) are also rarely observed there. *Prorocentrum lima* is observed routinely in this region at high concentrations, but is not commonly associated with toxin accumulation in shellfish. Other species, such as *Alexandrium pacificum, Dinophysis acuminata* and *Karenia mikimotoi* have been found in highest numbers in Southern NSW. In Port Phillip Bay, Victoria most species have been observed, but *Gymnodinium catenatum* and *Prorocentrum lima* are rare and *Dinophysis acuta* has not been recorded.

Monitoring of waters of Southeast Australia shows all the HAB species analysed here are most commonly found at background environmental levels, below aquaculture trigger levels (**Figure 3**). Two species, *Dinophysis acuta* and *Karenia mikimotoi* have never been above regulatory thresholds in any region. In Northern NSW, *Prorocentrum lima* is most commonly above regulatory thresholds (16.2%) and *Dinophysis acuminata* exceeds thresholds 6.0% of the time. In Central NSW three species exceeded their trigger levels about 3.5% of the time - *Alexandrium minutum, Alexandrium pacificum* and *Dinophysis caudata*. In Port Phillip Bay, HAB species are only rarely recorded above trigger levels.

Interestingly, there was a consistent pattern spatially in terms of the overall frequency of species recorded above trigger levels. It was greatest in the north and declined moving south: Northern NSW (2.0%), Central NSW (1.1%), Southern NSW (0.6%) and Port Phillip Bay (0.2%). There is also evidence of potential increases in the abundance of some HAB species in some regions. In Northern NSW, the abundance of *Prorocentrum lima* has increased, being regularly above trigger levels in recent years (although toxins are not elevated in these events). In Central NSW, *Alexandrium minutum* and *Karenia mikimotoi* have been observed more often at higher abundances, while *Alexandrium australiense* abundances have not. In Southern NSW there were also increases in *Alexandrium pacificum, Dinophysis caudata* and *Karenia mikimotoi. **Karenia mikimotoi*** in fact appears to have increased in abundance throughout mainland Southeast Australia.

Using the first principal component (PC1) based on the abundance of the 12 dinoflagellate species to summarise long-term trends, we observed a slight change over time in most regions (**Figure 4**). In recent years there was an increase in the abundance of HAB species in Northern NSW, and a weak increase in Southern NSW. By contrast, Central NSW and Port Phillip Bay showed relatively stable trends in the abundance of HAB species over the past 10 years.

---

[6] Records of *Dinophysis acuta* are so rare, and numbers so low, that unequivocal identification of this species has not been possible

Implications for people and ecosystems

We found the key dinoflagellate HAB species analysed here that are problematic for the Australian shellfish industry are widely distributed around the coast of mainland Southeast Australia. The seasonal cycles of HAB species vary across Southeast Australia. The species most commonly above the levels that trigger a management response are *Dinophysis acuminata, Dinophysis caudata* and *Prorocentrum lima,* with each of those species having a different risk profile based on actual toxin production and accumulation in shellfish. Key HAB species have increased in abundance slightly over the past 10 years in Southern and Northern NSW, but show a weaker trend in Central NSW and are relatively stable in Port Phillip Bay.

Monitoring of harmful species is vital for protection of human health, and the reputation and value of our export markets. HABs can cause significant economic impact either through toxin production, non-toxin related impacts on the health of farmed and wild-caught species, or through loss of amenity. There is increased concern for changes in the frequency, intensity, and duration of HAB events in light of our changing marine environment. *"Improved information on the linkages between HABs and climate will emerge only through the establishment and maintenance of long-term phytoplankton monitoring programmes adequately supported by environmental monitoring. At present, our understanding and ability to predict how climate may select for HABs are severely limited by the scarcity of long-term records"* (Pitcher et al. 2018). Better understanding of environmental triggers for blooms and toxin production will improve monitoring and reduce risk around harvest closures and re-opening and is the focus of both research and management agencies.

Acknowledgments

We would like to thank and acknowledge Hornsby Shire Council (NSW), NSW Food Authority and EPA Victoria for making this data available.

Data Sources

Australian Phytoplankton Database available through the AODN.
https://portal.aodn.org.au/search?uuid=75f4f1fc-bee3-4498-ab71-aa1ab29ab2c0

References

Ajani, P and Murray, S (2016) "A Review of Toxic Algal Species towards Improving Management of Toxic Blooms in New South Wales" Climate Change Cluster University of Technology Sydney doi: 10.13140/RG.2.1.3816.2160

Davies, C. H., Coughlan, A., Hallegraeff, G., Ajani, P., Armbrecht, L., Atkins, N., . . . Richardson, A. J. (2016). A database of marine phytoplankton abundance, biomass and species composition in Australian waters. ***Scientific Data, 3***, 160043. doi:10.1038/sdata.2016.43

Hallegraeff, G. M. (2010). Ocean climate change, phytoplankton community responses, and harmful algal blooms: A formidable predictive challenge. ***Journal of Phycology, 46***(2), 220-235. doi: 10.1111/j.1529-8817.2010.00815.x

Moestrup, Ø., Akselmann, R., Fraga, S., Hoppenrath, M., Iwataki, M., Komárek, J., . . . Zingone, A. E. (2009-2019). IOC-UNESCO Taxonomic Reference List of Harmful Micro Algae.

NSW Food Authority. (2015). Marine Biotoxin Management Plan: http://www.foodauthority.nsw.gov.au/_Documents/industry/marine_biotoxin_management_plan. pdf

VICTORIAN MARINE BIOTOXIN MANAGEMENT PLAN (2015) https://vfa.vic.gov.au/aquaculture/publications/shellfish-quality-asurance/marine-biotoxin-management-plan

Wells, M. L., Trainer, V. L., Smayda, T. J., Karlson, B. S. O., Trick, C. G., Kudela, R. M., . . . Cochlan, W. P. (2015). Harmful algal blooms and climate change: Learning from the past and present to forecast the future. ***Harmful Algae, 49***, 68-93. doi: 10.1016/j.hal.2015.07.009

IMOS

Integrated **Marine**
Observing System

IMOS
Integrated Marine Observing System

State and Trends of Australia's Oceans | Report

3.5 Time series of harmful algal blooms in New South Wales

Case Study 1: *Dinophysis* time series at South Ballina Beach

Hazel Farrell[1], Penelope Ajani[2], Shauna Murray[2], Phil Baker[1], Grant Webster[1], Steve Brett[3] and Anthony Zammit[1]

Case Study 2: *Alexandrium pacificum* in Twofold Bay

Abanti Barua[1,4], Penelope Ajani[2], Hazel Farrell[1], Anthony Zammit[1], Steve Brett[3], David Hill[3] and Shauna Murray[2]

[1] New South Wales Food Authority, New South Wales Department of Primary Industries, Biosecurity and Food Safety, Newington, NSW, Australia
[2] Climate Change Cluster (C3), University of Technology Sydney, Sydney, NSW, Australia
[3] Microalgal Services, Ormond, Vic, Australia
[4] Noakhali Science and Technology University, Noakhali, Bangladesh

Summary

Time-series of harmful algal blooms in New South Wales are important to manage the potential risks to human health as well as both domestic and export shellfish markets. We present two harmful bloom case studies, *Dinophysis* at South Ballina Beach and *Alexandrium pacificum* in Twofold Bay, to highlight the fluctuating and seasonal nature of harmful blooms along this coastline. There is an ongoing need for a more comprehensive understanding of the triggers of these events to safeguard the industry and consumers alike.

Key Data Streams

Australian Ocean
Data Network

State and Trends of Australia's Ocean Report
www.imosoceanreport.org.au

Time-Series published
10 January 2020

doi: 10.26198/5e16acea49e84

Rationale

Bivalve shellfish sold for human consumption in New South Wales (NSW) are sourced from wild or cultured (farmed) shellfish stocks. The high quality of freshly harvested shellfish is largely due to the healthy, productive coastal waters of NSW that supply phytoplankton, the main diet of filter-feeding oysters, mussels, cockles and pipis ('clams'). Some phytoplankton species produce biotoxins, which can bioaccumulate in shellfish and potentially threaten public health if contaminated shellfish are consumed. Monitoring programs for biotoxins routinely sample both water from shellfish growing areas and shellfish meat to manage potential risks from harmful algal blooms (HABs) to both domestic and export markets. Here we present two case studies – one for *Dinophysis* and the other for *Alexandrium* – to highlight the value of time series of harmful algal blooms.

Methods

In NSW, routine monitoring of commercial shellfish harvest (aquaculture for oysters and mussels) and wild harvest shellfish collection (pipis and cockles) are conducted in accordance with the NSW Food Authority Biotoxin Management Plan (NSW Food Authority, 2015) and the Australian Shellfish Quality Assurance Program (ASQAP) Manual (ASQAAC, 2016). If the phytoplankton action levels specified in the Biotoxin Management Plan for potentially harmful species were exceeded (e.g., >500 cells/L *Dinophysis* spp. or >200 cells L^{-1} for *Alexandrium pacificum*) then shellfish samples were collected for biotoxin analyses (see Farrell et al. 2018) for a more detailed description of sampling and biotoxin analysis).

Here we present two case studies of the value of time series monitoring for HABs in the context of shellfish harvesting. The first case study is from South Ballina Beach. Pipis (*Plebidonax deltoides*) are mainly collected from open ocean beaches on the mid-north and north coast beaches of NSW, including South Ballina beach. Here water samples for phytoplankton identification were collected weekly during the pipi harvest season from 1998-2003 (identified to species level) and 2012-2018 (to genus level). Samples were not collected between 2004 and 2011, as there was no commercial wild harvest. From 2012-2018, monitoring focused on June-December each year. Initially sampling consisted of a 1 L water sample, with an accompanying algal net tow sample. In 2012, the method changed to a 50 L water sample filtered with a 20 µm mesh phytoplankton net. Samples were collected and preserved with Lugol's iodine by fishers at various locations along South Ballina Beach, depending on where pipi stocks were available.

The second case study is from Twofold Bay, NSW. Here water samples comprising 500 – 1000 ml grab samples and a 20 µm mesh phytoplankton net surface drag sample were collected fortnightly and preserved with Lugol's iodine by trained industry samplers. In the laboratory, these samples were concentrated by gravity-assisted membrane filtration (5 µm) prior to microscopic analysis to species. Simultaneous phytoplankton net haul samples were used to assist with species identification. For the purpose of this case study, three day mean sea surface temperature (SST) and average sea surface temperature anomaly data for Twofold Bay was obtained for 24 October 2016 courtesy of Charitha Pattiaratchi, Integrated Marine Observing System (IMOS) Ocean Glider Facility.

Results and Interpretation

Case Study 1: *Dinophysis* time series at South Ballina Beach

This case study focuses on the dinoflagellate genus *Dinophysis*, which is a concern for shellfish food safety monitoring programs, as certain species produce diarrhetic shellfish toxins (DSTs: okadaic acid and dinophysistoxins). These toxins may cause gastrointestinal symptoms if contaminated shellfish are consumed. Acute cases generally subside within a few days. Some DST compounds, in laboratory studies on rodents, can cause tumours, but the effects of chronic exposure to DSTs is not well known. In NSW estuaries, long-term phytoplankton and biotoxin monitoring since 2005 have demonstrated a low incidence of *Dinophysis* spp. and DSTs in shellfish aquaculture areas (Farrell et al., 2018; Farrell et al., 2015; NSW Food Authority, 2017). However, reports of DSTs from *Dinophysis* spp. in wild harvest pipis collected from open beaches in NSW are more frequent (Farrell et al., 2018; Farrell et al., 2015). Monitoring data from South Ballina Beach on the northern coast of NSW have demonstrated a history of toxic *Dinophysis* blooms.

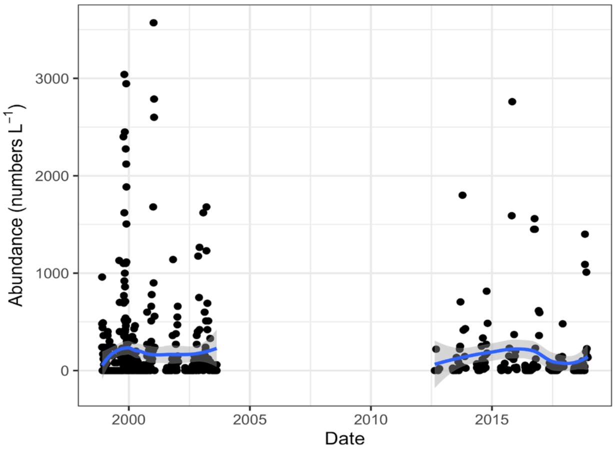

Figure 1. Time series of total *Dinophysis* spp. abundance for South Ballina Beach (1998-2018). Note that routine monitoring did not occur between 2004 and 2011, as shellfish were not collected for human consumption during this time. Blue line= least squares regression (smoothed); grey= confidence interval (as standard error) around the fitted line.

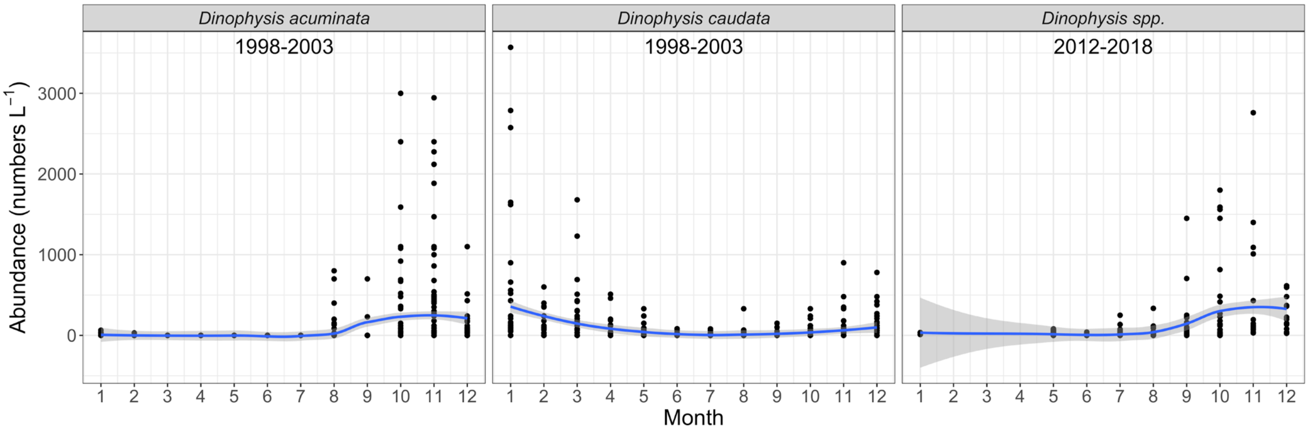

Figure 2. Seasonal cycles of *Dinophysis acuminata* (1998-2003), *Dinophysis caudata* (1998-2003) and *Dinophysis* spp. (2012-2018) from South Ballina Beach. Blue line = loess smoother; grey= confidence interval around the fitted line.

Total *Dinophysis* abundances across the two sampling periods on South Ballina Beach show concentrations up to 3,560 cells L^{-1} (**Figure 1**). Two distinct seasonal patterns were observed. *Dinophysis acuminata* and *Dinophysis caudata*, both known to produce DSTs, were reported from routine phytoplankton monitoring at South Ballina Beach between 1998 and 2003 (**Figure 2**). Peak abundances of *D. acuminata* (up to 3,000 cells L^{-1}) were observed between August and December (spring-summer), and peak abundances of *D. caudata* (up to 3,560 cells L^{-1}) were observed between December and March (summer-autumn). A similar seasonal pattern has been reported for these species in NSW oyster producing estuaries (Ajani et al., 2013; Ajani et al., 2016; Farrell et al., 2018). It should be noted that when *D. caudata* has been documented from toxic events in other locations it generally co-occurs with other toxic *Dinophysis* species (Reguera et al., 2012). While species level data were unavailable between 2012 and 2018, peak *Dinophysis* abundances were up to 2,760 cells L^{-1} between September-December (**Figure 2**). It is likely that *D. acuminata* was the main species present during these months based on its seasonal pattern between 1998 and 2003, and observations of *Dinophysis* species in NSW oyster producing estuaries at the same time (Ajani et al., 2013; Ajani et al., 2016; Farrell et al., 2018).

As biotoxin testing was primarily targeted when *Dinophysis* spp. exceeded action levels, the dataset returned a high percentage (41% of 117 samples) of positive results (**Figure 3**). In addition, pipis tend to have a slower natural depuration process for algal toxins in comparison to other shellfish (MacKenzie et al., 2002). Positive DST results were ≥50% each year between 1999 and 2003 (**Figure 3**). During 2012 and 2013, 25 and 78% of samples were positive, respectively. Biotoxin samples were not collected during 2014, as pipi collection on South Ballina Beach ceased following detection of elevated *Dinophysis* results. Data collected between 2015-2018 included samples collected directly from South Ballina Beach and from a shellfish end-product market survey (Farrell et al., 2018).

Except for 2017, positive results were reported each year. Where quantitative data were available, maximum biotoxin concentrations were reported during October 2013: 0.4 mg kg^{-1} okadaic acid (regulatory limit = 0.2 mg kg^{-1}) (Farrell et al., 2015).

Although these data reflect the fluctuating and seasonal nature of the wild harvest beach fishery, they also highlight the seasonal and episodic nature of *Dinophysis* blooms on NSW beaches. Further investigation is required to confirm that *D. acuminata* is the main source of DSTs in pipis in wild harvest shellfish and to establish the origin of the blooms and transport mechanisms for *Dinophysis* spp. along the coast of NSW.

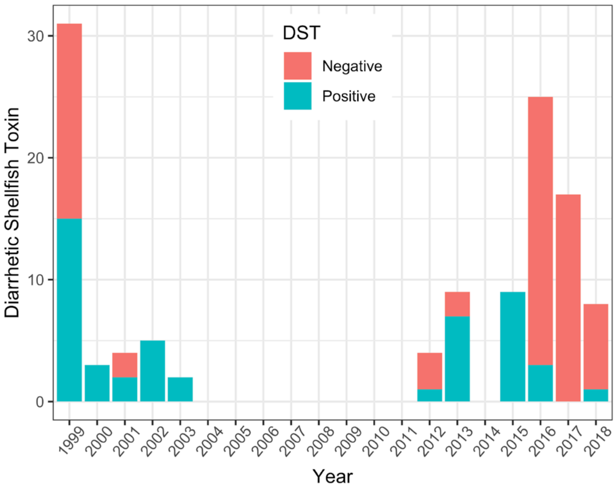

Figure 3. Time series of the number of positive and negative diarrhetic shellfish toxin (DST) results from shellfish samples from South Ballina Beach (1999-2018). Samples were collected following reports of elevated *Dinophysis* results. Data were not collected between 2004 and 2011, as shellfish were not collected for human consumption during this time. Biotoxin sample results from 2015-2017 (Farrell et al. 2018) and 2018 (ongoing end-product market survey) for South Ballina Beach are also included in the figure.

Case Study 2: *Alexandrium pacificum* in Twofold Bay

Twofold Bay is an open oceanic embayment on the south coast of New South Wales and supports a significant Blue Mussel industry. *Alexandrium* spp. accounts for >50% of all algal-related aquaculture harvest area closures in NSW (Farrell et al., 2013). This genus is included in the routine monitoring program for NSW shellfish production areas (Ajani et al., 2013; Farrell et al., 2013) to manage the potential risks of paralytic shellfish toxins (PSTs) for shellfish consumers. PSTs are another group of phycotoxins that can result in tingling of the lips, tongue, fingers and toes, muscular weakness and breathing difficulty (Ajani et al., 2017; Deeds et al., 2008). Death can occur due to respiratory failure in extreme cases (Deeds et al., 2008).

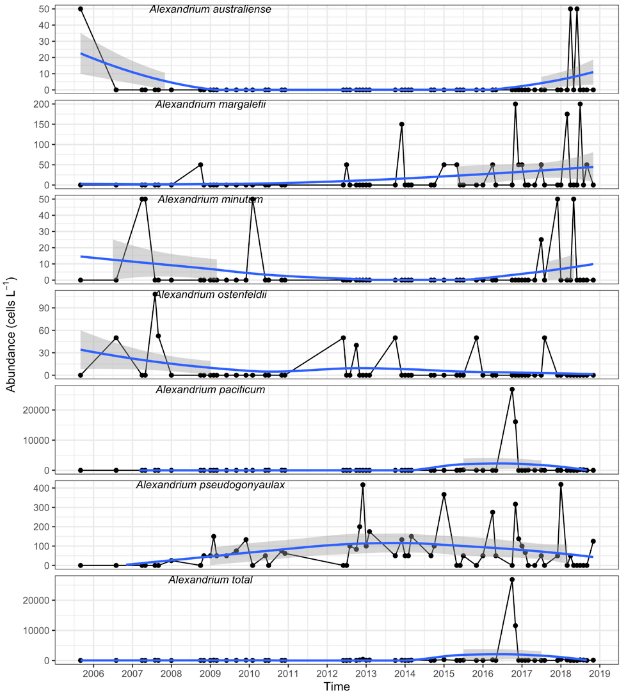

Figure 4. Abundance of *Alexandrium* spp. including *A. pacificum* from Twofold Bay, NSW. Note the different abundance scales for each species, and for total *Alexandrium*. Blue line = loess smoother; grey= confidence interval around the fitted line.

Harmful algae and their biotoxins have been routinely monitored within Twofold Bay since 2005. Historically, there is a low incidence of *Alexandrium* blooms in NSW (**Figure 4**). During October 2016, an unprecedented bloom of *Alexandrium pacificum* was detected within Twofold Bay reaching a maximum cell abundance of 89,000 cells L^{-1}, exceeding the alert level to issue a public health warning of 5000 cells L^{-1} (Barua et al. unpublished data) (**Figure 4**). The bloom persisted for at least eight weeks, with the regulatory limit for PSTs exceeded in nine Blue Mussel (*Mytilus galloprovincialis*) samples collected from within the bay (maximum 7.2 mg kg^{-1}; regulatory limit 0.8 mg kg^{-1} PST saxitoxin equivalent, **Figure 5**). Although highest cell concentrations of *Alexandrium* were detected within Twofold Bay, cell abundances ranging from 1,200 - 15,000 cells L^{-1} were detected up to 13 km north and 21 km south along the adjacent coastline. Further evidence of the bloom was detected as far as the Georges River to the north, and Wonboyn Lake to the south. SST data on 24 October 2016 indicates cold water (in the bottom 20th percentile) extending north from Bass Strait and influencing Twofold Bay (**Figure 6**), after a prolonged period of warmer than usual conditions (**Figure 7**). This cold, nutrient-rich water, is likely to have stimulated phytoplankton growth in the Bay at this time.

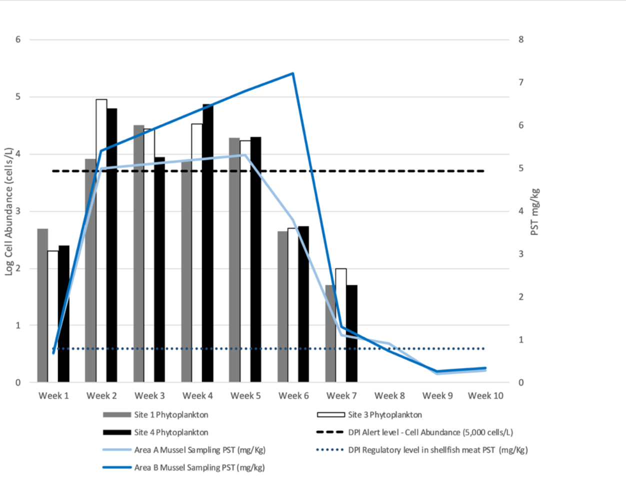

Figure 5. *A. pacificum* cell abundance, paralytic shellfish toxins concentrations, and regulatory limits for the October 2016 bloom.

The mussel harvest areas within Twofold Bay were closed during the 2016 bloom event and no shellfish exceeding the regulatory limits for PST were marketed. Advice from the regulatory authority during the bloom recommended that people not consume shellfish, sea urchins or fin fish species that are consumed whole (e.g., sardines), and to avoid consumption of the viscera from crustaceans (e.g., lobster) and gastropods (e.g., abalone) collected or caught from Twofold Bay. As a result of these warnings, no illnesses were reported from seafood consumers.

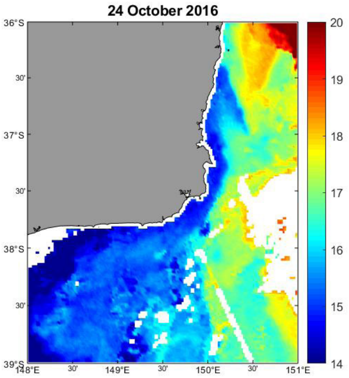

Figure 6. Three day mean sea surface temperature of the south-eastern Australian coastline on 24 October 2016 showing warm sea-surface temperature extending from the north as red and cold nutrient- rich water extending from Bass Strait in the south as blue (Figure courtesy of Charitha Pattiaratchi, Integrated Marine Observing System (IMOS) Ocean Glider Facility)

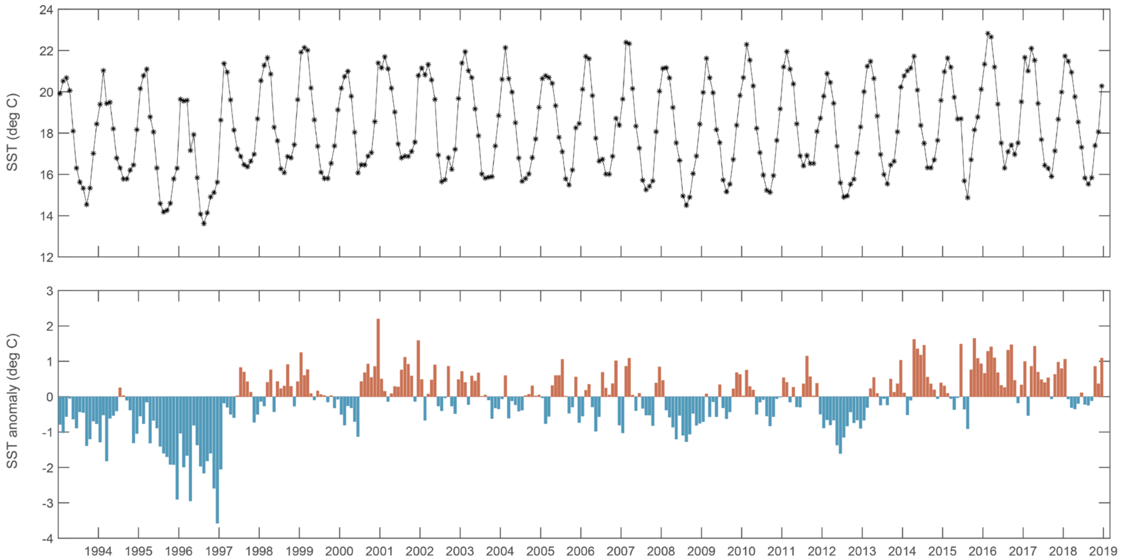

Figure 7. Mean monthly Sea Surface Temperature (SST) and SST anomaly (°C) at Twofold Bay, NSW from 2000 to 2019. (Figure courtesy of Charitha Pattiaratchi, Integrated Marine Observing System (IMOS) Ocean Glider Facility)

Implications for people and ecosystems

These time series are two examples of local monitoring programs designed to manage potential food safety risks from algal toxins when shellfish for human consumption are being collected from wild harvest areas or aquaculture operations. Wild harvest beaches or shellfish aquaculture areas are routinely closed if potentially harmful algae and/or algal toxins are detected above regulatory limits. In NSW, there were outbreaks of illness from DSTs in pipis in 1997 (northern NSW coast; 102 cases including, 46 anecdotal (Quaine et al., 1997)) and in 1998 (mid north NSW coast; >20 cases (Ajani et al, 2001; MacKenzie et al., 2002)). Since the establishment of routine monitoring for commercial wild harvest of pipis, there have been no reports of illness. Similarly, since the establishment of routine phytoplankton and biotoxin monitoring in NSW aquaculture growing areas, no illnesses related to algal toxins has been reported. In Twofold Bay, the *Alexandrium* bloom observed in 2016 resulted in the closure of the mussel harvest areas. Health warnings from the regulatory authority were extended to other species that may potentially have accumulated toxins, with the outcome that no illnesses were reported from seafood consumers.

In addition to human illness, the cost of harmful algal outbreaks can be significant and can include a loss of stock, a loss of market access, and damage to the reputation of the seafood industry. For example, the NSW oyster industry, which constitutes half of the Australian oyster industry, is valued at $55 million (2017-2018). There are ~25 closures per year due to HABs, with each closure lasting one week on average. At a conservative estimate of $100,000 per closure (NSW DPI), this equates to $2.5 million loss to the industry per year. Early warning of HABs will result in increased profit to the shellfish farmers and an increased confidence of Australian shellfish consumers. A more comprehensive understanding of the triggers of these events, and the potential impact of climate change (Glibert & Burford, 2017), is critical so that we can improve the forecasting and management of these toxic episodes, safeguarding the industry and consumers alike.

Acknowledgements

The authors wish to acknowledge Mario Puglisi and Chris Boyton for their assistance with this work.

Data Sources

Australian Phytoplankton Database available through the AODN.

https://portal.aodn.org.au/search?uuid=75f4f1fc-bee3-4498-ab71-aa1ab29ab2c0

New South Wales Food Authority
https://www.foodauthority.nsw.gov.au/

References

Ajani, P., Brett, S., Krogh, M., Scanes, P., Webster, G., & Armand, L. (2013). The risk of harmful algal blooms (HABs) in the oyster-growing estuaries of New South Wales, Australia. ***Environmental Monitoring and Assessment, 185***(6), 5295-5316. doi:10.1007/s10661-012-2946-9

Ajani, P., Hallegraeff, G., & Pritchard, T. (2001). Historic overview of algal blooms in marine and estuarine waters of New South Wales, Australia. ***Proceedings of the Linnean Society of New South Wales, 123***, 1-22. Retrieved from <Go to ISI>://WOS:000174087300002

Ajani, P., Larsson, M. E., Rubio, A., Bush, S., Brett, S., & Farrell, H. (2016). Modelling bloom formation of the toxic dinoflagellates Dinophysis acuminata and Dinophysis caudata in a highly modified estuary, south eastern Australia. ***Estuarine, Coastal and Shelf Science, 183***, 95-106. doi: 10.1016/j.ecss.2016.10.020

Ajani, P. A., Harwood, D. T., & Murray, S. A. (2017). Recent trends in marine phycotoxins from Australian coastal waters. ***Marine Drugs, 15***, 33. doi:doi:10.3390/md15020033

ASQAAC. (2016). The Australian Shellfish Quality Assurance Program Operations Manual. In (pp. 46). Canberra, Australia: Australian Shellfish Quality Assurance Advisory Committee.

Deeds, J. R., Landsberg, J. H., Etheridge, S. M., Pitcher, G. C., & Longan, S. W. (2008). Non-traditional vectors for paralytic shellfish poisoning. ***Marine Drugs, 6***(2), 308-348.

Farrell, H., Ajani, P., Murray, S., Baker, P., Webster, G., Brett, S., & Zammit, A. (2018). Diarrhetic Shellfish Toxin Monitoring in Commercial Wild Harvest Bivalve Shellfish in New South Wales, Australia. ***Toxins, 10***(11), 446. doi:10.3390/toxins10110446

Farrell, H., Brett, S., Ajani, P., & Murray, S. (2013). Distribution of the genus Alexandrium (Halim) and paralytic shellfish toxins along the coastline of New South Wales, Australia. ***Marine Pollution Bulletin, 72***(1), 133-145. doi:10.1016/j.marpolbul.2013.04.009

Farrell, H., Brett, S., Webster, G., Baker, P., & Zammit, A. (2015, 27-31 October 2014). ***A summary of harmful algal bloom monitoring and risk assessment within shellfish harvest areas in New South Wales, Australia.*** . Paper presented at the 16th International Conference on Harmful Algae, Wellington, New Zealand.

Glibert, P. M., & Burford, M. A. (2017). Globally changing nutrient loads and harmful algal blooms: Recent advances, new paradigms, and continuing challenges. ***Oceanography and Marine Biology, Vol 38, 30***(1), 58-69.

MacKenzie, L., Holland, P., McNabb, P., Beuzenberg, V., Selwood, A., & Suzuki, T. (2002). Complex toxin profiles in phytoplankton and Greenshell mussels (Perna canaliculus), revealed by LC–MS/MS analysis. ***Toxicon, 40***(9), 1321-1330. doi: 10.1016/S0041-0101(02)00143-5

NSW Food Authority. (2015). ***Marine Biotoxin Management Plan***. Retrieved from Newington, NSW: http://www.foodauthority.nsw.gov.au/_Documents/industry/marine_biotoxin_management_plan.pdf

NSW Food Authority. (2017). ***Phytoplankton and biotoxins in NSW shellfish aquaculture areas: risk assessment***. Retrieved from http://www.foodauthority.nsw.gov.au/_Documents/scienceandtechnical/phytoplankton_and_biotoxin_risk_assessment.pdf

Quaine, J., Kraa, E., Holloway, J., White, K., McCarthy, R., Delpech, V., . . . McAnulty, J. (1997). ***Outbreak of gastroenteritis linked to eating pipis***. Retrieved from

Reguera, B., Velo-Suárez, L., Raine, R., & Gil Park, M. (2012). ***Harmful Dinophysis species: A review*** (Vol. 14).

State and Trends of
Australia's Oceans
Report

3.6 Range expansion of the red tide dinoflagellate *Noctiluca scintillans*

Gustaaf Hallegraeff[1], Claire Davies[2] and Wayne Rochester[3]

[1] Institute for Marine and Antarctic Studies, University of Tasmania, Hobart, TAS, Australia
[2] CSIRO Oceans and Atmosphere, Hobart, TAS, Australia
[3] CSIRO Oceans and Atmosphere, Queensland Biosciences Precinct (QBP), St Lucia, QLD, Australia

Summary

The dinoflagellate *Noctiluca* exhibited a range expansion and biomass increase in the Australian region from the 1990s onwards, putatively driven by eutrophication promoting diatom prey (NSW), strengthening of the East Australian Current (Tas) and ship ballast water transport (Darwin, Rottnest, Cairns).

Key Data Streams

Ships of Opportunity

National Reference Stations

State and Trends of Australia's Ocean Report
www.imosoceanreport.org.au

Time-Series published
10 January 2020

doi: 10.26198/5e16ad2e49e85

Rationale

Noctiluca scintillans is a conspicuous, large (200 – 1000 µm diameter) dinoflagellate that commonly forms red tide surface slicks (**Figure 1**) and spectacular bioluminescent spectacles. It does not photosynthesise, but ingests small cells and particles. *Noctiluca* was first documented in Australian waters in Sydney Harbour in 1860. Up till the end of the 1980s, it was rarely seen, but had been newly reported from Moreton Bay and the Gulf of Carpentaria. Since the 1990s, *Noctiluca* prevalence has changed from rarely forming blooms to now becoming one of the most prominent red-tide organisms in Sydney and Tasmanian coastal waters. This range expansion and biomass increase raises concerns for beach tourism, grazing competition with zooplankton and larval fish, and ichthyotoxicity for finfish aquaculture.

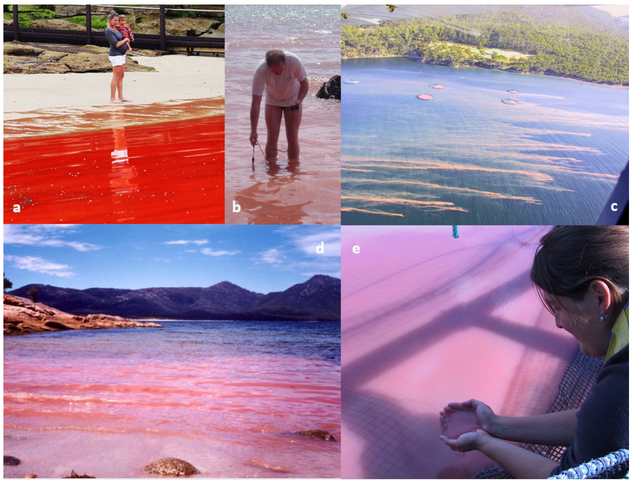

Figure 1. *Noctiluca* red tides in Australian waters. a. Clovelly Beach, Sydney, Nov 2012, Daily Telegraph; b, c, e. Tasman Peninsula, March 2002; photos G. Hallegraeff and J. Marshall; d. Freycinet Peninsula, Feb 2004, photo: E. Watson.

Methods

Historical observations of *Noctiluca* by plankton researchers, environmental agencies and the public were collated in the Australian Phytoplankton Database (Davies et al., 2017). Recent observations were drawn from the Integrated Marine Observing System (IMOS) Australian Continuous Plankton Recorder Survey, the Southern Ocean Continuous Plankton Recorder Survey, and phytoplankton and zooplankton samples from the IMOS National Reference Stations (Eriksen et al., 2019). All data were sourced from the IMOS Australian Ocean Data Network (AODN) (https://portal.aodn.org.au/; see the datasets "IMOS - AusCPR: Phytoplankton Abundance", "Southern Ocean Continuous Zooplankton Records", "The Australian Phytoplankton Database (1844 - ongoing) - abundance and biovolume" and "IMOS National Reference Station (NRS) - Zooplankton Abundance").

As *Noctiluca* can be a voracious feeder on phytoplankton and on copepod nauplli, *Noctiluca* can compete with and exert predatory pressure on copepods. We thus explored whether the expansion of *Noctiluca* in Australian waters could be negatively impacting the abundance of copepods. For data from Port Hacking and Maria Island National Reference Stations, we explored the relationship between *Noctiluca* and copepod abundances by removing the climatology signal from the abundance data and comparing residual values. A negative relationship between *Noctiluca* abundance and copepod abundance would mean that higher abundances of *Noctiluca* co-occur with lower abundances of copepods, implying *Noctiluca* is having negative competitive and/or predatory effects on copepods.

Results and Interpretation

Noctiluca scintillans has significantly expanded its distribution around Australia since the 1980s and increased its biomass (**Figure 2**). *Noctiluca* was first reported in Australia in 1860 in Sydney Harbour (Bennett, 1860). From 1950-1979, there was extensive phytoplankton sampling around Australia, but *Noctiluca* was only recorded in Sydney Harbour and Lake Macquarie. In the 1980s, the only new location for *Noctiluca* was the Gulf of Carpentaria (Burford, Rothlisberg, & Wang, 1995). Therefore, before the 1990s, *Noctiluca* appeared to be a rare and ephemeral species in warmer waters of Australia.

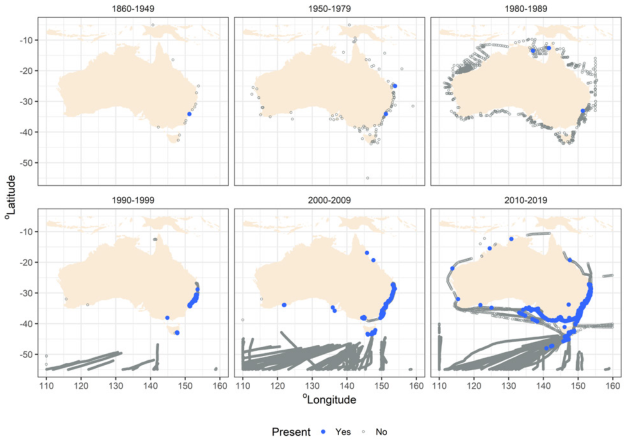

Figure 2. Expansion in the distribution of *Noctiluca scintillans* in Australian waters from 1860-2018. Blue dots show where Noctiluca has been detected, grey circles show the sampling effort within each time period.

In the 1990s, *Noctiluca* expanded its distribution into southern NSW and Moreton Bay (Heil, M.J., Miller, & Dennison, 1998), putatively stimulated by eutrophication of coastal estuaries promoting seed populations (Dela-Cruz, Ajani, Lee, Pritchard, & Suthers, 2002). It was first observed in Tasmania in 1994, apparently carried by the East Australian Current (EAC), and has since established overwintering populations (G. Hallegraeff, Hosja, Knuckey, & Wilkinson, 2008). In 2008, IMOS sampling observed *Noctiluca* off Townsville in Queensland, at Esperance in Western Australia, and at Kangaroo Island in South Australia. In 2010, *Noctiluca* was observed in the Southern Ocean for the first time, the most southerly record globally.

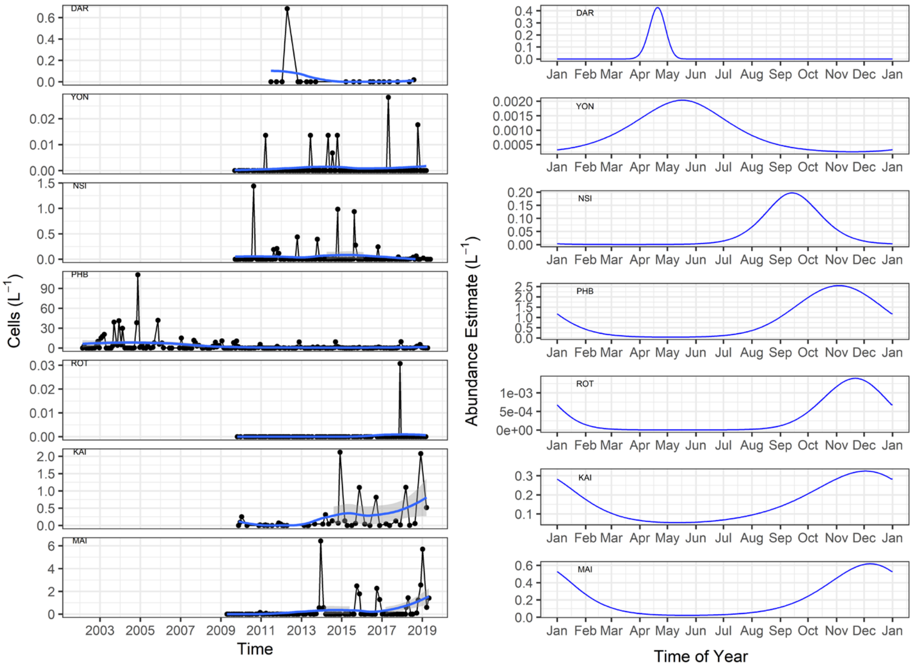

Figure 3. Time series (left) and seasonality (right) of *Noctiluca* for NRS stations. The estimated seasonal abundance used model predictions from data collected

It was transported south by a warm-core eddy, a likely consequence of the increased poleward penetration of the EAC (McLeod, Hallegraeff, Hosie, & Richardson, 2012). In 2013, *Noctiluca* was observed even further south in the Southern Ocean. In 2014, *Noctiluca* was reported for the first time from Darwin Harbour. In 2017, *Noctiluca* was observed at Rottnest Island for the first time. Interestingly, a mixotrophic green *Noctiluca,* different to the heterotrophic form we have seen here, hosts green flagellate symbionts. Green *Noctiluca* forms nuisance blooms in the Arabian Sea, but has never yet been observed in Australian waters.

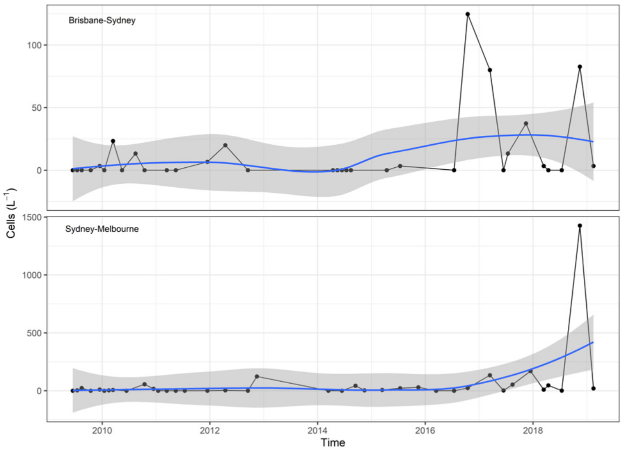

Figure 4. IMOS Continuous Plankton Recorder observations of *Noctiluca* from the Brisbane to Sydney and Sydney to Melbourne routes, between 2009 and early 2019.

Noctiluca has now been found at all IMOS National Reference Stations (NRS) (see Common Methods) and is common during spring (**Figure 3**). There is some evidence of an increase in *Noctiluca scintillans* abundance at Yongala and its recent appearance at Rottnest Island is noteworthy (**Figure 3**). Although Port Hacking typically has the highest concentrations of *Noctiluca* of all the NRS, there has been a weak decline in abundance over the past 16 years. In 2017 and 2018, there was some evidence of an increase in *Noctiluca scintillans* abundance off South-eastern Australia from the CPR transects from Brisbane to Sydney, and Sydney to Melbourne (**Figure 4**). In terms of the seasonal cycle, there is a clear relationship between bloom timing and latitude, with *Noctiluca* blooms earlier in the year further north. *Noctiluca* blooms in autumn and winter in tropical Australia, in spring in the subtropics, and in summer in temperate waters (**Figure 3**). In Sydney waters, most *Noctiluca* blooms are in spring and late summer (Dela-Cruz et al., 2002) as water temperatures warm to 19-24°C, while in Tasmania although *Noctiluca* is present through the year, even in winter-spring at temperatures of 10-13°C, largest blooms are in summer (18-20°C).

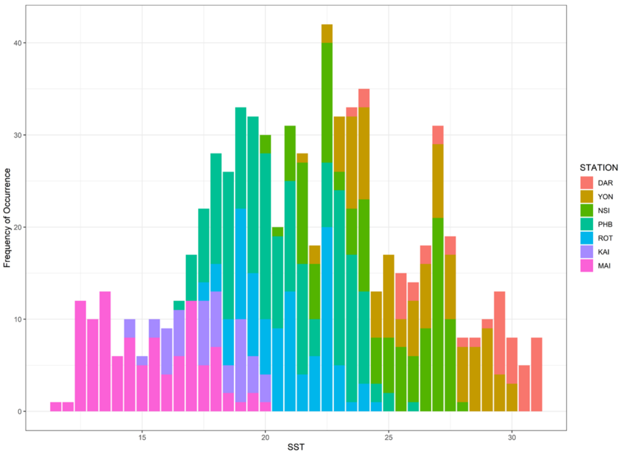

Figure 5. Frequency of occurrence of *Noctiluca* at the NRS (2008 – 2018) and associated Sea Surface Temperature (SST) for each observation.

doi: 10.26198/5e16ad2e49e85

While *Noctiluca* blooms are largely driven by prey availability, these seasonal responses indicate that temperature plays an important role in distribution. Acclimatised Tasmanian *Noctiluca* cultures under optimal conditions showed cell division at 10°C. But there was limited survival at 7°C, and *Noctiluca* were unable to thrive at Sydney summer temperatures of 25°C (G. M. Hallegraeff et al., 2019). This variability in temperature tolerance is supported by frequency of occurrence data from the IMOS NRS (**Figure 4**). While Tasmanian *Noctiluca* are favoured by summer temperatures, improved food availability is likely to maintain its occurrence throughout the rest of the year.

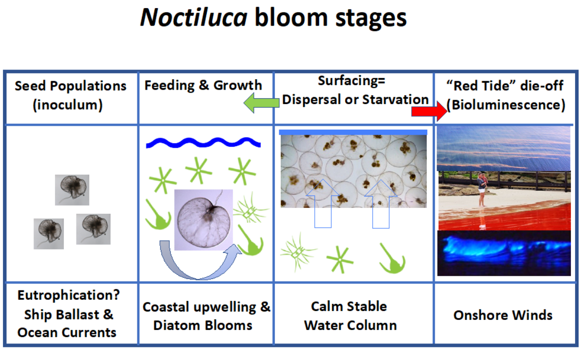

Figure 6. *Noctiluca* "blooms" start from small estuarine seed populations, that capitalise on feeding on dense diatom prey. Under calm stable water column conditions, *Noctiluca* can no longer access food and moves to surface. If successfully dispersed into new food areas, growth continues (green arrow). In the absence of feeding activity, populations die and generate red (often bioluminescent) coastal slicks (red arrow).

The relationship between *Noctiluca* and copepod abundances from Port Hacking and Maria Island National Reference Stations was positive and significant, after removing their seasonal cycles (**Figure 6**). This was contrary to expectations and indicates that *Noctiluca* is not having a negative impact on copepod populations. The positive relationship is probably a consequence of similar drivers; numbers of both *Noctiluca* and copepods are stimulated by greater phytoplankton abundance. The relationship was similar if total zooplankton was used in the analysis, rather than copepods.

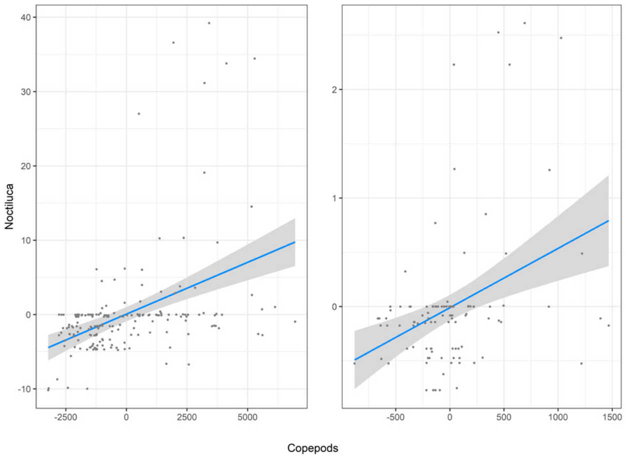

Figure 7. Relationship of the residual abundances of copepods to *Noctiluca* after removing the climatologies at a) Port Hacking and b) Maria Island National Reference stations.

Implications for people and ecosystems

Since the 1980s, *Noctiluca* has clearly expanded its geographic range and increased its bloom frequency. There are likely to be several potential mechanisms responsible for the range expansion of *Noctiluca*: 1. Stimulation of seed populations in estuaries by eutrophication (NSW); 2. Warmer water temperatures (southeast Australia); 3. Ship ballast water transport (WA, SA, Qld); and 4. Changes in prey abundance. Since the 1990s, waters in southern Australia have become warm enough to support *Noctiluca*. It can also be transported into the Southern Ocean in warm-core eddies that spin off from the EAC (McLeod et al., 2012). As the EAC is projected to continue to strengthen and transport more warm-core eddies further south, and as the Southern Ocean warms, *Noctiluca* may be able to establish in the Southern Ocean in the future, leading to potential competition with zooplankton grazers for phytoplankton.

Whilst *Noctiluca* is not having a negative effect on the abundance of copepods (**Figure 6**), the continued range expansion and increase in abundance of *Noctiluca* could have negative impacts on aquaculture and fisheries. *Noctiluca* has been implicated in the decline of fisheries in the Indian Ocean (Bhimachar & George, 1950) and can negatively impact caged fish production. Fortunately, compared to other fish-killing algae, the dinoflagellate *Noctiluca* would rank as the least ichthyotoxic. Only surface slicks of 1,000,000 to 2,000,000 cells per litre pose a risk to finfish aquaculture, both in terms of high ammonia and reduced oxygen (G. M. Hallegraeff et al., 2019). There is anecdotal evidence of shellfish tasting like ammonia in association with *Noctiluca* slicks and showing slower growth due to lack of phytoplankton food.

Acknowledgements

Data was sourced from Australia's Integrated Marine Observing System (IMOS) which is enabled by the National Collaborative Research Infrastructure Strategy (NCRIS).

Data Sources

IMOS National Reference Stations.
http://imos.org.au/facilities/nationalmooringnetwork/nrs/

IMOS Ships of Opportunity.
http://imos.org.au/facilities/shipsofopportunity/

doi: 10.26198/5e16ad2e49e85

References

Bennett, G. (1860). ***Gatherings of a naturalist in Australasia***: Currawong Press, Australia

Bhimachar, B. S., & George, P. C. (1950). Abrupt set-backs in the fisheries of the Malabar and Kanara coasts and “red water” phenomenon as their probable cause. ***Proceedings of the Indian Academy of Sciences, Series B 31***, 339-350.

Burford, M. A., Rothlisberg, P. C., & Wang, Y. G. (1995). Spatial and temporal distribution of tropical phytoplankton species and biomass in the Gulf of Carpentaria, Australia. ***Marine ecology progress series, 118***(1-3), 255-266. Retrieved from <Go to ISI>://A1995QP42600024

Davies, C. H., Coughlan, A., Hallegraeff, G., Ajani, P., Armbrecht, L., Atkins, N., . . . Richardson, A. J. (2017). A database of marine phytoplankton abundance, biomass and species composition in Australian waters. ***Scientific Data, 4***, 170042. doi:10.1038/sdata.2017.42

Dela-Cruz, J., Ajani, P., Lee, R., Pritchard, T., & Suthers, I. (2002). Temporal abundance patterns of the red tide dinoflagellate ***Noctiluca scintillans*** along the southeast coast of Australia. ***Marine ecology progress series, 236***, 75-88.

Eriksen, R. S., Davies, C. H., Bonham, P., Coman, F. E., Edgar, S., McEnnulty, F., . . . Richardson, A. J. (2019). Australia’s long-term plankton observations: the Integrated Marine Observing System National Reference Station network. ***Frontiers in Marine Science, 6***(Article 161), 17.

Hallegraeff, G., Hosja, W., Knuckey, R., & Wilkinson, C. (2008). Recent range expansion of the red-tide dinoflagellate ***Noctiluca scintillans*** in Australian coastal waters. ***Harmful Algae News, 38,*** 10-11.

Hallegraeff, G. M., Albinsson, L., Dowdney, J., Holmes, A. K., Mansour, P., & Seger, A. (2019). Prey selection, environmental tolerances and ichthyotoxicity by the red-tide dinoflagellate ***Noctiluca scintillans*** cultured from Tasmanian waters. ***Journal of Plankton Research, 41***, 407-418.

Heil, C. A., M.J., O. D., Miller, C. A., & Dennison, W. C. (1998). Phytoplankton community response to a flood event. In I. R. Tibbetts, N. J. Hall, & W. C. Dennison (Eds.), ***Moreton Bay and Catchment*** (pp. 569-584). School of Marine Science, The University of Queensland.

McLeod, D. J., Hallegraeff, G. M., Hosie, G. W., & Richardson, A. J. (2012). Climate-driven range expansion of the red-tide dinoflagellate ***Noctiluca scintillans*** into the Southern Ocean. ***Journal of Plankton Research, 34***(4), 332-337. doi:10.1093/plankt/fbr112

Integrated **Marine**
Observing System

IMOS
Integrated Marine Observing System

State and Trends of Australia's Oceans
Report

4.1 The response of the copepod community to long-term warming along the east coast of Australia

Anthony J. Richardson[1,2], Claire Davies[3] and Ruth Eriksen[3]

[1] CSIRO Oceans and Atmosphere, Queensland Biosciences Precinct (QBP), St Lucia, QLD, Australia

[2] Centre for Applications in Natural Resource Mathematics (CARM), School of Mathematics and Physics, The University of Queensland, St Lucia, QLD, Australia

[3] CSIRO Oceans and Atmosphere, Hobart, TAS, Australia

Summary

Warmer-water copepod species down Australia's east coast (at Maria Island, Port Hacking and Yongala) are now more common compared with the community 50-100 years ago. Warm-water copepods are generally smaller and lighter and are thus a poor food source for fish, seabirds and marine mammals.

Key Data Streams

Ships of Opportunity

National Reference Stations

State and Trends of Australia's Ocean Report
www.imosoceanreport.org.au

Time-Series published
10 January 2020

doi: 10.26198/5e16ad7949e86

Rationale

Copepods, the most abundant zooplankton, are sensitive indicators of climate change, as temperature regulates their physiology and influences their interactions with other species (Richardson, 2008). Ultimately, warmer temperatures alter species' ranges, timing of blooms, diversity, composition, and size structure. Examples of poleward movement of species (Beaugrand et al., 2002), earlier timing (Edwards & Richardson, 2004), higher diversity (Richardson, 2008), change toward a community that prefers warmer waters (Poloczanska et al., 2013) and smaller species (Campbell, 2018) have been described in many areas in the northern hemisphere with long-term datasets, but there are few examples from Australian waters. Now we have over ten years of zooplankton data from the Integrated Marine Observing System (IMOS) National Reference Stations, we can start to explore how climate change might be impacting Australian zooplankton communities.

Surface waters off the east coast of Australia have warmed by up to 2°C over the past 70 years, with greater warming in the south (e.g., Maria Island) than further north (e.g., Port Hacking) (**Figure 1**). This is a consequence of global warming and its influence on the intensification of the poleward-flowing East Australian Current (EAC) (Cai et al., 2005), which is distributing more warm-water to southern Australia (Ridgway, 2007). This increasing strength of the EAC has contributed to ocean warming off southeast Australia ~3–4 times the global average (Ridgway, 2007).

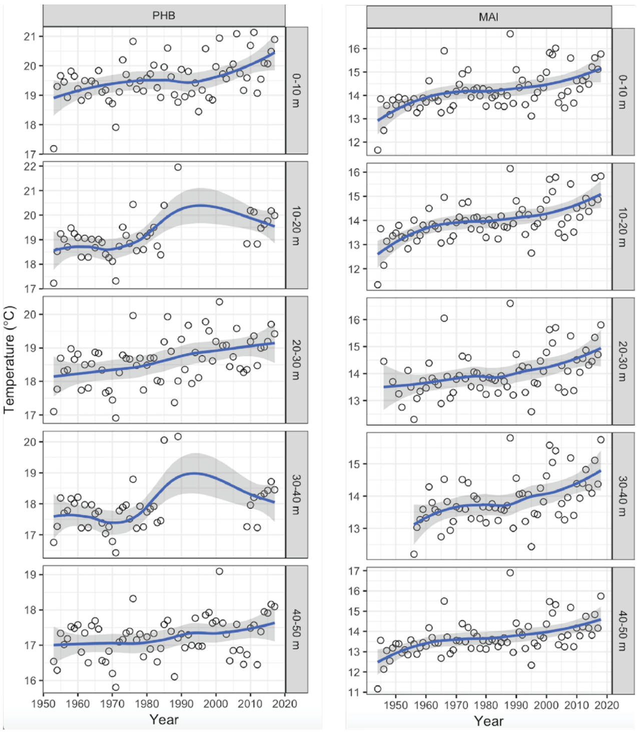

Figure 1. Mean annual temperatures (°C) from Maria Island (MAI) and Port Hacking (PHB) National Reference Stations in three depth strata (0-10 m, 20-30 m, 40-50 m) in the top 50 m, showing long-term warming since 1940s/50s. Data are not shown from Yongala because no long-term data exists from there.

Here we compare the IMOS copepod data from three National Reference Stations in eastern Australia – Maria Island (42.6°S), Port Hacking (34.1°S) and Yongala (19.3°S). We chose these regions because there was historical zooplankton data in each region to assess whether there is a signature of warming in the copepod community.

Methods

To investigate whether warming has impacted the copepod community, we compared the preferred temperature of copepods from historical samples to that from recent samples using the Community Temperature Index (CTI) (Stuart-Smith et al., 2015). The CTI is the overall temperature preference of species in a sample, weighted by their abundance, so that more abundant species have greater influence. It has been used to assess the temperature preference of communities of microbes, butterflies, fish and benthic invertebrates (Stuart-Smith et al., 2015 and references therein). We chose the CTI because it is sensitive to large-scale changes in temperature and is relatively robust to variations in sampling methods, as it is most responsive to relative and not absolute changes in abundance.

We performed three separate analyses – one for Maria Island, one for Port Hacking, and one for Yongala. All analyses compare current IMOS data with historical data from the Australian Zooplankton Database (Davies et al., 2014). For Port Hacking, IMOS samples from 2009-2018 were compared with two historical datasets. The first was 29 samples collected monthly from January 1931 to March 1932 by Dakin & Colefax (1940). The second was more recent; 71 samples were collected monthly from 2001-2008 (by the NSW Environment Agency). The 2001-2008 data were counted in the same way and by the same people as the 2009-2018 IMOS (104 samples). Only the most abundant 15 species were reported historically from 1931-1932, so these same species were extracted from the more recent data for comparison using the CTI.

For Maria Island, the historical dataset was collected monthly from August 1971 to May 1973 over a grid off the east coast of Tasmania by Nyan Taw (1975). We retained samples in our analysis that were within 150 km of Maria Island and <200 m depth to ensure similar conditions to the current IMOS National Reference Station. We then compared these data with IMOS data collected from January 2009 to the present. As the 1971-1973 data included only 25 copepod species, we selected the same species from the 2009-2018 period.

For Yongala, we use copepod data the 1928-1929 GBR expedition (Farran, 1949), Peter Liston's PhD thesis (Liston, 1990), sampling in the early 2000s (Mckinnon et al. 2005), and IMOS data since 2009.

doi: 10.26198/5e16ad7949e86

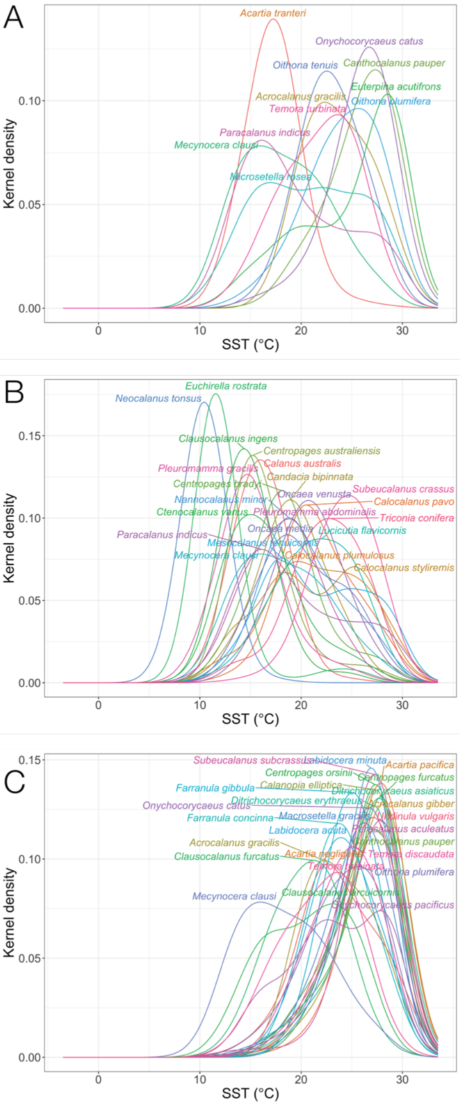

Figure 2. Kernel density plots showing the temperature preferences of the copepods in the analysis for A. Port Hacking between for 15 species, and B. Maria Island for 25 species. C. Yongala for species present across the studies.

To estimate the preferred temperature for each of the copepod species in the analyses, we used data on the abundance of copepods from 20,000 samples collected as part of the IMOS National Reference Stations, the Australian Continuous Plankton Recorder survey, and the Southern Ocean Continuous Plankton Recorder survey (Eriksen et al., 2019; Hosie et al., 2003). We assigned each sample a temperature based on a weekly composite from remote sensing data, and plotted the abundance of each species vs temperature in 0.5°C temperature bands and fitted kernel density models (**Figure 2**). The preferred temperature for each species is called the species temperature index and is defined as the temperature of maximum abundance (Stuart-Smith et al. 2015).

To calculate the CTI for each sample (i.e., the overall temperature preference of the copepods in a sample), we multiplied the abundance of each species by its thermal preference (i.e., species temperature index), and divided by the total abundance of these species in the sample (Stuart-Smith et al. 2015). As the same species are used to compare with historical and current data, any changes in the CTI are due to the relative changes in abundance of cold and warm-water species, and not to the influx of new warm-water species. This is a cautious approach, as it is less biased by differences in the ability to sample and identify rare species.

The last part of the analysis was to use a linear model to test whether there had been an increase in the CTI fover time as the waters are warming. We adjusted for the seasonal cycle in the analysis by including Month in the linear model. Historical data were sourced from the "The Australian Zooplankton Database" (Davies et al. 2014; data available at https://figshare.com/articles/Data_Paper_Data_Paper/3560811). Recent data (from IMOS) were sourced from the AODN (dataset "IMOS National Reference Station (NRS) - Zooplankton Abundance").

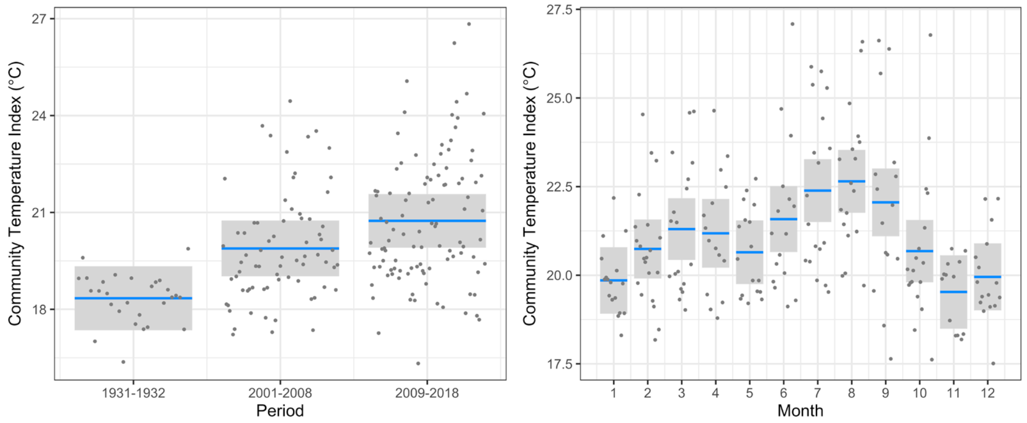

Figure 3. The linear model at Port Hacking of the Community Temperature Index (response) and the Period and Seasonal cycle (predictors).

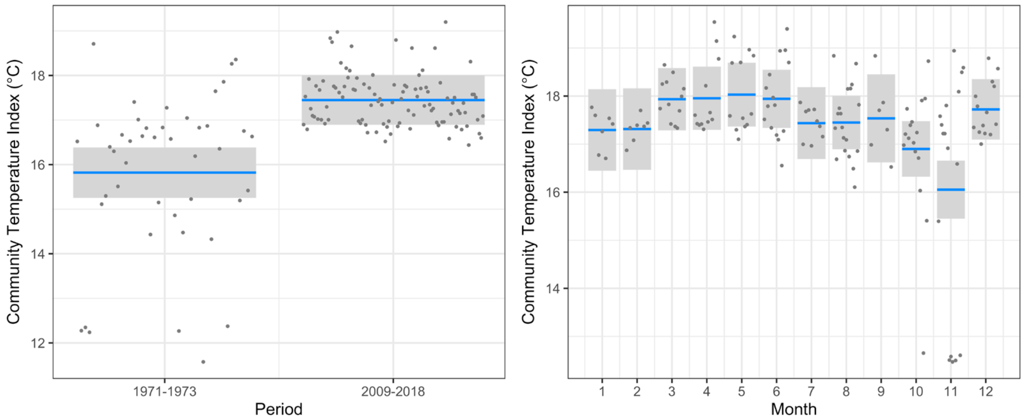

Figure 4. The linear model at Maria Island of the Community Temperature Index (response) and the Period and Seasonal cycle (predictors).

Results and interpretation

Copepod species at Port Hacking and Maria Island have a range of thermal preferences, with some preferring colder waters and some warmer waters (**Figure 2**). As expected, species from Port Hacking (**Figure 2a**) generally have warmer temperature preferences than those from Maria Island (**Figure 2b**).

At Port Hacking, the linear model clearly showed a significant increase in the CTI of 1.5°C from 1931-1932 to 2001-2008, and then a further increase of 0.9°C to 2009-2018 (r^2=35.9%, **Figure 3**). This increase in CTI is similar in magnitude to the warming since the 1930s, and implies that warm-water copepod species have increased in abundance whilst cold-water copepods have decreased. The increase in CTI is accompanied by some samples having extremely warm-water affinities with CTIs around 26°C, about 6°C warmer than the warmest communities observed in 1931-1932. There was a clear seasonal cycle in CTI at Port Hacking, with highest values in July-September, and lowest values in November-January.

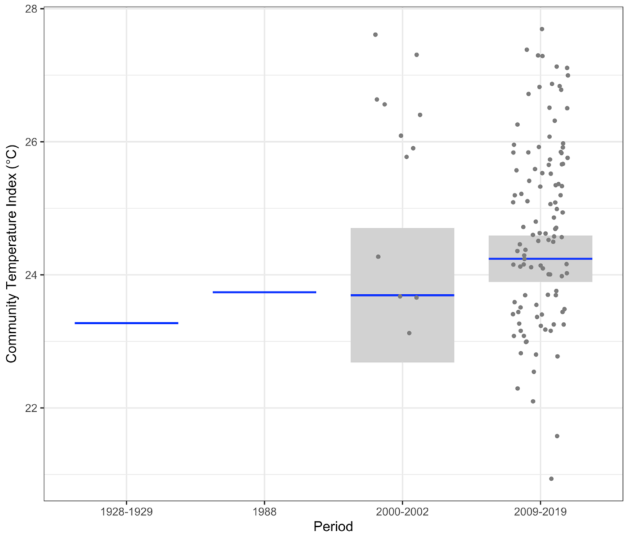

Figure 5 The linear model at Yongala of the Community Temperature Index (response) and the Period (predictor).

At Maria Island, the linear model clearly showed a significant increase in the CTI of 1.6°C from 1971-1973 to 2009-2018 (r^2=47.7%, **Figure 4**). This increase in CTI is similar in magnitude to the warming over the same period, and implies that warm-water copepod species have increased in abundance whilst cold-water copepods have decreased. There was a clear seasonal cycle in CTI, with highest values in March-June, and lowest values in October and November. The very low values of CTI (~12.5°C) seen in October and November in the 1970s (spring) is a consequence of high abundances of a single species – *Neocalanus tonsus*, a large cold-water copepod indicative of intrusions of Southern Ocean water. Despite nearly 10 years of monthly IMOS sampling since 2009, we have not seen *Neocalanus tonsus* in similar large numbers at Maria Island, potentially because of the increased flow of the EAC and reduced incursions of Southern Ocean water in the region.

At Yongala, the linear model clearly showed a significant increase in the CTI of nearly 1°C from 1928-1929 to 2009-2019 (**Figure 4**). This is similar to the 0.75°C warming observed in the region, based on Hadley ISST data from the UK Met Office. Data from two surveys – one in 1988 and the other 2000-2002 show intermediate values of CTI.

Implications for people and ecosystems

This is the strongest evidence to date that global warming is affecting zooplankton composition in response to warming in Australian waters. The increased abundance of warm-water taxa is consistent with what is happening in other systems including the North Atlantic (Beaugrand et al., 2002; Bonnet et al., 2005; Lindley & Daykin, 2005) and North Pacific (Poloczanska et al., 2013). Such a change from cold- to warm-water zooplankton species off southeast Australia is likely to have repercussions for higher trophic levels. Warm-water copepod communities generally have smaller individuals and lower biomass (Richardson & Schoeman, 2004) and are thus inferior food for fish, seabirds and marine mammals

doi: 10.26198/5e16ad7949e86

(Beaugrand et al., 2003). Ongoing IMOS observations of zooplankton ensure we are well placed to identify future changes in the zooplankton community around Australia.

Acknowledgements

Data was sourced from Australia's Integrated Marine Observing System (IMOS) which is enabled by the National Collaborative Research Infrastructure Strategy (NCRIS).

Data Sources

IMOS National Reference Stations.

http://imos.org.au/facilities/nationalmooringnetwork/nrs/

IMOS Ships of Opportunity.

http://imos.org.au/facilities/shipsofopportunity/

References

Beaugrand, G., Reid, P. C., Ibanez, F., Lindley, J. A., & Edwards, M. (2002). Reorganization of North Atlantic marine copepod biodiversity and climate. ***Science, 296***(5573), 1692-1694. Retrieved from <Go to ISI>://000175976200060

Beaugrand, G., Souissi, S., Reid, P. C., Brander, K. M., & Alistair Lindley, J. (2003). Plankton effect on cod recruitment in the North Sea. ***Nature, 426***(6967), 661-664.

Bonnet, D., Richardson, A., Harris, R., Hirst, A., Beaugrand, G., Edwards, M., . . . Fernandez de Puelles, M. L. (2005). An overview of Calanus helgolandicus ecology in European waters. ***Progress in Oceanography, 65***(1), 1-53. doi: 10.1016/j.pocean.2005.02.002

Cai, W., Shi, G., Cowan, T., Bi, D., & Ribbe, J. (2005). The response of the Southern Annular Mode, the East Australian Current, and the southern mid-latitude ocean circulation to global warming. ***Geophysical Research Letters, 32***(23). doi:L2370610.1029/2005gl024701

Campbell, M. (2018). ***Testing macroecological patterns that drive community structure using zooplankton in the global ocean.*** (Honours thesis). University of Queensland,

Dakin, W. J., & Colefax, A. (1940). The plankton of the Australian coastal waters off New South Wales Part I. ***Publications of the University of Sydney***, 210.

Davies, C. H., Armstrong, A. J., Baird, M., Coman, F., Edgar, S., Gaughan, D., . . . Richardson, A. J. (2014). Over 75 years of zooplankton data from Australia. ***Ecology, 95***(11), 3229-3229. doi:10.1890/14-0697.1

Edwards, M., & Richardson, A. J. (2004). Impact of climate change on marine pelagic phenology and trophic mismatch. ***Nature, 430***(7002), 881-884. doi: 10.1038/nature02808 Eriksen, R. S., Davies, C. H., Bonham, P., Coman, F. E., Edgar, S., McEnnulty, F., . . . Richardson, A. J. (2019). Australia's long-term plankton observations: the Integrated Marine Observing System National Reference Station network. ***Frontiers in Marine Science, 6***(Article 161), 17.

Farran, G. P. (1949). The seasonal and vertical distribution of the copepoda. In ***Scientific Reports*** (Vol. Great Barrier Reef Expedition 1928 - 1929 Volume 2).

Hosie, G. W., Fukuchi, M., & Kawaguchi, S. (2003). Development of the Southern Ocean Continuous Plankton Recorder survey. ***Progress in Oceanography, 58***(2-4), 263-283. doi:10.1016/j.pocean.2003.08.007

Lindley, J. A., & Daykin, S. (2005). Variations in the distributions of Centropages chierchiae and Temora stylifera (Copepoda: Calanoida) in the north-eastern Atlantic Ocean and western European shelf waters. ***ICES Journal of Marine Science, 62***(5), 869-877. doi:10.1016/j.icesjms.2005.02.009

Liston, P. W. (1990). ***Spatial variability and covariability of chlorophyll and zooplanktn on the Great Barrier Reef.*** (PhD). James ook University,

Mckinnon, A. D., Duggan, S., & De'ath, G. (2005). Mesozooplankton dynamics in nearshore waters of the Great Barrier Reef. ***Estuarine, Coastal and Shelf Science, 63***(4), 497-511. doi:10.1016/j.ecss.2004.12.011

Poloczanska, E. S., Brown, C. J., Sydeman, W. J., Kiessling, W., Schoeman, D. S., Moore, P. J., . . . Richardson, A. J. (2013). Global imprint of climate change on marine life. ***Nature Climate Change, 3***, 919. doi:10.1038/nclimate1958

Richardson, A. J. (2008). In hot water: zooplankton and climate change. ***ICES Journal of Marine Science, 65***(3), 279-295. doi:10.1093/icesjms/fsn028

Richardson, A. J., & Schoeman, D. S. (2004). Climate impact on plankton ecosystems in the northeast Atlantic. ***Science, 305***(5690), 1609-1612. doi:10.1126/science.1100958

Ridgway, K. R. (2007). Long-term trend and decadal variability of the southward penetration of the East Australian Current. ***Geophysical Research Letters, 34***(13). doi:10.1029/2007gl030393

Stuart-Smith, R. D., Edgar, G. J., Barrett, N. S., Kininmonth, S. J., & Bates, A. E. (2015). Thermal biases and vulnerability to warming in the world's marine fauna. ***Nature, 528***, 88. doi:10.1038/nature16144

Taw, N. (1975). ***Studies on the zooplankton and hydrology of south-eastern coastal waters of Tasmania.*** University of Tasmania, Hobart.

doi: 10.26198/5e16ad7949e86

IMOS

Integrated **Marine**
Observing System

IMOS
Integrated Marine Observing System
State and Trends of Australia's Oceans
Report

4.2 The impact on zooplankton of the 2011 heatwave off Western Australia

Anthony J. Richardson[1,2], Jessica Savage[3], Frank Coman[1], Claire Davies[4], Ruth Eriksen[4], Felicity McEnnulty[4], Anita Slotwinski[1], Mark Tonks[1] and Julian Uribe-Palomino[1]

1 CSIRO Oceans and Atmosphere, Queensland Biosciences Precinct (QBP), St Lucia, QLD, Australia

2 Centre for Applications in Natural Resource Mathematics (CARM), School of Mathematics and Physics, The University of Queensland, St Lucia, QLD,, Australia

3 The University of Queensland, St Lucia, QLD, Australia

4 CSIRO Oceans and Atmosphere, Hobart, TAS, Australia

Summary

The 2011 WA marine heatwave led to a substantial decline in zooplankton biomass, abundance and size, and an increase in diversity at Rottnest Island. The poor food environment, which persisted for several months before resetting, could have caused poor feeding conditions and recruitment failures in higher trophic levels.

Key Data Streams

National Reference Stations

Western Australia Moorings

State and Trends of Australia's Ocean Report
www.imosoceanreport.org.au

Time-Series published
10 January 2020

doi: 10.26198/5e16adc449e87

Rationale

Extreme climate events such as heatwaves and floods can have pronounced ecosystem and evolutionary impacts because they provide little opportunity for organisms to acclimate or adapt. With climate change, extreme climate events are becoming more frequent and more intense (Herring et al., 2018). In early 2011, an extreme La Niña event caused an intense marine heatwave (MHW) in Western Australia, unprecedented in the 140-year local record (Wernberg et al., 2013). The Leeuwin Current accelerated, bringing warm oligotrophic water down the west coast of Australia. The MHW persisted for months along most of the west coast of Australia, with temperatures up to 5°C above average. This led to coral bleaching, death of kelp forests, mortality of seagrass meadows, fish kills, collapse of fisheries, and southwards shifts manta rays and whale sharks (Babcock et al., 2019; Wernberg et al., 2013). Despite the extensive work on the marine heatwave, its effect on plankton have not yet been studied. A better understanding of the impacts on plankton could potentially help to explain impacts of the heatwave on higher trophic levels.

Methods

As part of the Integrated Marine Observing System (IMOS) National Reference Station (NRS) facility, physical, chemical and biological samples have been collected monthly off Rottnest Island since 2009. To investigate the impact of the 2011 marine heatwave on zooplankton in the region, we ianalysed zooplankton biomass, abundance and diversity (AODN datasets: “IMOS National Reference Station (NRS) - Zooplankton Biomass” and “IMOS National Reference Station (NRS) - Zooplankton Abundance”). To place the 2011 marine heatwave in context, we used temperature data throughout the water column from the CTD (AODN dataset: “IMOS - Australian National Mooring Network (ANMN) - CTD Profiles”) and chlorophyll-a data from (AODN dataset: “IMOS National Reference Station (NRS) - Phytoplankton HPLC Pigment Composition Analysis”).

We tested the impact of the heatwave by using a linear model with the chlorophyll-a, zooplankton biomass, zooplankton abundance, the Shannon copepod diversity and the Pielou copepod evenness index as separate response variables. As predictors in each model, we used Condition, with two levels (Heatwave: Jan-Apr 2011) and non-heatwave (all other months) and a Month term to adjust for seasonality.

Finally, we compared the size spectrum of the zooplankton community during the heatwave and outside the heatwave. We estimated the size spectrum of the sample using ZooScan, a high-performance water-proof scanner (Gorsky et al., 2010). The size spectrum is a plot of the biovolume of all particles in a sample against size bins, from small to large particles.

Results and interpretation

The 2011 marine heatwave had a distinct temperature signal at Rottnest Island, compared with all other times. The extremely warm conditions extended throughout the water column (**Figure 1**). Water temperature was up to 24°C in the top 45 m.

The marine heatwave had a large impact on many aspects of the Rottnest Island ecosystem (**Figure 2**, **Figure 3**). The heatwave had significantly higher SOI values than usual. The high SOI values in the lead up to the heatwave are also clear. Surface temperature was significantly warmer than usual. There was no significant difference in Chl-a within the heatwave and outside that period.

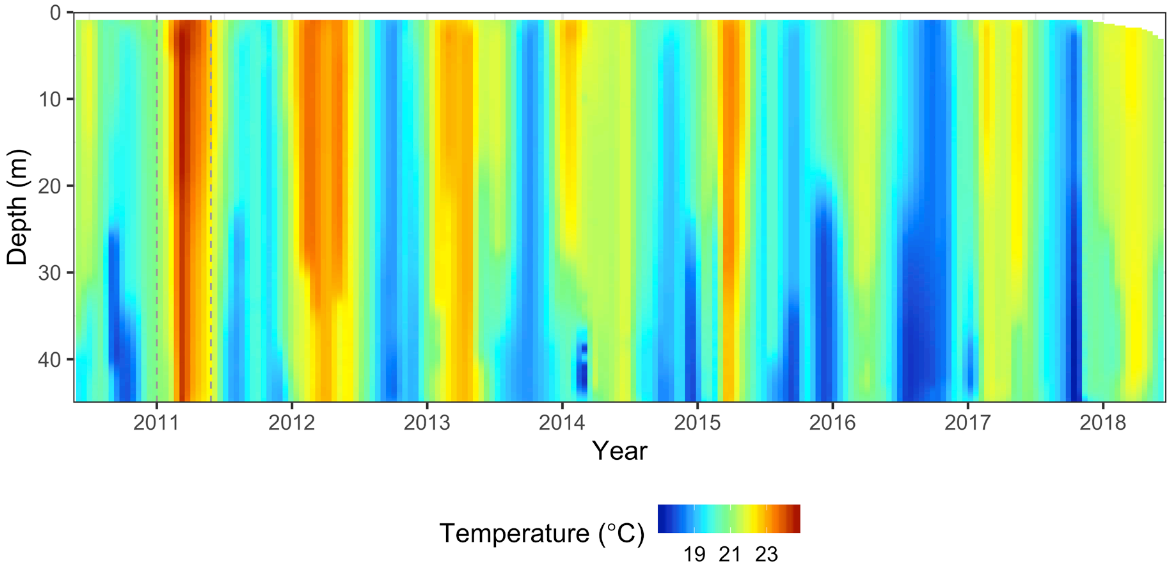

Figure 1. Contour plot of the temperature at Rottnest Island, Western Australia. The heatwave, from January 2011 to April 2011 is represented by the dashed lines.

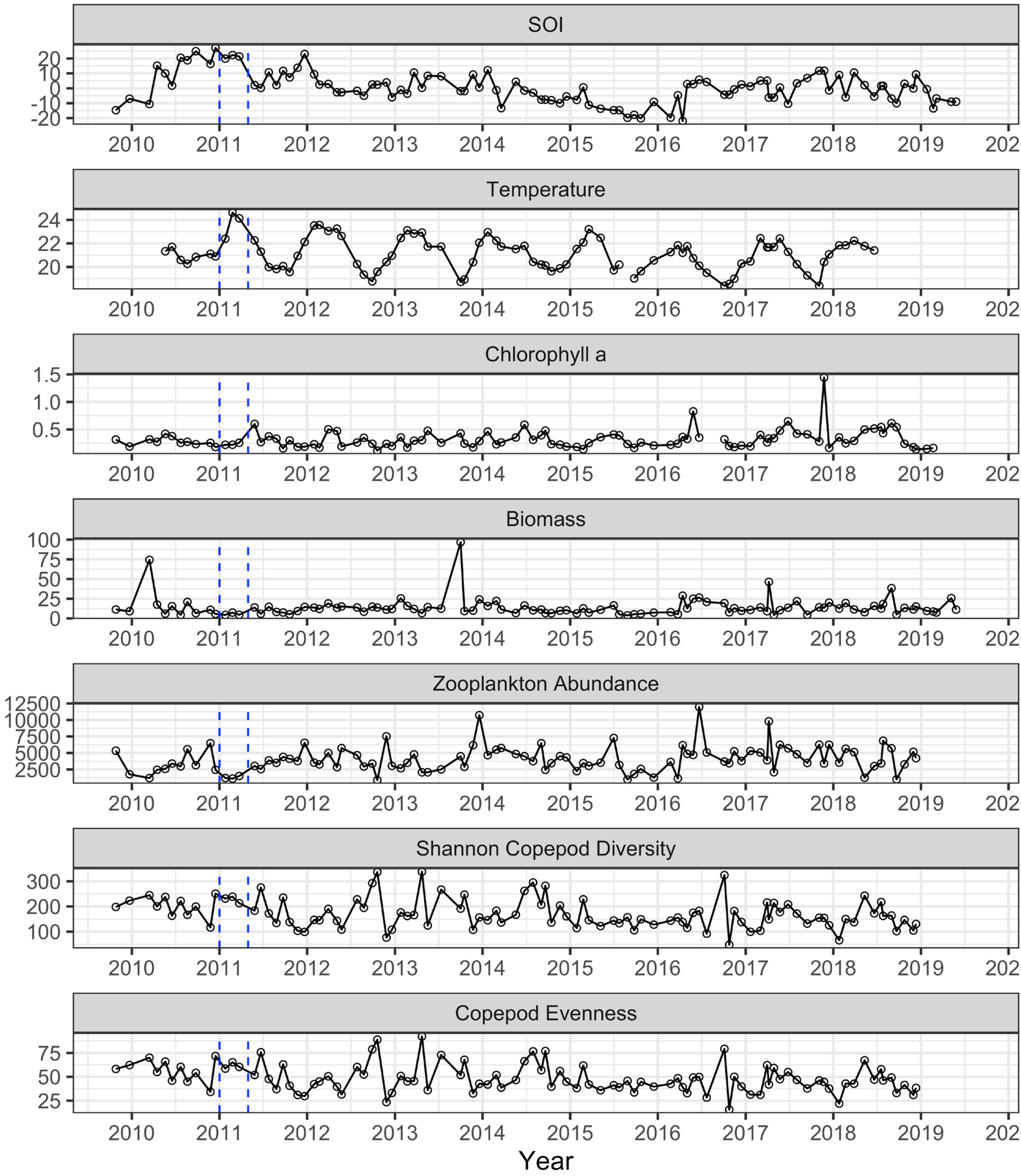

Figure 2. Time series of the Southern Oscillation Index, temperature (°C), surface chlorophyll-a (mg.m^{-3}), zooplankton biomass (mg.m^{-3}), zooplankton abundance (m^{-3}), copepod diversity, and evenness at Rottnest Island, Western Australia. The heatwave is represented by blue lines, from January 2011 to April 2011.

doi: 10.26198/5e16adc449e87

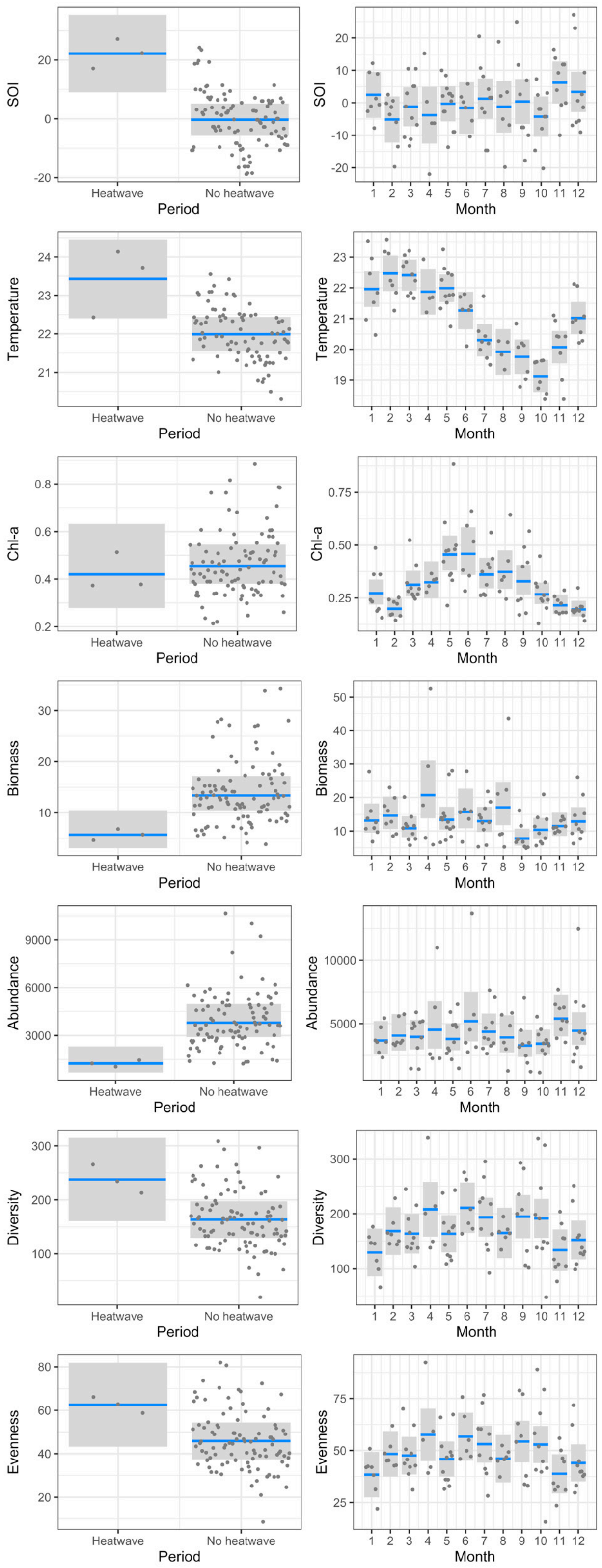

Figure 3. Linear models of different response variables, with predictors of Period (Heatwave, No heatwave) and Month.

By contrast, zooplankton biomass and abundance were significantly lower than usual. The copepod community had high significantly higher diversity during the heatwave, but similar evenness.

The size spectrum of zooplankton shifted lower during the marine heatwave (**Figure 4**). All zooplankton size classes declined, but particularly those in smaller size classes. Thus, the mean size of members of the zooplankton community declined.

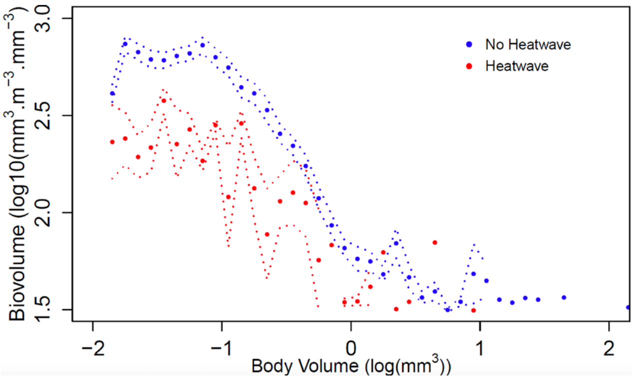

Figure 4. Biovolume for heatwave and non-heatwave samples. Dotted lines show standard error. Non-overlapping standard errors imply statistical significance.

Implications for people and ecosystems

We found that the 2011 marine heatwave had a major impact on the zooplankton at Rottnest Island. There was a substantial decline in zooplankton biomass, abundance and size, and an increase in diversity.

These responses are all consistent with our understanding of how zooplankton communities respond to warmer temperatures. The significant decrease in the biomass and abundance is most likely because the accelerating Leeuwin Current carried down fewer species in it, as plankton tends to be less abundant and smaller in the tropics (Daufresne, Lengfellner, & Sommer, 2009; Giani et al., 2012; Martin, Harris, & Irigoien, 2006). Similar results were found in another study in North West Australia, during the 1998-99 La Niña, where the greater influence of the Leeuwin Current resulted in a significant decrease in the abundance of copepods (McKinnon, Duggan, Carleton, & Bottger-Schnack, 2008). Further, tropical waters have higher diversity (Chaudhary, Saeedi, & Castello, 2016).

We also found that the zooplankton community bounced back quickly following the heatwave. Some of the impacts on higher trophic levels might not only be a consequence of the direct impacts of warm-water, but on the marked reduction in zooplankton productivity during the heatwave.

Acknowledgements

Data was sourced from Australia's Integrated Marine Observing System (IMOS) which is enabled by the National Collaborative Research Infrastructure Strategy (NCRIS).

Data Sources

IMOS National Reference Stations.
http://imos.org.au/facilities/nationalmooringnetwork/nrs/

IMOS Western Australia Moorings.
http://imos.org.au/facilities/nationalmooringnetwork/wamoorings/

References

Babcock, R. C., Bustamante, R. H., Fulton, E. A., Fulton, D. J., Haywood, M. D. E., Hobday, A. J., Vanderklift, M. A. (2019). Severe continental-scale impacts of climate change are happening now: extreme climate events impact marine habitat forming communities along 45% of Australia's coast. *Frontiers in Marine Science, 6*(411). doi:10.3389/fmars.2019.00411

Chaudhary, C., Saeedi, H., & Castello, M. J. (2016). Bimodality of latitudinal gradients in marine species richness. *Trends in Ecology & Evolution, 31*(9), 670-676. doi:10.1016/j.tree.2016.06.001

Daufresne, M., Lengfellner, K., & Sommer, U. (2009). Global warming benefits the small in aquatic ecosystems. *Proceedings of the National Academy of Sciences of the United States of America, 106*(31), 12788-12793. doi:10.1073/pnas.0902080106

Giani, M., Djakovac, T., Degobbis, D., Cozzi, S., Solidoro, C., & Umani, S. F. (2012). Recent changes in the marine ecosystems of the northern Adriatic Sea. *Estuarine Coastal and Shelf Science, 115*, 1-13. doi:10.1016/j.ecss.2012.08.023

Gorsky, G., Ohman, M. D., Picheral, M., Gasparini, S., Stemmann, L., Romagnan, J.-B., . . . Prejger, F. (2010). Digital zooplankton image analysis using the ZooScan integrated system. *Journal of Plankton Research, 32*(3), 285-303. doi:10.1093/plankt/fbp124

Herring, S. C., Christidis, N., Hoell, A., Kossssin, J. P., Schreck, C. J., & Stott, P. A. (2018). Introduction to exlaining extreme events of 2016 from a climate perspective. *Bulletin of the American Meteorological Society, 99*(1), S1-S6. doi:10.1175/bams-d-17-0284.1

Martin, E. S., Harris, R. P., & Irigoien, X. (2006). Latitudinal variation in plankton size spectra in the Atlantic Ocean. *Deep-Sea Research Part Ii-Topical Studies in Oceanography, 53*(14-16), 1560-1572. doi:10.1016/j.dsr2.2006.05.006

McKinnon, A. D., Duggan, S., Carleton, J. H., & Bottger-Schnack, R. (2008). Summer planktonic copepod communities of Australia's North West Cape (Indian Ocean) during the 1997-99 El Nino/La Nina. *Journal of Plankton Research, 30*(7), 839-855. doi:10.1093/plankt/fbn043

Wernberg, T., Smale, D. A., Tuya, F., Thomsen, M. S., Langlois, T. J., de Bettignies, T., . . . Rousseaux, C. S. (2013). An extreme climatic event alters marine ecosystem structure in a global biodiversity hotspot. *Nature Climate Change, 3*(1), 78-82. doi:10.1038/nclimate1627

IMOS

Integrated Marine
Observing System

IMOS
Integrated Marine Observing System
State and Trends of Australia's Oceans
Report

4.3 Use of Zooplankton communities to estimate the relative strength of the East Australian Current

Wayne Rochester[1], Frank Coman[1], Claire Davies[2], Ruth Eriksen[2], Felicity McEnnulty[2], Anita Slotwinski[1], Mark Tonks[1], Julian Uribe[1] and Anthony J. Richardson[1,3]

[1] CSIRO Oceans and Atmosphere, Queensland Biosciences Precinct (QBP), St Lucia, QLD, Australia
[2] CSIRO Oceans and Atmosphere, Hobart, TAS, Australia
[3] Centre for Applications in Natural Resource Mathematics (CARM), School of Mathematics and Physics, The University of Queensland, St Lucia, QLD, Australia

Summary

A time series of a water temperature index estimated from biological data alone was calculated from the semi-regular AusCPR transects of copepod species composition in the East Australian Current. This time series can potentially help detect changes in the EAC or monitor ecosystem responses to year-to-year variation and long-term trends in the physical and chemical environment, associated with EAC changes, ENSO and climate change.

Key Data Streams

Ships of Opportunity

Satellite Remote Sensing

State and Trends of Australia's Ocean Report
www.imosoceanreport.org.au

Time-Series published
10 January 2020

doi: 10.26198/5e16ae6149e88

Rationale

The East Australian Current (EAC) is the major boundary current in Australia and transports warm water poleward along the east coast of Australia (K. Ridgway, Coleman, Bailey, & Sutton, 2008). In recent decades the EAC has extended further south, increasing the rate of warming in the Tasman Sea (K. R. Ridgway, 2007). The EAC has marked seasonality – its strength peaks in summer (February) and is weakest in winter (K. R. Ridgway & Godfrey, 1997). By transporting organisms from tropical to temperate Australia, the EAC is a major driver of the distribution of marine communities along the east coast of Australia (Poloczanska et al., 2007).

As zooplankton have short generation times and are not exploited, they are sensitive indicators of temperature and different water masses, especially copepods, the most abundant multicellular animals (Hays, Robinson, & Richardson, 2005). One might expect variation in copepod communities down the east coast of Australia, with warmer-water communities in the north and cooler-water ones in the south. More subtly, warmer-water communities could penetrate further south when the EAC is strongest. And we might also expect a signature of the interannual variation in the EAC – which has peaks and troughs about four years apart (K. Ridgway et al., 2008) – might be reflected in changes in the copepod community.

Here we explore whether long-term (2010-2018) changes in the copepod community along the east coast of Australia could be used as an index of the seasonal and inter-annual strength of the EAC. The Integrated Marine Observing System (IMOS) Australian Continuous Plankton Recorder (AusCPR) survey dataset is ideal for this because ships regularly traverse this route towing CPRs. If we can develop an index of the relative strength of the EAC along the CPR route down the east coast, then this could provide a large-scale metric independent of physical measurements and not estimated at a single cross-section across the current.

Methods

Copepod data were collected between Brisbane and the border between New South Wales and Victoria, a distance of ~1600 km (**Figure 1**). The AusCPR dataset comprised 766 samples (transect segments) from 56 trips from 2010 to 2018 and included 180 copepod species (https://portal.aodn.org.au/; see the dataset "IMOS - AusCPR: Zooplankton Abundance"). SST data were obtained from the IMOS Regional Australian Multi-Sensor SST Analysis dataset (Beggs et al., 2011); https://portal.aodn.org.au/; see the dataset "IMOS - SRS - SST - L4 - RAMSSA – Australia").

We calculated a time series of an index of copepod species composition that was purposefully correlated with sea surface temperature (SST). We first conducted a multivariate redundancy analysis (RDA) of copepod species on SST, which ensures the multivariate index is maximally correlated with SST. We then used these sample scores from the multivariate RDA analysis as the univariate response in a generalised additive model, with latitude, day of year, and year as predictors (See Appendix for more details). Predictions from this model allowed us to produce a time series that reflects the copepod composition along the east coast of Australia. This time series included the seasonal, interannual and residual variation, but with the latitude effect removed. The anomalies and climatology can be plotted and interpreted analogously to, for example, the regional SST anomaly.

We have devised the EAC Copepod Composition Index to reflect changes in copepod communities down the east coast of Australia and thus to hopefully reproduce the relative strength of the EAC. If the index works, then the EAC should be stronger and the index more positive when warmer-water copepod communities are distributed further south. By contrast, the EAC should be weaker and the index more negative when warmer-water communities are confined to the north, and cooler-water communities dominate further south.

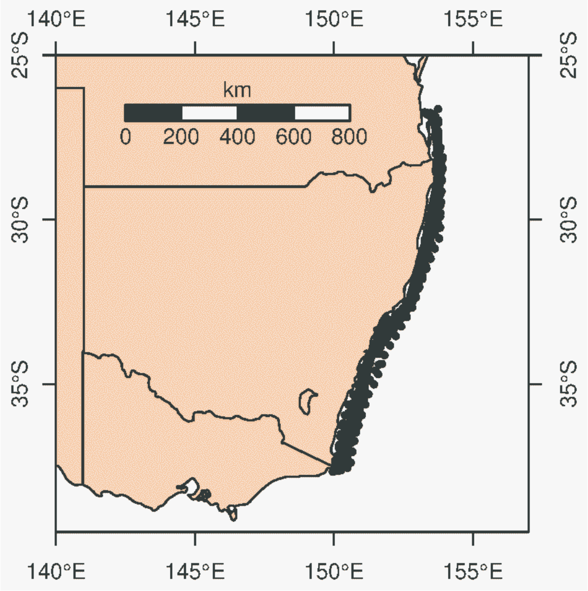

Figure 1. Locations of the CPR samples used in the analysis (nominal locations of transect segments).

Results and interpretation

As expected, the EAC Copepod Composition Index anomaly is positively related to the general trends in the SST anomaly along the east coast from 2010-2018 (R=0.60, p<0.0001, n=39), showing that the index reflects changes in SST. The EAC Copepod Composition Index was driven by real changes in copepod communities: higher values of the Index equated to more warmer-water species such as *Canthocalanus pauper*, *Temora turbinata* and *Centropages furcatus*; and lower values equated to more cooler-water species such as *Oncaea venusta*, *Acartia danae* and *Oncaea media* (**Figure 2**).

doi: 10.26198/5e16ae6149e88

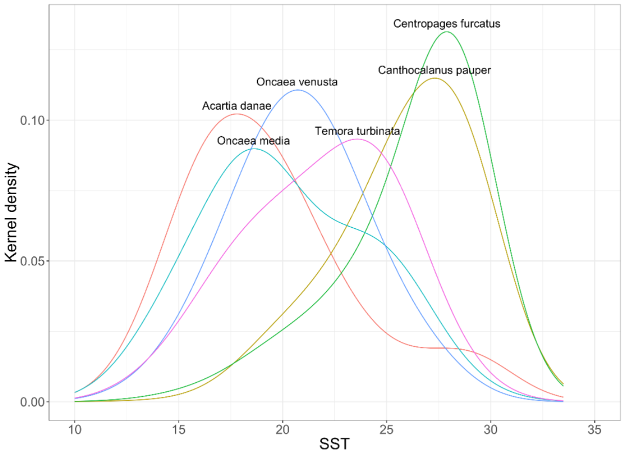

Figure 2. The temperature preferences of key species contributing to higher values of the EAC Copepod Composition Index (warm-water anomalies) included *Canthocalanus pauper*, *Temora turbinata* and *Centropages furcatus*; and those contributing to lower values of the EAC Copepod Composition Index (cool-water anomalies) included *Oncaea venusta*, *Acartia danae* and *Oncaea media*.

The EAC Copepod Composition Index appears to reflect three characteristics of the EAC (**Figure 3**). The first is the Index has a strong seasonal cycle (the dotted line in **Figure 3** is the climatology), with a peak in March and a trough in August, consistent with the known seasonality of the EAC (K. R. Ridgway & Godfrey, 1997) . The second characteristic is that deviations of the Index from the climatology are not random, but persist for extended periods (**Figure 3**). The anomalies indicate species compositions associated with cooler water from 2010-2012 (potentially weaker EAC flow), warmer water from 2014-2016 (potentially stronger EAC flow) and moderate water temperature from 2017-2018 (average EAC flow). From 1993-2006, K. Ridgway et al. (2008) found that the major interannual variation in strength of the EAC (peak-to-trough) was four years, similar to the three-year period we observed in the EAC Copepod Composition Index. Last, the Index is also weakly related to ENSO, with a stronger index under El Niño conditions (R=-0.38, p=0.02, n=39), similar to other studies that have shown similar weak relationship between EAC flow and ENSO (Holbrook, Chan, & Venegas, 2005).

Implications for people and ecosystems

It is difficult to measure the EAC strength along its whole extent, with most physical oceanographic methods estimating the flow over a cross section at a particular point. There are also breaks in the time series measurements. Developing an index based on biology could provide an independent along-EAC estimate of its strength, and potentially help to fill gaps in physical time series. Further, the EAC Copepod Composition Index tells us how the copepod community along the east coast is changing, providing a potentially valuable index for monitoring impacts of climate change. This could be especially valuable considering that the EAC is projected to continue increasing in strength in the future (Cai, Shi, Cowan, Bi, & Ribbe, 2005).

Regular transects by IMOS CPRs enable us to monitor changes in the offshore marine ecosystem that may be associated with year-to-year variation and long-term trends in the physical and chemical environment. These are potentially associated with changes in the EAC, ENSO and climate change. The next step is to further test the EAC Copepod Composition Index using model output (e.g., Bluelink) or measurements from the EAC array or proxy sources (e.g., XBT, CTD and satellite altimetry, Ridgway et al. (2008).

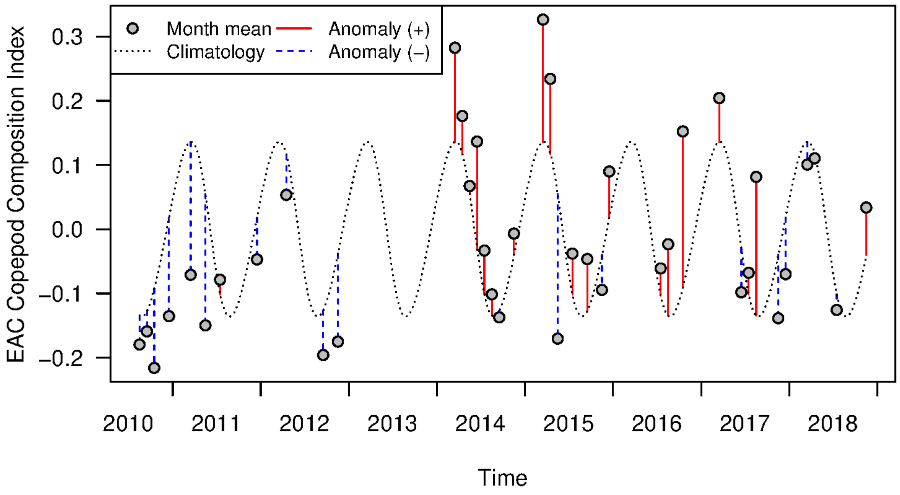

Figure 3. The time series of the EAC Species Composition Index Copepod species composition index. Positive values indicate species compositions associated with warmer water. The graph includes the climatology and anomalies of the index.

doi: 10.26198/5e16ae6149e88

Appendix – Extended Methods

In the calculation of the EAC Copepod Composition Index, we used a distance-based RDA (db-RDA), which transforms the community matrix with a transformation (here the Hellinger transformation) that both works well with species data and retains the Euclidean properties that enable the standard RDA method to be applied. Use of the Hellinger transformation implies that the analysis considered species composition only (i.e. percentage of sample animals in each species) and not absolute abundance. The outcome of this approach is that the value of the RDA score for a sample is the weighted average of the (transformed) percent contribution of each species to the sample total, with the species weights calculated (by the RDA) to ensure the score is correlated with SST.

As for SST, copepod species composition is correlated with latitude and season (**Figure 4**). To calculate our final index and anomalies from the RDA score, we removed the latitude component and calculated a climatology. We termed the final index the EAC Copepod Composition Index. Because the CPR deployment times are seasonal but often irregular because of shipping schedules, these steps could not be performed using simple calculations based on monthly averages. Instead, we used the following generalised additive model (GAM):

$$y = a + f_s(s) + f_l(l) + f_t(t) + e$$

where y is the RDA score, s is day of year, l is latitude, t is time (for trend across years), a is the intercept, e is the residual error and f_s, f_l and f_t are GAM spline functions (with f_s being cyclic). This model conveniently decomposed the RDA scores into components that we could combine by simple arithmetic to create the EAC Copepod Composition Index and climatology (**Figure 5**). We calculated the EAC Copepod Composition Index by subtracting the latitude component of the fitted values (i.e. $y' = y - f_l(l)$).

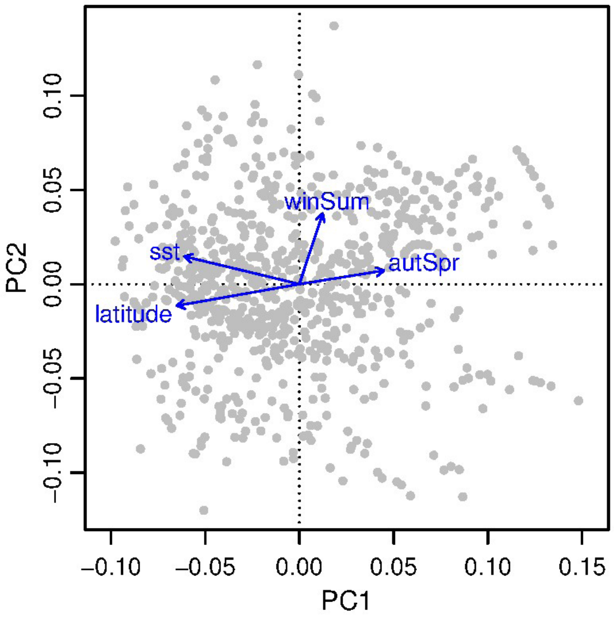

Figure 4. The correlation between copepod species composition (summarised with principal component analysis) and SST, latitude and season (as envfit vectors). The season components are winter–summer and autumn–spring.

The climatology was calculated as the sum of the day-of-year and intercept components of the GAM predicted values (i.e. $y_c = a + f_s(s)$). (Note that these calculations rely on fact that the GAM spline functions are constrained to sum to zero over the range of the data.) There is a clear climatology, with a stronger EAC copepod composition index during summer and weaker during winter (**Figure 5**). The latitudinal effect is nearly linear, but is steeper at more southern latitudes, implying the index is more sensitive to changes there than further north. The interannual time series shows there is longer-term persistent variation (**Figure 5**).

For plotting and further interpretation, the EAC Copepod Composition Index was aggregated to a monthly average. We then plot this output as the EAC Copepod Composition Index (**Figure 3**), and visualise it by including the climatology and anomalies from these.

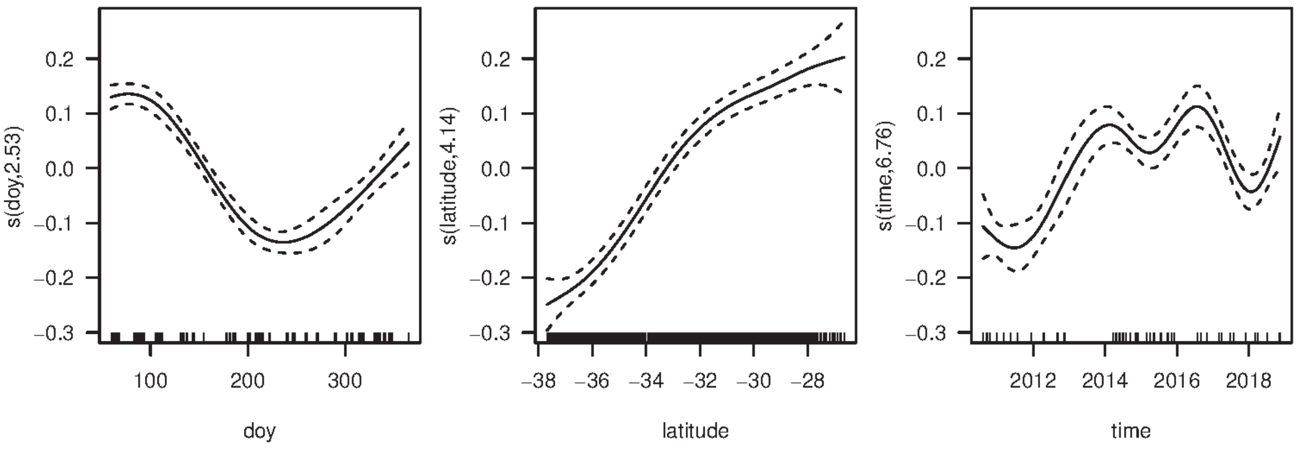

Figure 5. Spline curves for the GAM model terms. The season term (doy = day of year) is cyclic, so the curve connects smoothly between 31 December and 1 January.

Acknowledgements

Data was sourced from Australia's Integrated Marine Observing System (IMOS) which is enabled by the National Collaborative Research Infrastructure Strategy (NCRIS).

Data Sources

IMOS Ships of Opportunity.
http://imos.org.au/facilities/shipsofopportunity/

IMOS Satellite Remote Sensing.
http://imos.org.au/facilities/srs/

References

Beggs, H., Aihong, Z., Graham, W., Oscar, A., Brassington, G., & Pugh, T. (2011). *RAMSSA-An operational, high-resolution, Regional Australian Multi-Sensor Sea surface temperature Analysis over the Australian region* (Vol. 61).

Cai, W., Shi, G., Cowan, T., Bi, D., & Ribbe, J. (2005). The response of the Southern Annular Mode, the East Australian Current, and the southern mid-latitude ocean circulation to global warming. *Geophysical Research Letters, 32*(23). doi:L2370610.1029/2005gl024701

Hays, G. C., Robinson, C., & Richardson, A. J. (2005). Climate change and marine plankton. *Trends in Ecology and Evolution, 20*(6), 337-344.

Holbrook, N. J., Chan, P. S.-L., & Venegas, S. A. (2005). Oscillatory and propagating modes of temperature variability at the 3–3.5- and 4–4.5-yr time scales in the upper southwest Pacific Ocean. *Journal of Climate, 18 (719-736)*, 1637–1639.

Poloczanska, E. S., Babcock, R. C., Butler, A., Hobday, A., Hoegh-Guldberg, O., Kunz, T. J., Richardson, A. J. (2007). Climate change and Australian marine life. *Oceanography and marine biology: an annual review, 45*, 407-478. Retrieved from <Go to ISI>://WOS:000252476600008

Ridgway, K., Coleman, R., Bailey, R., & Sutton, P. (2008). Decadal variability of East Australian Current transport inferred from repeated high-density XBT transects, a CTD survey and satellite altimetry. *113*. doi:10.1029/2007JC004664

Ridgway, K. R. (2007). Long-term trend and decadal variability of the southward penetration of the East Australian Current. *Geophysical Research Letters, 34*(13), 1-5. doi:L1361310.1029/2007gl030393

Ridgway, K. R., & Godfrey, J. S. (1997). Seasonal cycle of the East Australian Current. *Journal of Geophysical Research: Oceans, 102*(C10), 22921-22936. doi:10.1029/97JC00227

IMOS

Integrated **Marine**
Observing System

IMOS
Integrated Marine Observing System
State and Trends of Australia's Oceans
Report

4.4 Ocean acidification and calcifying zooplankton

Anthony J. Richardson[1,2], Wayne Rochester[1]
and Bronte Tilbrook[3,4]

[1] CSIRO Oceans and Atmosphere, Queensland Biosciences Precinct (QBP), St Lucia, QLD, Australia

[2] Centre for Applications in Natural Resource Mathematics (CARM), School of Mathematics and Physics, The University of Queensland, St Lucia, QLD, Australia

[3] CSIRO Oceans and Atmosphere, Hobart, TAS, Australia

[4] Australian Antarctic Program Partnership, University of Tasmania, Hobart, TAS, Australia Partnership,

Summary

There is no evidence of a decline in calcifying zooplankton at the IMOS National Reference Stations over the past 10 years, suggesting ocean acidification over this time span is unlikely to be having a substantial impact on calcifying zooplankton. However, there is some evidence that calcifying zooplankton might at Maria Island and Yongala be sensitive to the aragonite saturation state at the range of values currently observed.

Key Data Streams

National Reference Stations

State and Trends of Australia's Ocean Report
www.imosoceanreport.org.au

Time-Series published
10 January 2020

doi: 10.26198/5e16b0b249e89

Rationale

A consequence of elevated carbon dioxide levels in the atmosphere is that more carbon dioxide dissolves in the ocean. This alters the carbonate balance, releasing more hydrogen ions into the water and lowering pH. There has been a decrease of 0.1 pH units since the Industrial Revolution, representing about a 30% increase in hydrogen ions. This is accompanied by a decrease in the dissolved carbonate ion concentration of the seawater (Doneyet al., 2005). These changes impact the ability of many ocean organisms to grow calcium carbonate structures, increasing maintenance costs, and reducing larval survival and growth (Bednarsek et al., 2019; Waldbusser et al., 2015). Among marine organisms with calcium carbonate shells (calcifiers), those with the aragonite form of calcium carbonate are more susceptible to acidification than those with calcite. The saturation state of both aragonite and calcite is decreasing in ocean waters around Australia. Superimposed on this variability is a strong seasonal cycle, particularly in temperate regions (Lentonet al., 2016).

Methods

To summarise trends in time series of abundance of calcareous groups at the Integrated Marine Observing System (IMOS) National Reference Stations, we plotted sample scores of the first component of a principal components analysis of the abundance time series of a suite of calcareous zooplankton groups (IMOS Australian Ocean Data Network (AODN) dataset: “IMOS National Reference Station (NRS) - Zooplankton Abundance”). The principal components scores can be interpreted as an index of abundance of the community, with a high positive score reflecting high abundances of calcifiers (Edwards & Richardson, 2004; Legendre & Legendre, 2012). Calcareous groups included in this analysis are: echinoderm larvae (starfish and sea urchins that have calcite structures with magnesium, which makes it 30 times more soluble than calcite alone (Raven et al., 2005); bivalve larvae that have shells of aragonite and calcite; several gastropods including Cavoliniids that have aragonite shells, *Limacina* spp. with aragonite shells, and prosobranchs (some which have calcite and others aragonite shells)).

We then corelated the principal component scores with the aragonite saturation state at each national reference station. We calculated aragonite saturation state based on calculations of saturation state made using measurements of total dissolved carbon dioxide and total alkalinity (AODN dataset: “IMOS National Reference Station (NRS) - Salinity, Carbon, Alkalinity, Oxygen and Nutrients (Silicate, Ammonium, Nitrite/Nitrate, Phosphate)”) following best practice recommendations (Dickson, Sabine, & Dore, 2007). If ocean acidification is impacting calcifiers over the time scale of sampling, one would expect a positive relationship between the abundance of calcifiers and the aragonite saturation state is lower.

Results and interpretation

The principal components analysis shows that there is considerable seasonal and inter-annual variation in abundance of calcifying zooplankton (**Figure 1**). Linear trend lines for each National Reference Station and for all stations combined show that there is no overall decline in abundance of calcifiers. There are modest increases in calcifier abundance at Maria Island, Port Hacking and Darwin, and slight declines at Yongala and Kangaroo Island, but no substantial declines.

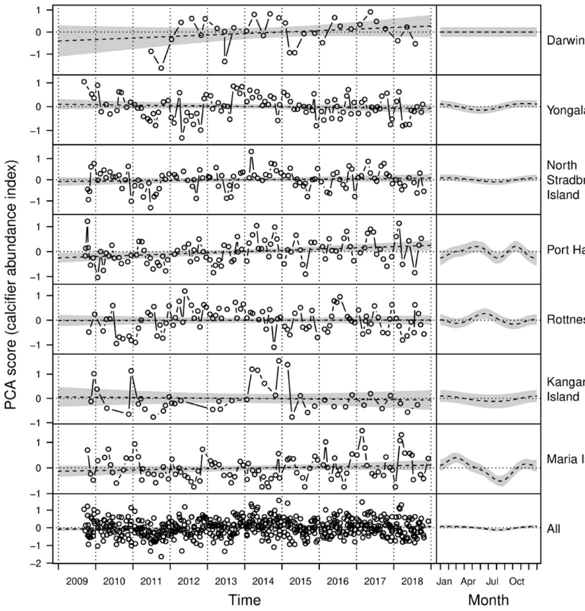

Figure 1. Time series of the scores on the first principal component of calcifying zooplankton (echinoderm larvae, bivalve larvae, Cavoliniid gastropods, and other shelled gastropods) and their seasonal cycles at the National Reference Stations. A linear trend was fitted to each NRS. The bottom plot shows the trend and seasonal cycle of zooplankton calcifiers for all stations combined.

There is strong seasonality in calcifier abundance at some stations. Warmer more tropical stations (Darwin, Yongala, North Stradbroke Island) have little seasonality, but colder-water stations (especially Maria Island, Rottnest and Kangaroo Island) are strongly seasonal. There is a clear spring and autumn bloom in calcifiers in Port Hacking, and a summer and autumn peak in Maria Island.

Calcifier abundance does not appear to be related to the range of aragonite saturation states observed at most National Reference Stations (**Figure 2**). However, there are significant positive relationships between the abundance of calcifiers (the first principal component) and the aragonite saturation state for Maria Island (r=0.34, p=0.007) and Yongala (r=0.32, p=0.001). This is likely to be a consequence of seasonal changes in aragonite saturation and calcifiers, but it could suggest that calcifiers in those regions might be sensitive to changes in aragonite saturation state. However, seasonal increases in temperature and saturation state coincide, so disentangling impacts of both is difficult.

doi: 10.26198/5e16b0b249e89

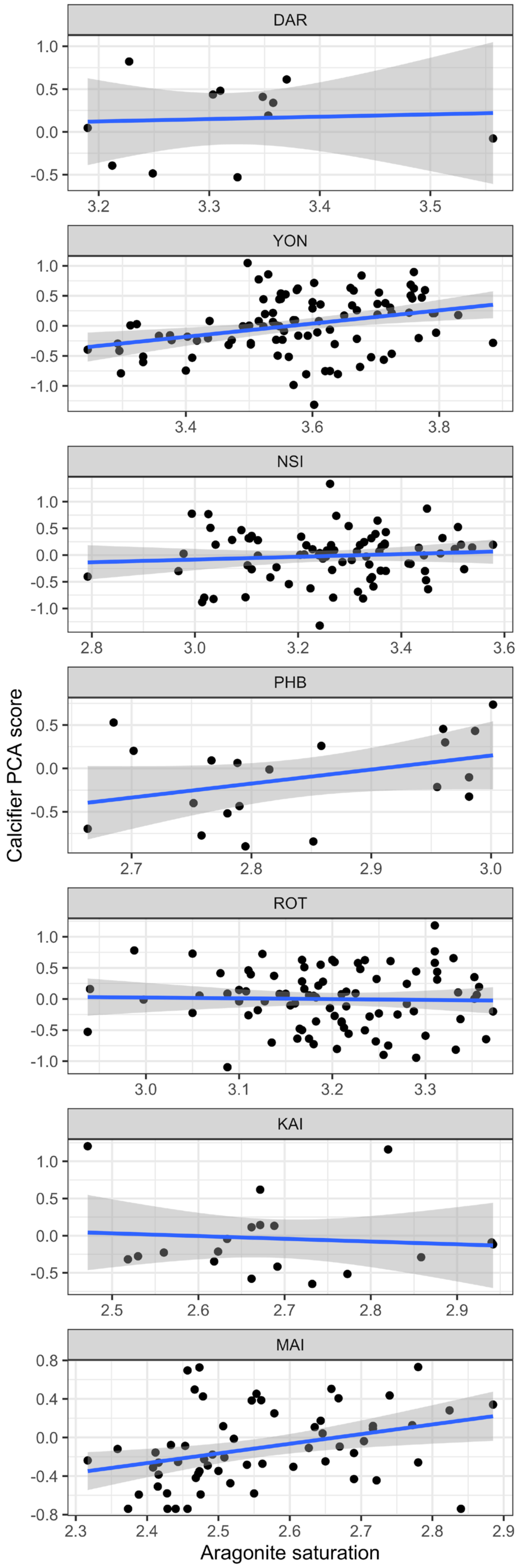

Figure 2. The relationship between the first principal component of calcifiers (echinoderm larvae, bivalve larvae, Cavoliniid gastropods, and other shelled gastropods) and the aragonite saturation state at the National Reference Stations.

Implications for people and ecosystems

There is no evidence of a decline in calcifying zooplankton at the IMOS National Reference Stations over the past 10 years. This suggests that ocean acidification over this time span is unlikely to be having a substantial impact on calcifying zooplankton. However, there is some evidence that at Maria Island and at Yongala that calcifiers might be sensitive to the aragonite saturation state at the range of values currently observed. It is also not clear if the changes that have occurred since the 1870s in the Australian region (Lenton et al., 2016) may have already impacted on zooplankton abundance. As the seawater aragonite saturation state continues to decrease in the future, the IMOS network is well placed to provide an early warning system of the impact of ocean acidification on calcifying zooplankton and other species.

Acknowledgements

Data was sourced from Australia's Integrated Marine Observing System (IMOS) which is enabled by the National Collaborative Research Infrastructure Strategy (NCRIS).

Data Sources

IMOS National Reference Stations.
http://imos.org.au/facilities/nationalmooringnetwork/nrs/

References

Bednarsek, N., Feely, R. A., Howes, E. L., Hunt, B. P. V., Kessouri, F., Leon, P., . . . Weisberg, S. B. (2019). Systematic review and meta-Aanalysis toward synthesis of thresholds of ocean acidification impacts on calcifying pteropods and interactions with warming. *Frontiers in Marine Science, 6*, 16. doi:10.3389/fmars.2019.00227

Dickson, A., Sabine, C., & Dore, J. (2007). Guide to best practices for ocean CO2 measurements

Doney, S. C., Fabry, V. J., Feely, R. A., & Kleypas, J. A. (2009). Ocean acidification: the other CO^2 problem. *Annual Review of Marine Science, 1*, 169-192. doi:10.1146/annurev.marine.010908.163834

Edwards, M., & Richardson, A. J. (2004). Impact of climate change on marine pelagic phenology and trophic mismatch. *Nature, 430*(7002), 881-884. Retrieved from 10.1038/nature02808

Legendre, P., & Legendre, L. (2012). *Numerical ecology. 3rd edition. 1006 pp.* (3rd ed. Vol. 24).

Lenton, A., Tilbrook, B., Matear, R. J., Sasse, T. P., & Nojiri, Y. (2016). Historical reconstruction of ocean acidification in the Australian region. *Biogeosciences, 13*(6), 1753-1765. doi:10.5194/bg-13-1753-2016

Raven, J., Caldeira, K., Elderfield, H., & Hoegh-Guldberg, O. (2005). *Ocean acidification due to increasing atmospheric carbon dioxide*. Retrieved from

Waldbusser, G. G., Hales, B., Langdon, C. J., Haley, B. A., Schrader, P., Brunner, E. L., . . . Gimenez, I. (2015). Saturation-state sensitivity of marine bivalve larvae to ocean acidification. *Nature Climate Change, 5*(3), 273-280. doi:10.1038/nclimate2479

IMOS

Integrated **Marine**
Observing System

IMOS
Integrated Marine Observing System

State and Trends of Australia's Oceans
Report

4.5 Sounding out life in Australia's twilight zone

Rudy Kloser[1] and Haris Kunnath[1]

[1]CSIRO Oceans and Atmosphere, Hobart, TAS, Australia

Summary

There is an increasing decadal trend in the Southern Australian Ocean twilight zone (200-1000 m depth) animals reflected sound. The twilight zone animals of fish, squids and zooplankton are an important aspect of the oceans, acting as predators and prey, storing carbon and as a potential food resource for humans. We now need to solve who, why and implication.

Key Data Streams

Ships of Opportunity

State and Trends of Australia's Ocean Report
www.imosoceanreport.org.au

Time-Series published
10 January 2020

doi: 10.26198/5e16b0ef49e8a

Rationale

The world's oceanic mesopelagic habitat (200–1000 m depth) is probably the largest unexplored region of the Earth (St. John et al., 2016). Recent research has highlighted that the fish biomass in the mesopelagic twilight zone – where there is very little light – could be between 2 to 20 billion tonnes. Most mesopelagic fish are currently unexploited, and it is likely that they will be increasingly harvested in the future for food and fish meal (St John et al., 2016). The mesopelagic zone also contributes substantially to active carbon sequestration (Davison et al., 2015; Proud et al., 2018), through vertical migration by fish, squid and zooplankton swimming toward the surface to feed during the night and returning to depth each day. This daily migration is the largest on Earth (**Figure 1**). To better understand the present biomass and structure of mesopelagic food webs, and how these change through time, we need long-term acoustic estimates. This information can inform ecosystem, carbon and Earth system models.

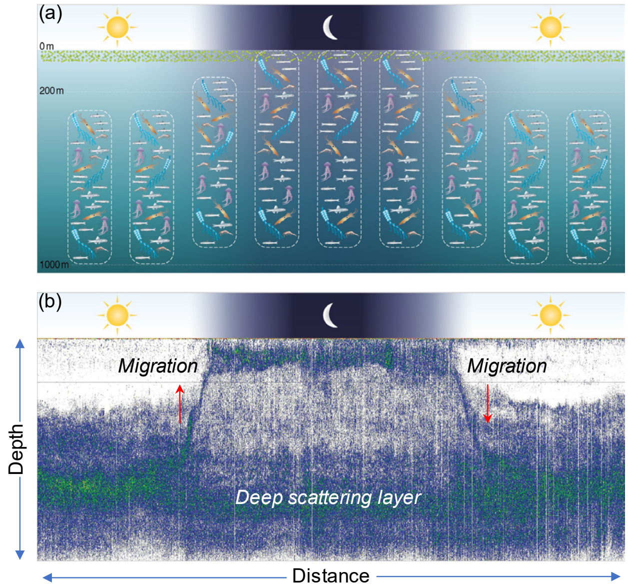

Figure 1. An example of diel vertical migration in the mesopelagic zone. (a) A stylised micronekton ecosystem (fish, squid, jellyfish and other zooplankton ~2-20 cm in size), many of which exhibit daily vertical migration. (b) Acoustic observations at 38 kHz (the deep scattering layer is indicated).

Methods

The Integrated Marine Observing System (IMOS) Ships of Opportunity Bio-Acoustics Facility provides ocean basin scale calibrated acoustic data, with snapshots of mesopelagic communities (**Figure 2**, Kloseret al., 2009). The main goal of the Bio-Acoustic Facility, operating since 2010, is to provide repeated observations for the status and trend of micronekton using echosounders on ships of opportunity. Key transects have been repeated across the Tasman Sea, Southern Ocean and the Indian Ocean. The Tasman Sea is separated into western, central and eastern regions (Flynn and Kloser 2012). Acoustic data are calibrated (Demer et al., 2015), quality-controlled (Ryan et al., 2015) and have a resolution of 1 km in distance and 10 m in depth (Figure 1b). Since 2010, ~513,219km of data from 18 vessels have been processed and reside in the Australian Ocean Data Network (AODN) (www.aodn.org.au). Historical data (2004-2009) for the Tasman Sea were also sourced and processed in the same way (Kloser et al., 2009). Derived data are calibrated area backscattering coefficient s_a (m^2 m^{-2}) that under appropriate conditions is linearly proportional to the density of dominant scattering organisms. Data are summarised into epipelagic (20–200 m), upper mesopelagic (200–400 m) and lower mesopelagic (400–800 m) layers. Although multiple frequencies are collected, only the 38 kHz data series constituting 82% of the total data is used here. Data are tagged with location, date, time of day, and an estimate of net primary production (NPP, from a Vertically Generalized Production Model) averaged for the year prior to acquiring the acoustic data.

Results and Interpretation

The 38 kHz acoustic backscatter data highlight large spatial variations at the basin scale that generally follow the Longhurst bioregions based on NPP (**Figure 2**). However, there are notable differences at the boundaries and within several regions for the lower mesopelagic layer (e.g. the low nutrient central south Pacific and Indian southern subtropical gyre province around Mauritius). The IMOS data have been used to test the current Longhurst pelagic bioregions (Longhurst, 2007; Proud et al., 2017), and as more data are collected, they can be used to produce a more refined pelagic bioregionalisation around Australia and the Southern Ocean.

From 2004-2018, there is an increasing linear trend in winter acoustic backscatter (with different magnitudes) in the Western (by 42%), Central (105%) and Eastern regions (100%) of Tasman Sea (**Figure 3a-c**). The increasing trend is also evident for the water column from 20–1200 m, as the lower mesopelagic represents 60-70% of the total acoustic backscatter. Trends in annual-averaged NPP at the sampling locations have either no trend or are slightly negative compared to the increasing acoustic trend for all three Tasman Sea regions. Correlation between annual NPP and snapshot acoustic data may not reflect the different temporal and spatial scales of the NPP and biology responsible for the acoustic scattering. The 38 kHz acoustic data are measuring a biological response from resonant scattering of fish and siphonophores in the gas-bladder size range of ~0.4-1.0 mm equivalent spherical radius (Kloser et al., 2016). Due to their age, these animals may have been transported some distance from the original primary production source.

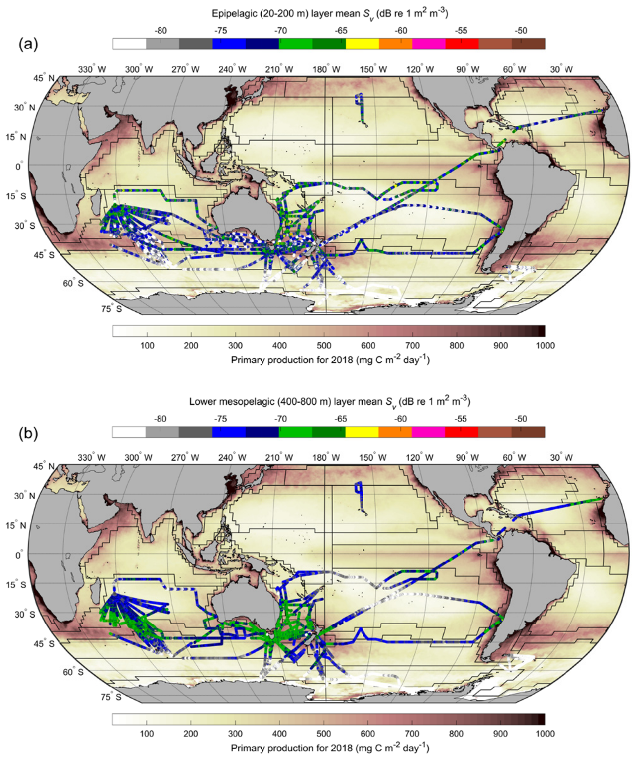

Figure 2. The mean volume backscattering strength S_v (dB re 1 m^2 m^{-3}) at 38 kHz for the IMOS BASOOP data. (a) Epipelagic layer (20–200 m depth) highlighting basin-scale diel vertical migration. (b) The lower mesopelagic layer (400–800 m depth). The 2018 annual averaged net primary production (mgC/m^2/d) is shaded in brown and Longhurst bioregions as black lines. Acoustic data in Scotia Sea were sourced from www.mesopp.eu.

For the Southern Ocean region (**Figure 3d**), there is an increasing trend (by 77% from 2010-2018) in acoustic data in late summer to autumn, but there is no clear trend in NPP (**Figure 3d-iv**).

The most plausible explanation for the increasing trend in the acoustic signal is that the number of organisms that have resonant gas bladders in the size range ~0.4 to 1.0 mm has increased in the lower mesopelagic regions sampled (Kloser et al., 2016). It appears the rate of increase is greatest for the Southern region (**Figure 3d-ii**). Although there are other potential explanations for the rise in backscatter, it is unlikely to be driven by measurement bias, given the temporal scale and diversity of vessels used. The validity of this interpretation, the mechanism causing this increase, and its significance need to be confirmed through net and acoustic/optical probe sampling.

Implications for people and ecosystems

Open ocean mesopelagic communities are a key ocean resource with an extremely large biomass that links pelagic and benthic systems. They also play an active role in carbon sequestration. The IMOS data provide the first decade-long, publicly accessible time series of mesopelagic bioacoustics anywhere in the world. The bio-acoustic time series of the structure and change of key components of the biology to 1200 m highlights a significant increasing trend (between 40–105% from 2004-2018) in the acoustic backscatter (400–800 m) for the Tasman Sea and Southern Ocean Time Series region. This likely increase in organisms may increase the active process of carbon sequestration. There has been some interest in harvesting these communities for protein and oils, though currently not in Australian waters. However, fishery sustainability and ecological impacts would need to be assessed prior to any activity or significant harvesting.

Figure 3. Trend in the acoustic time series for the Tasman Sea [(a) Western, (b) Central, and (c) Eastern regions] and (d) Southern Ocean highlighting, (ii) lower mesopelagic layer (400–800 m), (iii) full measured water column (20–1200 m) and, (iv) the annual net primary production. A fit to a linear trend (dashed line) with, correlation coefficient (*r*) and significance (*p*-value) in red, the 25 and 75% quantile of the data values are shaded as light blue.

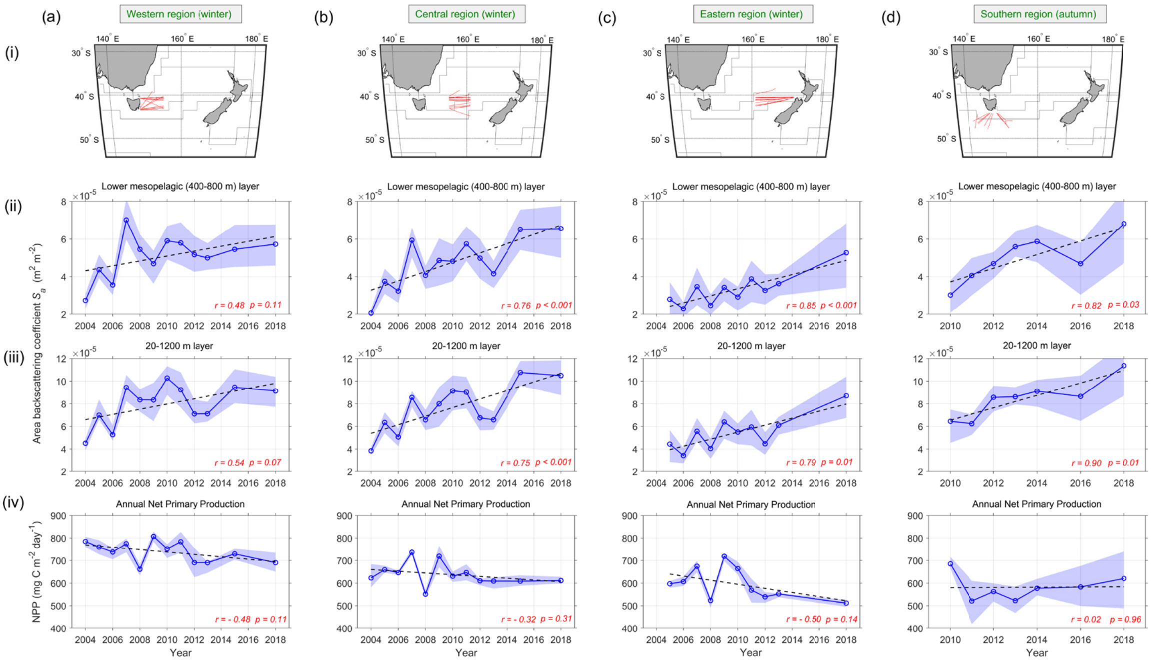

Acknowledgements

Data was sourced from Australia’s Integrated Marine Observing System (IMOS) which is enabled by the National Collaborative Research Infrastructure Strategy (NCRIS).

Data Sources

IMOS Ships of Opportunity.
http://imos.org.au/facilities/shipsofopportunity/

References

Davison, P. C., Koslow, J. A., & Kloser, R. J. (2015). Acoustic biomass estimation of mesopelagic fish: backscattering from individuals, populations, and communities. ***ICES Journal of Marine Science, 72***(5), 1413-1424. doi:10.1093/icesjms/fsv023

Demer, D., Berger, L., Bernasconi, M., Bethke, E., Boswell, K., Chu, D., . . . Gauthier, S. (2015). Calibration of acoustic instruments. ***ICES Cooperative Research Report, 326***, 133.

Flynn, A., & Kloser, R. (2012). Cross-basin heterogeneity in lanternfish (family Myctophidae) assemblages and isotopic niches ($\delta^{13}C$ and $\delta^{15}N$) in the southern Tasman Sea abyssal basin. ***Deep Sea Research Part I: Oceanographic Research Papers, 69***, 113-127.

Kloser, R. J., Ryan, T. E., Keith, G., & Gershwin, L. (2016). Deep-scattering layer, gas-bladder density, and size estimates using a two-frequency acoustic and optical probe. ***ICES Journal of Marine Science, 73***(8), 2037-2048. doi:10.1093/icesjms/fsv257

Kloser, R. J., Ryan, T. E., Young, J. W., & Lewis, M. E. (2009). Acoustic observations of micronekton fish on the scale of an ocean basin: potential and challenges. ***ICES Journal of Marine Science, 66***(6), 998-1006. doi:10.1093/icesjms/fsp077

Longhurst, A. R. (2007). ***Ecological Geography of the Sea*** (Second ed.): Academic Press.

Proud, R., Cox, M. J., & Brierley, A. S. (2017). Biogeography of the global ocean’s mesopelagic zone. ***Current Biology, 27***(1), 113-119.

Proud, R., Handegard, N. O., Kloser, R. J., Cox, M. J., Brierley, A. S., & Handling editor: David, D. (2018). From siphonophores to deep scattering layers: uncertainty ranges for the estimation of global mesopelagic fish biomass. ***ICES Journal of Marine Science***. doi:10.1093/icesjms/fsy037

Ryan, T. E., Downie, R. A., Kloser, R. J., & Keith, G. (2015). Reducing bias due to noise and attenuation in open-ocean echo integration data. ***ICES Journal of Marine Science, 72***(8), 2482-2493. doi:10.1093/icesjms/fsv121

St. John, M. A., Borja, A., Chust, G., Heath, M., Grigorov, I., Mariani, P., . . . Santos, R. S. (2016). A Dark Hole in Our Understanding of Marine Ecosystems and Their Services: Perspectives from the Mesopelagic Community. ***Frontiers in Marine Science, 3***(31). doi:10.3389/fmars.2016.00031

IMOS
Integrated Marine Observing System

State and Trends of
Australia's Oceans
Report

4.6 Temporal and spatial changes in larval fish

Ana Lara-Lopez[1,2], Charlie Hinchliffe[3], Iain M. Suthers[4],
Anthony J. Richardson[5,6] and Paloma A. Matis[4,7]

[1] Integrated Marine Observing System (IMOS), University of Tasmania, Hobart, TAS, Australia
[2] Institute for Marine and Antarctic Studies, University of Tasmania, Hobart, TAS, Australia
[3] School of Life Sciences, University of Technology Sydney, Broadway, NSW, Australia
[4] Sydney Institute of Marine Science, Building 19, Chowder Bay Road, Mosman, NSW , Australia
[5] CSIRO Oceans and Atmosphere, Queensland Biosciences Precinct (QBP), St Lucia, QLD, , Australia
[6] Centre for Applications in Natural Resource Mathematics (CARM), School of Mathematics and Physics, The University of Queensland, St Lucia, QLD, Australia
[7] Evolution and Ecology Research Centre, University of New South Wales, Sydney, NSW , Australia

Summary

Historical data and contemporary larval fish observations from the IMOS larval fish monitoring along the East Coast of Australia indicate the EAC may be affecting the larval fish community composition by distributing warm-water communities further south. This restructuring of the larval fish community is an expected impact of climate change that can have ecological and economic implications for the region.

Key Data Streams

Ships of Opportunity

National Reference Stations

State and Trends of Australia's Ocean Report
www.imosoceanreport.org.au

Time-Series published
10 January 2020

doi: 10.26198/5e16b12149e8b

Rationale

Most marine fish inhabit the upper water column during their early life, with eggs and larvae developing as part of the plankton. During this early life stage, fish are sensitive to environmental changes, with many oceanographic, biological and anthropogenic processes (e.g., eutrophication, pollution, climate change and fisheries) influencing their distribution, abundance and survival (Cowen et al., 2007, Hsieh et al., 2006, Keane and Neira, 2008). This makes the monitoring of larval fish a valuable tool for assessing ecosystem changes, and a relatively low-cost and efficient means for monitoring fish populations and communities (Koslow and Couture, 2013, Koslow and Wright, 2016). Larval fish time series can reflect long-term changes in the fish community, including the influence of large-scale oceanographic drivers of fish species distributions (Booth et al., 2011, Last et al., 2011, Vergés et al., 2016), and may also provide a valuable fishery-independent indicator of stock size and stock boundaries (Leis and McGrouther, 1996). Here we combine historical data on fish larval abundance, diversity and distribution with contemporary data from the Integrated Marine Observing System (IMOS) to investigate the distribution of larval abundance and richness down the east coast of Australia. We analyse seasonal changes in the latitudinal distribution of larval fish abundance and richness down the east coast. We also investigate whether climate change is having an effect on larval fish distributions by comparing the distribution of richness down the east coast before 1998 with the contemporary estimates after 1998. Our hypothesis is that as climate change has strengthened the East Australian Current (EAC) (Ridgway, 2007, Ridgway et al., 2008), larval fish communities should be more similar down the east coast now than in previous years (see Section on “Using zooplankton communities to estimate the relative strength of the East Australian Current” by Rochester et al. for a similar investigation).

Methods

We analysed data on larval fish assemblages from 11 surveys and programs from 1983-present in temperate and subtropical Australian pelagic waters (**Figure 1**). Samples were collected on the continental shelf (<200 m) and fish larvae were classified to the lowest possible taxonomic resolution. Historical data were compared with modern data from IMOS National Reference Stations (NRS) at Maria Island, Port Hacking and Stradbroke Island since 2009 off the east coast of Australia (Smith et al., 2018). Data were sourced from (Smith et al., 2018), the updated dataset will be available in the IMOS Australian Ocean Data Network (AODN) (https://portal.aodn.org.au/) in the near future.

We used generalised additive models to explore how spatial patterns in larval fish abundance and richness changed through time, using season and latitude as covariates. To assess changes in the larval community, we used Principal Coordinates Analysis on a square-root transformed Bray-Curtis dissimilarity matrix of larval fish assemblages, after removing rare species.

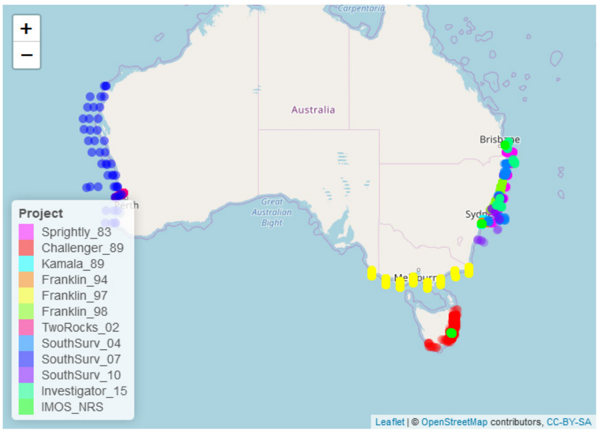

Figure 1. Locations of data for each Survey and the IMOS National Reference Stations (IMOS NRS) at which monthly sampling of larval fishes is ongoing are indicated.

Results and interpretation

Larval fish density was generally lower off the west coast, and higher off the east coast of Australia (**Figure 2**). In the west highest densities were off Perth, and in the east highest densities were off the New South Wales coast.

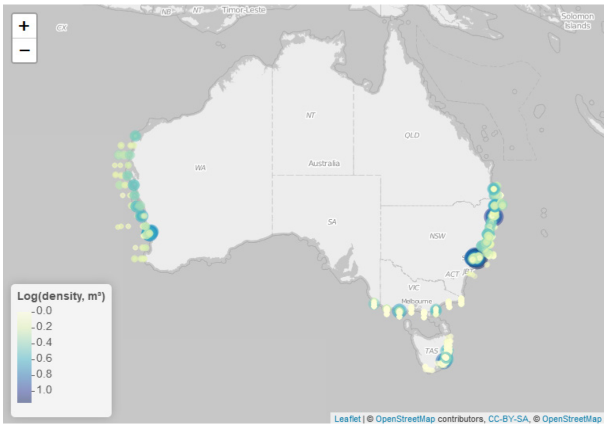

Figure 2. Density of larval fish (ind. m^{-3}) around Australia from historical datasets and IMOS NRS stations in Maria Island, Port Hacking and Stradbroke Island.

There was a strong latitudinal trend in species richness in most seasons, with higher species richness in tropical northern regions and a steep decline in abundance south of 30°S (**Figure 3**). This decline in richness with increasing latitude is typical for most species (Chaudhary et al., 2017). The only season that did not show this decline in richness with latitude was summer when species richness appears to be more similar down the east coast (**Figure 3a**). This is likely due to local spawning during summer near Tasmania, with the strengthening of the EAC perhaps playing some role, although, this cannot be confirmed at this stage.

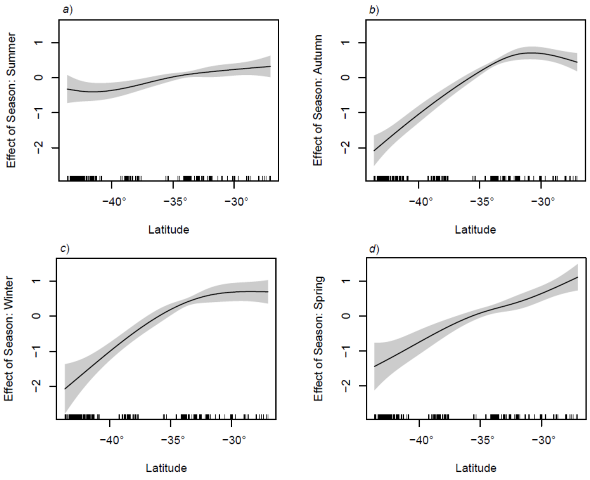

Figure 3. Seasonal effect of latitude on larval fish species richness in relation to the mean, after accounting for the effects of bathymetry, sampling depth, gear type (data not shown). The solid line represents the regression spline fitted in a GAM with 95% confidence intervals for the mean fit.

Similarly, total abundance showed a strong latitudinal trend in most seasons, with higher larval abundances in the north, although summer again was the only exception (**Figure 4**). In summer, there was little change in abundance down the east coast. Again, this is due to local spawning driving the increase in abundance in the higher latitudes, reflecting the strong seasonal character in fish spawning for this region.

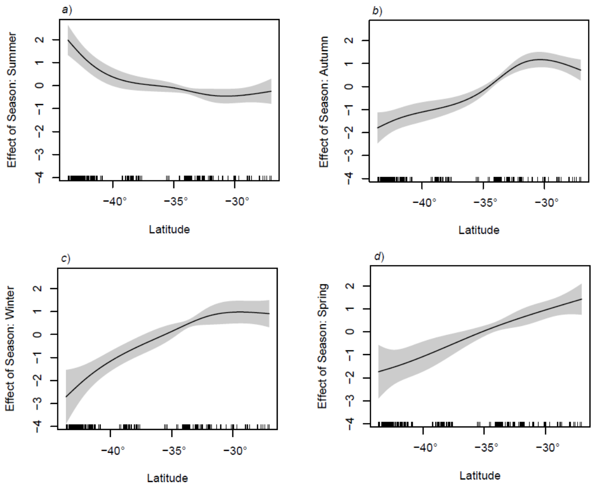

Figure 4. Effect of latitude on larval fish abundance in relation to the mean, after accounting for the effects of bathymetry, sampling depth, gear type. Data were grouped into terrestrial seasons. The solid line represents the regression spline fitted in a GAM with 95% confidence intervals for the mean fit.

Based on the first Principal Coordinate Analysis, the larval fish community has varied over time down the east coast of Australia (**Figure 5**). Before 1998, there is a marked difference in Principal Coordinate Analysis scores between northern and southern Australia. By contrast, after 1998, the Principal Coordinate Analysis scores varied less with latitude. Thus, the larval fish assemblage south of 35°S appears more similar to the northern assemblages post-1998. This might suggest that post-1998 fish larval assemblages at southern latitudes became more similar to the northern assemblages compared to those before 1998, an expected outcome under a warming climate. However, at this point in time, data from Tasmanian waters after the 1998 El Nino benchmark event is limited. Therefore, these trends needs further investigation, and the continuation of IMOS larval fish observations is crucial to ascertain if this trend is real.

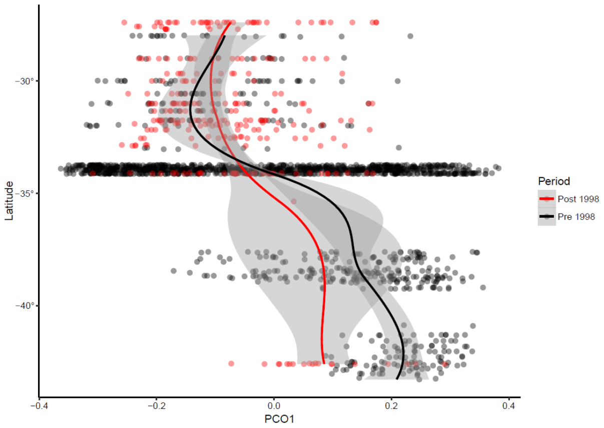

Figure 5. PCO1 loadings from each sample plotted against latitude. The red line is fitted using loess smoother for the post-1998 data with 95% confidence intervals, and the black line is loess smoother for the pre-1998 data with 95% confidence intervals.

Implications for people and ecosystems

Here we show that the abundance and diversity of fish larvae decline towards the south of the east Australian coast. Furthermore, we found that the EAC may be playing an important role in what appears to be a weakening of the latitudinal gradient of the larval fish assemblage post-1998. This trend, is in agreement with the gradients found in copepod communities along the east coast of Australia, with warm-water communities being distributed further down the east coast during summer (see State and Trends of Australia's Ocean Report 4.3: Use of zooplankton communities to estimate the relative strength of the East Australian Current). Collectively, these findings highlight the strong structuring role that the EAC is having on pelagic communities down the east coast of Australia.

The behaviour of the EAC also explains the long-term changes in the distribution of fish larvae in response to climate change we observed. The increase in the strength of the EAC has driven a poleward shift in species distribution, which is superimposed on local warming, promoting the transport of warmer-water fish species further south (Booth et al., 2011, Booth et al., 2007, Ridgway, 2007, Johnson et al., 2011, Last et al., 2011). This explains why we observe more similar communities of fish larvae down the east coast after 1998 compared with years beforehand.

The shift in the distribution of marine organisms is one of the main expected impacts of climate change and can have ecological and economic consequences (Pecl et al., 2017, Booth et al., 2011, Last et al., 2011). Ecologically, the movement of species causes the reshuffling of existing communities (Booth et al., 2011, Vergés et al., 2016). The southward shift in fish larval distributions may suggest that spawning regions are shifting as the ocean warms due to climate change – and although probably thermally suitable, the impacts on recruitment are unclear. Thus, this shift in the distribution of fish larvae could have an economic effect, with some commercial species shifting away from current fishing areas while presenting new opportunities in new regions.

The IMOS larval fish monitoring program fills a unique gap in Australian marine science. It is the only monthly fisheries-independent dataset for understanding the spawning of fish that are of commercial and non-commercial importance. As the time series grows, the IMOS larval fish monitoring program will provide new insights into not only how fish larval assemblages are changing their distribution with climate change, but also how the timing of spawning might be impacted.

Acknowledgements

Data was sourced from Australia's Integrated Marine Observing System (IMOS) which is enabled by the National Collaborative Research Infrastructure Strategy (NCRIS).

Data Sources

IMOS National Reference Stations.
http://imos.org.au/facilities/nationalmooringnetwork/nrs/

IMOS Ships of Opportunity.
http://imos.org.au/facilities/shipsofopportunity/

References

Booth, D. J., Bond, N., & Macreadie, P. (2011). Detecting range shifts among Australian fishes in response to climate change. *Marine and Freshwater Research, 62*(9), 1027-1042.

Booth, D. J., Figueira, W. F., Gregson, M. A., Brown, L., & Beretta, G. (2007). Occurrence of tropical fishes in temperate southeastern Australia: Role of the East Australian Current. *Estuarine, Coastal and Shelf Science, 72*(1-2), 102-114. Retrieved from http://www.sciencedirect.com/science/article/B6WDV-4MFKDD0-1/2/e36241f1aac00e308e22cc27586632c8

Chaudhary, C., Saeedi, H., & Costello, M. J. (2017). Marine species richness is bimodal with latitude: A reply to Fernandez and Marques. *Trends in Ecology & Evolution, 32*, 234-237.

Cowen, R. K., Gawarkiewicz, G., Pineda, J., Thorrold, S. R., & Werner, F. E. (2007). Population connectivity in marine systems an overview. *Oceanography, 20*(3), 14-21.

Hsieh, C.-h., Reiss, C. S., Hunter, J. R., Beddington, J. R., May, R. M., & Sugihara, G. (2006). Fishing elevates variability in the abundance of exploited species. *Nature, 443*(7113), 859.

Johnson, C. R., Banks, S. C., Barrett, N. S., Cazassus, F., Dunstan, P. K., Edgar, G. J., . Taw, N. (2011). Climate change cascades: Shifts in oceanography, species' ranges and subtidal marine community dynamics in eastern Tasmania. *Journal of Experimental Marine Biology and Ecology, 400* (1-2), 17-32. doi:10.1016/j.jembe.2011.02.032

Keane, J. P., & Neira, F. J. (2008). Larval fish assemblages along the south-eastern Australian shelf: linking mesoscale non-depth-discriminate structure and water masses. *Fisheries Oceanography, 17*(4), 263-280.

Koslow, J. A., & Couture, J. (2013). Ocean sciences: Follow the fish. *Nature News, 502*(7470), 163.

Koslow, J. A., & Wright, M. (2016). Ocean sciences: Follow the fish. *Nature News, 502*, 163.

Last, P. R., White, W. T., Gledhill, D. C., Hobday, A. J., Brown, R., Edgar, G. J., & Pecl, G. (2011). Long-term shifts in abundance and distribution of a temperate fish fauna: a response to climate change and fishing practices. *Global Ecology and Biogeography, 20*(1), 58-72. doi:10.1111/j.1466-8238.2010.00575.x

Leis, J., & McGrouther, M. (1996). Regional larval fish archives now in operation: availability of an important fisheries resource. *Australian Society for Fish Biology, Inc. Newsletter, 26*, 25-31.

Pecl, G. T., Araujo, M. B., Bell, J. D., Blanchard, J., Bonebrake, T. C., Chen, I. C., . . . Williams, S. E. (2017). Biodiversity redistribution under climate change: Impacts on ecosystems and human well-being. *Science, 355*(6332), 9. doi:10.1126/science.aai9214

Ridgway, K., Coleman, R., Bailey, R., & Sutton, P. (2008). Decadal variability of East Australian Current transport inferred from repeated high-density XBT transects, a CTD survey and satellite altimetry. *Journal of Geophysical Research, 113*, 18pp.

Ridgway, K. R. (2007). Long-term trend and decadal variability of the southward penetration of the East Australian Current. *Geophysical Research Letters, 34*(13), 1-5. doi:L13613

10.1029/2007gl030393

Smith, J. A., Miskiewicz, A. G., Beckley, L. E., Everett, J. D., Garcia, V., Gray, C. A., . . . Lara-Lopez, A. (2018). A database of marine larval fish assemblages in Australian temperate and subtropical waters. *Scientific data, 5*, 180207.

Vergés, A., Doropoulos, C., Malcolm, H. A., Skye, M., Garcia-Pizá, M., Marzinelli, E. M., Vila-Concejo, A. (2016). Long-term empirical evidence of ocean warming leading to tropicalization of fish communities, increased herbivory, and loss of kelp. *Proceedings of the National Academy of Sciences, 113*(48), 13791-13796.

IMOS
Integrated Marine Observing System
State and Trends of Australia's Oceans | Report

4.7 | Continental-scale shark migrations

Michelle Heupel[1], Vic Peddemors[2], Mario Espinoza[1],
Amy Smoothey[2] and Colin Simpfendorfer[3]

[1] Australian Institute of Marine Science, Townsville, QLD, Australia
[2] Fisheries New South Wales, NSW Department of Primary Industries, Sydney Institute of Marine Science, Mosman, NSW, Australia
[3] Centre for Sustainable Tropical Fisheries and Aquaculture, College of Marine and Environmental Sciences, James Cook University, Townsville, QLD, Australia

Summary

Understanding movement and connectivity of populations is critical to management and conservation efforts. Through the IMOS Animal Tracking Facility the movements of bull sharks were tracked along the east coast of Australia between Sydney Harbour and the central Great Barrier Reef (GBR). This continental-scale tracking data identified previously unknown population connections with large numbers of bull sharks making return trips between Sydney and the GBR and revealing the importance of both of these regions for this species.

Key Data Streams

Acoustic Telemetry

State and Trends of Australia's Ocean Report
www.imosoceanreport.org.au

Time-Series published
10 January 2020

doi: 10.26198/5e16b18449e8c

Rationale

Movement and connectivity of marine populations is increasingly important as human use and environmental change alter ocean ecosystems. Identifying movement patterns is particularly important for species that move long distances and thus link ecosystems (e.g., coastal and offshore regions). The ability to move across state or national boundaries is also a topic of concern for management and conservation efforts. Large predators are key components of ecosystems due to their ability to directly (through predation) and indirectly (through fear affecting prey movements and distribution) affect other species. Here we investigate the capacity for large predators to connect habitats and affect an array of communities. In addition, understanding how they move, connect habitats and interact with other species can help define their role in ecosystems, which can help identify potential consequences of any population declines.

Methods

Movements of bull sharks were examined using acoustic telemetry receiver arrays along the east coast of Australia spanning from Sydney Harbour to the central Great Barrier Reef (GBR). Acoustic tracking data were obtained from the Integrated Marine Observing System (IMOS) Animal Tracking Facility and examined to define the extent and timing of movement of tagged sharks (Australian Ocean Data Network dataset: "IMOS - Animal Tracking Facility - Acoustic Tracking - Quality Controlled Detections (2007 -2017)"). A total of 114 bull sharks were fitted with acoustic transmitters – 75 in NSW and 39 in QLD (**Figure 1**). Straight line distances between detection locations were determined to approximate movement along the coast. To examine the level of connectivity among acoustic receiver arrays, a chord diagram was compiled to define incoming and outgoing movements of individuals.

Figure 1. Measuring and tagging a captured bull shark in QLD.

Results and Interpretation

Approximately half (n = 36) of the bull sharks tagged in NSW moved north into tropical regions. Seventeen individuals moved north and did not return to NSW. Both males and females were recorded undertaking long-range movements. Straight line distances were estimated at 60 – 1770 km one way (**Figure 2**). Several individuals were recorded making multiple, repeat movements between NSW and QLD, in some cases as many as five subsequent trips. The majority of repeat movements were completed by female sharks. Larger individuals were more likely to move than smaller individuals, suggesting differences in behaviour by life stage. By contrast, only one shark tagged in QLD moved into NSW, but 25% of QLD tagged sharks moved to southern reefs or inshore habitats. Some of the individuals tagged in QLD remained resident in the area throughout the study period and 50% of individuals that left their tagging area (central GBR) returned to the area. Connectivity analysis reflected the high degree of movement among locations and the scale of movement exhibited by this species (**Figure 3**).

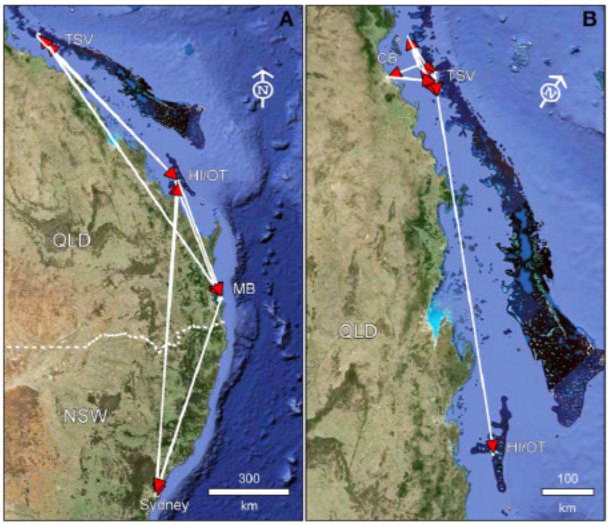

Figure 2. Straight line movements of an individual released in (A) NSW and (B) QLD based on detections on acoustic arrays beyond their capture location. Sourced from Heupel et al., 2015.

These results reveal complex linkages along the east coast of Australia, which suggest a tropical reef-based population comprised of individuals that migrate to multiple regions. Continental-scale acoustic telemetry systems can help define long-range movements and connectivity of broadly moving species such as large sharks. This analysis also revealed the importance of the GBR for adult bull sharks, which was previously unknown. The scale of movement and capacity to connect coastal temperate habitat to tropical reef habitat through movement suggest bull sharks could play a key role in ecosystem functions and energy linkage along the east coast of Australia.

doi: 10.26198/5e16b18449e8c

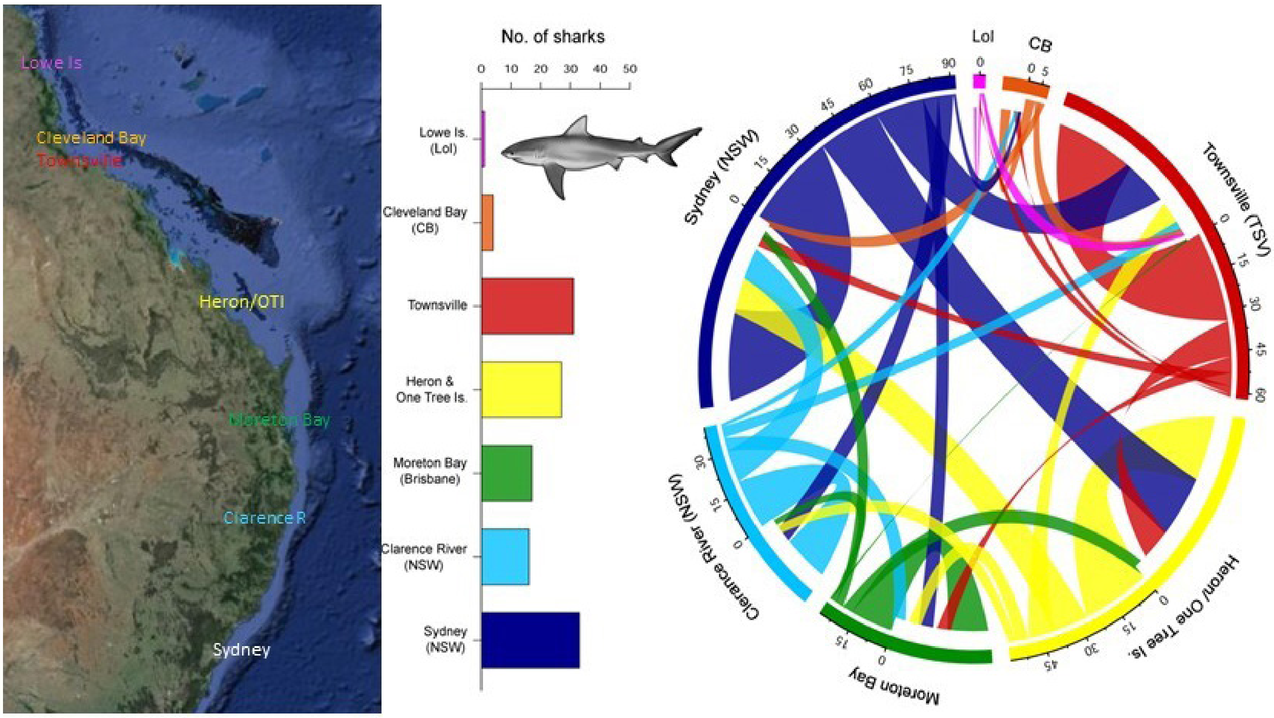

Figure 3. Map indicating the location of acoustic receiver arrays along the east coast of Australia and associated connectivity plot (chord diagram), indicating movement of individuals between receiver arrays. Sourced from Heupel et al., 2015.

Implications for people and ecosystems

The previously unknown importance of bull sharks in large marine ecosystems has been elucidated through data obtained via the IMOS Animal Tracking Facility. The analysis of bull shark movements highlights the complex challenges faced by managers when species move broadly and cross jurisdictional boundaries. Movement across state boundaries emphasises the need for cooperation among management agencies to ensure sharks receive adequate protection during their migrations. These data underscore the potential for sharks to move outside Australian waters and that this should be considered in international management agreements. This study reveals the capacity of acoustic telemetry networks to obtain valuable movement data can guide effective management and conservation policies for highly mobile species.

Acknowledgements

Data was sourced from Australia's Integrated Marine Observing System (IMOS) which is enabled by the National Collaborative Research Infrastructure Strategy (NCRIS).

Data Sources

IMOS Acoustic Telemetry.
http://imos.org.au/facilities/animaltracking/acoustictelemetry/

References

Heupel, M.R., Simpfendorfer, C.A., Espinoza, M., Smoothey, A.F., Tobin, A., Peddemors, V. 2015. Conservation challenges of sharks with continental scale migrations. *Frontiers in Marine Science*. doi: 10.3389/fmars.2015.00012.

IMOS

Integrated **Marine**
Observing System

IMOS
Integrated Marine
Observing System

State and Trends of
Australia's Oceans

Report

4.8 Tracking elephant seal population trends in the Southern Ocean

Clive McMahon[1], Rob Harcourt[2] and Mark Hindell[1]

[1] Institute for Marine and Antarctic Studies, University of Tasmania, Hobart, TAS, Australia

[2] Marine Predator Research Group, Department of Biological Sciences, Faculty of Science and Engineering, Macquarie University, North Ryde, NSW, Australia

Summary

Using satellite tagged southern elephant seals equipped with in situ data loggers we show that the decrease in the Macquarie Island population is related to increasing sea ice concentrations in forging grounds along the Victoria Land Coast. Seals that feed in the relatively stable sub-Antarctic however (representing approximately 40% of the Macquarie Island population) are experiencing population growth. A predicted continued increase in sea ice in Antarctic foraging regions indicates that southern elephant seal populations will continue to decrease in the southern Pacific Ocean.

Key Data Streams

Animal Tagging

State and Trends of Australia's Ocean Report
www.imosoceanreport.org.au

Time-Series published
10 January 2020

doi: 10.26198/5e16b1ec49e8d

Rationale

For over sixty years, the southern elephant seal population at Macquarie Island has been decreasing at an average rate of 1.2% per year (**Figure 1**). Macquarie Island has the sole breeding population in the southern Pacific Ocean and is one of the four distinct stocks of southern elephant seals found around the southern hemisphere. These four stocks are genetically distinct, with limited mixing among populations. Currently, only the Macquarie Island population is decreasing and the explanation for this is that food availability is regulating population growth, although the proximate mechanism of how food availability affects population growth remains unclear. The most likely explanation is that population growth in southern elephant seals is determined by a combined response of individuals using a patchwork of habitats resulting in variable foraging and ultimately breeding success, the sum total of which is an overall slow, decline in the population. A major challenge for testing this hypothesis is to quantify links between individual maternal foraging zones and pup weaning mass (i.e., food quality in those zones) and the contribution to population growth for a large sample of animals.

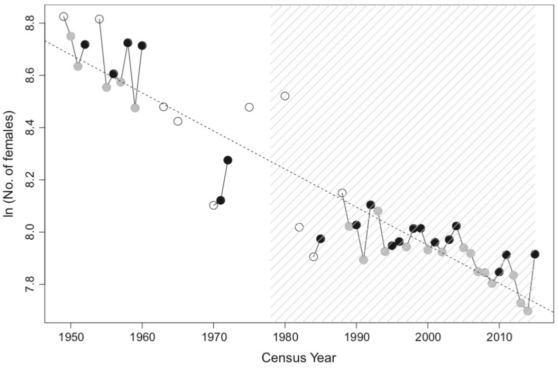

Figure 1. Decline in elephant seals at Macquarie Island (adapted from Hindell et al., 2017, Global Change Biology, hatched areas are period with satellite environmental data).

Methods

Much of what we now know about elephant seal migration and foraging behaviour comes from biotelemetry. Satellite trackers or data-loggers can be attached to individual animals to follow their movements during the long post-breeding and post-moult periods at sea (80 and 280 days respectively) and to record foraging depths and prey encounter rates. Such studies can be logistically difficult or expensive and often samples are restricted to few individuals. The challenge is knowing how representative these samples (typically <500 individuals) are of the population being studied.

The Integrated Marine Observing System (IMOS) has been instrumental in resolving the vexing question of where seals forage and how this may be linked to long-term population growth. Female southern elephant seals were tagged at Macquarie island to investigate where seals fed and to assess the quality of these feeding areas (**Figure 2**). We used *in situ* environmental data collected by seals (Conductivity, Temperature and Depth) to describe the water masses where seals were feeding and linked this to broader indices of environmental state including sea-ice extent (Hindell et al., 2017; McMahon, Harcourt, Burton, Daniel, & Hindell, 2017).

Figure 2. A Weddell seal in the Ross Sea sports a Conductivity, Temperature and Depth Satellite Relay Data Logger (Photo Clive R. McMahon).

Results and interpretation

The study lead by Mark Hindell (2017) at the Institute for Marine and Antarctic Studies (IMAS) found that there were three main groups of seals specialised in feeding in different ocean realms, the sub-Antarctic, the Ross Sea and the Victoria Land Coast (**Figure 3**). Physical and climate attributes (e.g., wind strength, sea surface height, ocean current strength) varied amongst the realms and also displayed different temporal trends over the last four decades. Most notably, sea ice extent increased in the Victoria Land realm, while it decreased overall in the Ross Sea realm. Indeed, this increase in sea-ice along the Victoria Land Coast is one of the few regions in the Antarctic where sea-ice is increasing. Using a species distribution model, mean residence times (i.e., the time the seals spent in each 50 by 50 km grid cell) was related to nine climate and physical co-variates. By predicting the seal residence times spatially, the core feeding regions used by the seals could be identified across the Southern Ocean from 120°E to 120°W (**Figure 4**).

Interestingly, the seal population size at Macquarie Island was negatively correlated with ice concentration within the core habitat of seals using the Victoria Land Coast, where the sea-ice is increasing, and predicted to continue to increase over the next decades. Consequences of these changes on the Antarctic biota are unknown. But what is known is that for elephant seals there is a negative relationship between seal numbers at Macquarie Island and increased sea-ice, implying that the population in the southern Pacific Ocean will continue to decrease. However, despite this negative relationship between sea-ice and population numbers, 40% of the Macquarie Island females fed in the relatively stable sub-Antarctic region. In this region there is a positive relationship with population growth; this positive relationship may buffer the Macquarie population against longer-term regional changes in habitat quality.

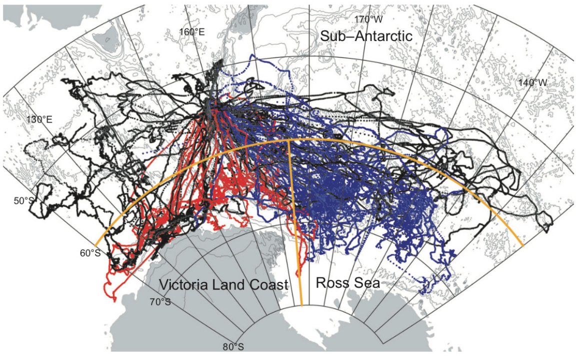

Figure 3. 67 seal tracks colour coded by specialist group; Red = Victoria Land Coast, Black = Sub-Antarctic; Blue = Ross Sea adapted from Hindell et al., 2017).

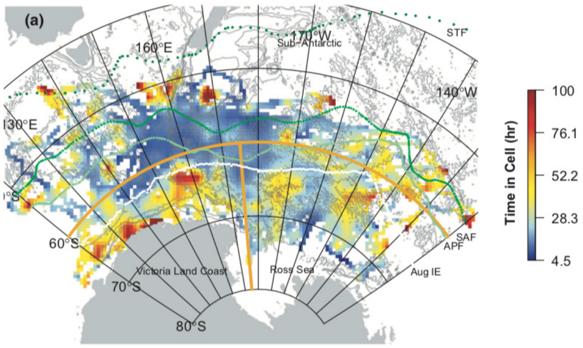

Figure 4. Mean seal residence time per 50 km x 50 km grid, with a colour scale ranging from 4.5 hr to 327 hr. APF is Antarctic Polar Front; SAF is Sub-Antarctic Front, STF is Sub-Tropical Front (adapted from Hindell et al., 2017, Global Change Biology).

Implications for people and ecosystems

In the Anthropocene, wild animals now make up <4% of the world's animal biomass. Identifying how these remaining animals might respond to on-going human activities needs strong, evidence-based science and innovative approaches. This study has shown that by combining new approaches to tracking animals that enable us to quantify their behaviours while simultaneously measuring the physical attributes of their remote feeding areas, we can put our finger on the underlying drivers of population change of even these most enigmatic of animals inhabiting the world's remote Southern Ocean.

Acknowledgements

Data was sourced from Australia's Integrated Marine Observing System (IMOS) which is enabled by the National Collaborative Research Infrastructure Strategy (NCRIS).

Data Sources

IMOS Animal Tagging.
http://imos.org.au/facilities/animaltracking/animaltracking-animaltagging/

References

Hindell, M. A., Sumner, M., Bestley, S., Wotherspoon, S., Harcourt, R. G., Lea, M.-A., . . . McMahon, C. R. (2017). Decadal changes in habitat characteristics influence population trajectories of southern elephant seals. *Global Change Biology, 23*(12), 5136-5150. doi:10.1111/gcb.13776

McMahon, C. R., Harcourt, R. G., Burton, H. R., Daniel, O., & Hindell, M. A. (2017). Seal mothers expend more on offspring under favourable conditions and less when resources are limited. *Journal of Animal Ecology, 86*(2), 359-370. doi:10.1111/1365-2656.12611

IMOS

Integrated Marine
Observing System